Mechanistic Studies on Enzymes of Secondary Metabolism:

5'-Fluoro-5'-deoxyadenosine synthase and 1-Deoxy-D-xylulose-5-phosphate reductoisomerase

A thesis presented for the degree of Doctor of Philosophy to the University of St. Andrews on the 17th April 2006

by

Cosimo Damiano Cadicamo

To my parents, to my grandfather Attilio Oliva,
and to my friends Antonio Marucci and Giuseppe Galati

Declaration

I, Cosimo Damiano Cadicamo, hereby certify that this thesis, which is approximately 32,000 words in length, has been written by me, that it is the record of work carried out by me and that it has not been submitted in any previous application for a higher degree.

Date....2/6/06....Signature of Candidate..

I was admitted as a research student in June 2002 and as a candidate for the degree of Doctor of Philosophy in June 2002, the higher study for which this is a record was carried out at the University of St Andrews between June 2002 and December 2005.

Date....2/6/06.....Signature of Candidate....

I hereby certify that the candidate has fulfilled the conditions of the Resolution and Regulations appropriate for the Degree of Doctor of Philosophy in the University of St Andrews and that the candidate is qualified to submit this thesis in application for that degree.

Date.2/6/06.....Signature of Supervisor.. ....

Copyright

In submission of this thesis to the University of St. Andrews I understand that I am giving permission for it to be made available for use in accordance with the regulation of the University Library for the time being in force, subject to any copyright vested in the work not being affected thereby. I understand that the title and abstract will be published and a copy of the work may be made and supplied to any *bona fide* library or research worker.

Date..2/6/06.....Signature of Candidate...

Acknowledgements

To start I would like to thank my supervisor Professor David O'Hagan who gave the opportunity to study in St Andrews and for all his support during my PhD.

I would like also thank all people that were involved in my projects: Dr Hai Deng and Dr Abdel Meddour (Orsay, Paris) for the "Stereochemical Study", Dr David Robinson and Andy McEwan for "Halide binding studies" and Dr. Russell Cox and Dr. U. Wong (at Bristol University) for "DXR inhibition assays".

I am extremely grateful to all the following people for technical support: Dr. Alexandra Slawin for X-ray analysis, Sylvia Williamson for elemental analysis, Caroline Hosburgh for mass spectrometry, and Melanja Smith for NMR spectroscopy. But I am most grateful to Dr Tomas Lebl for his valuable help with NMR analyses.

I would next like to thank all the past and present DOH members, who made the lab an enjoyable environment in which to work. A special thanks goes to Dr Luke Hunter and to my "academic daughter" (*figlia*) Mayca Onega who read early drafts of the thesis.

Last but not least, I would like to thank all my friends I have met over St Andrews. Thank you all of you for your friendship and for the time we spent together.

Contents

List of Abbreviations

Ac	Acetyl
AIBN	Azo-bis-*iso*-butyronitrile
ATP	Adenosine tri-phosphate
br s	Broad singlet
BuLi	Butyl-lithium
BzCl	Benzoyl-chloride
CI	Chemical ionization
d	Doublet
DCC	Dicyclohexyl-carbodiimide
DMSO	Dimethyl-sulfoxide
de	Diastereomeric excess
dec	Decompose
DXP	1-Deoxy-D-xylulose-5-phosphate
DXR	1-Deoxy-D-xylulose-5-phosphate reductoisomerase
eq.	Equivalent
Et	Ethyl
ES-MS	Electrospray mass spectrometry
5'-FDA	5'-Fluoro-5'-deoxy-adenosine
5'-FDI	5'-Fluoro-5'-deoxy-inosine
5-FDR	5-Fluoro-5-deoxy-D-ribose
5-FDRP	5-Fluoro-5-deoxy-D-ribose-1-phosphate
g	Gram
GC-MS	Gas chromatography mass spectrometry
h	Hour

HPLC	High pressure liquid chromatography
Hz	Hertz
IR	Infrared spectroscopy
J	Coupling constant
kDa	Kilo Dalton
LDA	lithium diisopropylamide
m	Multiplet
M	Molar
Me	Methyl
MEP	2-*C*-Methyl-D-erythritol-4-phosphate
mg	Milligram
min	Minute
mL	Millilitre
mM	Millimolar
mmol	Millimol
mp	Melting point
Ms	Mesyl
µl	Microlitres
NAD^+	Nicotinamide adenine dinucleotide (oxidised form)
NMR	Nuclear magnetic resonance
PEP	Phosphoenoylpyruvate
Ph	Phenyl
PBLG	Poly-γ-benzyl-L-glutamate
PLP	Pyridoxal phosphate
PNP	Purine nucleoside phosphorylase

PPh_3	Triphenyl-phosphine
ppm	Parts per million
Pyr	Pyridine
q	Quartet
s	Singlet
SAH	*S*-Adenosyl-L-homocysteine
SAM	*S*-Adenosyl-L-methionine
t	Triplet
TBAF	Tetrabutyl ammonium fluoride
t-BuOH	*tert*-butanol
t-BuSH	*tert*-butanthiol
TFA	Trifluoro-acetic acid
THF	Tetrahydrofuran
TLC	Thin layer chromatography
TMS	Trimethylsilyl
Tris	Tris(hydroxymethyl)aminoethane
TsCl	*p*-tosylchloride
UV	Ultra-violet

Abstract

A fluorination enzyme (fluorinase) has recently been isolated in St. Andrews from the bacterium *Streptomyces cattleya*. This enzyme mediates a reaction between fluoride ion and S-adenosyl-L-methionine (SAM) to generate 5'-fluoro-5'-deoxy-adenosine (5'-FDA). In this thesis the stereochemical course of biological fluorination has been evaluated. This involved the preparation of a stereospecifically labelled sample of ATP {(5'*R*)-[$^2H_1$]-ATP}. This substrate generated a stereospecifically labelled sample of 5'-FDA after a coupled enzyme reaction involving the SAM synthase and then the fluorinase. Evaluation of the absolute configuration of the chiral fluoromethyl group at the 5'-carbon of 5'-FDA (HDFC-) by ^2H-NMR analysis in a chiral liquid-crystalline medium, and by comparison with a stereospecifically labelled sample of (5'*S*)-[$^2H_1$]-FDA, established that the fluorinase catalyses fluorination with an inversion of configuration, consistent with an S_N2 reaction mechanism. This is discussed in detail in **chapter 4**.

An investigation into halide binding prior to nucleophilic substitution of SAM was also addressed. This involved the preparation of a sample of 9-(β-D-*erythro*-furanosyl)adenosine, a compound which was co-crystallised with the fluorinase. An enzyme crystal structure with 9-(β-D-*erythro*-furanosyl)adenosine was obtained, although the chloride ion was not evident. This is discussed in **chapter 3**.

The DXR is an enzyme on the non-mevalonate pathway to isopentenyl diphosphate and dimethylallyl diphosphate that catalyses the conversion of 1-deoxy-D-xylulose 5-phosphate (DXP) to 2-*C*-methyl-D-erythritol 4-phosphate (MEP). A candidate inhibitor was designed and prepared to explore the mechanism of this enzyme. This is discussed in detail in **chapter 6**.

Chapter 1

Introduction

Secondary metabolites have always been a central theme in organic chemistry. Their structures have challenged organic chemists and have driven methodology in synthesis, and this continues today. Exploring the origin of secondary metabolites has also driven much of our current understanding of enzyme mechanism. The number of natural products that have been isolated and characterised has risen dramatically in the last 20/30 years. This is clearly the result of the development of analytical techniques such as mass spectrometry and NMR, but it is also the result of increased collaboration across various disciplines such as biochemistry, molecular biology, chemistry and computational chemistry.

One of the major aspects of the study of secondary metabolites is the investigation of their biosynthetic pathways. A metabolic pathway can be understood at several levels:[1] a) In terms of the sequence of reactions by which a specific metabolite is converted to a product; b) in terms of the mechanisms by which each intermediate is converted to its successor; c) in terms of the control mechanisms that regulate the flow of metabolites through the pathway.

In particular, the mechanistic investigation of the biosynthetic steps requires the isolation and characterization of specific enzymes that catalyse each reaction.[1] As enzymatic reactions are essential for the metabolism of all living systems, enzymes may clearly be an important target for medicinal chemists that wish to prepare drugs that are active in the

organisms. Thus, mechanistic studies of these proteins are important not just to shed light on a specific metabolic pathway, but they are also fundamental for the rational design of biological active compounds.

1.1 Primary and secondary metabolites

Natural products can be subdivided in two classes. These are primary and secondary metabolites.[2] Primary metabolites include proteins, nucleic acids, sugars and lipids. These molecules are essential for the survival of the organism and they are common to all living systems. However, their biosynthetic pathways can vary widely across different organisms.

Secondary metabolites, instead, can be classified as non-essential molecules produced from a small number of key intermediates, which are formed during the anabolism (production) or catabolism (degradation) of primary metabolites. These include compounds that are unique to a particular species or are of relatively limited occurrence. For example, the alkaloid morphine **1** comes from just two species of poppy, *Papaver somniferum* and *Papaver setigerum*.[2] The role of secondary metabolites is not always clear, but obviously their biosynthesis must confer a selective advantage to the organism. Many of these compounds have been established to play an important role in inter- and intra- species interactions. This area of study is known as "ecological chemistry".[2] For example, several plants species produce the very toxic metabolite fluoroacetate **2** in high concentrations, presumably as a means of defence against grazing herbivores (section 2.1.1).[3]

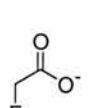

2

Secondary metabolites are characterised by a staggering variety of structural motifs, as represented by the examples reported in Figure 1.1.

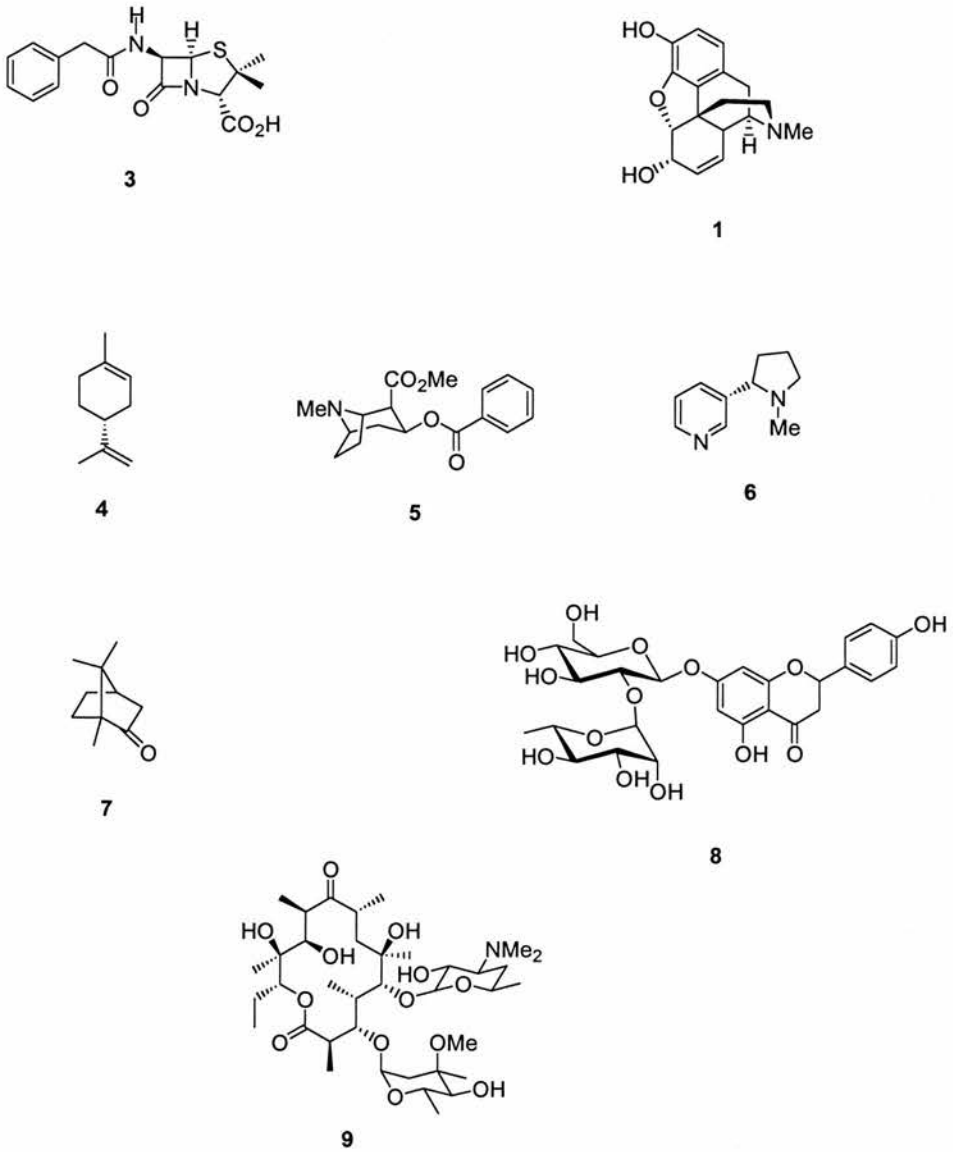

Figure 1.1. Examples of secondary metabolites: the alkaloids morphine **1**, cocaine **5**, and nicotine **6**; the polyketide erythromycin A **9**; the isoprenoids camphor **7** and (+)-limonene **4**; the amino acid metabolite penicillin G **3**; and the flavonoid naringin **8**.

They are biosynthesised from four principal building blocks.[2] These are a) acetate, in the form of its coenzyme A thioester, which contributes to many polyketide aromatics and

fatty acid metabolites like the prostaglandins and leukotrienes; b) isopentenyl diphosphate and dimethylallyl diphosphate, which are the progenitors of the steroidal isoprenoids; c) shikimic acid, which is involved in the production of cinnamic acid derivatives, lignans, flavonoids and other aromatic compounds; and finally c) the amino acids, which are the biosynthetic precursors of a diversity of N and S containing compounds such as the alkaloids and the penicillins.

1.2 Exploring biosynthetic pathways

The elucidation of a metabolic pathway and its metabolite intermediates is a complex process, involving contributions from a variety of disciplines. Nevertheless, the new techniques evolved in the last 40-50 years have enabled scientists to shed light on many biosynthetic routes. The use of metabolic tracers to follow paths of specific atoms and molecules through the metabolic maze has become routine.[1] A more biochemical approach involves blocking of a metabolic step by mutation and subsequently studying the effect of the mutation on the growth or on the production of metabolic intermediates.

1.2.1 Use of isotopes

A common strategy to elucidate the biosynthetic origin of secondary metabolites involves the use of isotopically enriched precursors which are administered to growing organisms or to cell-free extracts.[1,2] The resulting product is then isolated, purified and analysed for isotopic content. If the incorporation of isotope has occurred in the predicted fashion, cautious acceptance of the precursor/metabolite relationship can be assumed.[2]

Early studies involved the use of radioactive isotopes (^{14}C, ^{3}H)-β-emitters to carry out feeding experiments. These isotopes are unstable and undergo to radioactive decay involving the emission of electrons (β particles).[1] Some of the most common isotopes used in biosynthesis studies are reported in Table 1.1. Radioactive nuclei emit radiation with characteristic energies and they have also characteristic half-lives. The radiation emitted can be detected and quantified by using a variety of techniques, the most common involving liquid scintillation counting.

Radioactive Isotopes		
Nucleus	Radiation type	Half-Life
^{3}H	β	12.32 years
^{14}C	β	5715 years
^{32}P	β	14.28 days
^{35}S	β	87.2 days

Table 1.1. Most common radioactive isotopes used in biochemical experiments.[1]

The use of radiolabelled compounds has been advantageous due to the low level of incorporation required for their detection, especially in those cases where intermediates accumulate poorly in biosynthetic pathways. However, these unstable isotopes have clear disadvantages. First of all, they need to be handled with great caution as they can cause genetic damage upon ingestion.[1] Secondly, the isolated radiolabelled metabolite must be degraded chemically to provide information about the centres of enrichment, and it may be necessary to degrade the sample to a single carbon entity in order to determine the position

of label with complete certainty. Because each degradative step reduces the amount of metabolite available for further degradation, it is usually impossible to obtain a complete labelling pattern for the molecule.[2] Finally, legislative controls render their use administratively burdensome.

Due to these limitations, radioactive isotopes have been widely replaced by stable isotopes, even though the use of such isotopes requires higher isotope concentrations compared to those (trace) required for radiolabelled feeding experiments. Stable isotope utility has improved dramatically due to the development of NMR spectroscopy and to the advent of pulsed Fourier-transform spectrometers, which constitute now a viable method to study compounds for isotopic content.[2] The most common stable isotopes used in biochemical experiments are reported in Table 1.2.

Stable Isotopes		
Nucleus	Natural Abundance (%)	I= spin
^{2}H	0.015	1
^{13}C	1.10	1/2
^{15}N	0.37	1/2
^{18}O	0.20	0

Table 1.2. The most common stable isotopes used to trace metabolic pathways.[1]

The ^{13}C-isotope has been widely used for the elucidation of many metabolic pathways. Feeding experiments with ^{13}C labelled precursors can lead to the formation of isotopically enriched metabolites that give ^{13}C-NMR spectra containing peaks enhanced compared to

others. If the natural abundance spectrum has been assigned, the enhanced peaks can be also assigned to a single carbon of the metabolite, and hence the regiospecific incorporation can be deduced without recourse to degradative chemistry.[2]

The ^{2}H-isotope is also widely used. The fate of deuterium atoms during a biosynthesis can be detected directly by ^{2}H-NMR spectroscopy or indirectly by ^{13}C-NMR spectroscopy.[4,5] Poor resolution is frequently a limitation of ^{2}H-NMR spectroscopy because the peaks are normally broad and the spectral dispersion is low. Thus the indirect approach is preferred. Generally, in the indirect method the deuterium is attached to a ^{13}C nucleus, the resonance of which is shifted upfield (α-shift) and shows deuterium coupling.[4] However, for quantitative measurements of deuterium enrichment this technique has the disadvantage that the signal of the ^{2}H-bearing carbon is reduced by poor relaxation, signal multiplicity, and loss of nuclear Overhauser relaxation (NOE).[4] A deuterium atom placed at a β-position to the ^{13}C nucleus is often more readily detectable, as the upfield shift (β-shift) is still present but the coupling between the two nuclei is negligible (<1 Hz).[4]

One example of such isotopic labelling studies, involving ^{15}N-label, is depicted in Figure 1.2.[1] This investigation was carried out by D. Shemin and D. Rittemberg in 1945. By feeding experiments with ^{15}N-labelled precursors, they demonstrated that the nitrogen atoms of heme **10** are derived from glycine **11**. No isotopic label was detected when the experiment was carried out with ^{15}N-labelled proline **12**, leucine **13**, glutamic acid **14** or ammonia **15**.

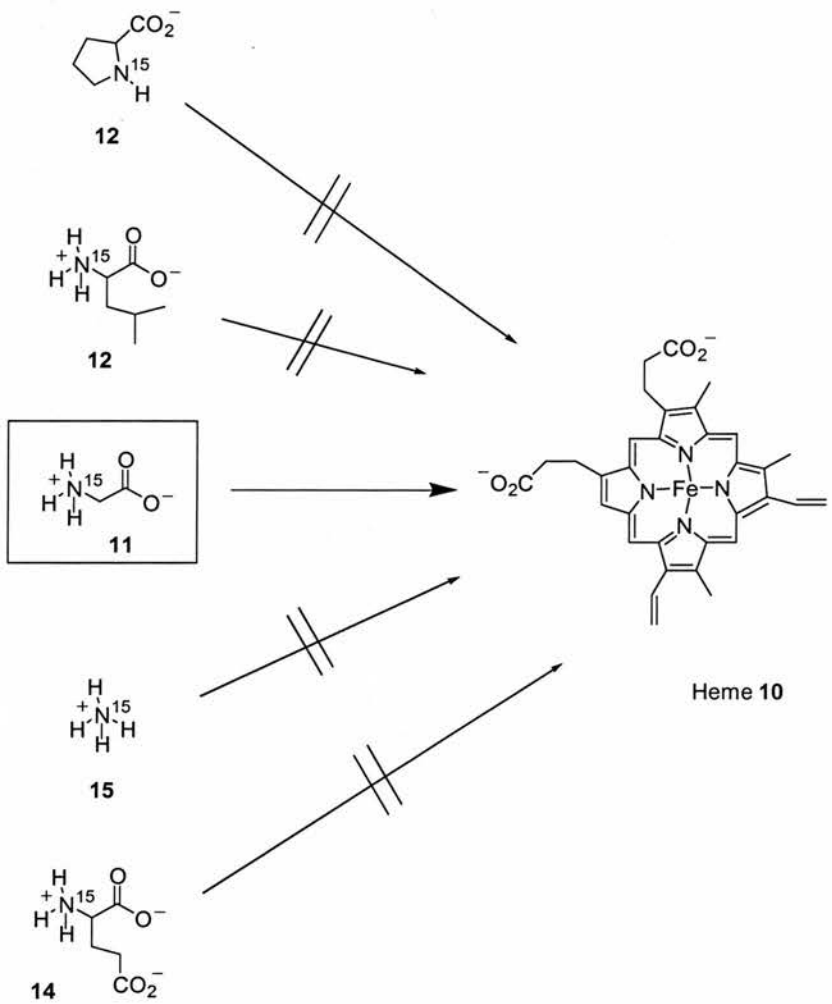

Figure 1.2. Study of the metabolic origin of the nitrogen atoms in heme **10**.[1]

1.2.2 Metabolic block

A different approach to the study of metabolic pathways consists of blocking a metabolic step in order to favour the build up of potential intermediates.[1,2] The isolation and characterization of such intermediates can offer key information for the elucidation of a specific biosynthetic pathway. One of the methods employed to block a metabolic step involves the use of chemical inhibitors. These have proven successful for biochemical

studies. For instance, the discovery that iodoacetate causes yeast extracts to accumulate fructose-1,5-bisphosphate, and that fluoride causes the building up of 3-phosphoglycerate and 2-phosphoglycerate was fundamental to elucidate the glycolytic pathway in yeast.[1]

The other general method to generate a metabolic block involves the genetic manipulation of micro-organisms.[1] An induced mutation in a specific micro-organism can generate a mutant strain that is deficient in the expression of a particular enzyme of a specific biosynthetic pathway. In this case, the mutant strain may accumulate metabolites, which are then isolated and characterised. The mutation can be induced by a random process, for instance by exposition to UV and X-ray irradiation. This of course has some limits as the mutation can affect also other enzymes. However the use of modern genetic engineering techniques eliminates such problems and allows targeting of desired enzymes at the gene level.[1]

1.3 Mechanistic investigation of enzymes

Each step of a metabolic pathway is catalysed by a specific enzyme. Like all catalysts, enzymes have the ability to lower the activation energy by helping stabilize the transition state.[6] They can viewed to act as a surface for the reaction, bringing the substrate or substrates together and holding them in an optimal position for reaction.

The decrease of the activation energy is the result of a contribution of a number of mechanisms and factors that are involved in the enzymatic action. First of all we need to consider the formation of the complex substrate/enzyme. When the substrate enters the active site, it forces the latter to change shape (Koshland's Theory of Induced fit).[6] This

moulding process is crucial for the enzymatic reaction. In fact, this may force the substrate in the ideal conformation for the reaction to follow and may also weaken the very bonds which have to be broken.[6] The substrate is bound to the active site of enzymes by interactions with amino acids. These include mainly ionic and hydrophobic interactions, hydrogen bonding, and also dipole-dipole or induced-dipole interactions. The amino acids present in the active site are important not just to bind the substrate. They also play an active role in catalysing the biochemical reaction. For example the amino acid histidine **16** is responsible for acid/base catalysis. Histidine **16** is a weak base and is able to accept and donate protons in the reaction mechanism as shown in Figure 1.3.

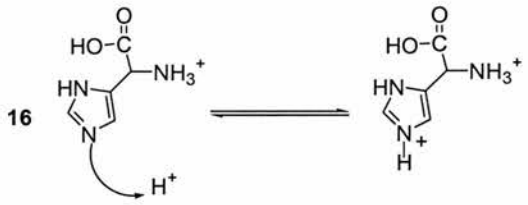

Figure 1.3. The amino acid histidine **16** is a weak base: it can accept and donate protons.[6]

Several enzymes require additional non-protein substances called cofactors for the reaction to take place. Cofactors include metal ions (e.g. Mn^{2+}, Mg^{2+}), and small molecules called co-enzymes that derive from water soluble vitamins.

The way cofactors and amino acid residues take part in enzyme reactions, and the way a substrate is transformed to a specific product is the main objective of the mechanistic investigation of a specific enzyme. A general approach to understanding the mechanism involves the use of the isotopes as described in section 1.2.1. The use of labelled substrates has proven successful for the elucidation of enzymatic mechanisms, and many examples are reported in the literature. In particular ^{13}C and ^{2}H are largely employed. ^{2}H-labelled substrates are often used to study the stereochemical features of a specific

enzyme. If the position of the label in the product is established after the enzymatic reaction, this will provide information about how the substrate has been processed.

Kinetic methods, X-ray diffraction data and computational studies are also involved in the study of enzyme-catalysed reactions. In particular, due to developments in protein expression, purification and crystallization, X-ray diffraction analyses of crystals of a specific enzyme may be a useful method to predict the mechanism of that enzyme. The general approach of this method involves the co-crystallization of the enzyme of interest with competitive inhibitors that are substrate or transition state mimics. The way such compounds are bound to the active site gives important information on how the enzyme acts.

Site-directed mutagenesis is a methodology widely employed in the study of enzymes. This has been also used to investigate the role of the amino acid residues of the active site, and it is often crucial to establish which of such residues is essential to the enzyme action.[7]

All these approaches proved fundamental to understand enzymatic reactions and form a solid basis for mechanistic postulations.

Investigation of enzyme mechanisms is also the main objective of the present thesis. In particular, the two enzymes, 5'-fluoro-5'-deoxyadenosine synthase (formally called "fluorinase") and 1-deoxy-D-xylulose-5-phosphate reductoisomerase (DXR), were explored. The fluorinase, recently purified from the actinomycete bacterium *S. cattleya* in the St Andrews lab, is the first native fluorination enzyme to have been identified, and it has given the first insight into the biosynthesis of fluorinated natural products.[8,9] Insights on the mechanism of this enzyme are discussed in chapters 3 and 4. The DXR is involved in the non-mevalonate pathway to isopentenyl diphosphate **17** and dimethylallyl

diphosphate **18**, a new route of isoprenoid biosynthesis discovered in 1993 by Rohmer and co-workers.[10]

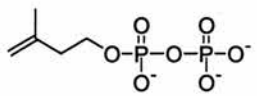

17

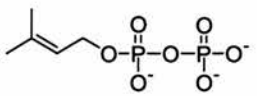

18

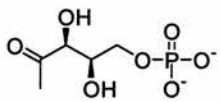

19

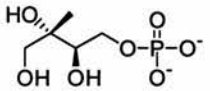

20

This enzyme catalyses an important step of the pathway in which 1-deoxy-D-xylulose-5-phosphate **19** (DXP) is converted to 2-*C*-methyl-D-erythritol-4-phosphate **20** (MEP). The design of a DXR inhibitor, based on mechanistic studies, is the aim of my second project and it is discussed in detail in chapter 6.

References Chapter 1

1. D. Voet and J. Voet, "Biochemistry", 2nd Ed., John Wiley & Sons, Inc.

2. J. Mann, "Chemical Aspects of Biosynthesis", 1st Ed. (1994), Oxford University Press.

3. D. O'Hagan and D. B. Harper, *J. Fluor. Chem.*, 1999, **100**, 127.

4. C. Abell and J. Staunton, *J. Chem. Soc., Chem. Commun.*, 1981, 856.

5. R. G. Brereton, M. J. Garson and J. Staunton, *J. Chem. Soc., Perkin I*, 1984, 1027.

6. G. L. Patrick, "An Introduction to Medicinal Chemistry", Oxford University Press, 2002.

7. T. Kuzuyama, S. Takahaschi, M. Takagi and H. Seto, *J. Biol. Chem.*, 2000, **275**, 19928.

8. H. Deng, D. O'Hagan and C. Schaffrath, *Nat. Prod. Rep.*, 2004, **21**, 773.

9. D. O'Hagan, C. Schaffrath, S. Cobb, J. T. G. Hamilton and C. D. Murphy, *Nature*, 2002, **416**, 279.

10. M. Rohmer, M. Knani, P. Simonin, B. Sutter and H. Sahm, *Biochem. J.*, 1993, **295**, 517.

Chapter 2

Fluorine-containing natural products

2.1 Introduction

The biosynthesis of halogenated secondary metabolites has attracted a lot of interest in recent years. The number of halogen-containing natural products isolated has increased significantly over the last thirty years (more than 4,000), as reported in a recent review by Gribble *et al.*[1] The majority of these compounds contain either a chlorine (2300) or a bromine (2100) atom. Both chlorinated and brominated natural products have been found to originate from a variety of sources (e.g. plant, bacterial) but the largest number have been isolated from marine sources.[1-3] Some examples of brominated and chlorinated secondary metabolites are shown in Figure 2.1.

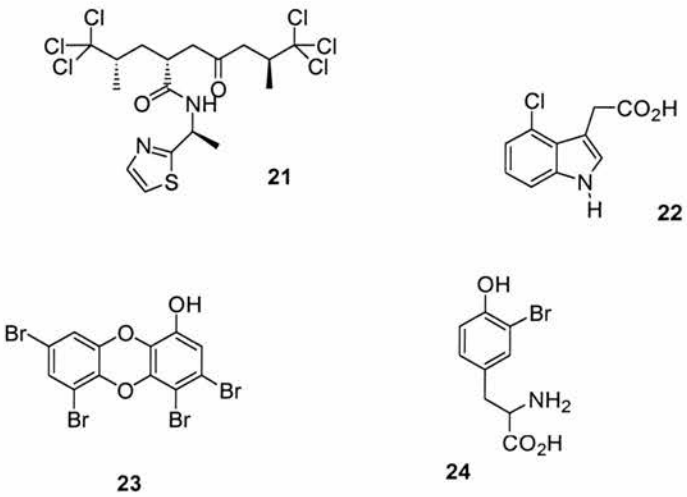

Figure 2.1. Selected chlorine and bromine containing secondary metabolites: Nordysidenin **21**, 4-chloroindole-3-acetic acid **22**, bromo-tyrosine **24** and spongiadioxin **23**.

Natural products containing iodine are relatively rare. This small sub-group includes tyrosine derivatives including the human thyroid hormone, thyroxine **25** (T_4),[4] nucleoside derivatives[5], and also fatty acid[6] and terpene derivatives.[7]

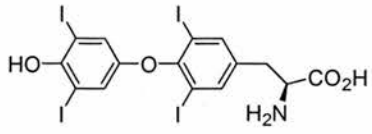

25

Surprisingly the most abundant halogen in the earth's crust, fluorine, has been identified as a component of only 13 secondary metabolites of which eight are ω-fluorinated homologues of long chain fatty acids found as co-metabolites in the seeds of the same plant. So formally only six discrete fluorinated natural products have been isolated excluding these fatty acid homologues.[8] The main reason for this lack of fluorine containing natural products is that seawater typically contains only 1.3 ppm fluoride in comparison to 1900 ppm of chloride.[9] Another important factor that limits the participation of fluorine in biochemical processes is the high heat of hydration of the fluoride ion. In fact fluoride ion in water is heavily hydrated, and therefore its nucleophilicity is poor. So it appears clear that fluorination reaction by nucleophilic displacement in water is not straightforward. However, probably the most important factor restricting the biosynthesis of organofluorine compounds is the high redox potential required for the oxidation of fluoride which does not permit oxidation of fluoride ion to radical fluorine or F^+, by reduction of hydrogen peroxide. This precludes the incorporation of fluorine by the haloperoxidase reaction, the main route for formation of the other organohalogen compounds.[10,11]

2.1.1 Fluoroacetate 2

2

Fluoroacetate **2** was the first organo-fluorine compound to be identified. Marais reported the metabolite from the Southern African plant *Dichapetalum cymosum* in 1943.[12,13] This plant was known to be very toxic, and its fresh leaves can accumulate levels of fluoroacetate **2** to 250 ppm. Fluoroacetate **2** has subsequently been found at varying concentrations in a variety of plants throughout the world, mostly in Africa but also in Australia and to a lesser extent South America.[8,14] In Australia the toxin has been identified in 35 species from three genera of Leguminosae, especially *Gastrolobium* and *Oxylobium.* These plants, however, do not have a wide geographic distribution and are generally confined to the south west of Western Australia. The most toxic plant reported to date, found in central Africa, belongs to the genus *Dichapetalum. D. braunii* can contain up to 8000 ppm of fluoroacetate **2** within its seeds, and it is extremely toxic.[8,15] The reason why several plant species are capable of accumulating fluoroacetate **2** to very high concentrations, is presumably related to defence against foraging animals.

2.1.2 Fluorocitrate 26

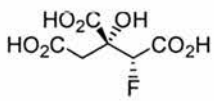

26

In 1953, the British biochemist Sir Rudolph Peters was the first to propose a mechanism

for the toxicity of fluoroacetate **2**.[8,16] He proposed that its toxicity arises from its *in vivo* conversion of fluoroacetate **2** to fluorocitrate **26**, a process that was named the "lethal synthesis". Fluorocitrate **26** is formed after the condensation of fluoroacetyl-CoA **27** with oxaloacetate **28** catalysed by citrate synthase, an important enzyme of the citric acid cycle. This reaction is completely stereoselective and produces only the toxic (2*R*,3*R*)-stereoisomer of fluorocitrate **26**.[8] The other three possible stereoisomers are not toxic. This was demonstrated by Kun and Dummell, who prepared and purified all of the stereoisomers, and showed that only the (2*R*,3*R*)-isomer inhibits citrate synthase.[17] Aconitase, the enzyme that succeeds citrate synthase in the citric acid cycle, converts fluorocitrate **26** to fluoro-*cis*-aconitate **29**, which, in the enzyme-bound form, is attacked by hydroxide in an S_N2' process, to generate 4-hydroxy-*trans*-aconitate **30** (Scheme 2.1).[8,18] This compound is a potent competitive inhibitor of aconitase, which explains the biochemical origin of fluoroacetate **2** toxicity. The crystal structure of aconitase with the inhibitor supports this mechanism unequivocally.[18]

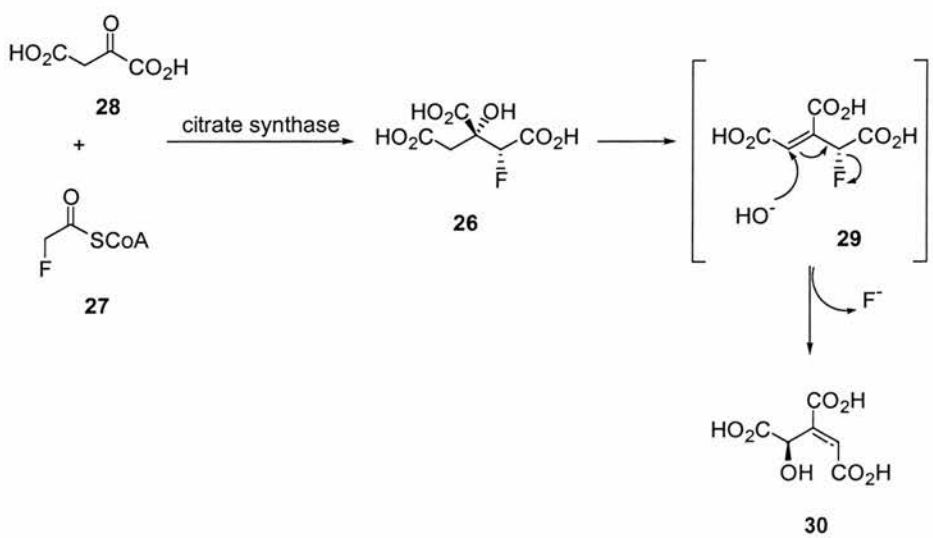

Scheme 2.1. Conversion of fluoroacetyl-CoA **27** to 4-hydroxy-*trans*-aconitate **30**, a potent inhibitor of aconitase.

2.1.3 Fluoroacetone 31

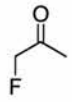

31

The existence of fluoroacetone **31** was reported by Peters and Shorthouse in the late 1960's, while they were exploring fluoride metabolites in the plants *Acacia georginae*.[19,20] When volatiles of the plant grown in fluoride solution, were passed through a dinitrophenylhydrazine (DNP) derivatising solution, approximately 13% of the volatilised fluorine was trapped as the fluorinated 2,4-dinitrophenylhydrazone derivative which showed an identical retention time on paper chromatography to the hydrazone derivative of fluoroacetone **31**.[20] However, as admitted by the authors, this conclusion is tentative and the existence of fluoroacetone **31** needs to be revisited and supported by more consistent experiments.

2.1.4 Fluorinated fatty acids

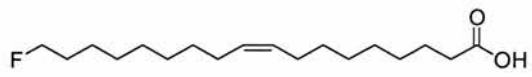

32

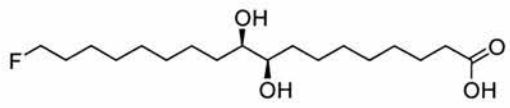

33

In 1959, Sir Rudolph Peters and co-workers[21,22] found that the seeds of *Dichapetalum toxicarium*, a plant from Sierra Leone in West Africa, contain up to 1800 μg g^{-1} of organic fluorine. The major fluorinated constituent was identified as ω-fluorooleic acid **32** ($C_{18:1}$),

and small traces of ω-fluoropalmitic acid ($C_{16:0}$) were also isolated. Further and more detailed analysis by GS-MS has revealed the presence of a range of ω-fluorofatty acids at much lower concentrations ($C_{16:1}$, $C_{18:0}$, $C_{18:2}$, $C_{20:0}$ and $C_{20:1}$).[23] *Threo*-18-Fluoro-9,10-dihydroxystearic acid **33** has also been isolated from *D. toxicarium* seed oil accounting for about 1% of the organic fluorine present.[8] By correlation to the non-fluorinated fatty acids, the ω-fluoro compounds probably arise from a common precursor, presumably fluoroacetyl-CoA **27**. A hypothetical biosynthetic pathway to these fluorinated fatty acids is summarised in Scheme 2.2.

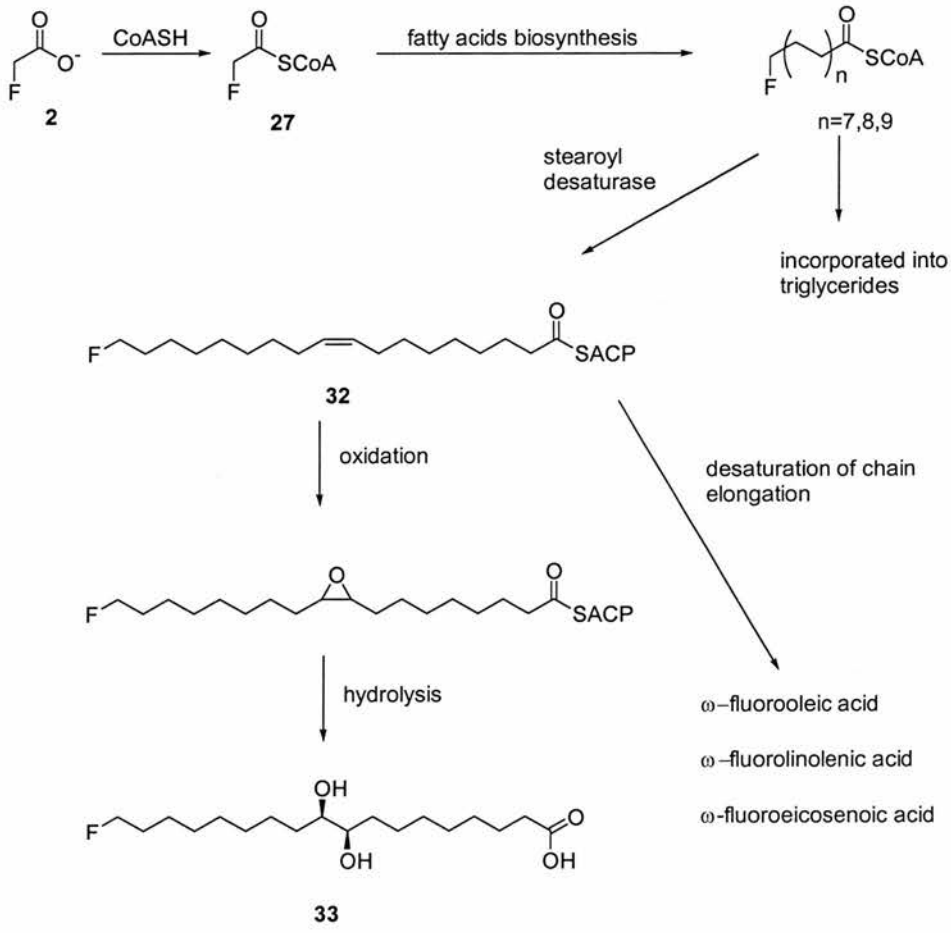

2 **27** **32** **33**

Scheme 2.2. Putative biosynthetic pathway to ω-fluorofatty acids in *D. toxicarium*.

2.1.5 5'-Fluorouracil derivatives

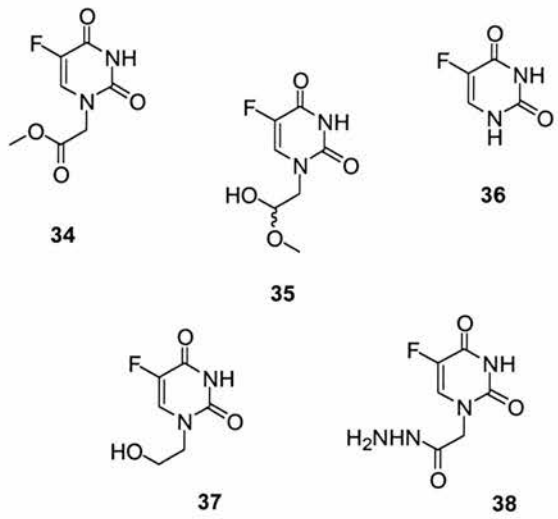

Figure 2.2. 5'-Fluorouracil derivatives identified from the sponge *Phakellia fusca* **34-38**.

More recently (2003) some fluorinated metabolites were reported from the marine sponge *Phakellia fusca*.[24] The *Phakellia* sponges have been reported to yield alkaloids, peptides and polyether acids and it was during attempts to isolate new biologically active molecules that a series of 5'-fluorouracil derivatives **34-38** (Figure 2.2) were identified. It is not clear if and how these compounds have accumulated in the sponge, but their structures all contain the motif of the chemotherapeutic drug 5'-fluorouracil **36**, which raises the possibility that they are products of industrial contamination and metabolic derivatisation rather than new biosynthetic products.[25] This hypothesis is strengthened by the fact that sponges filter feed.

2.1.6 Nucleocidin 39

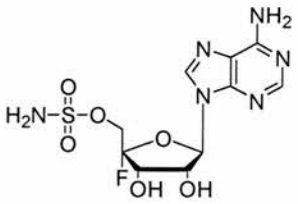

39

Two bacteria have been reported that are able to biosynthesise organo-fluorine compounds. The first of these is the nucleoside antibiotic nucleocidin **39**. This nucleoside was isolated originally in 1957 from the bacterium *Streptomyces calvus*, which was obtained from an Indian soil sample.[26] However, the presence of a fluorine atom in the molecule was not appreciated until 1969, when the structure 4′-fluoro-5′-*O*-sulfamoyl-adenosine was proposed for nucleocidin **39**.[27] Subsequent work by Shuman *et al.*[28] supported a β-D configuration of the ribose moiety in the proposed structure as upon heating in DMF, nucleocidin was converted to an N^3,5'-anhydronucleoside **40**. Finally, in 1976, the structure of nucleocidin **39** was confirmed by a total synthesis.[29,30] The location of fluorine at the 4'-position is somewhat unexpected due to anomeric destabilization, however this doesn't appear to be a problem. It is also intriguing to speculate on how nucleocidin **39** is biosynthesised. Unfortunately, recent attempts in several laboratories to re-isolate this metabolite from cultures of *S. calvus* have failed.[29]

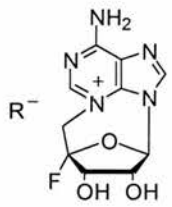

40

2.1.7 Fluorinated natural products in *S. cattleya*

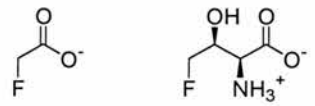

2 41

The first evidence of organo-fluorine compounds in *S. cattleya* was reported 1986 by a research group at Merck, N. Jersey (USA).[31] The bacterium produces the β-lactam antibiotic thienamycin,[32] and during optimization of the thienamycin fermentation they discovered the capacity of *S. cattleya* to produce fluorinated metabolites, when a particular soya bean casein was used as a feed stock.[25] The casein had high levels of fluoride. The compounds were identified as fluoroacetate **2** and 4-fluorothreonine **41**. The importance of this discovery is quite clear if we consider the failure to re-isolate the fluorinated antibiotic nucleocidin **39** from the bacterium *Streptomyces calvus*. This is only the second microorganism able to elaborate an organo-fluorine compound, and it allowed researchers to carry out studies exploring the origin of the carbon-fluorine bond *via* an enzymatic reaction. This is discussed in detail in section 2.2.

2.1.8 The first reported enzymatic C-F bond formation

The first reported enzymatic C-F bond formation involved mutants of a glycosidase enzyme from *Agrobacterium* sp.[33,34,35] In this enzyme the catalytic glutamate residue, which stabilises the intermediate oxocarbenium ion prior to disaccharide formation, was replaced, by site directed mutagenesis, with either an alanine or serine residue arresting any glycosidic bond cleavage. However, in the presence of a high concentration of fluoride (2 M), the enzyme's activity was restored. Fluoride, in fact, is able to quench the

oxocarbenium ion in these mutants and generates a transient α-fluoroglycoside **42** which is then subject to a second nucleophilic displacement to generate **43** (Scheme 2.3).

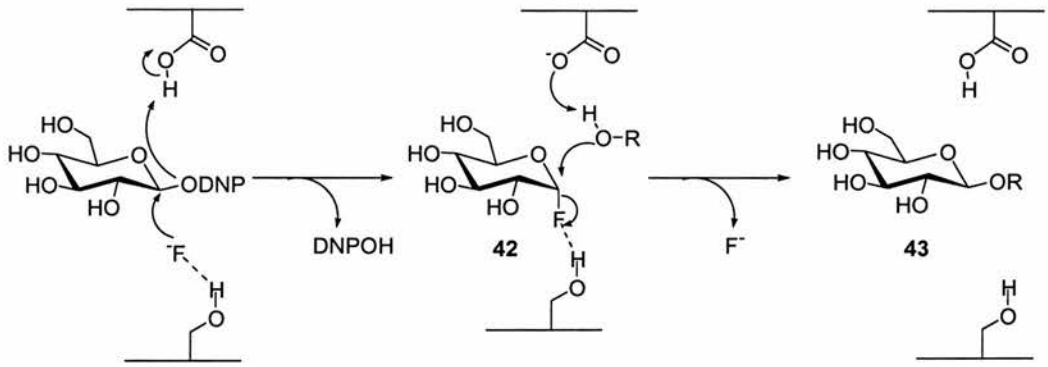

Scheme 2.3. Enzymatic C-F bond formation reactivates glycosidase activity in a mutant glycosidase enzyme.

These experiments with mutant enzymes are exciting and demonstrated for the first time that a nucleophilic fluorination to generate a C—F bond, can be enzymatically catalysed in an aqueous environment, albeit at high fluoride ion concentrations.

2.2 Elucidation of biological fluorination in *S. cattleya*

2.2.1 Labelling studies exploring fluoroacetate 2 and 4-fluorothreonine 41

In order to elucidate the metabolic pathway for the biosynthesis of fluoroacetate **2** and 4-fluorothreonine **41**, O'Hagan and co-workers[10] explored the incorporation of isotopically (^{13}C and/or ^{2}H) labelled compounds into the fluorinated metabolites **2** and **41**. Incubation of whole cell suspensions of *S. cattleya* with [2-^{13}C]- and [1,2-$^{13}C_2$]-glycine **11** resulted in a high incorporation of the labelled carbons into C-1 and C-2 of fluoroacetate **2** and into the [C-2, C-3 and C-4] fragment of 4-fluorothreonine **41** (Scheme 2.4). Incorporations were of a similar magnitude in both cases and were established principally by ^{19}F-NMR spectroscopy, but also by GC-MS.

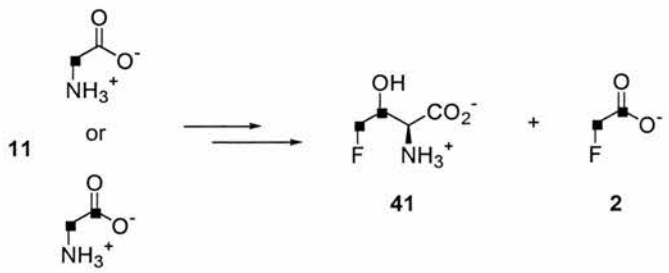

Scheme 2.4. Incorporation of [2-^{13}C]- and [1,2-$^{13}C_2$]-glycine **11** into fluoroacetate **2** and 4-fluorothreonine **41**.

In all of these experiments, no label was contributed by the carboxylate carbon of glycine **11**, indicating that it is lost during the biosynthetic process. This incorporation pattern was rationalised by the conversion of glycine **11** to serine **44** and then to a C-3 metabolite related to pyruvate **45**, and into the glycolytic phosphate pathway. Glycine **11** is first cleaved to form N^5,N^{10}-methylenetetrahydrofolate, the methylene group being contributed by C-2 of serine **44**. This then condenses with another molecule of glycine **11** to form

serine **44**, mediated by the enzyme serine-hydroxymethyl transferase. Serine **44** is subsequently converted to pyruvate **45** by serine dehydratase.[8] Evidence for this was supported also by the observation that C-2 and C-3 of pyruvate **45** are efficiently incorporated into both **2** and **41** in a regiospecific manner.[10] It was proposed that pyruvate **45** is then converted to oxaloacetate **28** by the action of pyruvate carboxylase.[10] To explore the involvement of oxaloacetate **28** in the biosynthesis, experiments involving [$^2H_4$]-succinate **46** were carried out.[10] A single deuterium atom was retained in the fluoromethyl groups of each fluorometabolite, an observation consistent with succinate **46** being processed *via* the citric acid cycle through fumarate **47** and malate **48** prior to oxidation to oxaloacetate **28**.[10] The enzyme phosphoenoylpyruvate carboxykinase converts oxaloacetate **28** to phosphoenoylpyruvate **49** (PEP) and this provides an entry into the glycolytic pathway. The enolate then generates 2-phosphoglycerate **50**, before further processing to glyceraldehyde-3-phosphate **51** as shown in Scheme 2.5.[36]

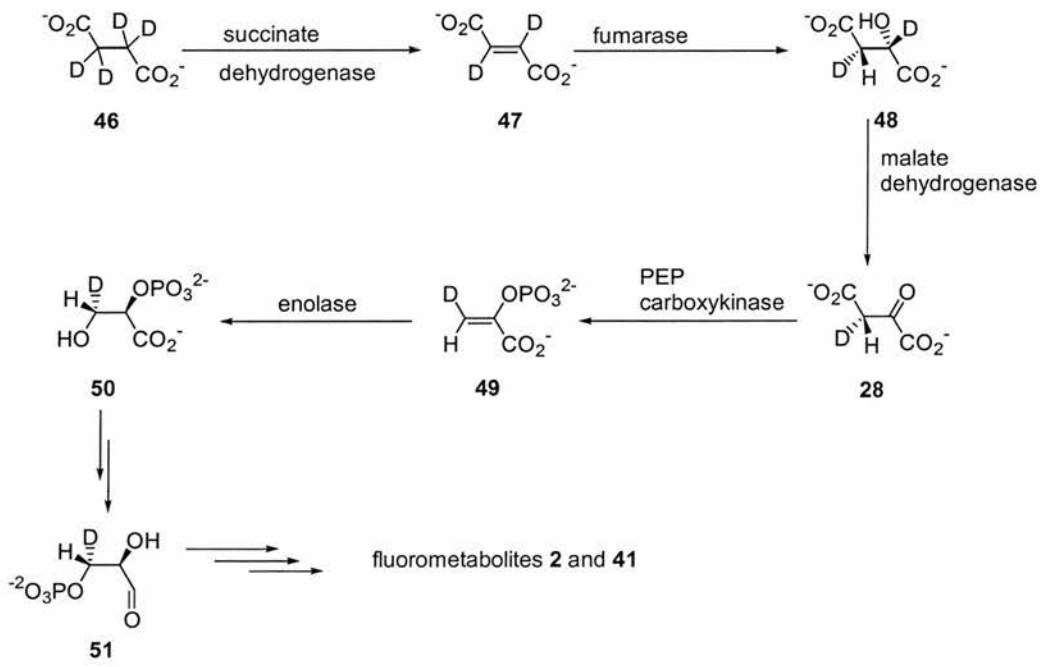

Scheme 2.5. [$^2H_4$]-Succinate **46** is metabolised to fluorometabolites **2** and **41** *via* the glycolytic pathway.

Further evidence of the involvement of oxaloacetate **28** was probed with [$^2H_3$]-aspartate **52**,[10] which is transaminated *in vivo* to **28**. The two fluorometabolites **2** and **41** retained both deuterium atoms in their fluoromethyl groups. These labelling studies are rationalised in Scheme 2.6.

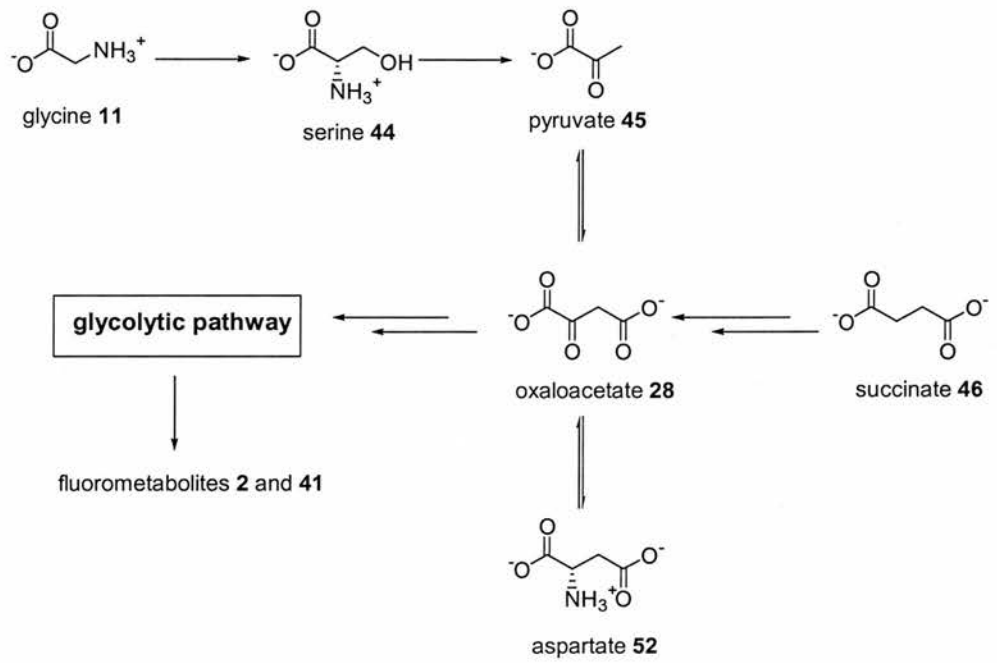

Scheme 2.6. Overview of the metabolic pathway for the biosynthesis of fluoroacetate **2** and 4-fluorothreonine **41**.

Soda and co-workers[37] showed in 1995 that [2-^{13}C]-glycerol **53** efficiently labelled C-1 of fluoroacetate **2** in *S. cattleya*, which also pointed attention to the involvement of the glycolytic pathway for the fluorometabolite biosynthesis. A stereochemical study involving (2*R*)-[1-$^2H_2$]- and (2*S*)-[1-$^2H_2$]-glycerol **53** was carried out by O'Hagan *et al.*[38] Interestingly they noted that only (2*R*)-[1-$^2H_2$]-glycerol **53** resulted in isotope incorporation into fluoromethyl groups of fluoroacetate **2** and 4-fluorothreonine **41**, indicating that it is the *pro-R* hydroxymethyl group of glycerol **53** that becomes incorporated into the

fluorometabolites and that the *pro-S* is cleaved during the biosynthesis (Scheme 2.7).[25,38]

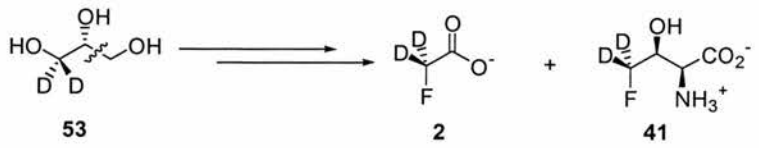

Scheme 2.7. The *pro-R* hydroxymethyl group of glycerol **53** is incorporated into fluoroacetate **2** and 4-fluorothreonine **41**.

From all of the labelling experiments described above it emerged that 4-fluorothreonine **41** and fluoroacetate **2** derive from a common intermediate, as the level of incorporation and isotopic labelling patterns into these metabolites was always identical in every labelling experiment. It follows that there is a single fluorinating enzyme in *S. cattleya*.

2.2.2 The role of fluoroacetaldehyde 54

It became clear from the labelling studies reported above that fluoroacetaldehyde **54** emerged as a candidate for the common intermediate in fluorometabolite biosynthesis. An oxidation reaction could generate fluoroacetate **2**, and a condensation with glycine **11** would afford 4-fluorothreonine **41**. To explore the role of fluoroacetaldehyde **54**, Moss *et al.*[39] prepared a synthetic sample of **54**, which was incubated with resting cell cultures of *S. cattleya*. Analysis of the culture supernatant by ^{19}F NMR spectroscopy revealed an almost stoichiometric conversion of fluoroacetaldehyde **54** to fluoroacetate **2** after only 3 h. Further investigations in cell-free extracts revealed that the enzymatic oxidation required NAD^+, demonstrating that an aldehyde dehydrogenase in *S. cattleya* mediates this conversion. The aldehyde dehydrogenase was the first enzyme of the fluorometabolite pathway to be isolated and characterised.[40] Addition of fluoroacetaldehyde **54** to resting

cells of *S. cattleya* resulted in the increased production of 4-fluorothreonine **41**, measured by monitoring its concentration in culture supernatant, using an HPLC assay.[39] To further investigate the relationship between fluoroacetaldehyde **54** and 4-fluorothreonine **41** a synthetic sample of [1-^{2}H]-fluoroacetaldehyde **54** was prepared by Moss *et al.*[39] This sample was administrated to cell suspensions of *S. cattleya* and the incorporation of deuterium into C-3 of 4-fluorothreonine **41** was monitored by GC-MS over time. The GC-MS results showed a significant incorporation of a single deuterium atom into the C-2—C-3—C-4 fragment of 4-fluorothreonine **41** after 7 h. The C-1—C-2 fragment didn't show any labelling, which indicated that the deuterium must be incorporated into C-3 or C-4 of 4-fluorothreonine **41**. This experiment strongly supported the origin of the C-3 hydrogen of 4-fluorothreonine **41** from the C-1 hydrogen of fluoroacetaldehyde **54** (Scheme 2.8).

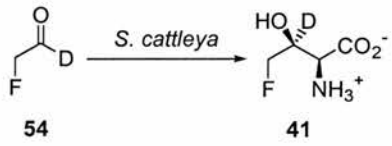

54 **41**

Scheme 2.8. [1-^{2}H]-Fluoroacetaldehyde **54** is efficiently incorporated into 4-fluorothreonine **41**.

Murphy and co-workers[41] reported that 4-fluorothreonine **41** derives from the direct condensation of fluoroacetaldehyde **54** with L-threonine **55**. In fact, incubation of a cell-free extract of *S. cattleya* with L-threonine **55**, pyridoxal 5'-phosphate (PLP), and fluoroacetaldehyde **54** gave rise to the production of 4-fluorothreonine **41**, as detected by ^{19}F-NMR spectroscopy. Based on this assay, the PLP-dependent enzyme responsible for this transaldolase activity was then purified and tested with several amino acids; however 4-fluorothreonine **41** was only detected when L-threonine **55** was employed. Glycine **11** was not a substrate. Scheme 2.9 shows a proposed mechanism for this transaldol reaction. In the first step the co-factor PLP forms the imine **56** with a molecule of L-threonine **55**.

Acetaldehyde **57** is cleaved off and replaced by fluoroacetaldehyde **54** as result of a retroaldol/aldol reaction sequence to give intermediate **58**. Finally, hydrolysis of the imine **58** affords 4-fluorothreonine **41**.

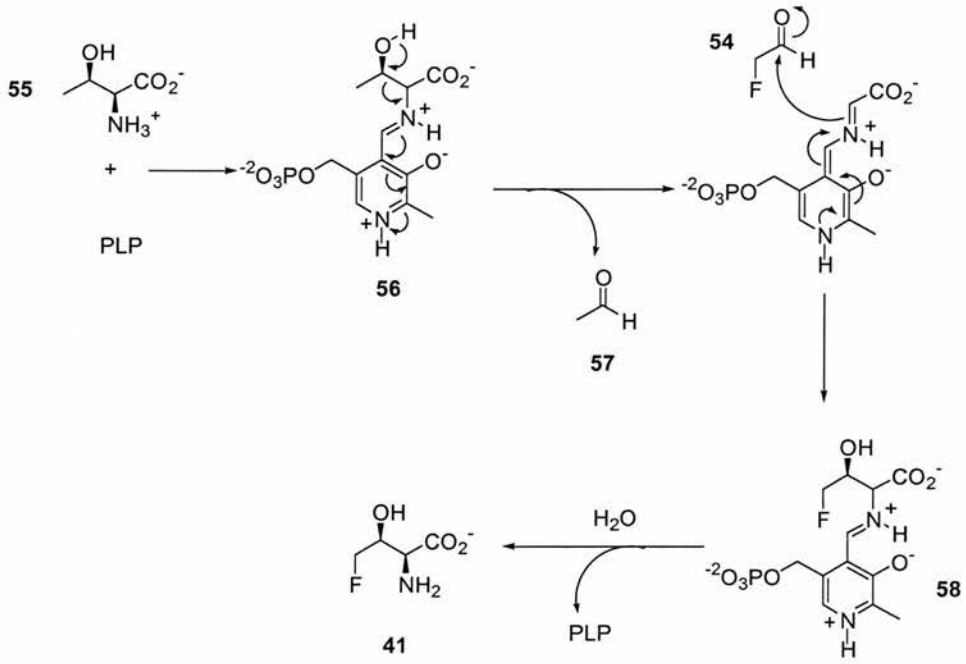

Scheme 2.9. A mechanism for the conversion of L-threonine **55** and fluoroacetaldehyde **54** to 4-fluorothreonine **41** catalysed by a PLP transaldolase.[41]

2.2.3 Identification of 5'-fluoro-5'-deoxyadenosine synthase (fluorinase)[42]

In order to identify the C-F forming enzyme, Schaffrath *et al.*[43] (at St Andrews University) carried out a series of experiments by incubating cell-free extracts, prepared under a variety of conditions with various co-factors, buffers and fluoride ion and the reactions were monitored by ^{19}F-NMR spectroscopy. Interestingly, it was noticed that when the whole cells were incubated with glycerol **53** and KF, low levels of fluorophosphates in the culture medium were detected after 5 days at 28 °C. It was considered at that time that

fluorophosphates may overcome the problem of transporting the heavily hydrated fluoride ion within the cell.[44] The potential role of fluorophosphates in the formation of the fluorometabolites was investigated by incubation of ATP **59** and other nucleotides (UTP, GTP and CTP) with fluoride ion in a cell-free extract of *S. cattleya*. It was found that only ATP **59** gave rise to the production of three organo-fluorine products, as shown in Figure 8.[43] The ^{19}F-NMR spectrum showed a signal (triplet), which was assigned to fluoroacetate **2**, and two other signals (both doublets of triplets) corresponding to two unknown compounds, A and B.

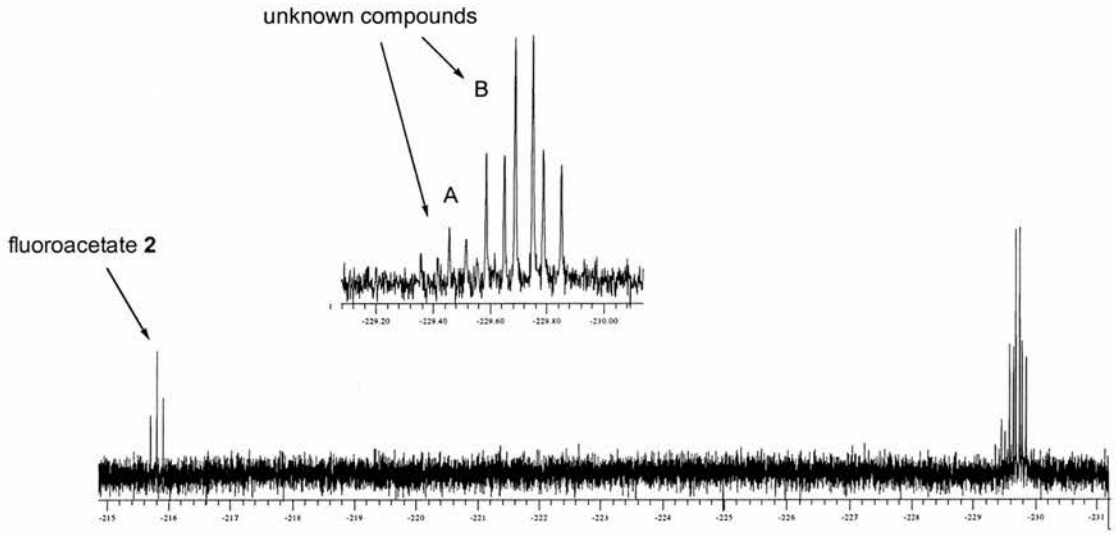

Figure 2.3. ^{19}F-NMR spectrum obtained after incubation of ATP **59** in a cell-free extract of *S. cattleya*.

Subsequent to these results and after isolation and correlation with synthetic material, 5'-fluoro-5'-deoxyadenosine **60** (5'-FDA) was assigned to compound A. Compound A was the first organofluorine compound produced in *S. cattleya*. 5'-FDA **60** arises from the displacement of the triphosphate of ATP **59** by a fluoride ion (Scheme 2.10).

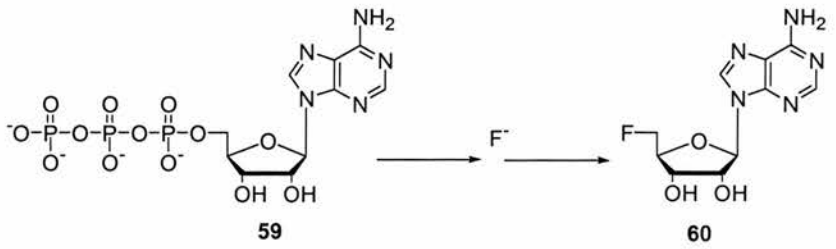

Scheme 2.10. 5'-FDA **60** was proposed as first formed fluorometabolite derived from ATP **59**.

Further biochemical investigations showed an increased production of fluorometabolites when the amino acid L-methionine **61** was administrated to the cell-free extract. This result was rationalised by the conversion of ATP **59** to *S*-adenosyl-L-methionine **62** (SAM) and 5'-FDA **60** being actually generated from SAM **62** and not directly from ATP **59**. The ubiquitous enzyme, SAM synthase, catalyses the conversion of ATP **59** and L-methionine **61** to SAM **62**.[45] Fluoride ion would then attack SAM **62** and displace L-methionine **61** to afford 5'-FDA **60**, catalysed by the fluorinase. This hypothesis is illustrated in Scheme 2.11.

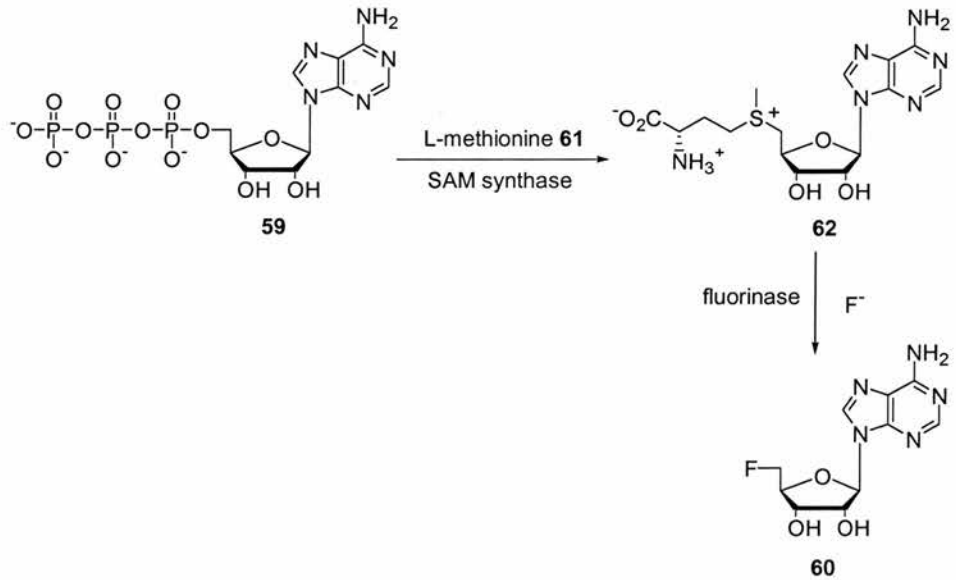

Scheme 2.11. 5'-FDA **60** formation in *S. cattleya* from ATP **59**.

Incubation of a cell-free extract of *S. cattleya* with SAM **62** and KF gave the same fluorinated products as that derived from ATP **59**.[25,46,47] In the presence of iodoacetamide this compound arrested fluoroacetate **2** formation by inhibiting the aldehyde dehydrogenase, but resulted in the build up of the two fluorometabolites A and B. A sample of compound B was obtained by preparative HPLC. ^{1}H- and ^{19}F-NMR analysis of this compound was very similar to 5'-FDA **60**, however ES-MS analysis showed a mass, one mass unit greater than 5'-FDA **60**. A deamination process involving the conversion of 5'-FDA **60** to 5'-fluoro-5'-deoxyinosine **63** (5'-FDI) was explored. An experiment carried out with labelled water ($H_2{}^{18}O$) confirmed this hypothesis.[25] Mass spectrometry analysis showed that the oxygen-18 had become incorporated into compound B, as a result of hydrolytic deamination (Scheme 2.12).

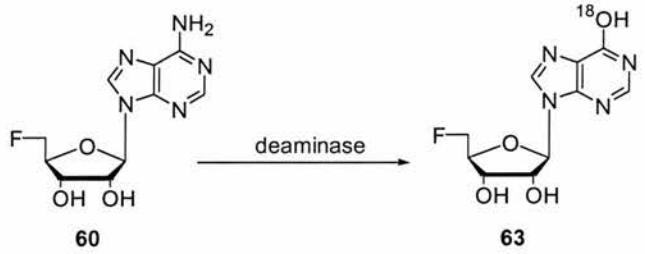

60 **63**

Scheme 2.12. Incorporation of $H_2{}^{18}O$ into 5'-FDI **63** (compound B).

A synthetic sample of 5'-FDI **63** confirmed the cell free production of **63**.[47] In order to prove that 5'-FDA **60** was the immediate product of the fluorination enzyme, a synthetic sample of 5'-FDA **60** was incubated with the cell-free extract and the *in vitro* bio-transformation was monitored by ^{19}F-NMR analysis.[46,47] The result showed again the production of fluoroacetate **2** and 5'-FDI **63**. Therefore peak A was confidently assigned to 5'-FDA **60** and peak B to 5'-FDI **63**. A further experiment was carried out involving incubation of the cell-free extract with **63**. No fluorometabolites were formed indicating

that 5'-FDI **63** is an adventitious shunt product and does not support fluorometabolites biosynthesis. 5'-FDI **63** Does not accumulate in whole cell experiments and is only formed in the cell free extract. With the role of 5'-FDA **60** established as the product of the fluorinase, an HPLC-based assay was established to monitor the production of 5'-FDA **60** from SAM **62**.[48] This allowed the fluorinase to be purified using standard protein purification protocols. After purification, the gene of the fluorinase enzyme was then identified and cloned and over-expressed by Dr. J. Spencer and his co-workers at Cambridge University, using a reverse genetics strategy.[49] An amino acid sequence to design PCR primers was obtained after N-terminal amino acid analysis and trypsin digestion of the native protein. The fluorinase gene was cloned in a suitable plasmid and over-expressed in *E. coli*. The availability of the over-expressed fluorinase has allowed a full crystallographic and mechanistic investigation of the enzyme to be completed. Details of the crystal structure of the fluorinase are discussed in chapter 3.

2.2.4 Further investigations on biological fluorination

The purification of the fluorinase and the identification of 5'-FDA **60** as the first committed intermediate in biological fluorination gave some insight into the origin of the C-F bond in living systems. The next challenge was of course to reveal the intermediates between 5'-FDA **60** and fluoroacetaldehyde **54** to obtain a more complete picture of the biosynthesis. 5-Fluoro-5-deoxyribose **64** (5-FDR) was proposed as the next intermediate after 5'-FDA **60**, a compound which could arise as a result of depurination.[50] However, incubation studies with the cell-free extract and a synthetic sample of 5-FDR **64** didn't show production of fluoroacetate **2** and 4-fluorothreonine **41**. 5-Fluoro-5-deoxyribose-1-

phosphate **65** (5-FDRP) was then explored. In this case, incubation of **65** with the cell-free extract did result in the accumulation of fluoroacetate **2** indicating *in vitro* biotransformation and supporting the role of 5-FDRP **65** as an intermediate on the biosynthetic pathway. (Scheme 2.13).[50]

The purine nucleotide phosphorylase (PNP) responsible for this transformation was purified and the gene identified. Interestingly, this gene lies immediately adjacent to the fluorinase gene on the *S. cattleya* genome.

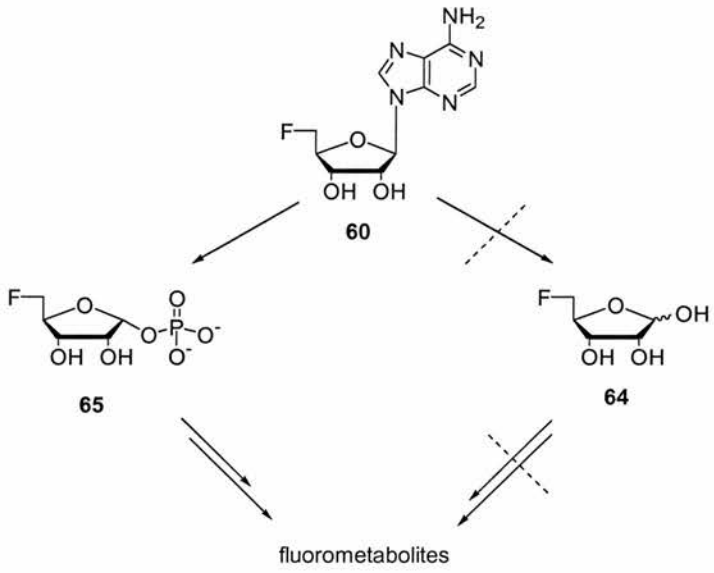

Scheme 2.13. Metabolic fate of 5'-FDA **60** in *S. cattleya via* 5-FDRP **65**. 5-FDR **64** is not a biosynthetic intermediate.

The details of the transformation of 5-FDRP **65** to fluoroacetaldehyde **54** remain to be characterised at the biochemical level. A current hypothesis is that 5-fluoro-5-deoxyribulose-1-phosphate **66** is a potential intermediate after 5-FDRP **65**, arising as a result of an isomerase activity.[25] The idea comes from the known metabolism of 5'-methylthioadenosine **67**, in the L-methionine **61** salvage pathway (Scheme 2.14).

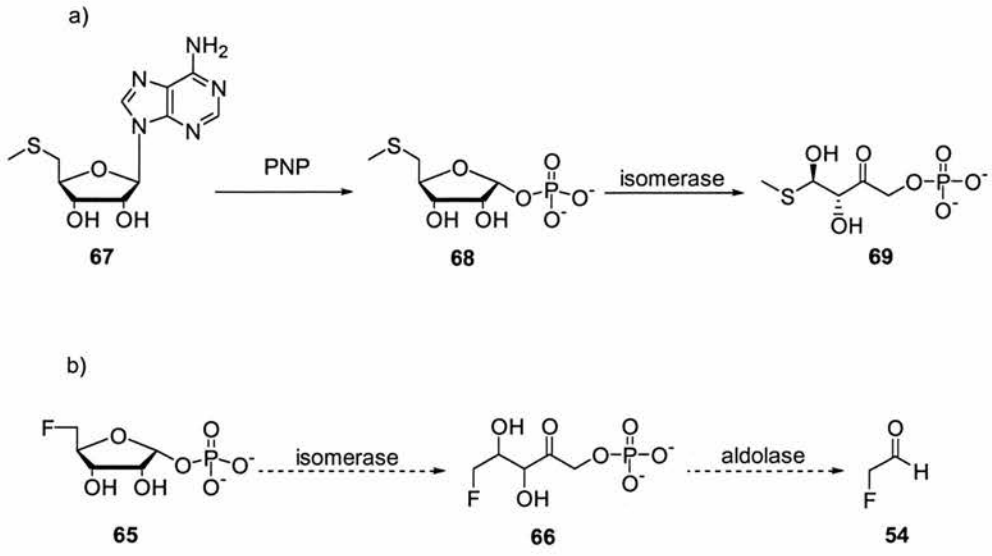

Scheme 2.14. a) Section of the L-methionine **61** salvage pathway; b) an analogous reaction to (a) in *S. cattleya via* a putative isomerase activity.

On that pathway, 5'-methylthioadenosine **67** is also degraded by a PNP enzyme to generate 5-methylthio-5-deoxyribose-1-phosphate **68** in mammals. An isomerase enzyme then converts the sugar phosphate to the acyclic 5-methylthio-5-ribulose-1-phosphate **69**.[51] In a similar manner an isomerase present in *S. cattleya* may convert 5-FDRP **65** to 5-fluoro-5-deoxyribulose-1-phosphate **66**. Current work to test this hypothesis is in progress in St. Andrews.

An overview of the biological fluorination pathway in *S. cattleya* is represented in Scheme 2.15.

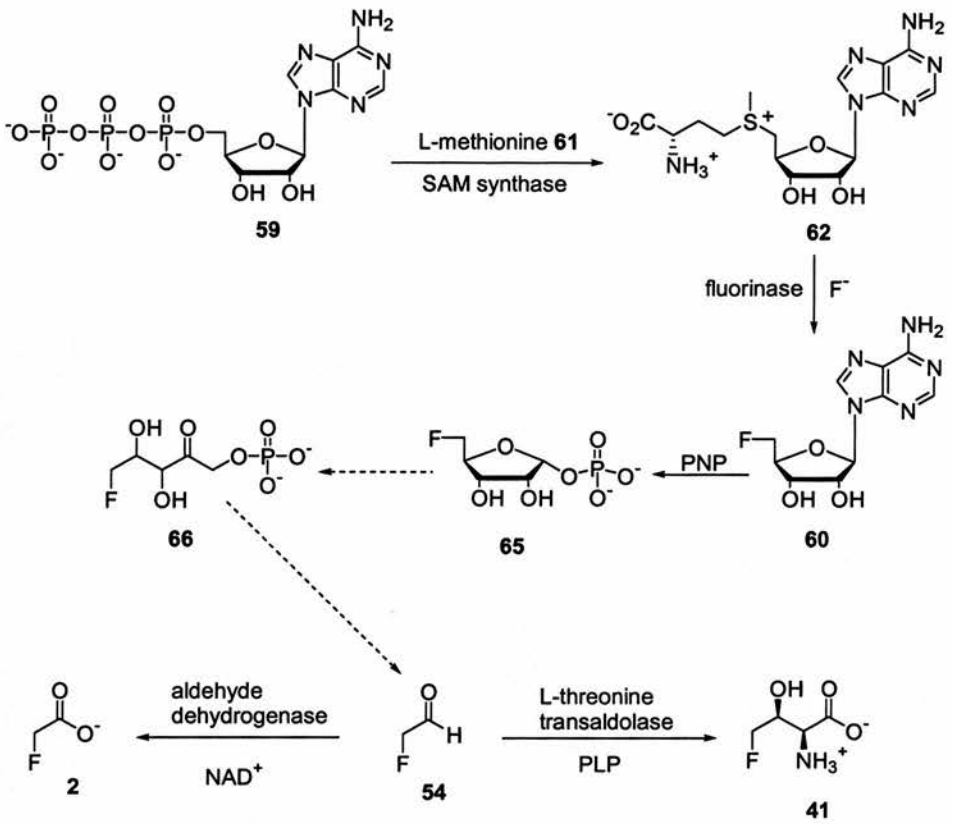

Scheme 2.15. Schematic representation of biological fluorination in *S. cattleya*.

2.3 Characterization of the fluorination enzyme

Kinetic analysis of the fluorinase[49] demonstrated a catalytic rate constant (k_{cat}) of 0.07/min and a K_m for fluoride ion of about 2.0 mM, a high value compared to the K_m calculated for SAM **62** (74 μM). This high K_m is probably related to the high energy of desolvation that must be overcome to secure fluoride ion binding at the active site of the enzyme.

Two SAM analogues, *S*-adenosyl-L-homocysteine **70** (SAH) and the antibiotic sinefungin **71**, have been explored as inhibitors of the fluorinase. SAH **70** is a potent inhibitor with a K_i of 29 μM, whereas sinefungin **71** showed weaker inhibition.[25]

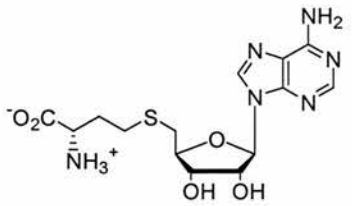

70

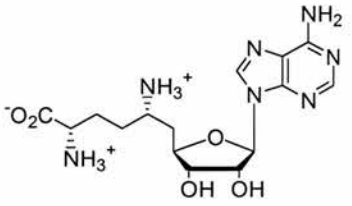

71

2.3.1 The fluorinase catalyses the reverse reaction[52]

The fluorination enzyme is able to catalyse the reverse reaction involving C-F bond cleavage (Scheme 2.16). This is notable because the C—F bond is the strongest covalent bond in organic chemistry. Incubation of the fluorinase with L-methionine **61** and 5'-FDA **60** led to the production of SAM **62** as established by ES-MS and HPLC analysis. This is an interesting observation, as the only reported enzyme capable of generating SAM **62** so far is SAM synthase.

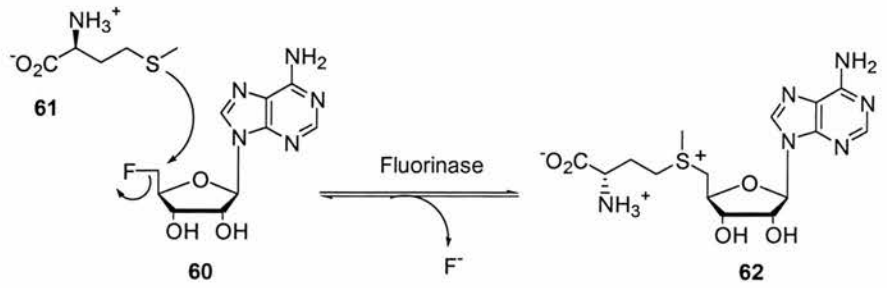

Scheme 2.16. C—F bond cleavage catalysed by the fluorination enzyme: conversion of 5'-FDA **60** to SAM **62**.

Further investigations on the reverse reaction were explored using a sample of 5'-chloro-5'-deoxyadenosine **72** (5'-ClDA) as a potential substrate of the fluorinase. Compound **72** was processed efficiently by the fluorinase and led to production of SAM **62** with concomitant release of chloride ion (Scheme 2.17).

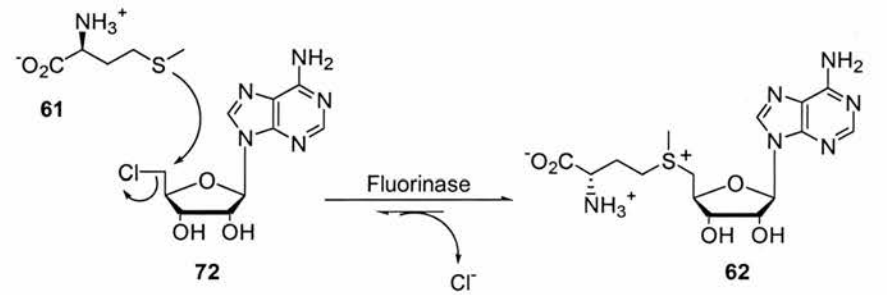

Scheme 2.17. Conversion of 5'-ClDA **72** to SAM **62** catalysed by the fluorination enzyme.

The V_{max} for both 5'-FDA **60** (0.7 nmol/g protein/min) and for 5'-ClDA **72** (4.0 nmol/g protein/min) showed that 5'-ClDA **72** is a more efficient substrate than the natural substrate.[47] This is most likely related to the fact that chloride ion is a better leaving group than fluoride.

An enhanced rate of the reverse reaction was also observed when the L-methionine **61** analogue, L-selenomethionine **73**, was used to carry out the experiment. In this case the

increased nucleophilicity of selenium over sulphur accelerates the nucleophilic substitution of fluoride to generate seleno-SAM **74**.

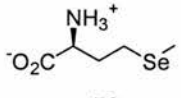

73

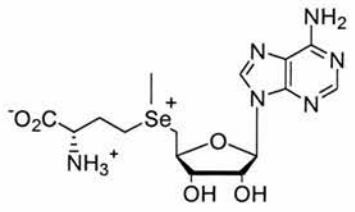

74

2.3.2 Substrate specificity of the fluorinase

The various crystal structures of the fluorinase with substrates or products bound at the active site, that are discussed in detail in next chapter, reveal that SAM **62** is bound in a high energy conformation where the ribose ring is planar.[49] Also all of the heteroatoms (except the oxygen ether of the ribose) are involved in hydrogen bonding contacts to the protein. Any modification on the substrate would be anticipated to result in a lower affinity towards the active site and more probably result in the loss of activity. The ability to run the reaction in the reverse direction opened up the opportunity to study in more detail the substrate specificity of the fluorinase, as 5'-FDA analogues are easier to prepare than SAM analogues. Accordingly, four positions of the 5'-halonucleosides **60** and **72** were identified for potential sites for modification[47] (6-amino, 2'-OH, 3'-OH, 2-H) as shown in Figure 2.4.

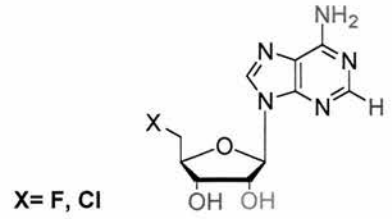

60, 72

Figure 2.4. The coloured groups of the 5'-halo-5'-deoxyadenosines **60** and **72** were identified as potential modification sites: 6-amino (red), 2-H (blue), 2'-OH (purple), 3'-OH (green).[47]

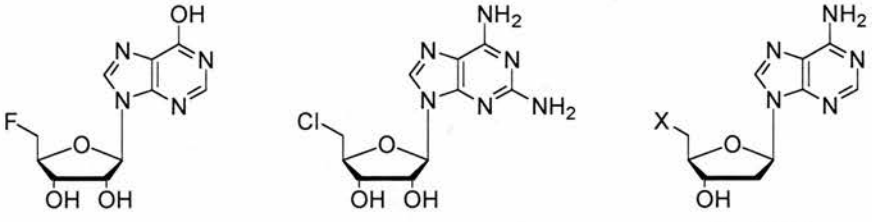

63 **75**

5'-FDI **63** was not a substrate for the fluorinase and revealed that the 6-amino group of the adenine is fundamental for binding and for the enzyme activity.

The fluorinase was able to tolerate the presence of an amino group at C-2 of the adenine ring, and in the event, 2-amino-5'-halo-5'-deoxyadenosine **75** gave rise to the production of 2-amino-SAM **78**, a novel SAM analogue (recent unpublished data).

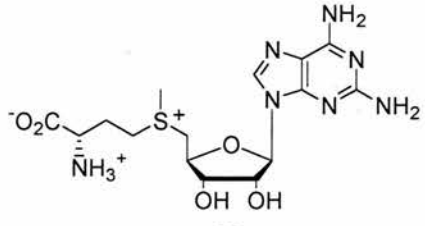

78

Removal of the 2'-hydroxyl group was explored.[53] The 5'-chloro- and 5'-fluoro-2',5'-dideoxyadenosines, **76** (2'dClDA) and **77** (2'dFDA) respectively, were both converted to 2'-deoxy-SAM **79** by the fluorinase (Scheme 2.18), but these substrates were processed

less efficiently than 5'-FDA **60**. The chloro- analogue, 2'dClDA **76**, was the more efficient of the two, as expected due to the better leaving group ability of chloride over fluoride. This data indicates that the 2'-hydroxyl group is not fundamental for the enzyme activity, which was a rather unexpected outcome.

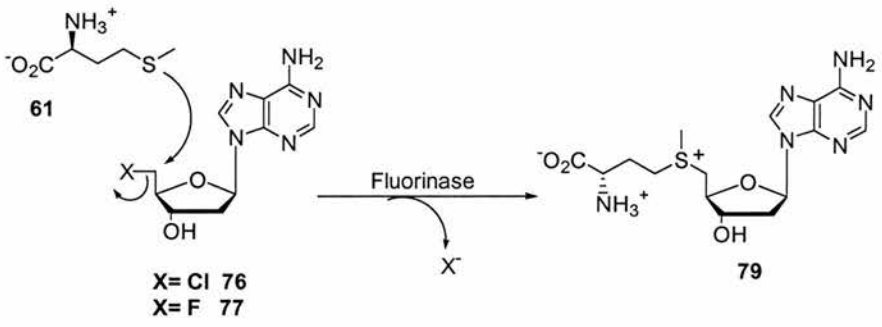

Scheme 2.18. Conversion of 2'dClDA **76** and 2'dFDA **77** to 2'dSAM **79** catalysed by the fluorination enzyme.

2.3.3 *Trans*-halogenation[47]

By exploiting the relative reactivity of chloride and fluoride, a *trans*-halogenation experiment was successfully carried out. This involved incubation of 5'-ClDA **72**, and either L-methionine **61** or L-selenomethionine **73** with the fluorinase in 20 mM fluoride. HPLC Analysis showed the production of 5'-FDA **60**. This result indicated that the production of 5'-FDA **60** must proceed *via* enzymatic fluorination of either transiently formed SAM **62** or seleno-SAM **74**, as represented in Scheme 2.18.

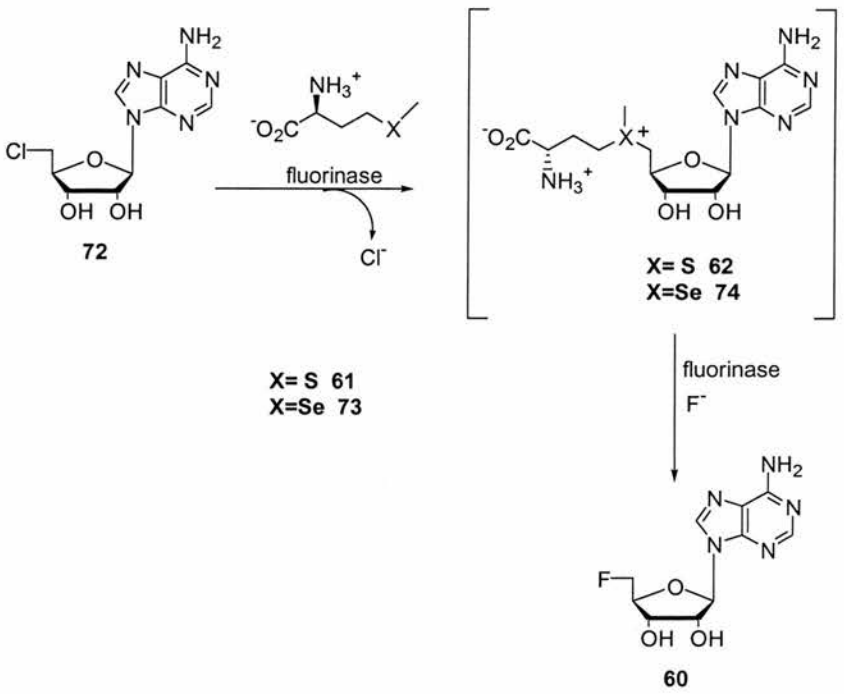

Scheme 2.18. *Trans*-halogenation reaction mediated by the fluorination enzyme.

The fact that 5'-FDA **60** is produced from 5'-ClDA **72** suggests that even with chloride as the better leaving group, fluoride is a better substrate/nucleophile in the forward reaction. A similar *trans*-halogenation reaction[53] also occurred when 2'dClDA **76** was used as a substrate under similar reaction conditions, to generate 2'dFDA **77**.

5'-Bromo-5'-deoxyadenosine **80** (5'-BrDA) has been also explored as a substrate and HPLC analysis showed the production of 5'-FDA **60**. Control experiments showed that the reaction did not occur in the absence of the fluorinase. However it was demonstrated that this *trans*-halogenation took place *without* either L-methionine **61** or L-selenomethione **73**. Presumably, the fluorination enzyme catalyses the displacement of 5'-BrDA **80** to 5'-FDA **60** without the intermediacy of SAM **62** (Scheme 2.19). The bromine atom has a large atomic radius, so it is unlikely that it sits in the active site in the same position as fluorine or chlorine, due to steric factors. It seems more reasonable that the bromine atom of 5'-

BrDA **80** is accommodated in the position where the sulphur atom of SAM **62** normally resides. If this is true, then 5'-BrDA **80** acts as SAM **62** mimic and is susceptible to direct fluoride attack to form 5'-FDA **60**.

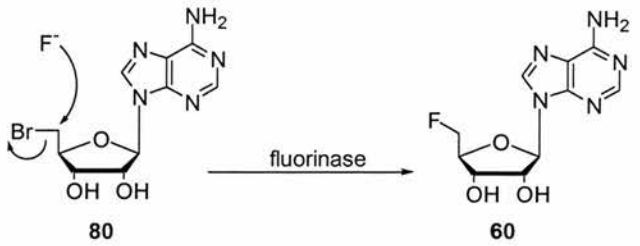

80 **60**

Scheme 2.19. Direct conversion of 5'-BrDA **80** to 5'-FDA **60** mediated by the fluorinase (without L-methionine **61**).

2.3.4 The fluorinase is a chlorinase[52]

5'-ClDA **72** has been used successfully as a substrate for the production of SAM **62**, in the reverse reaction, mediated by the fluorinase. However, initial experiments carried out by incubation of the fluorinase in the presence of SAM **62** and chloride ion to generate 5'-ClDA **72** failed. This was because the equilibrium is significantly in favour of the substrates rather than products. In order to demonstrate that the fluorinase is able to activate chloride ion towards nucleophilic attack, two different coupled enzyme assays were addressed to shift the equilibrium in favour of the products (Scheme 2.20). The first experiment involved the coupling of the fluorinase with an L-amino acid oxidase (*Bothrops atrox* venom, Sigma Chem. Co. Ltd.). This enzyme is able to convert L-methionine **61** into the α-oxo-acid **81**. Removal of L-methionine **61** from the equilibrium now favours 5'-ClDA **72** production and this was observed. In a second experiment, the fluorinase was coupled with an adenyl acid deaminase. In this reaction the resultant 5'-

ClDA **72** was converted to 5'-chloro-5-deoxyinosine **82** (5'-ClDI). The production of 5'-ClDI **82** was identified by HPLC/ES-MS analysis, against a reference compound.

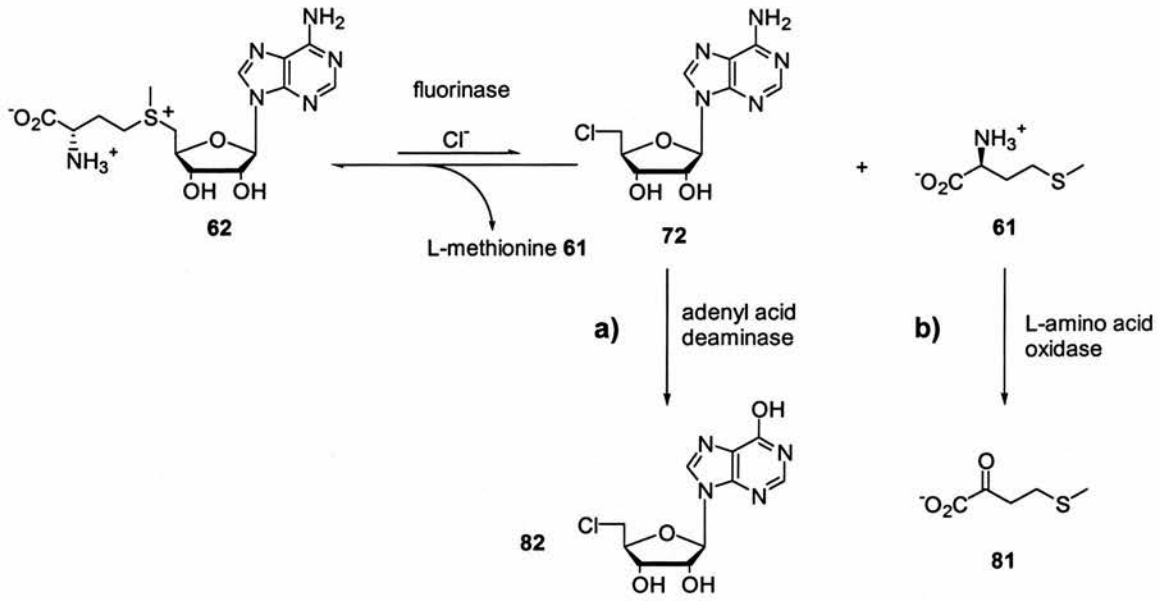

Scheme 2.20. Coupled enzyme assays with a) fluorinase-L-amino acid oxidase, and b) fluorinase-adenyl acid deaminase driving organochlorine synthesis.[52]

2.4 Aims of the project

Focus of the present project was to carry out further studies on biological fluorination using the over-expressed fluorinase. In the first study addressed, we explored the halide ion binding to the active site of the enzyme prior to nucleophilic substitution of SAM **62**. This investigation involved crystallization of the enzyme with an appropriate substrate and chloride ion, and is discussed in detail in chapter 3.

The over-expressed fluorinase also gave the opportunity to revaluate the stereochemical outcome reported in a previous study by O'Hagan and co-workers.[36] According to this study, the enzyme catalyses the displacement of the L-methionine **61** group of SAM **62** by fluoride ion with an inversion of configuration consistent with an S_N2 reaction mechanism. These experiments, however, had some limitations as they were carried out in the whole cells. A stereochemical investigation of biological fluorination, involving the enzyme directly, was addressed and is discussed in detail in chapter 4.

References Chapter 2

1. G. W. Gribble, *J. Chem. Educ.*, 2004, **81**, 1441.

2. K. Ballschmiter, *Chemoshpere*, 2003, **52**, 313.

3. G. W. Gribble, *Chemoshpere*, 2003, **52**, 289.

4. G. M. Salamonczyk, V. B. Oza and C. J. Sih, *Tetrahedron Lett.*, 1997, **38**, 6965.

5. R. Kazlauskas, P. T. Murphy, R. J. Wells, J. A. Baird-Lambert and D. D. Jamieson, *Aust. J. Chem.*, 1983, **36**, 165.

6. A. Durgrillion and R. Gaetner, *Eur. J. Endocrinol.*, 1995, **132**, 735.

7. P. G. Williams, W. Y. Yoshida, R. E. Moore and V. J. Paul, *Org. Lett.*, 2003, **5**, 4167.

8. D. O'Hagan and D. B. Harper, *J. Fluor. Chem.*, 1999, **100**, 127.

9. F. A. Cotton, and G. Wilkinson, "Advanced Inorganic Chemistry," 5th Ed. (1988), Wiley Interscience.

10. J. T. G. Hamilton, C. D. Murphy, M. R. Amin, , D. O'Hagan and D. B. Harper, *J. Chem. Soc., Perkin Trans. I*, 1998, 759.

11. S. L. Neidleman and J. Geigert, "Biohalogenation: Principles, Basic Roles and Applications", (1986), Ellis Horwood, Chichester.

12. J. S. C. Marias and J. Onderstepoort, *Vet. Sci. Amin. Ind.*, 1943, **18**, 203.

13. J. S. C. Marias and J. Onderstepoort, *Vet. Sci. Amin. Ind.*, 1944, **20**, 67.

14. J. Tannock, *Rhod. J. Agric. Res.*, 1975, **13**, 67.

15. D. O'Hagan, R. Perry, J. M. Lock, J. J. M. Meyer, L. Dasaradhi, J. T. G. Hamilton and D. B. Harper, *Phytochemistry.*, 1993, **33**, 1043.

16. R. A. Peters, R. W. Wakelin, P. Buffa and L. C. Thomas, *Proc. Roy. Soc. B*, 1953, **10**, 497.

17. E. Kun and R. J. Dummel, *Methods Enzymol.*, 1969, **13**, 632.

18. H. Luable, M.C Kennedy, M.H Emptage, H. Beinert, C.D. Stout, *Proc. Nat. Acad. Sci.* USA, **1996**, 93, 13699.

19. R. A. Peters and M. Shorthouse, *Nature*, 1967, **216**, 80.

20. R. A. Peters and M. Shorthouse, *Nature*, 1971, **231**, 123.

21. R. A. Peters, P. J. Hall, R. F.V. Ward and N. Sheppard, *Biochem. J.*, 1960, **77**, 17.

22. P. F. V. Ward and P. J. Hall and R. A. Peters, *Nature*, 1964, **201**, 611.

23. J. T. G. Hamilton and D. B. Harper, *Phytochemistry.*, 1997, **44**, 1179.

24. X.-H. Xu, G.-M. Yao, Y.-M. Li, J.-H. Lu, C.-J. Lin, X. Wang and C.-H. Kong, *J. Nat. Prod.*, 2003, **66**, 285.

25. H. Deng, D. O'Hagan and C. Schaffrath, *Nat. Prod. Rep.*, 2004, **21**, 773.

26. S. O. Thomas, V. L. Singleton, J. A. Lowery, R. W. Sharpe, L. M. Pruess, J. N. Porter, J. H. Mowat and N. Bohonos, *Antibiotics Annu.*, 1957, 716.

27. G. O. Morton, J. E. Lancaster, G. E. Van Lear, W. Fulmor and W. E. Meyer, *J. Am. Chem. Soc.*, 1969, **91**, 1535.

28. D. A. Shuman, R. K. Robins and M. J. Robins, *J. Am. Chem. Soc.*, 1969, **91**, 3391.

29. A. R. Maguire, W.-D. Meng, S. M. Roberts and A. J. Willets, *J. Chem. Soc., Perkin Trans. 1*, 1993, 1795.

30. I. D. Jenkins, J. P. H. Verheyden and J. G. Moffatt, *J. Am. Chem. Soc.*, 1976, **98**, 3346.

31. M. Sanada, T. Miyano, S. Iwadare, J. M. Williamson, B. H. Arison, J. L. Smith, A. W. Douglas, J. M. Leisch and E. Inamine, *J. Antibiotics*, 1986, **39**, 259.

32. D. F. Corbett, A. J. Eglington and T. T. Howarth, *Chem Commun.*, 1977, 953.

33. H. M. Senn, D. O'Hagan and W. Thiel, *J. Am. Chem. Soc.*, 2005, **127**, 13643.

34. O. Nashiru, D. L. Zechel, D. Stoll, T. Mohammadzadeh, R. A. J. Warren and S. G. Withers, *Angew. Chem. Int. Ed.*, 2001, **40**, 417.

35. D. L. Zechel, S. P. Reid, D. Stoll, O. Nashiru, R. A. J. Warren and S. G. Withers, *Biochemistry*, 2003, **42**, 7195.

36. D. O'Hagan, R. J. M. Goss, A. Meddour and J. Courtieu, *J. Am. Chem. Soc.*, 2003, **125**, 379.

37. T. Tamura, M. Wada, N. Esaki and K. Soda, *J. Bacteriol.*, 1995, **177**, 2265.

38. J. Neischalk, J. T. G. Hamilton, C. D. Murphy, D. B. Harper and D. O'Hagan, *Chem. Commun.*, 1997, 799.

39. S. J. Moss, C. D. Murphy, J. T. Hamilton, W. C. McRoberts, D. O'Hagan, C. Schaffrath and D. B. Harper, *Chem. Commun.*, 2000, 2281.

40. C. D. Murphy, S. J. Moss and D. O'Hagan, *Appl. Environ. Microbiol.*, 2001, **67**, 4919.

41. C. D. Murphy, D. O'Hagan and C. Schaffrath, *Angew. Chem. Int. Ed.*, 2001, **40**, 4479.

42. D. O'Hagan, C. Schaffrath, S. Cobb, J. T. G. Hamilton and C. D. Murphy, *Nature*, 2002, **416**, 279.

43. C. Schaffrath, "Biosynthesis and Enzymology of Fluorometabolite Production in Streptomyces Cattleya", PhD Thesis, University of St. Andrews, 2002.

44. D. B. Harper, D. O'Hagan and C. D. Murphy, "The Handbook of Environmental Chemistry", Vol. 3, Part P, 2003, 141.

45. T. C. Chou and P Talalay, *Biochemistry*, 1972, **11**, 1065.

46. C. Schaffrath, S. L. Cobb and D. O'Hagan, *Angew. Chem. Int. Ed.*, 2002, **41**, 3913.

47. S. L. Cobb, "The origin and metabolism of 5'-FDA in S. Cattleya", PhD Thesis, University of St. Andrews, 2005.

48. C. Schaffrath, H. Deng and D. O'Hagan, *FEBS Letters*, 2003, **547**, 111.

49. C. J. Dong, F. L. Huang, H. Deng, C. Schaffrath, J. B. Spencer, D. O'Hagan and J. H. Naismith, *Nature*, 2004, **427**, 561.

50. S. L. Cobb, H. Deng, J. T. Hamilton, R. P. McGlinchey and D. O'Hagan, *Chem. Commun.*, 2004, 592.

51. L. Y. Ghoda, T. M. Savarese, D. L. Dexter, R. E. Parks Jr., P. C. Trackman and R. H. Abeles, *J. Biol. Chem.*, 1984, **259**, 6715.

52. H. Deng, S. L. Cobb, A. McEwan, R. P. McGlinchey, J. H. Naismith, D. O'Hagan, D. A. Robinson and J. B. Spencer, *Angew. Chem. Int. Ed..*, 2006, **45**, 659.

53. S. L. Cobb, H. Deng, A. McEwan, J. H. Naismith, D. O'Hagan and D. A. Robinson, *Org. Biomol. Chem.*, 2006, **4**, 1458.

Chapter 3

Crystallization studies on the fluorinase

3.1 Introduction

With the fluorination enzyme purified and protein available after its over-expression in *E. coli*, crystallization of the enzyme was pursued. Crystals of the enzyme, suitable for X-ray crystallography, were obtained which subsequently led to a crystal structure and this has revealed the binding interaction between the substrate and the enzyme surface.[1] These crystallographic investigations have also revealed important insights into the mechanism of enzymatic fluorination, suggesting a nucleophilic displacement process. This conclusion is in total agreement with the stereochemical studies carried out in this study and discussed in detail in chapter 4.[2] Substrate analogues have also been prepared which were employed to explore the properties of this unusual enzyme.[3] Some of these substrates were co-crystallised with the fluorinase, and this has allowed a more detailed analysis of its substrate specificity, and the importance of certain interactions.

3.1.1 Crystal structure of the fluorinase

Crystallization of the fluorinase was initiated by Dr. C. Dong with the wild type enzyme in a collaboration in St. Andrews with Prof. J. H. Naismith, and this coupled with the over-expressed protein from *E. coli* (cloned in Cambridge) led to a successful diffraction study. A seleno-methionine enriched sample of the fluorinase was crystallised, and the structure

solved by anomalous scattering methods.[1] The structure showed a hexamer constructed as a dimer of trimers (Figure 3.1). The fold of the monomeric unit of the trimer is novel with no obvious relationship to any known protein super-family. This is consistent with its novel activity.

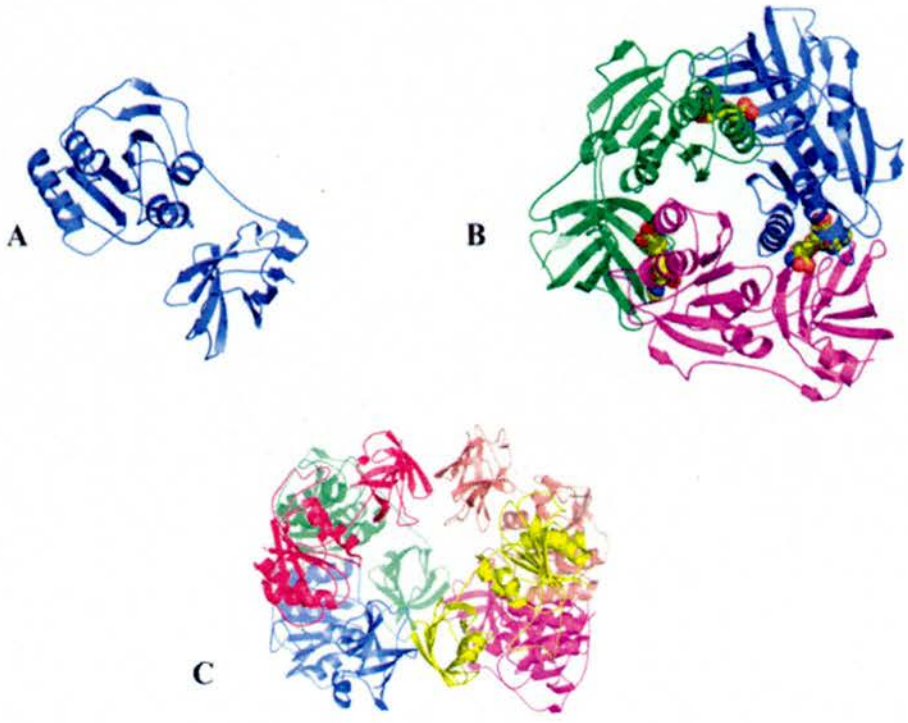

Figure 3.1. Structure of the fluorinase: **A**, monomer; **B**, trimer with SAM **62** bound at the interfaces; **C**, the overall hexameric structure which is a dimer of the trimer.[4]

The enzyme crystallised from *S. cattleya* contained three molecules of SAM **62** bound to the trimers at the interface with each monomer. Clearly, SAM **62** does not dissociate readily from the protein during purification. Figure 3.2 shows a schematic representation of SAM **62** bound to the active site of the enzyme. The recognition of SAM **62** is highly specific with the adenine ring, the ribose and the L-methionine **61** held by hydrogen bonds and van der Waals contacts. The ribose ring of SAM **62** is held in an unusual planar conformation by hydrogen bonds between the 2'- and 3'-hydroxyl groups and the

carboxylate of Asp-16. In this arrangement the C—O-3' and the C—O-2' bonds are eclipsed (torsion angle 1°). This results in an unusually planar conformation of the furanose ring.[1] The ether oxygen of the ribose ring is the only heteroatom of SAM **62** that is not involved in any hydrogen bonding interactions with the surface of the protein.

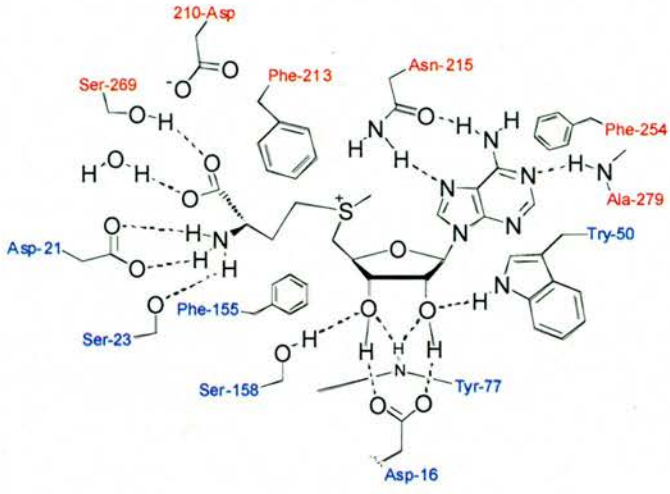

Figure 3.2. Topographical image of SAM **62** bound to the active site of the fluorinase with all of the H-bonding contacts shown.[1]

Incubation of SAM **62** with the fluorinase and fluoride ion gave rise to a co-crystal of the enzyme with the products 5'-FDA **60** and L-methionine **61**. The electron density map showed clearly that SAM **62** was broken into two fragments (Figure 3.3b).

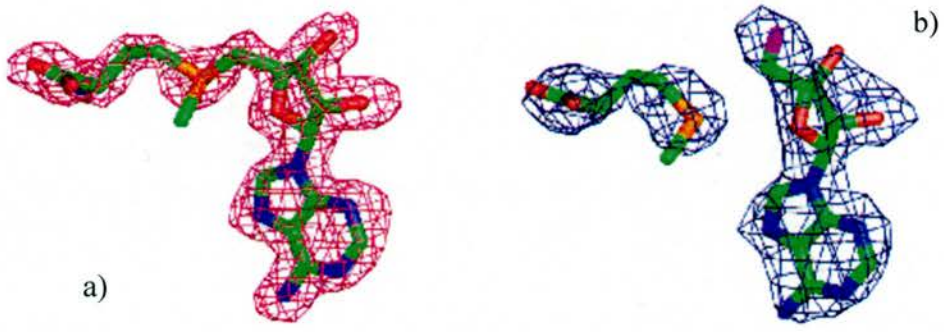

Figure 3.3. Electron density maps of the bound substrate/products. a) with SAM **62**; b) with 5'-FDA **60** and L-methionine **61**.[1]

A comparison of the diffraction data, both before and after the fluorination reaction, reveals very little difference between the two structures except in the bond forming/breaking region (Figure 3.4).[1,4] The orientation of the C-F bond of the product (5'-FDA **60**) is approximately antiperiplanar (~164°) to the C-S bond of the substrate (SAM **62**), indicative of a substitution reaction occurring with an inversion configuration (S_N2).

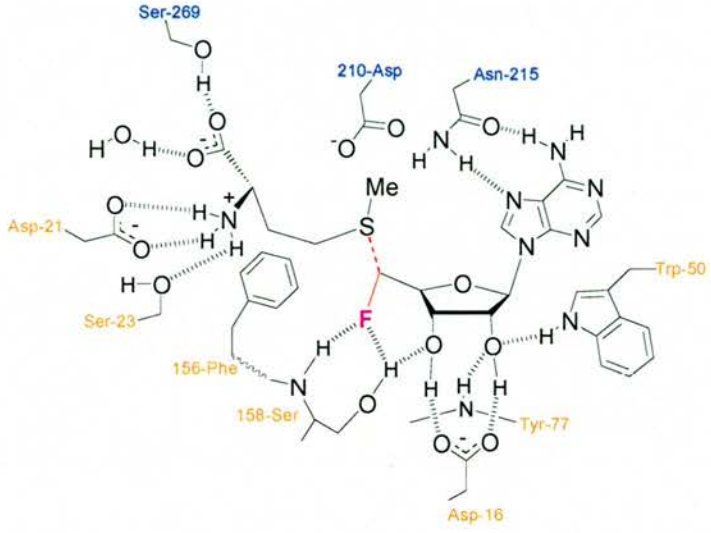

Figure 3.4. Topographical image of 5'-FDA **60** and L-methionine **61** bound to the active site of the fluorinase.[4]

Of course some care has to be taken in such cases as the ground state structures do not necessarily report the true orientation of the atoms immediately after reaction. However, a recent QM/MM theoretical study carried out by Thiel *et al.*[5], calculated the transition state geometry for this reaction, which was in agreement with the S_N2 mechanism suggested by the crystal structure (Figure 3.5). This study was based on the experimental X-ray structure of the SAM-enzyme complex. By manual insertion of fluoride, it was possible to obtain the reactant complex, the transition state and then the product complex. A comparison with the X-ray crystal structure of the enzyme/product complex revealed that the fluoromethyl group had rotated showing only the hydrogen bond from the Ser-158 backbone NH,

whereas the second hydrogen bond to Ser-158 side-chain OH had rotated away. The torsion angle between C-5'—C-4' varied between 162° and 174°, whereas this angle was just 108° in the simulated product structure.

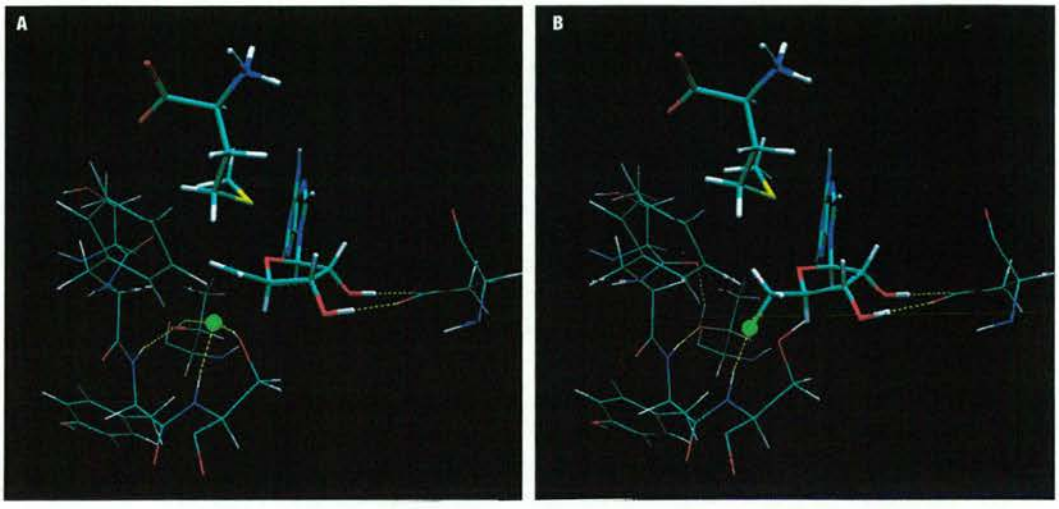

Figure 3.5. A) Simulation of the transition state for fluoride nucleophilic attack and b) the product complex.[5]

3.1.2 Crystal structures of the fluorinase with alternate substrates

Some of the substrate analogues, described in the previous chapter, have been co-crystallised successfully with the fluorinase. X-ray diffraction analysis of these crystals clearly gave further information about the substrate specificity of the enzyme. In a recent published work,[6] the crystal structure of the co-crystallised 2'dFDA-fluorinase complex has been obtained. The data show that 2'dFDA **77** sits in the active site in a slightly different conformation to that exhibited by 5'-FDA **60**, particularly around the ribose ring. The 3'-hydroxyl group has moved to accommodate a more central bifurcated hydrogen bond with both oxygens of Asp-16 carboxylate group (Figure 3.6).

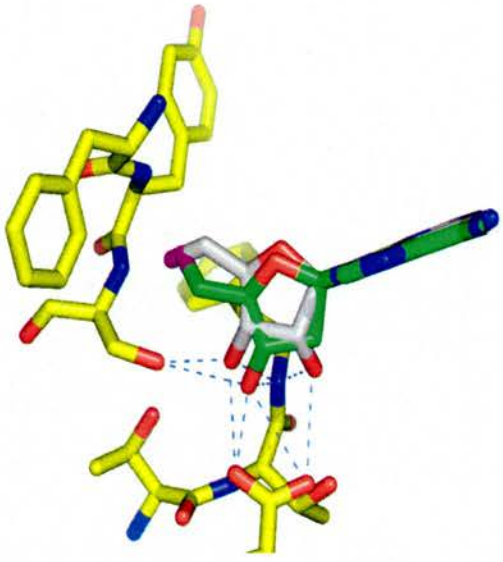

Figure 3.6. The structure of the 2'dFDA-fluorinase co-complex, superimposed with the structure of 5'-FDA **60**. The 2'dFDA **77** has the ribose C's coloured green, while in 5'-FDA **60** they are coloured white.[6]

Also the ether ring of the sugar is no longer planar. This was an interesting observation in that it showed that this planarity is not an important factor for the reactivity. This has also been corroborated by the theoretical study mentioned in section 3.1.1, where this ring strain was not judged important in lowering the reaction energy barrier.[5]

The chlorinated substrate 5'-ClDA **72** has been co-crystallised with the fluorinase in the absence of L-methionine **61** (by A. McEwan and Prof. J. H. Naismith).[7] In the resultant structure, the C-5'—Cl bond adopts two orientations locating the organo-chlorine atom in two different positions. The most relevant conformer is represented in Figure 3.7, in which 5'-ClDA **72** is bound to the active site of the fluorinase. Superimposed on this structure is the structure of 5'-FDA **60**, the natural substrate. It can be seen that the chlorine atom is displaced by 1.3 Å relative to fluorine in 5'-FDA **60**, as a consequence of its larger atomic radius. However, it still makes the same two hydrogen bonding contacts to Ser-158, observed in 5'-FDA **60**. Figure 3.8 shows both conformers of the 5'-ClDA **72**.

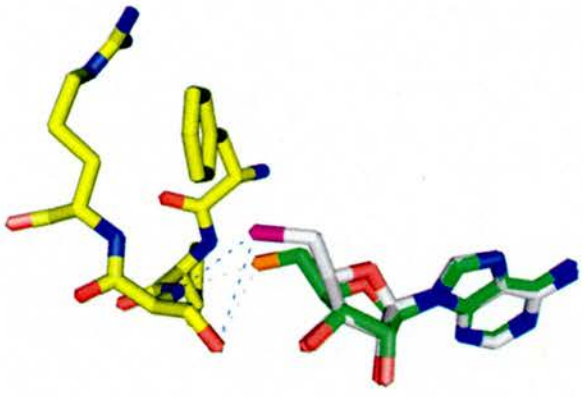

Figure 3.7. Structure of the 5'-ClDA-fluorinase co-complex, superimposed with the structure of 5'-FDA **60**. The chlorine is displaced by 1.3 Å relative to fluorine. The 5'-FDA **60** has the ribose C's coloured green, while in 5'-ClDA **72** they are coloured white.[7]

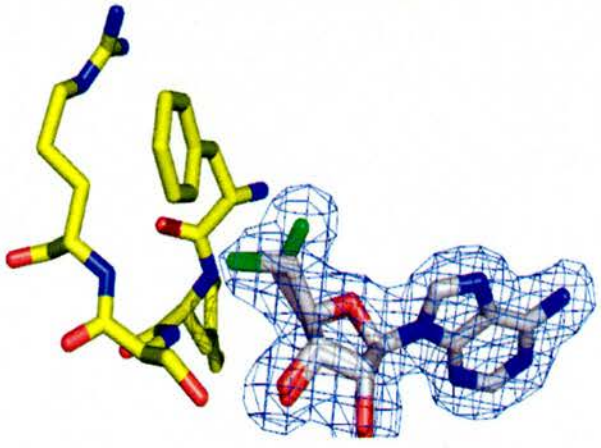

Figure 3.8. The structure of 5'-ClDA **72** bound to the fluorinase showing both conformations of the chlorine atom.

3.1.3 Further crystallographic investigation

The crystallographic study on the fluorinase has revealed important information regarding the interaction of 5'-FDA **60** with the active site of the enzyme.[1] The 5'-fluorine of 5'-FDA **60** is shown to make two hydrogen bonds with Ser-158: one with the NH of the

amide and the second with the OH of the side chain. This was a surprising observation, as fluorine is well known to be a relatively poor hydrogen-bonding acceptor. This pocket, which presumably binds fluoride ion prior to nucleophilic substitution, is unoccupied in the SAM structure and is quite hydrophobic in nature.[1] No water molecules are found in the vicinity of fluorine, which suggested that the fluoride nucleophile is fully dehydrated prior to C-F bond formation.[1] It is possible that the fluorinase may bind a molecule of SAM **62** initially, then fluoride ion may diffuse into the active site through a channel and attack the C-5' position of the substrate to generate 5'-FDA **60**.[1] However, a convincing channel that is wide enough to allow the passage of F^- anion, with SAM **62** bound, is not obvious, and perhaps fluoride ion may be bound first. It became a focus of this research to try to explore fluoride ion binding by crystallography.

3.2 Crystallographic investigation into halide ion binding

Observing fluoride ion bound to a protein is difficult by crystallography, because the number of electrons (ten) in F^- is identical to that of water and consequently they cannot easily be distinguished. However, in light of the fact that the fluorination enzyme is also able to catalyse a chlorination reaction (as reported in section 2.3.4), the identification of chloride ion on the enzyme surface is, in principle, a much easier prospect by crystallography. Furthermore, X-ray analysis of the co-crystallised 5'-ClDA-fluorinase complex, has shown that the C-5'—Cl bond of 5'-ClDA **72** adopts a similar orientation to the C-5'—F bond of 5'-FDA **60**.[7] This suggests that chloride will be bound to the active site in a similar manner to fluoride prior to nucleophilic substitution.

In order to carry out this study, a suitable substrate was required. The ideal compound must bind to the enzyme in a similar manner to that exhibited by SAM **62**, and at the same time should be able to inhibit enzymatic halogenation. In this context, 9-(β-D-*erythro*-furanosyl)adenosine **83**, emerged as a candidate substrate.

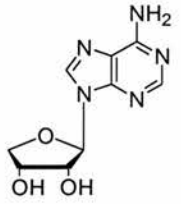

83

This compound has both the adenine and the ribose rings necessary for binding the enzyme, but, because the C-5' atom is missing, reaction clearly cannot take place (Scheme 3.1).

It was anticipated that a co-crystal of the fluorinase with **83**, L-methionine **61** and chloride ion, may allow chloride ion to be located at the active site.

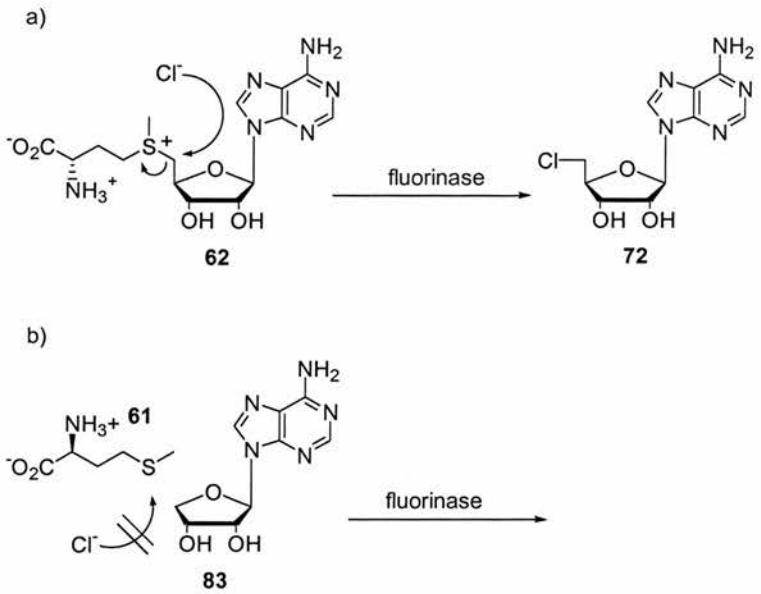

Scheme 3.1. a) Chloride displaces L-methionine **61** to generate 5'-ClDA **72**. b) The same reaction cannot take place with 9-(β-D-*erythro*-furanosyl)adenosine **83**, as the C-5' involved in the nucleophilic substitution is missing.

3.2.1 Approach to the synthesis of 9-(β-D-*erythro*-furanosyl)adenosine 83

The synthesis of 9-(β-D-*erythro*-furanosyl)adenosine **83** has been already described in the literature.[8,9,10] Some of the synthetic steps gave low overall yields and multiple products, which made them unattractive. An interesting approach, based on the trimethylsilyl method described by Vorbrüggen and co-workers,[11] has been reported by Serianni *et al.*[10] (Scheme 3.2).

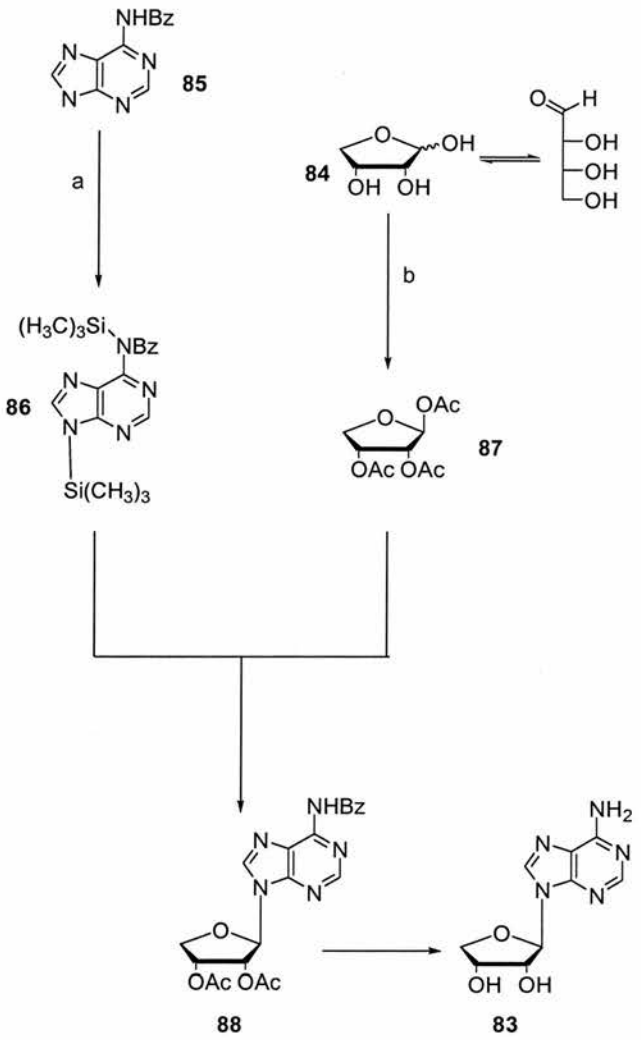

Scheme 3.2. Synthesis of 9-(β-D-*erythro*-furanosyl)adenosine **83** starting from D-erythrose **84** and N^6-benzoyladenine **85**.

This strategy involved a Friedel-Crafts reaction between the sugar donor, 1,2,3-triacetoxy-D-*erythro*-furanose **87**, and the silylated adenine **86** in the presence of the trimethylsilyl-trifluoromethanesulfonate as a catalyst.[10,11] This generated nucleoside **88**. Subsequent removal of the protecting groups afforded 9-(β-D-*erythro*-furanosyl)adenosine **83**. This route was reported to give a good overall yield (~39%), but involved relatively expensive starting materials (N^6-benzoyladenine **85** and D-erythrose **84**) and was therefore not addressed in this research. The procedure described above was based on known ionic

chemistry, and the desired product was obtained by coupling the sugar moiety with the adenine ring. A different approach towards the carbon skeleton of the sugar fragment involved the dehomologation of the ribose of the appropriate nucleoside, by breaking the C-4'—C-5' bond.

The carboxylic acid derivative of 2',3'-*O*-isopropylideneadenosine, compound **89**, emerged as an ideal precursor for this route, as a decarboxylation reaction would afford the dehomologated moiety.

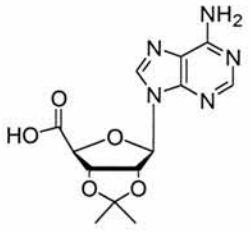

89

Radical decarboxylation has been widely described by Barton and co-workers.[12] This methodology involves the formation of thiohydroxamic esters (mixed anhydrides) as a source of disciplined radicals. According to this approach, the appropriate carboxylic acid is derivatised with *N*-hydroxy-2-thiopyridinone **90** to form a mixed anhydride such as **91**. This compound is then irradiated using a tungsten lamp and, in the presence of AIBN and tributyltin hydride **92**, forms a carboxyl radical **93** which spontaneously releases carbon dioxide. The radical intermediate can generate different compounds as a result of either an inter- or intra- molecular reaction or simply, as in our case, abstraction of a hydrogen atom (Scheme 3.3).

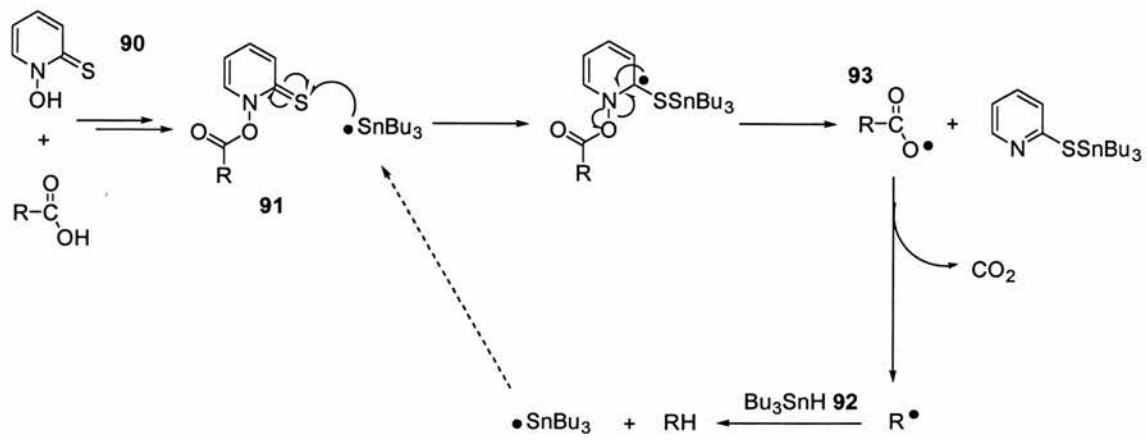

Scheme 3.3. Radical decarboxylation by irradiation of the thiohydroxamic ester **91** in the presence of AIBN and tributyltin hydride **92**.[12]

This strategy has already been described in adenosine systems, and in particular for the synthesis of (*S*)-sinefungin **71** (Scheme 3.4).[13] In this case, the 5'-oxyl radical **94** derived from the decarboxylation reaction, added to the appropriate electron deficient olefin **95**, to generate intermediate **96**, which was then converted to (*S*)-sinefungin **71**.

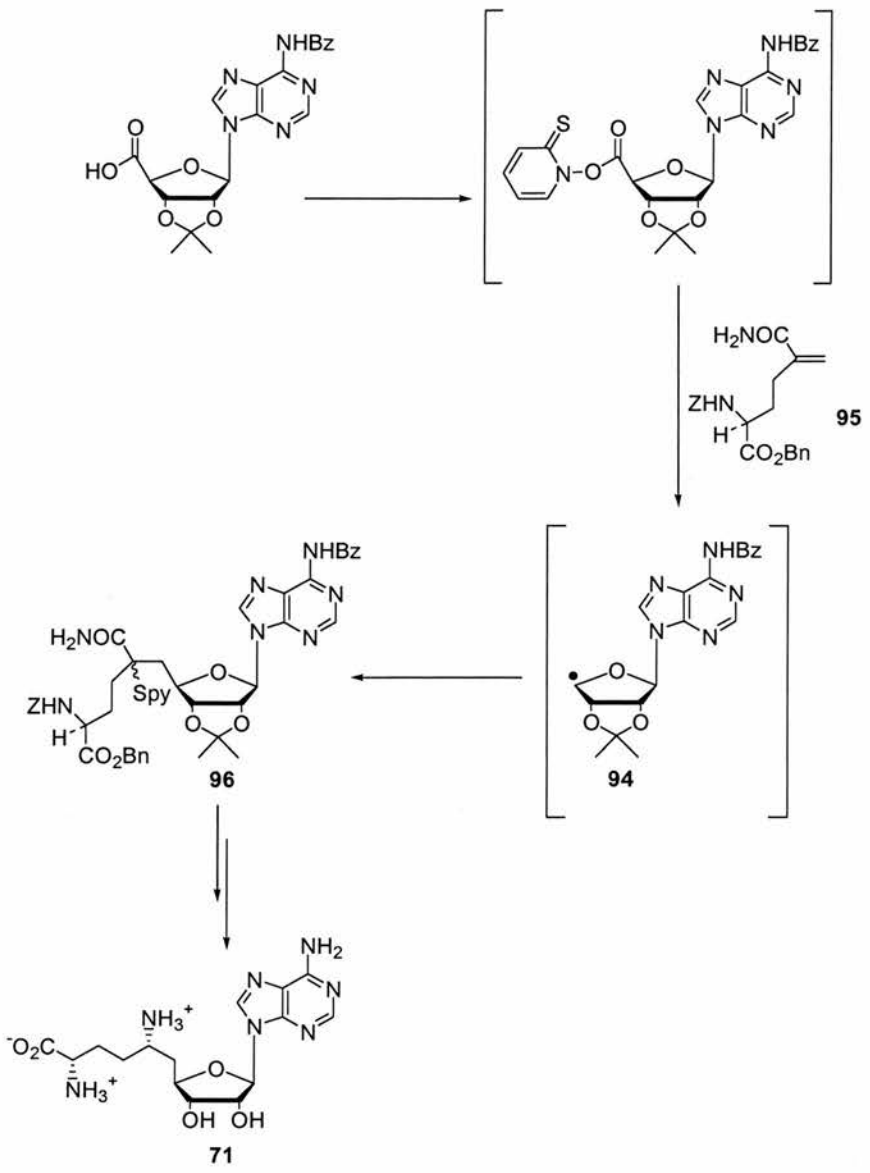

Scheme 3.4. Synthesis of (*S*)-sinefungin **71** *via* a radical reaction strategy.[13]

An alternative decarboxylation procedure has been reported for carboxylic acids in the presence of aza aromatic compounds with *tert*-butylthiol **97** (t-BuSH) as a hydrogen donor.[14] This method has been used successfully for the decarboxylation of primary, secondary and even tertiary aliphatic carboxylic acids. The aza aromatic compound used in those cases was acridine **98**, but other compounds were effective as well (phenanthridine, phenazine, DMAP, quinoline and 1,10- phenantroline). The mechanism for this

decarboxylation is not clear and there have been several proposals; for example, an ionic mechanism through an exciplex formed *via* π, π* singlet state by Nozaky,[15] an electron transfer mechanism by Davidson,[16] and a radical pair mechanism by Libman.[17] Probably, the most plausible mechanism is proposed by Okada *et al.*[14], as summarised in Scheme 3.5.

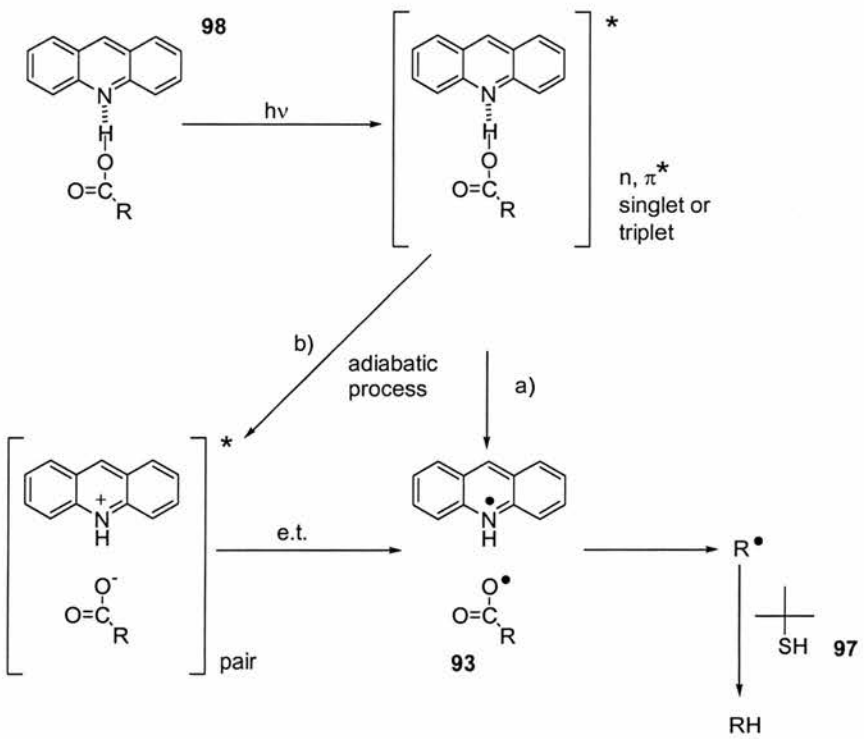

Scheme 3.5. Okada's mechanism for the decarboxylation of aliphatic carboxylic acids mediated by acridine **98**.[14]

Acridine **98** is a weak base and chelates the carboxylic acid. Excitation of this chelated complex produces the chelated excited states. The chelated n, π* singlet or the second triplet (n, π*) directly abstracts the chelated hydrogen (path a) to produce the carboxyl radical which in turn undergoes decarboxylation and abstracts hydrogen from t-BuSH **97** to give the alkane. Alternatively, adiabatic protonation through the chelated complex gives the excited ion pair (path b), which undergoes the electron transfer reaction to produce the

carboxyl radical.[14]

This method presented several advantages. Firstly, it does not require derivatization of the carboxylic acid, and secondly, it does not involve tributyltin hydride **92**, which makes the route attractive considering the high toxicity of tin reagents.

A dehomologation reaction, *via* a radical mechanism, could also be accessed using the 5'-*O*-nitro ester derivative of 2',3'-*O*-isopropylideneadenosine, compound **99**, as a starting material. This strategy has been described by Robins and co-workers[18], who reported the preparation of 9-(β-D-*erythro*-furanosyl)adenosine **83a** with a deuterium label at the C-4'.

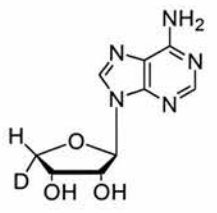

83a

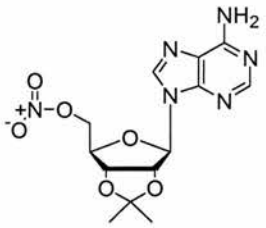

99

The synthesis of this labelled compound required just three steps and this was judged the most suitable for the preparation of our synthetic target **83**. A full discussion of the synthesis is reported below.

3.2.2 Synthesis of 9-(β-D-*erythro*-furanosyl)adenosine 83

The synthesis of **83** was successfully accomplished by employing a slight modification of Robins' strategy.[18] The first step of this procedure involved the derivatization of the primary alcohol moiety of 2',3'-*O*-isopropylideneadenosine **100**, to give the corresponding nitro ester **99** (Scheme 3.6).

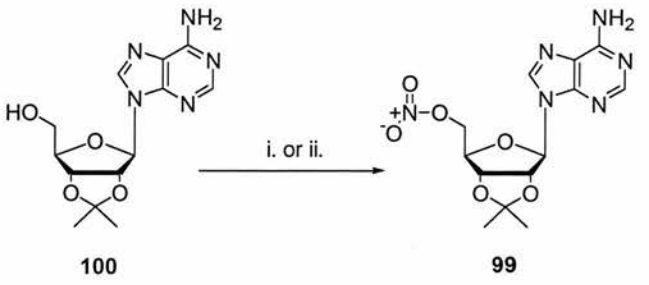

Scheme 3.6. i. 1-Nitropyrazole/triflic acid/CH_3CN (12%); ii. 60% nitric acid/acetic anhydride (50%).

In the first instance, the nitration was carried out using *N*-nitropyrazole as a nitrating transfer agent and triflic acid as a catalyst, as previously reported.[18,19] This reagent has been used successfully for the nitration of aromatic substrates, and was also found to be effective for the derivatization of uracil and nucleoside derivatives.[19,20] The nitration of adenosine **100** was reported to give a low yield (20%).[18] In our case the yield was also poor (12% best result) and could not be improved. The use of acetyl nitrate (generated by *in situ* by addition of nitric acid to acetic anhydride) at low temperature proved much better and resulted in an increased yield (50%) of the 5'-*O*-nitro ester **99**.[21] The best conditions for this reaction were found to involve 10:1 acetic anhydride:60% nitric acid mixture at -30 °C for 15 min.[21] The low temperature and the short reaction time were sufficiently mild for the acetonide protecting group to survive hydrolysis.

The β-scission of the C-4'—C-5' bond of the 5'-*O*-nitro-2',3'-*O*-isopropylideneadenosine **99** was then carried out *via* a radical reaction, using tributyltin hydride **92**, AIBN as initiator and *o*-xylene as the solvent.[18] The mechanism of this reaction is thought to involve the formation of the 5'-oxyl radical **101**. Radical **101** can then abstract a hydrogen atom, most probably from tributyltin hydride **92**, to give 2',3'-*O*-isopropylideneadenosine **100**, or it can release formaldehyde **102** to generate the 4'-glycosyl radical **103**, which subsequently gives nucleoside **104** after hydrogen transfer (Scheme 3.7).

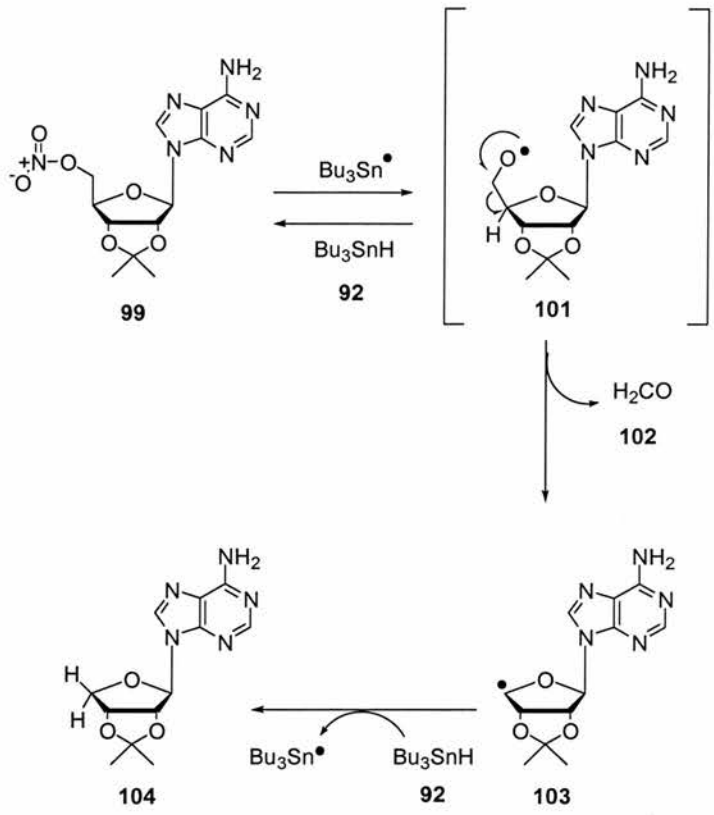

Scheme 3.7. β-Scission of the C-4'—C-5' bond of **101** *via* a radical mechanism.[18]

Some problems were encountered with the purification of **104**. Purification over silica gel gave a mixture of two products as shown by ^{1}H-NMR analysis (Figure 3.9). 9-(β-D-*erythro*-furanosyl)-2'3-O-Isopropylideneadenosine **104** co-eluted with a side product, which in the event had the same R_F on TLC. However, this unexpected compound could be isolated as a crystalline solid from the product mixture. Thus, after several crystallizations from methanol the side product was almost totally removed, affording compound **104** up to ~95% of purity. X-ray structure analysis of the side product showed this to be compound **105**.

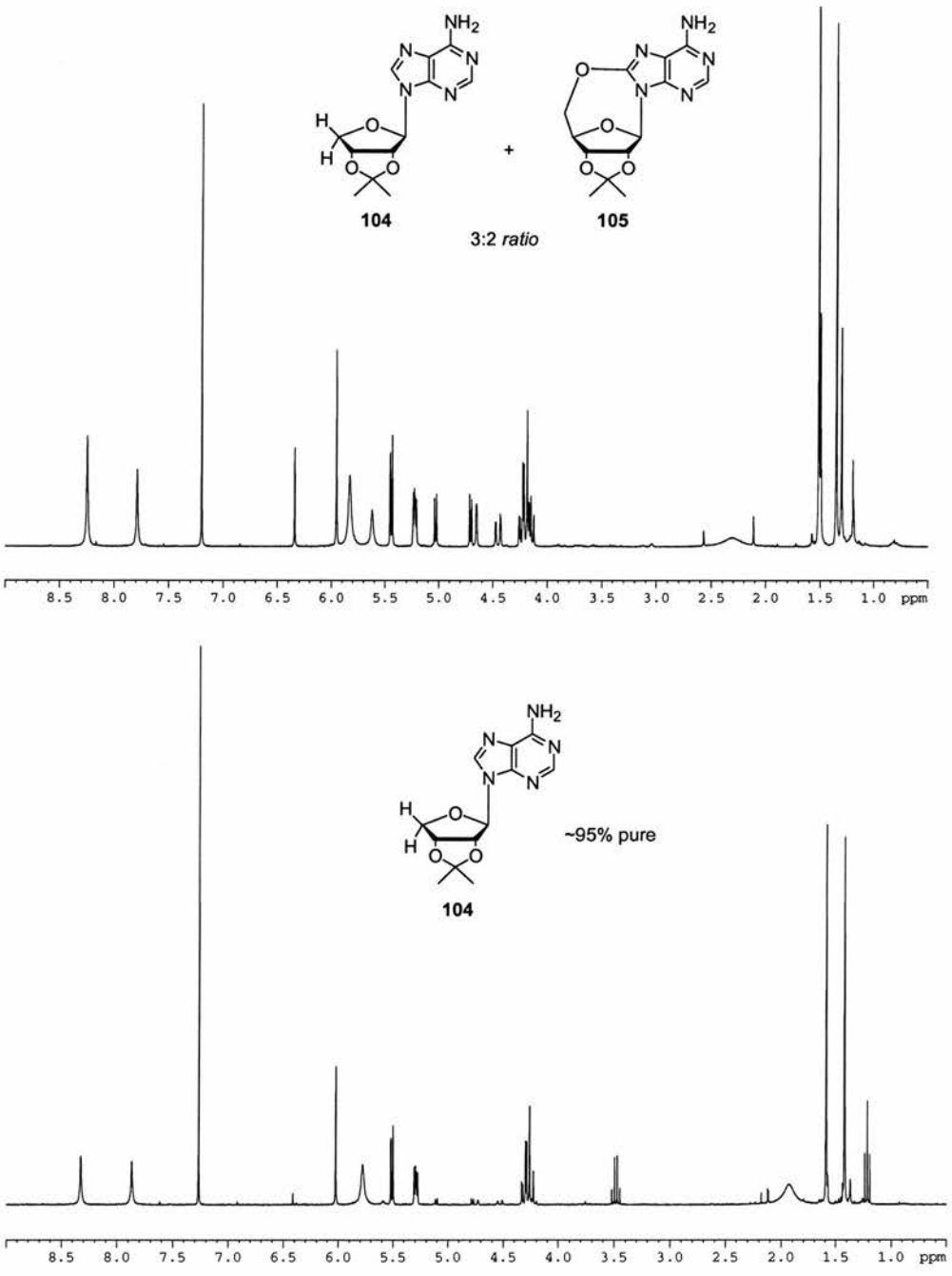

Figure 3.9. ^{1}H-NMR spectra of a) a mixture of **104** and **105** (3:2 *ratio*); and b) **104** ~95% pure.

This unexpected compound indicates that the 5'-oxyl radical **101** was quenched by an alternative pathway, by undergoing intramolecular attack to C-8 of the adenine ring to give the cyclic ether **105** (Figure 3.10).

A proposed mechanism of this intramolecular cyclization is presented in Scheme 3.8.

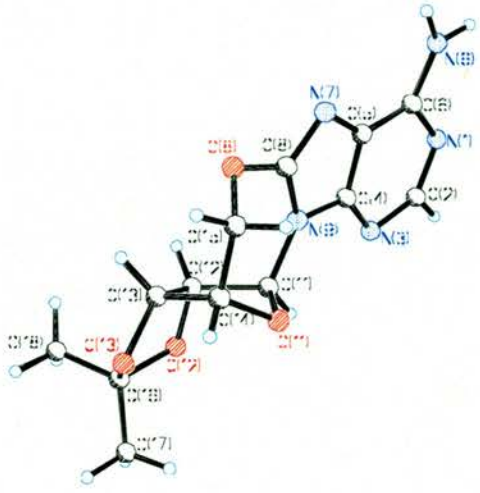

Figure 3.10. X-ray structure of 2',3'-*O*-isopropylidene-5',8-*O*-cycloadenosine **105**.

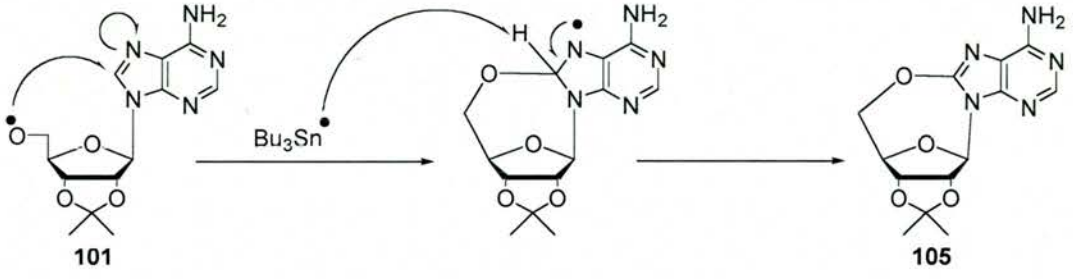

Scheme 3.8. Proposed mechanism for the formation of the side product **105** after the formation of 5'-oxyl radical **101**.

A modification of this radical reaction was also explored. Tin reagents are known to be toxic and they are difficult to be eliminated completely from reaction products. For these reasons, tris(trimethylsilyl)silane **106** has been used as a mediator for radical chain reactions in place of the organotin initiators.[22] The Si—H bond energy of **106** is low enough to be homolytically cleaved by heat (Scheme 3.9). This is probably due to the bonding interaction between β-silicon d-orbitals and the semi-occupied p-orbital on the

central silicon atom in the corresponding silyl radical derived from **106**.[22]

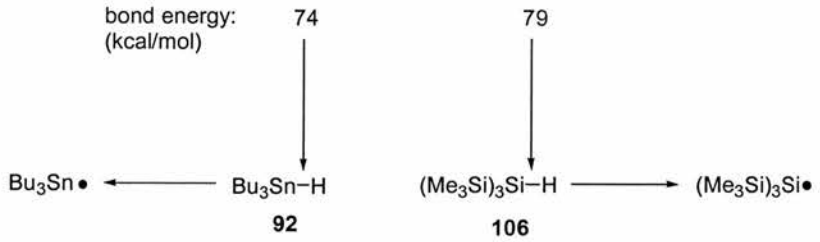

Scheme 3.9. The homolytic scission of the Si—H bond of **106** requires just 5 kcal/mol more energy than the Sn—H bond of **92**.[22]

However, in the event this reaction resulted in a very poor yield (~5%) of product when the silane reagent **106** was employed, and tributyltin hydride **92**, despite its problems, remained the reagent of choice.

The preparation of 9-(β-D-*erythro*-furanosyl)-2',3'-*O*-isopropylideneadenosine **104** *via* dehomologation of carboxylic acid **89** was also investigated. The required carboxylic acid was prepared by oxidation of the primary alcohol of 2',3'-*O*-isopropylideneadenosine **100** with excess of $KMnO_4$ in a KOH solution (Scheme 3.10).[23] The product **89** was recovered in 69% overall yield.

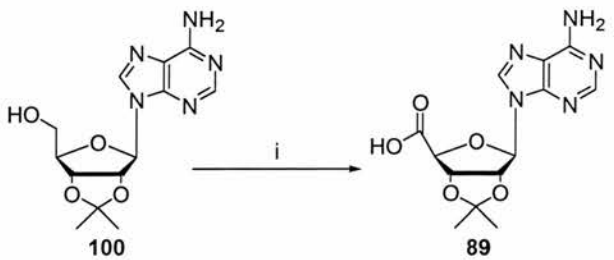

Scheme 3.10. i. $KMnO_4$, H_2O/KOH (69%).

Decarboxylation of **89** was then attempted following Barton's methodology[12,13] as described in section 3.2.2. The carboxylic acid **89** was activated for nucleophilic

substitution by derivatization with isobutyl chloroformate using *N*-methylmorpholine as a base (Scheme 3.11). The anhydride **107**, which is formed *in situ*, was then treated with the sodium salt of *N*-hydroxy-2-thiopyridinone **90**, which generated the mixed anhydride **108**. According to the literature procedure, this intermediate is not isolated but is irradiated directly with a 400 watt tungsten lamp, after addition of Bu_3SnH **92** and AIBN to the mixture. However, this reaction proved unsuccessful. Attempts to modify the reaction conditions (solvent, temperature, reaction time) were also unsuccessful.

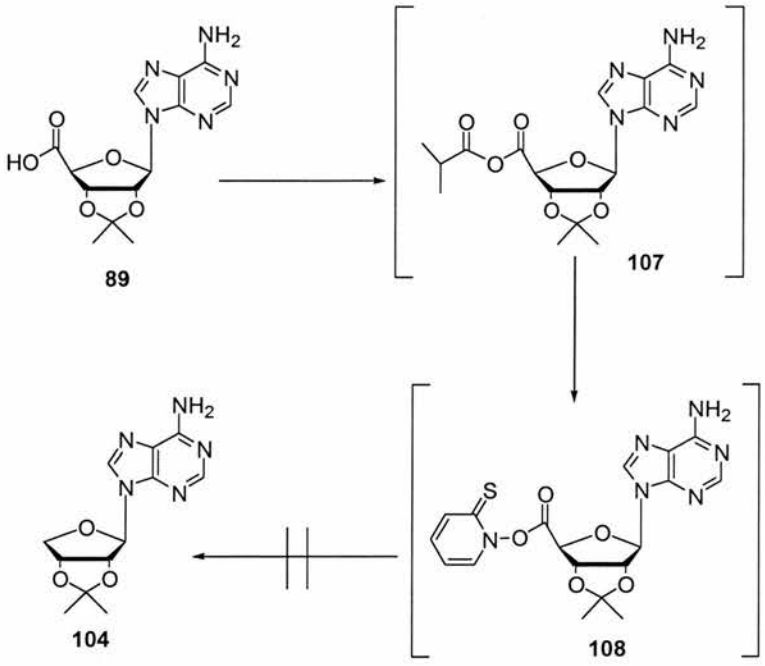

Scheme 3.11. Attempted dehomologation of carboxylic acid **89** by the Barton's methodology.

A further attempt involved the decarboxylation of **89** *via* an aza aromatic. Disappointingly, irradiation of the carboxylic acid **89** with a 400 watt tungsten lamp in the presence of acridine **98** and t-BuSH **97**, was unsuccessful. The same negative result was obtained when DMAP was used as the aza compound.

Of all the procedures attempted, Robins' methodology gave the best result and a sufficient

respect to each other, while the ribose ring adopts the usual planar conformation observed for other substrate analogues co-crystallised with the fluorinase. It is interesting to note that **83** sits in the active site in a conformation almost identical to that of 5'-FDA **60**. This is clearly shown in Figure 3.12 where **60** and **83** are superimposed.

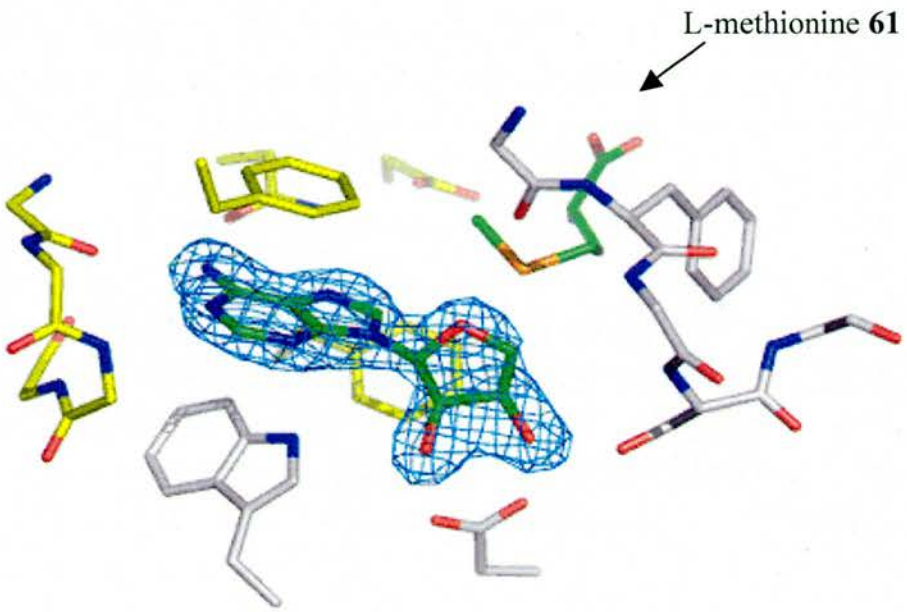

Figure 3.11. Crystal structure of 9-(β-D-*erythro*-furanosyl)adenosine **83** and L-methionine **61** bound to the active site of the fluorination enzyme.

Disappointingly, chloride ion was not observed in the active site of the enzyme.

In the co-crystallised SAM-fluorinase complex, the radius of the pocket where the halogen is thought to reside is roughly 1.4-1.6 Å (assuming hydrogen atoms at their calculated positions with a van der Waals radius of 1.0 Å).[1] This could explain why the large chloride ion doesn't appear in the active site. A more accurate investigation involved the same crystallization process without the L-methionine **61**. This in theory would allow chloride ion to accommodate the active site. However, the crystal structure obtained gave the same results as the previous experiment with **83** bound, but chloride was not evident.

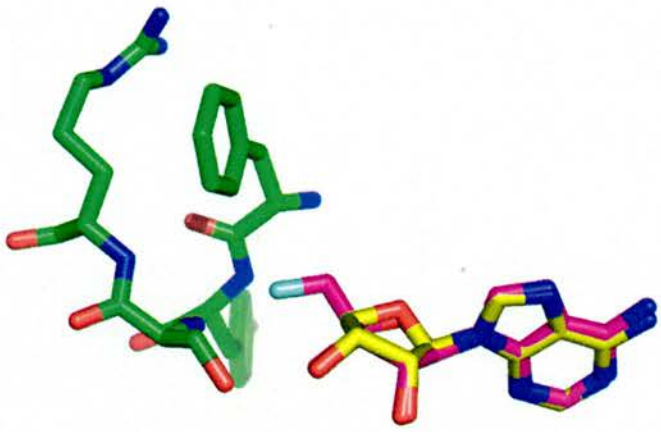

Figure 3.12. Crystal structure of 9-(β-D-*erythro*-furanosyl)adenosine **83** (with carbons depicted in yellow) superimposed to 5'-FDA **60** (with carbons depicted in purple).

3.2.4 Conclusion

The preparation of 9-(β-D-*erythro*-furanosyl)adenosine **83** was designed to carry out further crystallographic investigations of the fluorinase in order to explore chloride ion binding.

Compound **83** was prepared by a modification of a literature method[18], based on the β-scission of the C-4'—C-5' bond of adenosine. This compound was then used as a ligand in a co-crystallization trials with the fluorinase, in the presence of chloride and with/without L-methionine **61**. Although a structure of the modified substrate with the fluorinase was solved, the diffraction data did not indicate the presence of chloride ion. Clearly, further crystallographic experiments are required to shed light on the halide binding prior to the nucleophilic attack to SAM **62**, and these will involve different substrate analogues.

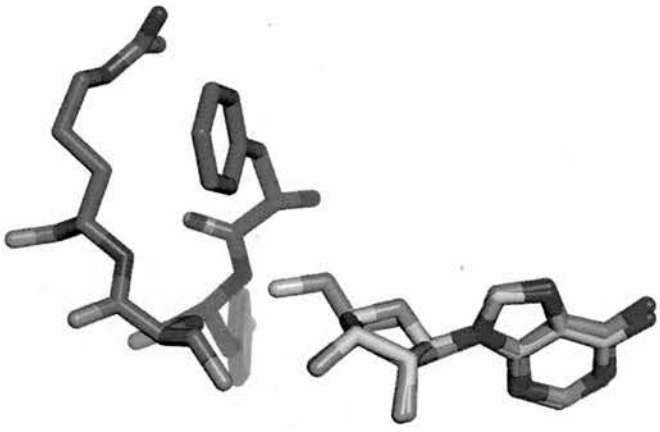

Figure 3.12. Crystal structure of 9-(β-D-*erythro*-furanosyl)adenosine **83** (with carbons depicted in yellow) superimposed to 5'-FDA **60** (with carbons depicted in purple).

3.2.4 Conclusion

The preparation of 9-(β-D-*erythro*-furanosyl)adenosine **83** was designed to carry out further crystallographic investigations of the fluorinase in order to explore chloride ion binding.

Compound **83** was prepared by a modification of a literature method[18], based on the β-scission of the C-4'—C-5' bond of adenosine. This compound was then used as a ligand in a co-crystallization trials with the fluorinase, in the presence of chloride and with/without L-methionine **61**. Although a structure of the modified substrate with the fluorinase was solved, the diffraction data did not indicate the presence of chloride ion. Clearly, further crystallographic experiments are required to shed light on the halide binding prior to the nucleophilic attack to SAM **62**, and these will involve different substrate analogues.

References Chapter 3

1. C. J. Dong, F. L. Huang, H. Deng, C. Schaffrath, J. B. Spencer, D. O'Hagan and J. H. Naismith, *Nature*, 2004, **427**, 561.

2. C. D. Cadicamo, J. Courtieu, H. Deng, A. Meddour and D. O'Hagan, *ChemBioChem.*, 2004, **5**, 685.

3. S. L. Cobb, "The origin and metabolism of 5'-FDA in S. Cattleya", PhD Thesis, University of St. Andrews, 2005.

4. H. Deng, D. O'Hagan and C. Schaffrath, *Nat. Prod. Rep.*, 2004, **21**, 773.

5. H. M. Senn, D. O'Hagan and W. Thiel, *J. Am. Chem. Soc.*, 2005, **127**, 13643.

6. S. L. Cobb, H. Deng, A. McEwan, J. H. Naismith, D. O'Hagan and D. A. Robinson, *Org. Biomol. Chem.*, 2006, **4**, 1458.

7. H. Deng, S. L. Cobb, A. McEwan, R. P. McGlinchey, J. H. Naismith, D. O'Hagan, D. A. Robinson and J. B. Spencer, *Angew. Chem. Int. Ed..*, 2006, **45**, 659.

8. D. H. Murray, and J Prokop, *J. Pharm. Sci.*, 1967, **56**, 867.

9. G. L. Szekeres, J. T. Witkowski and R. K. Robins, *J. Carbohydrates, Nucleosides, Nucleotides*, 1977, **4**, 147.

10. P. C. Kline and A. S. Serianni, *J. Org. Chem.*, 1992, **57**, 1772.

11. H. Vorbrüggen, K. Krolikiewicz and B. Bennua, *Chem. Ber.*, 1981, **114**, 1234.

12. D. H. R. Barton, D. Crich and W. B. Motherwell, *Tetrahedron*, 1985, **41**, 3901.

13. D. H. R. Barton, S. D. Géro, B. Quiclet-Sire and M. Samadi, *J. Chem. Soc. Perkin Trans. 1*, 1991, 981.

14. K. Okada, K. Okubo and M. Oda, *Tetrahedron Lett.*, 1989, **30**, 6733.

15. R. Noyori, M. Kato, M. Kawanishi and H. Nozaki, *Tetrahedron*, 1969, **25**, 1125.

16. D. R. G. Brimage, R. S. Davidson and P. R. Steiner, *J. Chem. Soc., Perkin 1*, 1973, 526.

17. J. Libman, *J. Chem. Soc., Chem. Commun.*, 1976, 198.

18. M. J. Robins, Z. Guo, M. C. Samano and S. F. Wnuk, *J. Am. Chem. Soc.*, 1999, **121**, 1425.

19. J. Giziewicz, S. F. Wnuk and M. J. Robins, *J. Org. Chem.*, 1999, **64**, 2149.

20. G. A. Olah, S. C. Narang and A. P. Fung, *J. Org. Chem.*, 1981, **46**, 2706.

21. F. W. Lichtenthaler and H. J. Müller, *Synthesis*, 1974, 199.

22. B. Giese and B. Kopping, *Tetrahedron Lett.*, 1989, **30**, 681.

23. R. R. Schmidt, U. Schloz and D. Schwille, *Chem. Ber.*, 1968, **101**, 590.

Chapter 4

Stereochemical studies

4.1 Introduction

The fluorinase enzyme mediates a reaction between inorganic fluoride and SAM **62** to generate 5'-FDA **60** (Scheme 4.1).[1] SAM **62** is of course derived from a reaction between ATP **59** and L-methionine **61** mediated by L-methionine adenosyltransferase. This enzyme catalyses a nucleophilic attack of the sulphur of L-methionine **61** to the C-5' carbon of ATP **59** to generate SAM **62**. It has been shown by Parry *et al.*[2] that this enzymatic reaction proceeds with an inversion of configuration, suggesting an S_N2 type reaction.

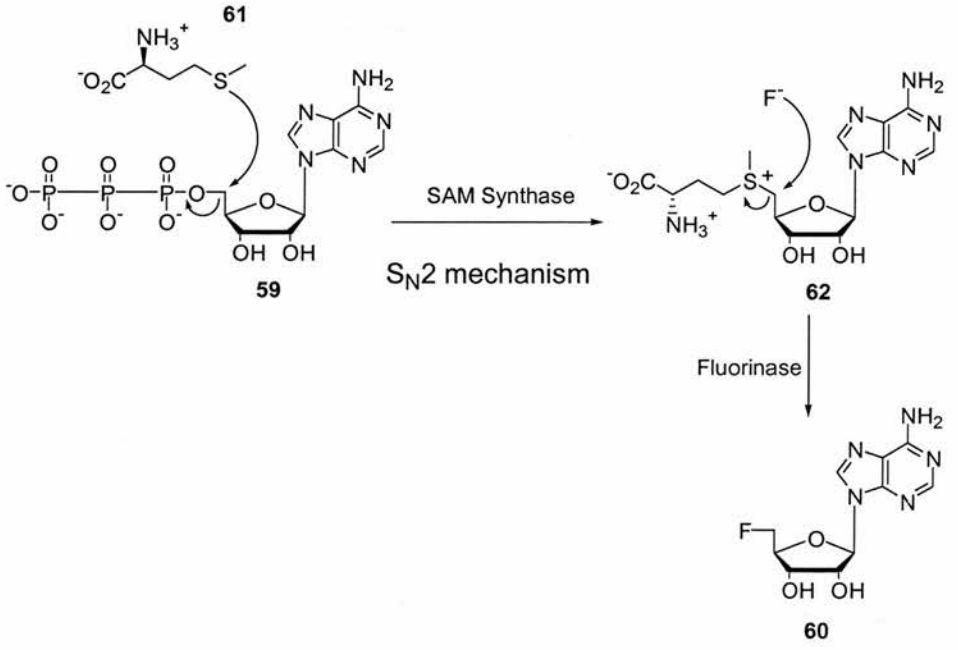

Scheme 4.1. Overview of enzymatic fluorination in *S. cattleya*.

Clearly a stereochemical analysis of biological fluorination will assist a mechanistic understanding of this unusual enzyme reaction. If the fluorinase enzyme mediates an S_N2 substitution of fluoride ion with SAM **62**, it will generate 5'-FDA **60**, with release of L-methionine **61**, with an inversion of configuration. Alternatively a sequence of events involving two S_N2 substitution reactions, perhaps involving a nucleophilic substituent on the enzyme, would result in an overall retention of configuration. Finally there is the possibility of an elimination reaction occurring on SAM **62** to generate an enzyme bound substrate with sp^2 hybridisation at C-5'. Fluoride addition to either face of such a double bond could result in either an inversion or retention of configuration.[3] However, this latter scenario appears to be a less likely process, as the anti-Markovnicov attack of HF to an enol ether is disfavoured (Scheme 4.2).

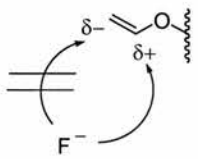

Scheme 4.2. In an enol-ether system, fluoride addition to the α-position is favoured over the β-position.

Some stereochemical details of biological fluorination had already been reported prior to this study.[3] These experiments carried out in whole-cells of *S. cattleya* are described in section 4.1.3. A more detailed analysis of the stereochemistry was obtained with over-expressed fluorinase.[4] Both stereochemical studies were based on the use of ^{2}H-NMR in a chiral lyotropic liquid crystalline phase generated from a chloroform (or DMF) solution of poly-γ-benzyl-L-glutamate **109** (PBLG). This proved to be an effective analytical method to determine the absolute configuration of the chiral deuterium labelled fluoromethyl group generated during the fluorination

reaction and it is discussed in more detail in section 4.2.[3]

4.1.1 Liquid-crystalline phase ^{2}H-NMR

Solutions of PBLG **109**, in various organic solvents, are known to produce lyotropic cholesteric liquid-crystalline solutions.[5,6]

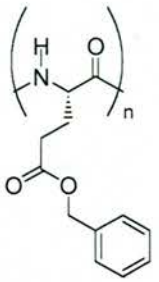

109

When placed in a strong magnetic field, B_o, the cholesteric pitch unwinds, and the solutions behave like a chiral nematic phase with the director aligned parallel to B_o.[6] The polypeptide chains of **109** exist in an *alpha* helical conformation (Figure 4.1).

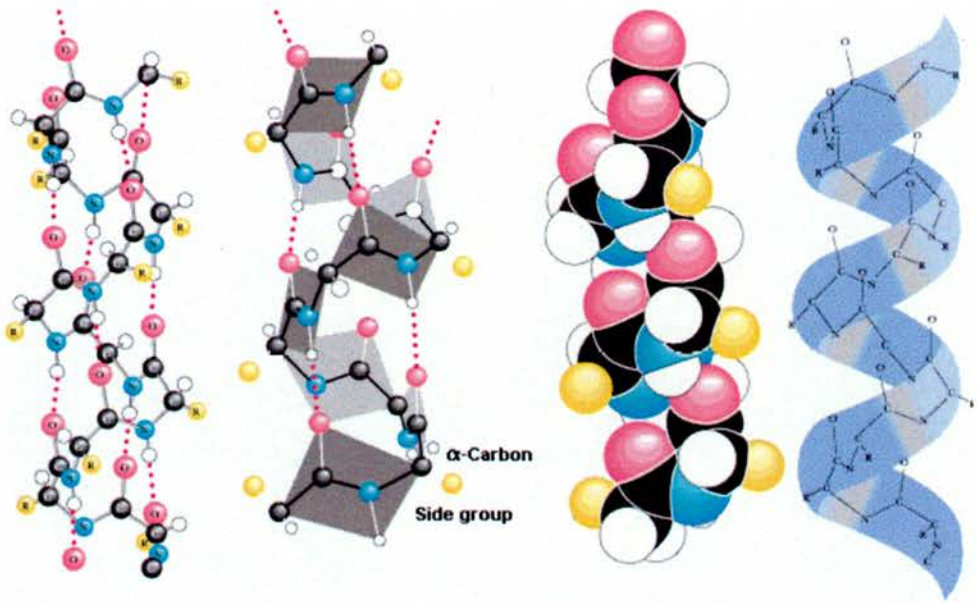

Figure 4.1. Representation of the *alpha* helix conformation similar to PBLG **109**.

The side chains, which branch from the main helix, form a secondary molecular helical structure that varies in a complex manner as a function of the solvent and the temperature. When molecules are dissolved in such a liquid crystalline system, they become partly ordered, and consequently their NMR spectra exhibit anisotropic interactions (the anisotropy of the chemical shifts, the dipolar couplings, and the quadrupolar splittings for spins larger than I= ½). The measure of these interactions is related to the degree of order of the solute molecule in the liquid-crystalline medium.[6] In the same way, enantiomers orient differently when dissolved in the PBLG **109**/organic solvent liquid crystals, and this enables their discrimination. In fact, we observe different ^{1}H-NMR spectra for the (*R*) and (*S*) enantiomers dissolved in such a system. The efficiency of chiral discrimination depends on the ability of the PBLG **109** to interact differently with the two enantiomers. The degree of polymerization (DP) of the PBLG **109** doesn't seem to be so crucial for the resolution as long the chains are long enough to produce a liquid-crystalline solution when dissolved in an organic solvent. Usually a DP between 515 and 1100 gives excellent results.[6]

4.1.2 ^{2}H-NMR analysis in a chiral liquid-crystalline phase

^{1}H-NMR spectra of ordered molecule become extremely complex when the number of nuclei becomes large, and interference may also be caused from the background resonances due to the solvent.[6] The use of proton decoupled ^{2}H-NMR of deuterium labelled chiral compounds provides a much more powerful tool for enantiomeric discrimination since the spectra are less complex. ^{13}C-NMR and ^{19}F-NMR in chiral liquid crystals have also been used successfully for enantiomeric discrimination.[7]

However, the sensitivity of this method is maximal for deuterium labelled compounds as the quadrupolar splittings associated with the deuterium nucleus (I=1) are large and thus the interactions with the electric field vector of the orientated polymer are maximal. A schematic representation of enantiomeric discrimination is reported in Figure 4.2. It should be pointed out that chiral discrimination could be obtained by any deuterium atom present in the molecule, and not just by a deuterium at the stereogenic centre.[6] This could be advantageous in cases where specific regiochemical labelling is synthetically difficult. Chiral discrimination by natural abundance deuterium $^{2}H\{^{1}H\}$-NMR in chiral liquid phases has been successfully addressed as well.[8] This has the advantage that no isotopic enrichment is needed, however, natural abundance NMR is characterised by its low sensitivity, therefore higher magnetic fields (B_0) and higher concentrations (often neat) of samples are required.

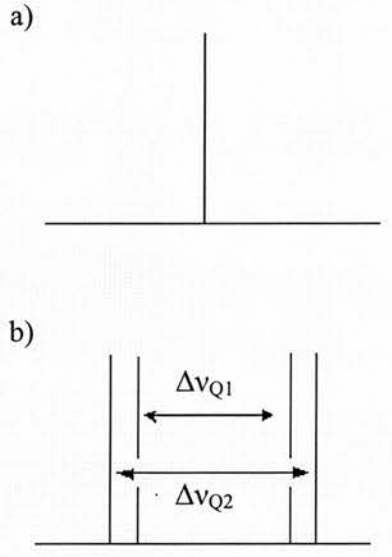

Figure 4.2. Schematic proton decoupled $^{2}H\{^{1}H\}$-NMR spectra of a monodeuterated racemic molecule in a) isotropic solvent, and b) chiral anisotropic solvent. $\Delta\nu_{Q1}$ And $\Delta\nu_{Q2}$ are the quadrupolar splittings for each enantiomer. Q represents the deuterium quadrupolar coupling constant.

4.1.3 First investigation on the stereochemistry of biological fluorination[3]

The first stereochemical study of biological fluorination involved the incubation of stereospecifically labelled precursors in the whole-cell suspensions of *S. cattleya*. As isotopically labelled glycerols had been shown to give high incorporations into the fluorometabolites **2** and **41**,[9,10] glycerols that were chiral by virtue of deuterium labelling were employed in that study. The diastereoisomers (1*R*, 2*R*) **53a** and (1*S*, 2*R*)-[1-$^2H_1$]-glycerol **53b** (95% and 87% e.e., respectively) were prepared where the diastereotopic hydrogens of the *pro-R* hydroxymethyl group were labelled separately by deuterium. These compounds were then added in separate experiments to cells of *S. cattleya*.

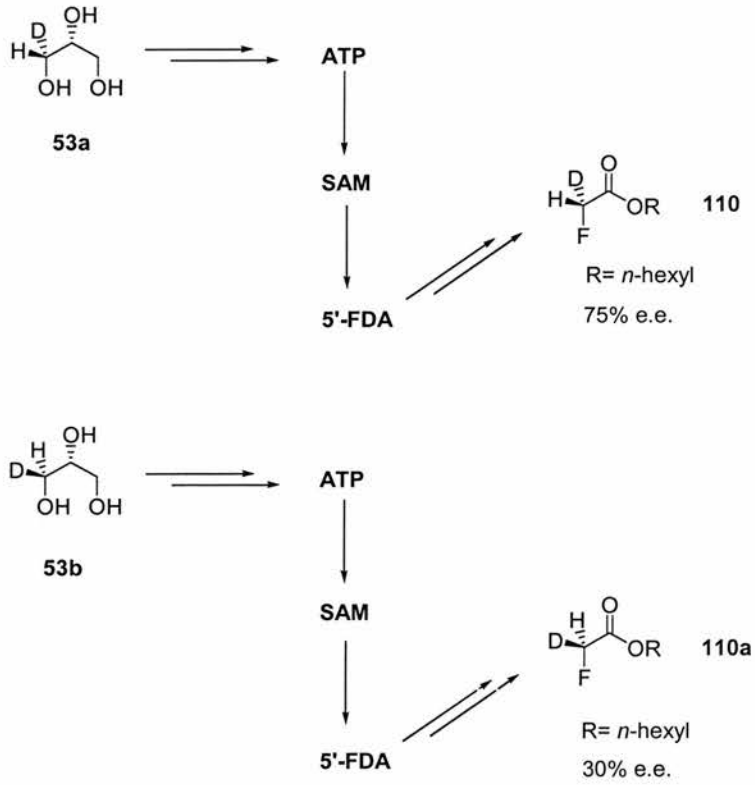

Scheme 4.3. Incorporation of chiral deuterium labelled glycerols **53a**, **53b** in whole cell incubations of *S. cattleya*, gave fluoroacetates with an overall retention of configuration.

Both labelled glycerols **53a** and **53b** gave rise to samples of enantiomerically enriched [2-$^2H_1$]-fluoroacetates **2a**, **2b**. These samples were first derivatised as their hexyl esters **110** and **110a**, and were then analysed by ^{2}H-NMR in PLBG **109** in chloroform. The absolute configuration of the two fluoroacetate esters was established by comparison with a standard sample of known configuration. The results from this ^{2}H-NMR analysis indicated that the labelled fluoroacetate products have retained their configuration throughout the biosynthetic experiment (Scheme 4.3). Taking into account the knowledge that SAM synthase operates with an inversion of configuration, the overall retention of configuration was deduced to be the result of a second inversion event occurring during the fluorination process. This stereochemical study revealed important information regarding the mechanism of biological fluorination, but it had several limitations. Firstly, this study relied on the correct metabolic and stereochemical interpretation of events as the isotope on the glycerol was assumed to enter the glycolytic pathway, and then pass into the pentose phosphate pathway prior to labelling ribose and becoming incorporated into the ribose ring at the C-5' position of ATP **59**, and then into SAM **62** prior to fluorination. Secondly, the isotope was analysed in the fluoroacetate products **2a**, **2b** and not in 5'-FDA **60**, the immediate product of the fluorination enzyme. The conclusion assumed that there was no configurational change during both the earlier and later stages of the biosynthesis in which 5'-FDA **60** is processed to fluoroacetate **2**.

With the purified and over-expressed fluorination enzyme available, it appeared appropriate to re-evaluate the mechanism of the fluorination reaction on the enzyme directly. These experiments are described in section 4.2. The biochemical aspects were carried out by my colleague Dr. H. Deng. The chiral ^{2}H-NMR analysis was

carried out by Dr. A. Meddour at Université Paris Sud, Orsay, in a collaboration with Professor J. Courtieu.

4.2 Stereochemical investigation of the fluorination enzyme

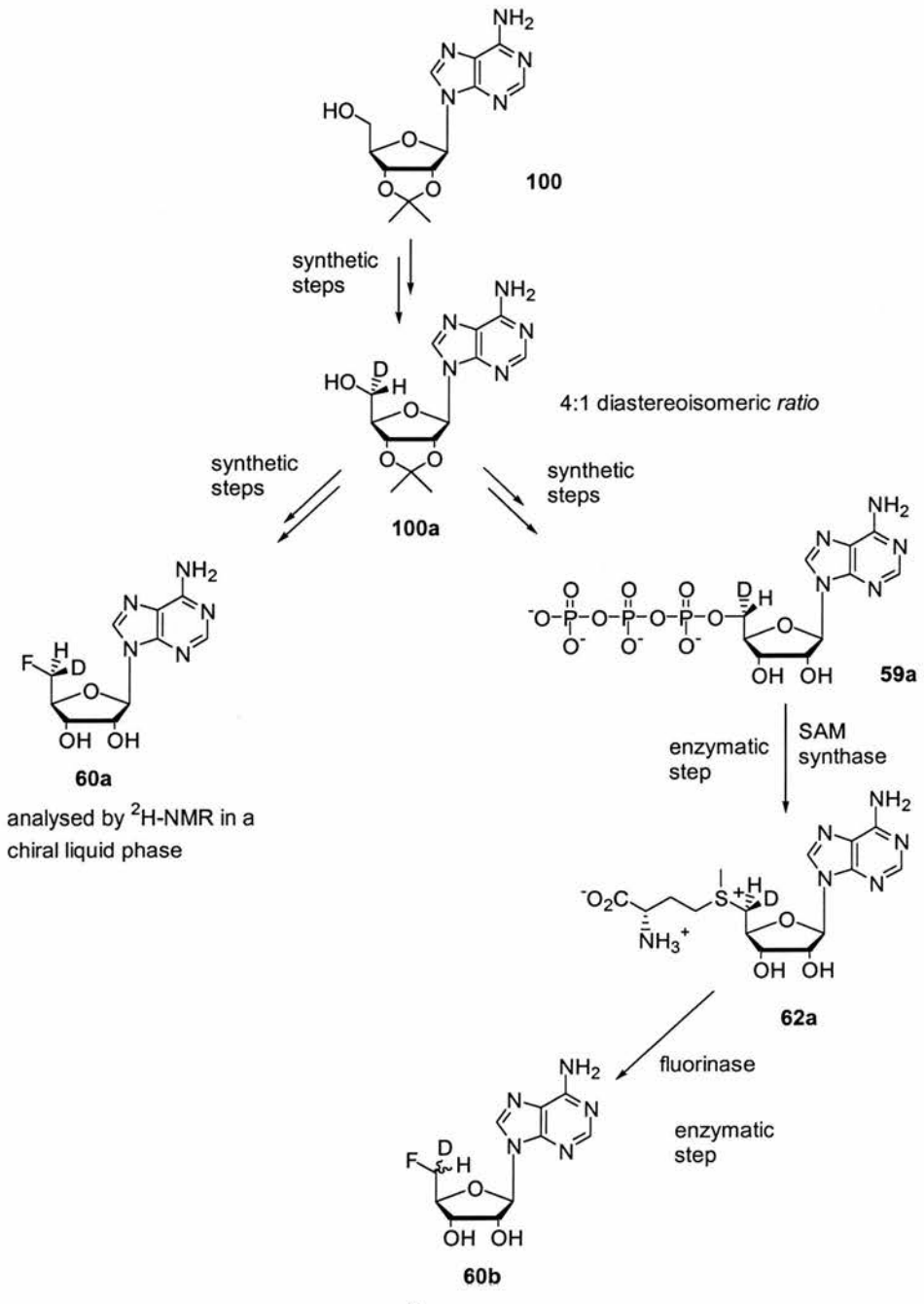

Scheme 4.4. Experimental approach to study the stereochemical course of the fluorination enzyme.

Our approach to evaluate the stereochemical course of the fluorination enzyme is outlined in Scheme 4.4. We envisaged a preparation of (5'*R*)-[$^2H_1$]-ATP **59a** followed by its incubation with SAM synthase to generate a sample of (5'*S*)-[$^2H_1$]-SAM **62a**. Treatment of this stereospecifically and isotopically labelled SAM **62a** with fluoride ion in the presence of the fluorinase should provide a sample of 5'-[$^2H_1$]-FDA **60b**, stereospecifically labelled at the C-5' position. With the knowledge that SAM synthase mediates a configurational inversion, the resultant configuration at C-5' of 5'-[$^2H_1$]-FDA **60b** in the coupled enzyme reaction, established by comparison with a synthetic sample of (5'*S*)-[$^2H_1$]-FDA **60a**, should allow the stereochemical course of the fluorination reaction to be deduced. The entire strategy relied on the use of ^{2}H-NMR in a chiral liquid-crystalline medium to determine the absolute stereochemistry of 5'-[$^2H_1$]-FDA.

4.2.1 Preparation of (5'*R*)-[$^2H_1$]-2',3'-*O*-isopropylideneadenosine 100a

(5'*R*)-[$^2H_1$]-2',3'-*O*-Isopropylideneadenosine **100a** emerged as an ideal common synthetic intermediate for the preparation of both the stereospecifically labelled 5'-FDA **60a** and ATP **59a**, as outlined in Scheme 4.4. The synthetic strategy, summarised in Scheme 4.5, proceeded as follows. 2',3'-*O*-Isopropylideneadenosine **100**, which is commercially available, was converted to **111** by treatment with benzoyl chloride in pyridine followed by selective hydrolysis of the 5'-*O*-benzoyl group with potassium hydroxide in aqueous pyridine.[11] N^6-Benzoylation of the adenosine **100** was carried out because 2',3'-*O*-isopropylideneadenosine-5'-aldehyde **112** is difficult to isolate. This problem is particularly acute because, as has been

shown,[12] such aldehydes readily epimerize at C-4' or eliminate the acetonide functionality giving 3',4'-unsaturated aldehydes upon attempted chromatography.

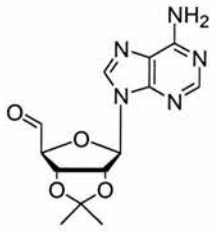

112

The presence of the benzoyl group avoids these problems and simplifies the isolation of the nucleoside aldehyde. Oxidation of the primary alcohol of N^6-benzoyl-2',3'-*O*-isopropylideneadenosine **111** was conveniently achieved by treatment with dimethyl sulfoxide (DMSO) and dicyclohexylcarbodiimide (DCC) in the presence of dichloroacetic acid.[13] As reported in the literature,[14] this kind of oxidation shows a maximum yield when 3 eq. of DCC and 0.5 eq. of dichloroacetic acid are used. Other attempted oxidations (e.g., Dess-Martin periodinate and Swern) failed. Trapping of the aldehyde **113** with *N,N'*-diphenylethylenediamine gave the 1,3-diphenylimidazolidine derivative **114**[13] which could be crystallized to purity from ethanol (78%). Treatment of derivative **114** with Dowex 50 (H^+) resin in aqueous THF readily regenerated the aldehyde as its stable hydrate **115** (73%).[13] In the literature the free aldehyde **113** was obtained after azeotrope with benzene using a Dean-Stark apparatus.[13] Because of the toxicity of benzene and because, as reported,[13] prolonged azeotropic treatment with benzene leads to the appearance of a less polar product, an alternative method to obtain the free aldehyde **113** was addressed. If the hydrate **115** is treated with ethanol, the insoluble starting material goes quite rapidly into solution in the aldehyde form **113**. Evaporation of the ethanol leaves **113** as a

foam. It is important to point out that the aldehydic form of **113** always co-occurs with a small amount of hydrate **115**.

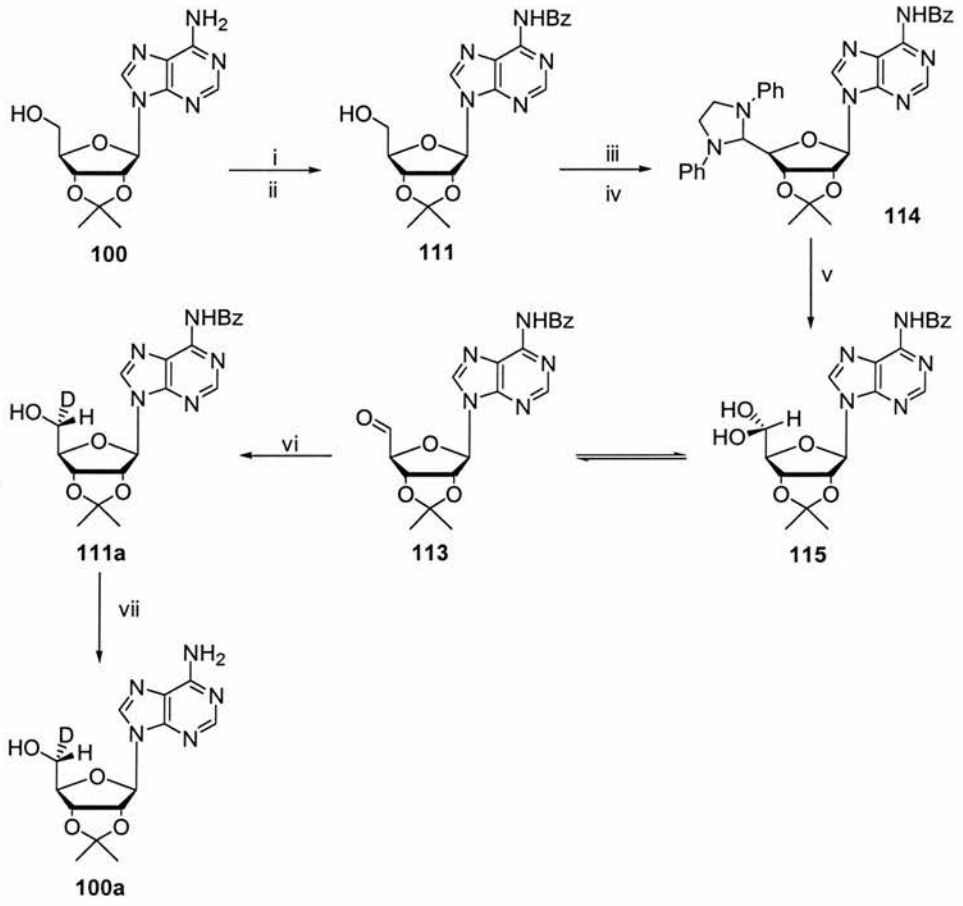

Scheme 4.5. i. BzCl/Pyr; ii. KOH/Pyr (50% over 2 step); iii. DMSO, DCC, dichloroacetic acid; iv. *N,N'*-Diphenyl-ethylene-diamine (78% over 2 step); v. Dowex H^+ (73%); vi. $LiAlD_4$ + t-amylalcohol/LiI -78 °C in THF for 3 h (36%); vii. NH_4OH/MeOH (1:1), 18 h (85%).

For the next step, the asymmetric reduction, a reaction with $NaBD_4$ at 0 °C was explored. The presence of the stereogenic centres in the ribose moiety of the adenosine influence the facial selectivity of aldehyde reduction. In the event the *ratio* between the two diastereoisomers was just 3:2 (optical purity at C-5' is *ca.* 20%) and was not sufficiently high for our stereochemical study. An asymmetric reduction of

aldehyde **113** has been reported by Dupre and Gaudemer[15], which gives a good *d.e.* of ~70%. This method involved the use of $LiAlD_4$ modified with a bulky chiral alcohol [(-)-isoborneol]. However this enantiomerically pure alcohol is quite an expensive material. An interesting method regarding the asymmetric reduction of ribose derivative aldehydes is reported in the literature, and it was also explored for the reduction of the nucleoside aldehyde **113**. Aldehyde **113** was conveniently reduced using $LiAlD_4$, modified with the bulky alcohol, *t*-amyl alcohol, and an excess of LiI (10-12 eq.) at -78 °C.[16] The lithium ion appears to play a crucial role in the asymmetric reduction,[17] probably because it co-ordinates between the carbonyl group and the oxygen atom of the ribose, directing the aluminium deuteride to attack preferentially the carbonyl group from the less hindered face. Some problems arose during the work up of this reaction. Addition of a 2N NaOH solution, to destroy excess $LiAlD_4$, led to formation of a gel that trapped the product and resulted in a poor recovery and a low overall yield (35%).

Figure 4.3 shows the ^{1}H-NMR spectra of (5'*R*)-[$^2H_1$]-N^6-benzoyl-2',3'-*O*-isopropylideneadenosine **111a** and the corresponding non labelled compound **111**. When one of the protons at C-5' is replaced by a deuterium atom, this results in a doublet for the major diastereoisomer and a separate doublet for the minor diastereoisomer. Furthermore the intensity of the upfield proton was much diminished: δ 3.77 (0.2 H, d, *J*2.5 Hz, 5'-H_a) and 3.91 (0.8 H, d, *J*2.0 Hz, 5'-H_b). It therefore appears that the diastereoisomeric purity of the reduction product **111a** is *ca.* 60% *de.*

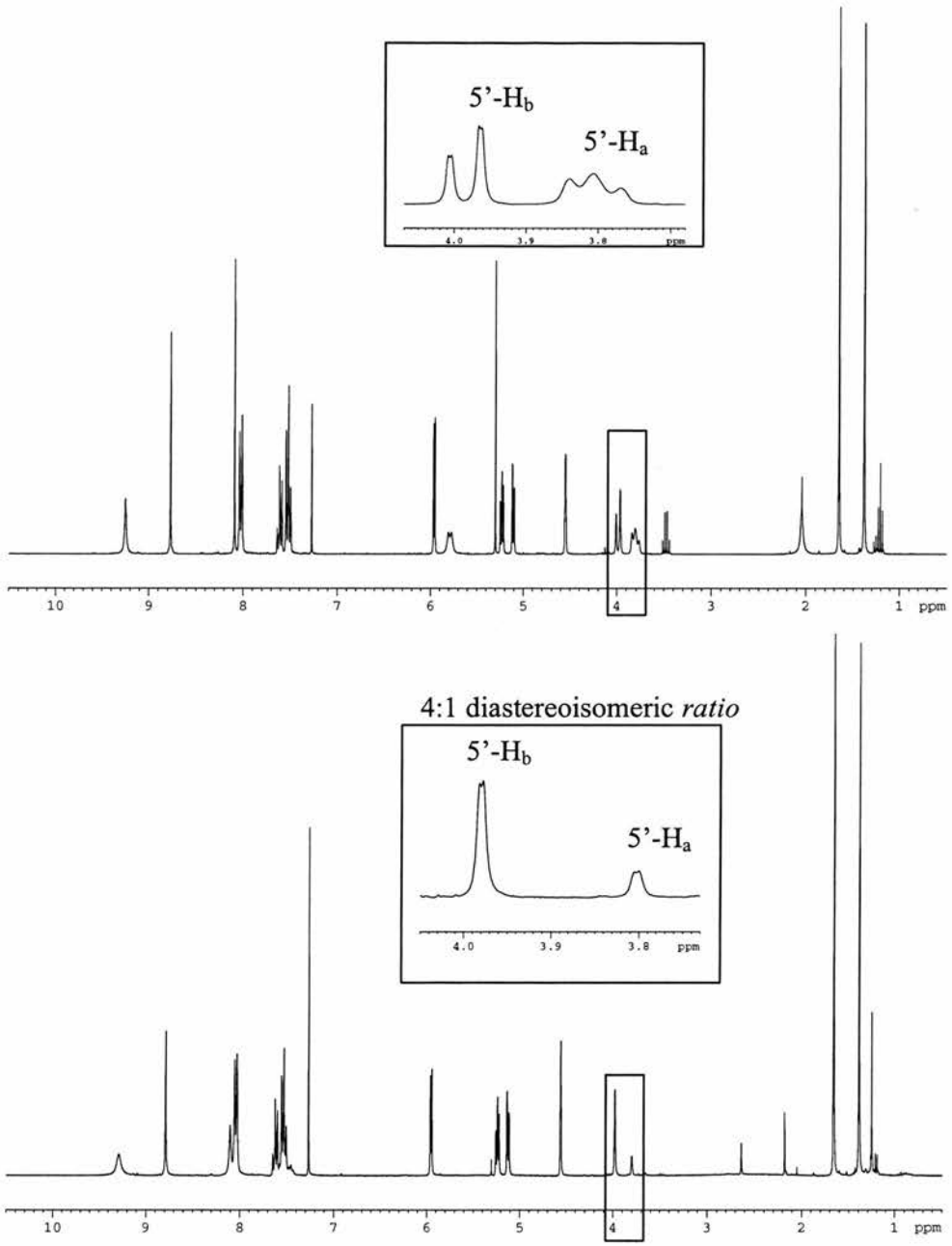

Figure 4.3. ^{1}H-NMR spectra of a) N^{6}-benzoyl-2',3'-*O*-isopropylideneadenosine **111** and b) (5'*R*)-[$^{2}H_{1}$]-N^{6}-benzoyl-2',3'-*O*-isopropylideneadenosine **111a** (4:1 diastereoisomeric *ratio*). The inserts highlight the signals for the protons at the C-5' position.

Comparison with the ^{1}H-NMR spectrum from the literature established that the major diastereoisomer has the (*R*)-configuration. This configuration was established

following the analysis of R. Parry in 1978.[18] They treated N^6-benzoyl-2',3'-*O*-isopropylideneadenosine **111** with methanesulphonyl chloride in pyridine to generate the 5'-mesyl derivative **116**. A stereospecific base induced elimination, mediated by treatment with potassium *t*-butoxide, gave **117** (Scheme 4.6).[11]

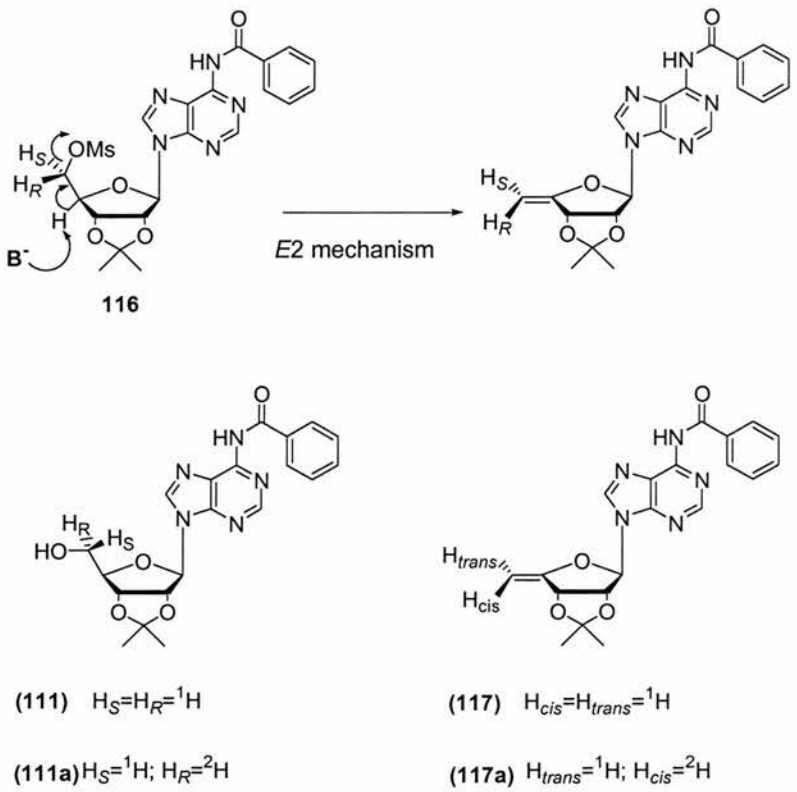

(111) $H_S=H_R={}^1H$

(111a) $H_S={}^1H$; $H_R={}^2H$

(117) $H_{cis}=H_{trans}={}^1H$

(117a) $H_{trans}={}^1H$; $H_{cis}={}^2H$

Scheme 4.6. R. Parry stereochemical analysis.[18]

The ^{1}H-NMR spectrum of **117** showed a doublet for one of the vinyl hydrogens at C-5' and a quartet for the other one at C-5': δ 4.53 (1 H, d, J_{gem} 2.5 Hz, 5-'H_a) and 4.67 (1 H, q, J_{gem} 2.5 Hz, $J_{3',5'b}$ 1 Hz, 5'-H_b). Since *trans* allylic coupling constants are generally larger than *cis* allylic coupling constants,[19] the C-5' hydrogen (5'-H_b), which appears as a quartet, can be assigned to the vinyl hydrogen which is *trans* to the C-3' hydrogen. Conversion of **111a** into **117a** and analysis of the ^{1}H-NMR spectrum of the latter compound showed a singlet for one vinyl hydrogen and a doublet for

the other. Furthermore, the intensity of the upfield proton was much diminished: δ 4.57 (0.15 H, s, H_{cis}) and 4.66 (0.85 H, d, $J_{3',5'b}$ 1.0 Hz, H_{trans}). Therefore, the deuterium in **117a** is concluded to be *cis* to C-3'. Since the formation of the deuterated olefin **117a** from the methane sulfonate almost certainly occurs *via* an *E2* elimination process, it follows that the deuteriated adenosine derivative **111a** has the (*R*)-configuration at C-5'.

In our case, the *ratio* between the two diastereoisomers of **111a** was 82:18 as deduced by ^{2}H-NMR analysis in a chiral liquid-crystalline solution generated from a chloroform solution of PBLG **109**, with a small amount of DMF (Figure 4.4).

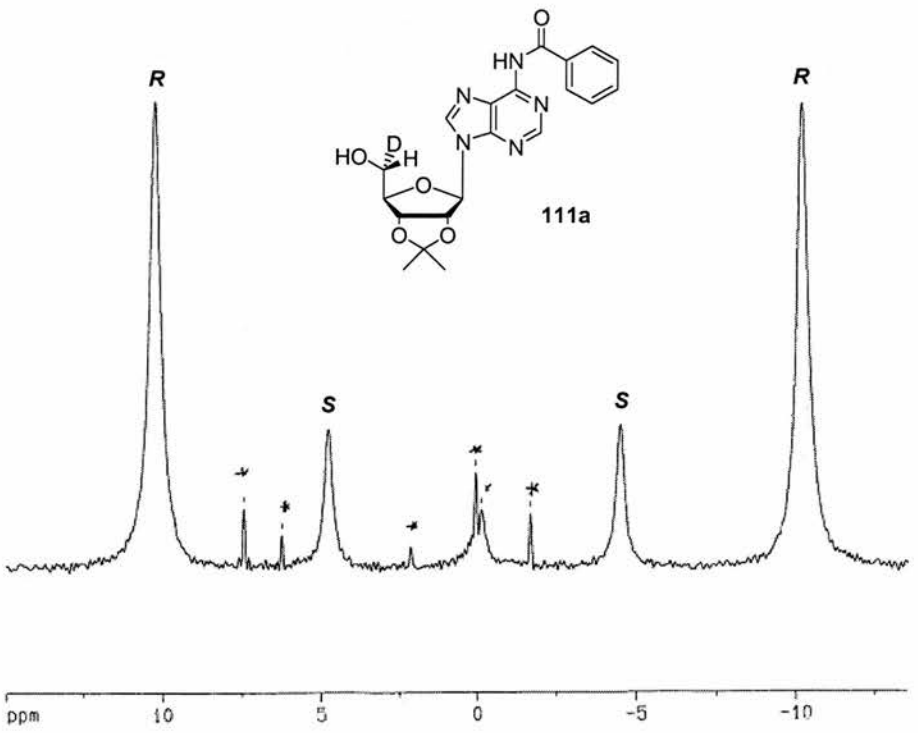

Figure 4.4. ^{2}H{^{1}H}-NMR spectrum of (5'*R*)-[$^2H_1$]-N^6-benzoyl-2',3'-*O*-isopropylideneadenosine **111a** (4:1 diastereoisomeric *ratio*) in a chiral liquid phase. The peaks labelled with asterisks highlight the natural abundance signals from the solvent (DMF).

The different ordering of the two diastereoisomers in the chiral system results in two sets of doublets in the ^{2}H-NMR spectrum: a large quadrupolar splitting (~1250 Hz) for the *R* diastereoisomer, and a smaller quadrupolar splitting (~570 Hz) for the *S* diastereoisomer.

After the asymmetric reduction, the benzoyl protecting group of **111a** was removed using 50% saturated methanolic ammonia,[11] and the product **100a** was purified by silica gel chromatography (85%). The acetonide protected adenosine **100a** was used as a precursor for the preparation of both (5'*S*)-[^{2}H$_1$]-FDA **60a** and (5'*R*)-[^{2}H$_1$]-ATP **59a**.

4.2.2 Preparation of (5'*S*)-[^{2}H$_1$]-5'-FDA 60a

The fluorination of the primary alcohol of **100a** was carried out by a slight modification of a route already established in our lab by Dr. S. L. Cobb (Scheme 4.7).[20] According to this strategy, (5'*R*)-[^{2}H$_1$]-2',3'-*O*-isopropylideneadenosine **100a** was converted initially into the mesylate derivative **116a** by treatment with methanesulfonyl chloride in pyridine.[21] The yield of this reaction was 73% after purification by silica gel chromatography. This mesylate was then treated with a TBAF solution (1 M in THF) in anhydrous acetonitrile. This resulted in a nucleophilic displacement reaction by fluoride ion to generate **118** with a chiral fluoromethyl group.

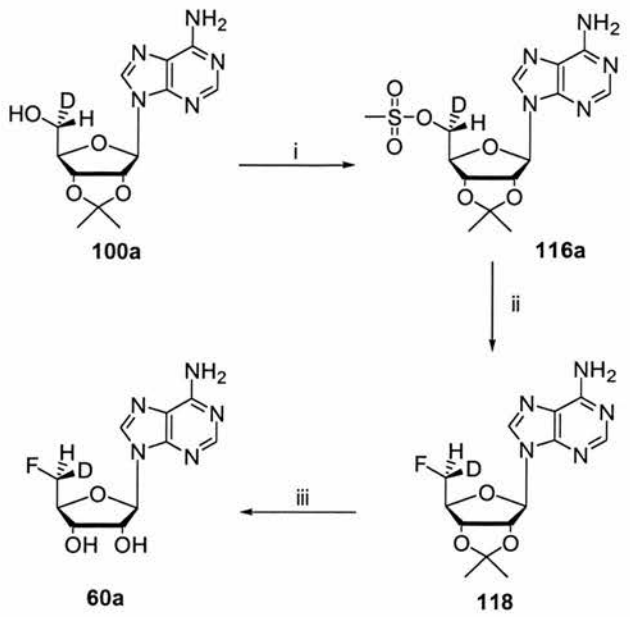

Scheme 4.7. i. MsCl/ Pyr 20 °C, 3 h (73%). ii. TBAF/CH_3CN reflux 3 h (35%); iii. TFA (90%), 30 min (81%).

It is assumed that the configuration at C-5' is inverted during the reaction consistent with fluoride displacement *via* a S_N2 process. The yield of this reaction is quite low (35%) and several factors contribute to the decreased efficiency of this nucleophilic substitution. Firstly, sulfonated precursors have been shown to be unstable due to a competing intramolecular reaction between N-3 of the adenine ring and C-5' to give cyclic nucleosides **119**.[22,23] This process is activated by the lone pair on the *exo*-cyclic N^6-nitrogen. Secondly, the fluoride ion of TBAF is a strong base and elimination products are formed from competing side reactions.

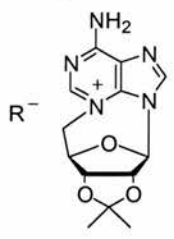

119

The $^{19}F\{^1H\}$-NMR spectrum of (5'*S*)-[$^2H_1$]-2',3'-*O*-isopropylidene-5'-fluorodeoxyadenosine **118** allowed discrimination between the two diastereoisomers, rendered non equivalent due to differential topic placement of deuterium at C-5'. Figure 4.5 reproduces this spectrum and shows two broad triplets (-229.31, 0.8 F, *J* 6.9; -229.29, 0.2 F, *J* 8.6) partly overlapped. The diastereomeric *ratio* is 4:1 in favour of the (*S*)-diastereoisomer as previously evaluated.

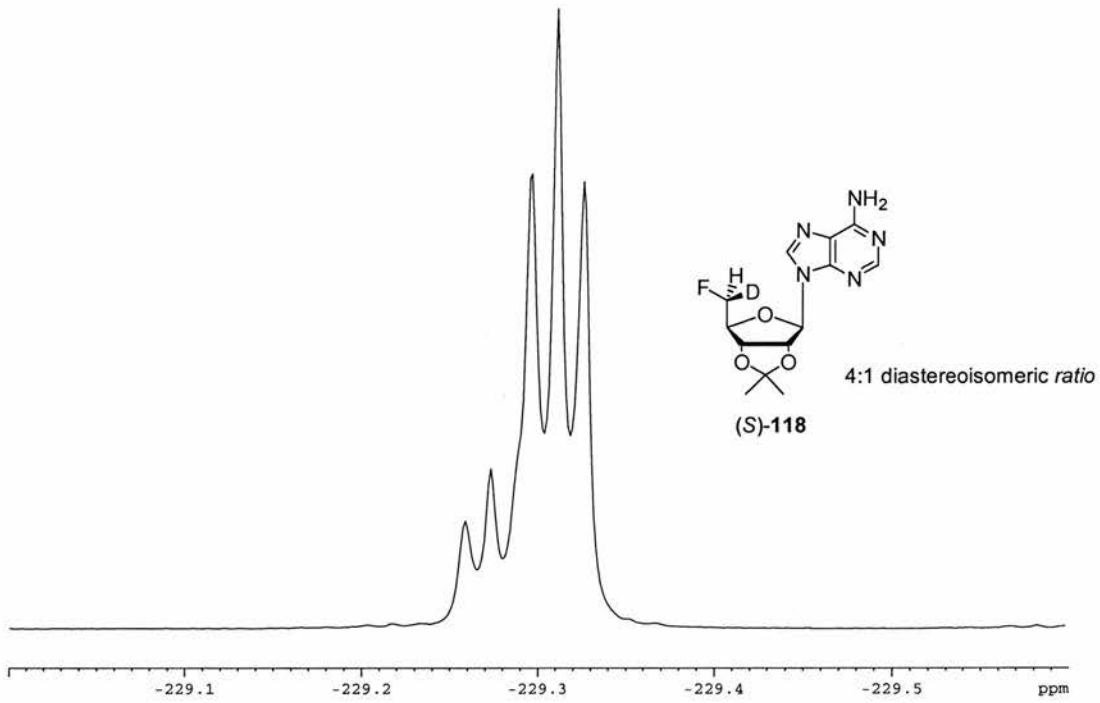

Figure 4.5. $^{19}F\{^1H\}$-NMR spectrum of (5'*S*)-[$^2H_1$]-2',3'-*O*-isopropylidene-5'-fluorodeoxyadenosine **118** (4:1 diastereoisomeric *ratio*). The two partly overlapping triplets originate from a F-D coupling.

The desired synthetic standard required for the stereochemical study, (5'*S*)-[$^2H_1$]-FDA **60a**, was finally obtained in good yield (~80%) and with a 60% *de* after removal of the acetonide group using trifluoroacetic acid-water (9:1).[13]

4.2.3 Chiral ^{2}H-NMR spectroscopy analysis of (5'*S*)-[$^2H_1$]-FDA 60a

(5'*S*)-[$^2H_1$]-FDA **60a** has been analysed by ^{2}H-NMR spectroscopy in a chiral liquid phase generated from a DMF solution of PBLG **109** [with a small amount of chloroform (Figure 4.6)] and used as a reference.

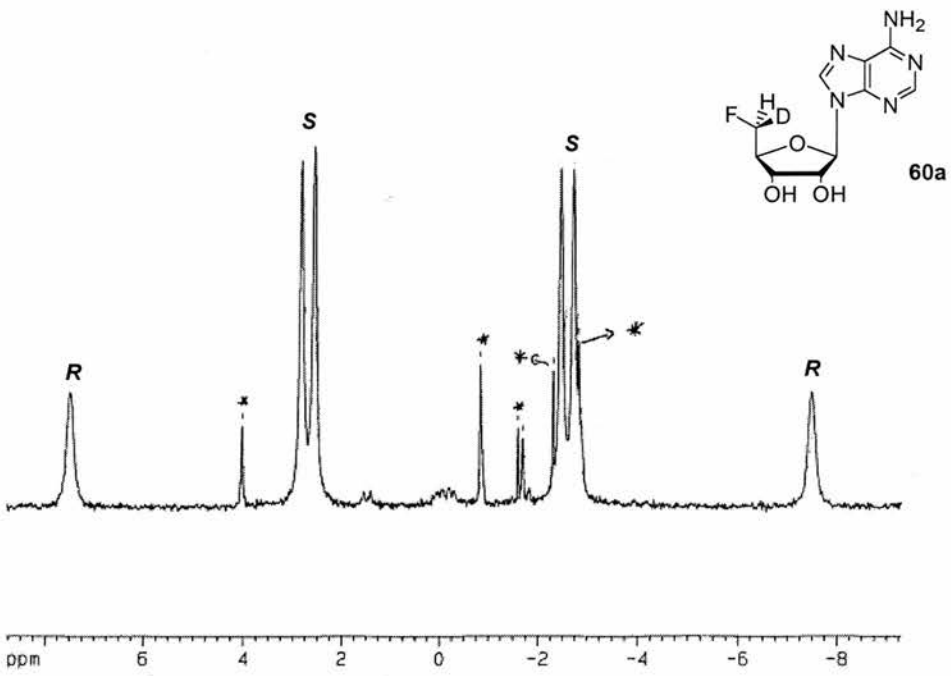

Figure 4.6. $^2H\{^1H\}$-NMR spectrum of synthetic (5'*S*)-[$^2H_1$]-FDA **60a** (4:1 diastereoisomeric *ratio*) in a chiral liquid phase. The peaks labelled with asterisks are the natural abundance signals from DMF.

The spectrum obtained shows a difference in the quadrupolar splitting of the (5'*R*)- and (5'*S*)-deuterium labelled compounds. The (5'*S*)-deuterium signal gives a doublet of doublets; the large splitting is the ^{2}H-quadrupolar splitting (~340 Hz) and the smaller splitting (~16 Hz) arises due to the total spin-spin coupling, T_{DF}, between the deuterium and the fluorine nuclei with $T_{DF}=2D_{DF} + J_{DF}$. In this expression, J_{DF} is the scalar coupling and D_{DF} is the dipolar coupling. The (5'*R*)-deuterium signal has the larger quadrupolar splitting (~950 Hz), but does not show any observable ^{2}H-^{19}F spin-

spin coupling. In this case the dipolar and scalar coupling are of opposite sign and that the dipolar coupling D_{DF} is about one half of the scalar coupling J_{DF}. The diastereoisomeric *ratio* obtained by integration is evaluated as 79:21 and is similar to that already established for **111a** after the asymmetric reduction, so there has been no change in the diastereoisomeric *ratio* during chemical fluorination. The spectrum also shows signals (labelled with asterisks) for natural abundance deuterium in DMF. These consist of three quadrupolar doublets centred on the chemical shifts of the three possible isotopomers of DMF, that is, the isotopomer in which the deuterium is at the aldehydic position and the two isotopomers in which the deuterium is on the non-equivalent methyl groups.

4.2.4 Synthesis of (5'*R*)-[^{2}H$_1$]-ATP 59a

For the synthesis of (5'*R*)-[^{2}H$_1$]-ATP **59a**, a method for adding the triphosphate group to the primary alcohol of (5'*R*)-[^{2}H$_1$]-2',3'-*O*-isopropylideneadenosine **100a** was explored, following a previously described protocol (Scheme 5).[24,25] Phosphorylation of the protected adenosine **100a** was easily achieved in a three step, one pot reaction. (5'*R*)-[^{2}H$_1$]-2',3'-*O*-Isopropylideneadenosine **100a**, dissolved in anhydrous pyridine and dioxane (or THF) and was treated initially with 2-chloro-4*H*-1,2,3-benzodioxaphosphorin-4-one to generate the cyclic phosphite **120**. The product was then treated with tributyl-ammonium pyrophosphate to afford the cyclic triphosphate derivative **121**.

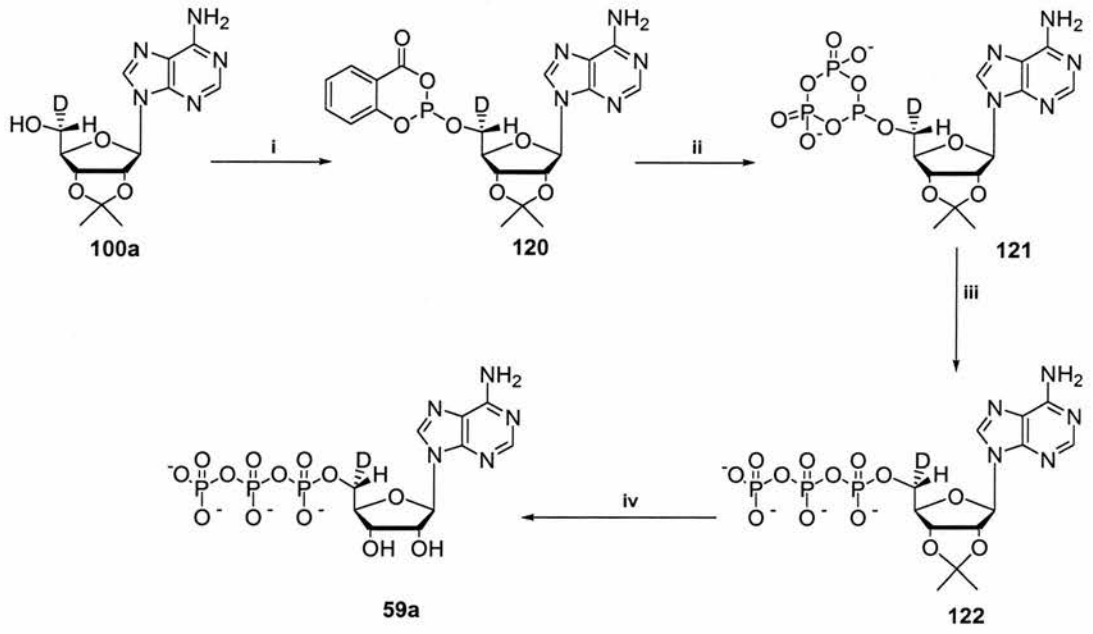

Scheme 4.8. i. 2-Chloro-4*H*-1,2,3-benzodioxaphosphorin-4-one in Dioxane (or THF)/Pyr, 15 min; ii. tributylammonium pyrophosphate in DMF/Et_3N, 30 min; iii. I_2 (1%) in Pyr/H_2O (98:2), 20 min; iv. TFA (25%), 30 min.

Finally oxidation using a solution of 1% iodine in pyridine/water (98:2) gave access to the desired triphosphate **122**. The conversion of **100a** to the corresponding triphosphate derivative does not involve any stereochemical inversion at C-5', therefore isopropylidene-ATP **122** was predominant in the (5'*R*)-configuration. The crude triphosphate-isopropylideneadenosine **122** was treated with an aq. solution of TFA (50%) to remove the acetonide group. After addition of aq. 0.1 N NaOH until pH 8.5, the solvent was evaporated to dryness *under vacuum*. The resultant residue was then treated with ethyl acetate and the product filtered. Analysis of the crude product by ^{31}P-NMR showed the presence of ATP **59a** as the major phosphorus containing compound.

4.2.5 Analysis of ATP 59a by biotransformation

Further confirmation of the synthesis of ATP **59a** was established by a biotransformation to organofluorine products. The product was incubated with a cell-free extract (CFE) from the bacterium *S. cattleya* plus L-methionine **61** and KF. After 3 h incubation the sample was heated to denature the proteins, and the proteins were then precipitated by centrifugation. Finally the supernatant was used for HPLC analysis. The chromatographic data showed the presence of the peak corresponding to 5'-FDI **63a**. This compound originates from a molecule of 5'-FDA **60b** by the *in situ* deaminase reaction (Scheme 4.9).

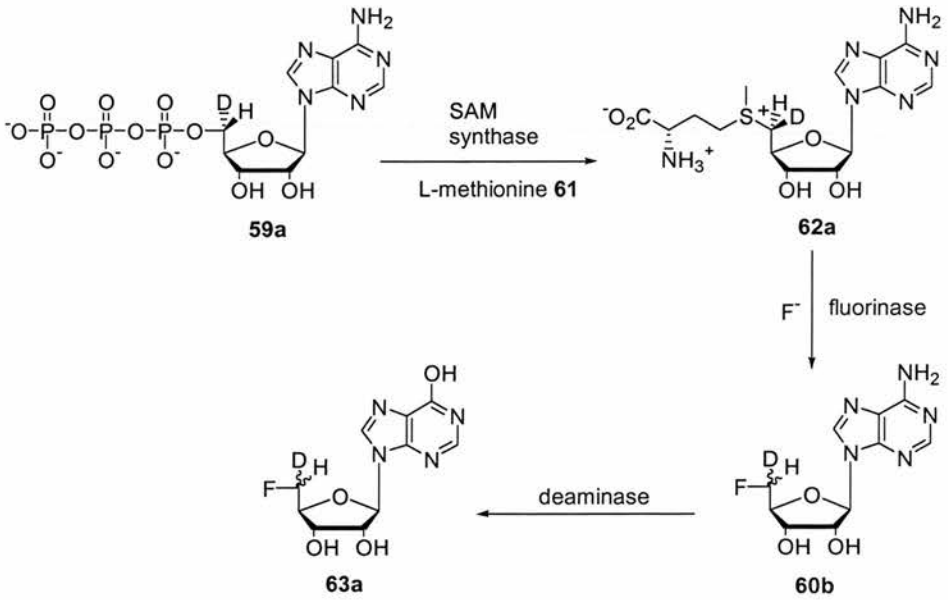

Scheme 4.9. Deamination of 5'-FDA **60b** to 5'-FDI **63a** in a CFE of *S. cattleya*.

The result of this experiment clearly confirmed the presence of ATP **59a**, as ATP **59a** was converted first to SAM **62a** by the enzyme L-methionine adenosyltransferase (SAM synthase), then to 5'-FDA **60b** by the fluorinase enzyme, as expected. Finally, a deaminase catalysed the conversion of 5'-FDA **60b** to 5'-FDI **63a** in the cell free

extract.

An important aspect revealed by this experiment was that the biochemical experiments could be carried out directly on the ATP product **59a**, taking advantage of the specificity of the enzymes. This avoided technically demanding purification procedures for the labelled (5'*R*)-[$^2H_1$]-ATP **59a**.

4.2.6 Assessing the stereochemistry of the fluorinase

With (5'*R*)-[$^2H_1$]-ATP **59a**, prepared as described in the previous paragraph, we were now in a position to study its enzymatic transformation and hence to access the stereochemistry of the fluorinase mechanism. Thus, **59a** was used for the next step involving the conversion of **59a** to SAM **62a** by SAM synthase.[4] This enzyme was partially purified from baker's yeast (*Saccharomyces cerevisae*). In the key experiment, (5'*R*)-[$^2H_1$]-ATP **59a** was treated with L-methionine **61**, Mg^{2+}, and KF in a coupled enzyme reaction with SAM synthase and the fluorinase. The resultant 5'-[$^2H_1$]-FDA **60b** was purified by semipreparative HPLC according to a standard protocol, and was finally analysed by ^{2}H-NMR spectroscopy under identical conditions to that used to analyse the synthetic reference. Figure 5 shows the $^2H\{^1H\}$-NMR spectra for 5'-[$^2H_1$]-FDA **60b** derived from the enzymatic reaction and that for the synthetic reference (5'*S*)-[$^2H_1$]-FDA **60a** (60% *de*), obtained in a PBLG **109** liquid-crystalline medium.

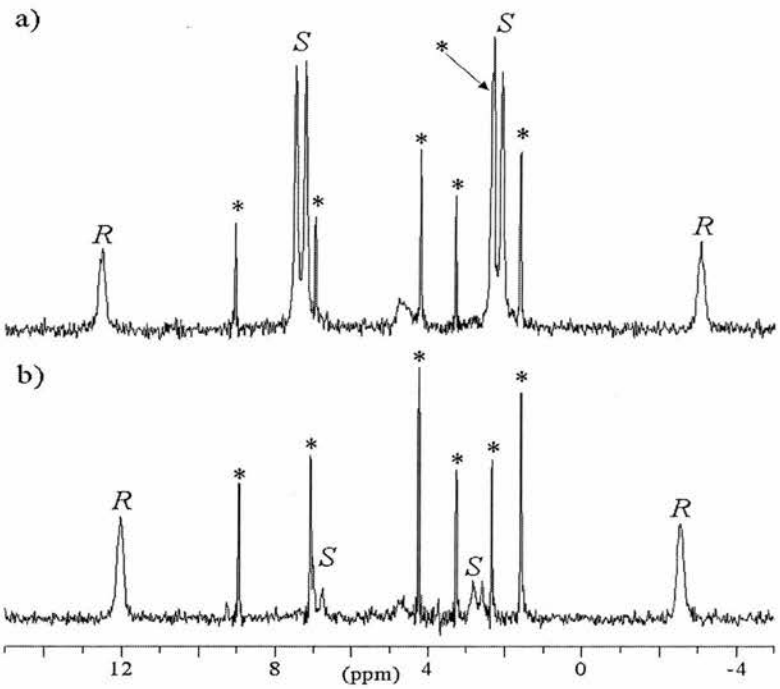

Figure 4.7. $^{2}H\{^{1}H\}$-NMR spectra of a) synthetic (5'*S*)-[$^{2}H_{1}$]-FDA **60a** (4:1 diastereoisomeric *ratio*) and b) (5'*R*)-[$^{2}H_{1}$]-FDA **60b** (4:1 diastereoisomeric *ratio*) prepared using coupled enzymatic reactions from (5'*R*)-[$^{2}H_{1}$]-ATP **59a**, in a chiral liquid-crystalline phase. The peaks labelled with asterisks are the natural abundance signals from DMF.

5'-[$^{2}H_{1}$]-FDA **60b** Derived from the coupled enzyme reaction shows the major diastereoisomer with the (*R*)-configuration at C-5', the same configuration as that in the starting material (5'*R*)-[$^{2}H_{1}$]-ATP **59a**. Taking into consideration that SAM synthase produced a molecule of [$^{2}H_{1}$]-SAM **62a** with the predominant (*S*)-configuration at C-5', the stereochemical outcome indicates that a second inversion of configuration was catalysed by the fluorination enzyme. The result is consistent with an S_N2 reaction mechanism operating during the fluorinase reaction and reinforces the earlier conclusion drawn after the whole-cell experiments with *S. cattleya*.[4]

It is interesting to note that not so many enzymatic reaction mechanisms operate by an S_N2 process. Furthermore, the nucleophilic substitution that occurs in

the fluorination enzyme is predicted to be a relatively difficult process. In fact, the nucleophilic substitution occurs at a β-oxygen (the ribose moiety) and in such cases the rate of S_N2 reactions slow down by up to an order of magnitude.[26] It was in fact reported that the nucleophilic substitution of bromine by iodide in a β-bromoethyl ether derivative proceeds 10 times slower than the displacement of bromine in an analogous system in which the oxygen is replaced by a carbon.[27]

inductive effect

Figure 4.8. The inductive effect (I-) exerted by the *beta*-oxygen disfavours the nucleophilic substitution.

This difference in reaction rate is clearly rationalised as the result of the inductive effect (I-) exerted by the oxygen through σ-bonds (Figure 4.8). The inductive effect in fact, strengthens the carbon-halogen bond rendering the nucleophilic substitution more difficult. Furthermore, the fluoride ion must become substantially desolvated to attack the C-5' of SAM **62**, a process predicted to require up to 400 kJ mol^{-1}, a high activation energy for the enzyme.[28] However, an interesting theoretical study carried out recently by Vincent and Hillier attempting to model the fluorinase reaction, has predicted that the solvated fluoride anion can be a good nucleophile.[29] Apparently, the charge on the organic substrate (S^+) is critical both in stabilizing the fluoride ion as it becomes partially desolvated, and in giving a reactant conformation appropriate for nucleophilic attack.

4.2.7 Conclusion

The availability of the over-expressed fluorination enzyme has allowed the stereochemical course of biological fluorination to be re-examined. The synthesis of isotopically labelled (5'*R*)-[$^2H_1$]-2',3'-*O*-isopropylideneadenosine **100a** (optical purity *ca* 60%) was crucial for this investigation. This compound was obtained by asymmetric reduction of the corresponding aldehyde **113**, using a different and less expensive reagent with respect to those described in the literature for the same reaction. (5'*R*)-[$^2H_1$]-2',3'-*O*-Isopropylideneadenosine **100a** has allowed the preparation of (5'*S*)-[$^2H_1$]-FDA **61a**, which was used as a stereochemical reference, and (5'*R*)-[$^2H_1$]-ATP **59a**, which was used as a precursor of (5'*R*)-[$^2H_1$]-FDA **60b** after treatment with SAM synthase and the fluorinase enzyme.

From this coupled enzymatic reaction, it emerged that the fluorination reaction takes place with an inversion of configuration consistent with an S_N2 mechanism. This result reinforces that obtained in a previous study, based on the whole-cell incubation of stereospecifically labelled precursors of the glycolytic pathway in *S. cattleya*, and is further supported by both X-ray structures of the fluorination enzyme with bound substrates and products, and a theoretical study.[30]

The stereochemical conclusions have been drawn through the use of $^2H_1$-NMR in a chiral liquid-crystalline medium. In such a solvent, enantiotopic or diastereotopic groups do not exhibit the same ordering properties due to the chirally orientated field. This differential ordering of enantiomers or diastereoisomers results in a difference that is often very large in the order-sensitive NMR interactions, such as quadrupolar splitting. The technique offers a powerful tool for examining the stereochemical

course of enzymatic reactions with appropriately labelled substrates.[4] The method developed in this research, is the only practical method available to date for assigning the absolute stereochemistry of chiral fluoromethyl (HDFC-) groups.

References Chapter 4

1. C. Schaffrath, S. L. Cobb and D. O'Hagan, *Angew. Chem. Int. Ed.*, 2002, **41**, 3913.

2. R. J. Parry and A. Minta, *J. Am. Chem. Soc.*, 1982, **104**, 871.

3. D. O'Hagan, R. J. M. Goss, A. Meddour and J. Courtieu, *J. Am. Chem. Soc.*, 2003, **125**, 379.

4. C. D. Cadicamo, J. Courtieu, H. Deng, A. Meddour and D. O'Hagan, *ChemBioChem.*, 2004, **5**, 685.

5. A. Abe and T. Yamasaki, *Macromolecules*, 1989, **22**, 2145.

6. I. Canet, J. Courtieu, A. Loewenstein, A. Meddour and J. M. Pechine, *J. Am. Chem. Soc.*, 1995, **117**, 6520.

7. V. Madiot, P. Lesot, D. Grée, J. Courtieu and R. Gree, *Chem. Commun.*, 2000, 169.

8. P. Lesot, D. Merlet, A. Loewenstein and J. Courtieu, *Tetrahedron: Asymmetry*, 1998, **9**, 1871.

9. T. Tamura, M. Wada, N. Esaki and K. Soda, *J. Bacteriol.*, 1995, **177**, 2265.

10. J. Neischalk, J. T. G. Hamilton, C. D. Murphy, D. B. Harper and D. O'Hagan, *Chem. Commun.*, 1997, 799.

11. I. D. Jenkis, J. P. H. Verheyden and J. G. Moffatt, *J. Am. Chem. Soc.*, 1976, **98**, 3346.

12. G. H. Jones and J. G. Moffatt, Abstracts, 158th National Meeting of the American Chemical Society, New York, N. Y., Sept 1969, CARB 16.

13. R. S. Ranganathan, G. H. Jones and J. G. Moffatt, *J. Org. Chem.*, 1974, **39**, 290.

14. K. E. Pfitzner and J. G. Moffatt, *J. Am. Chem. Soc.*, 1965, **87**, 5661.

15. M. Dupre and A. Gaudemer, *Tetrahedron Lett.*, 1978, **31**, 2783.

16. Y. Oogo, A. M. Ono and M. Kainosho, *Tetrahedron Lett.*, 1998, **39**, 2873.

17. Y. Mori, M. Kuhara, A. Takeuchi and M. Suzuki, *Tetrahedron Lett.*, 1988, **29**, 5422.

18. R. J. Parry, *Chem Commun.*, 1978, 294.

19. L. M. Jackman and S. Sternhell, "Applications of Nuclear Magnetic Resonance Spectroscopy in Organic Chemistry", 2nd edn., Pergamon, Oxford, 1969, 316.

20. S. L. Cobb, "The origin and metabolism of 5'-FDA in S. Cattleya", PhD Thesis, University of St. Andrews, 2005.

21. D. Giani and A. W. Johnson, *J. Chem. Soc., Perkin Trans. I*, 1982, 1197.

22. T. Ashton and P. J. Scammells, *Bioorg. & Med. Chem. Lett.*, 2005, **15**, 3361.

23. J. Uzawa and K. Anzai, *Can. J. Chem.*, 1985, **63**, 3537.

24. E. Trevisol, E. Defrancq, J. Lhomme, A. Laayoun and P. Cros, *Eur. J. Org. Chem.*, 2000, 211.

25. J. Ludwig and F. Eckstein, *J. Org. Chem.*, 1989, **54**, 631.

26. H. Deng, D. O'Hagan and C. Schaffrath, *Nat. Prod. Rep.*, 2004, **21**, 773.

27. F. B. Tutwiler and R. L. McKee, *J. Am. Chem. Soc.*, 1954, **76**, 6342.

28. C. J. Dong, F. L. Huang, H. Deng, C. Schaffrath, J. B. Spencer, D. O'Hagan and J. H. Naismith, *Nature*, 2004, **427**, 561.

29. M. A. Vincent and I. H. Hillier, *Chem. Commun.*, 2005, 5902.

30. H. M. Senn, D. O'Hagan and W. Thiel, *J. Am. Chem. Soc.*, 2005, **127**, 13643.

Chapter 5

Isoprenoids

5.1 Introduction

Isoprenoids are a large family of molecules present in all living organisms, and they play important roles in physiological and pathological processes.[1] The range of compounds that belong to this family includes essential metabolites (Figure 5.1), like sterols (membrane stabilizers, precursors for steroid hormones and bile acids in vertebrates), carotenoids (constituents of the photosynthetic apparatus in all the phototrophic organism), and quinones of electron transport chains (ubiquinone **124** and menaquinone **123** have long acyclic isoprenic chains).[2]

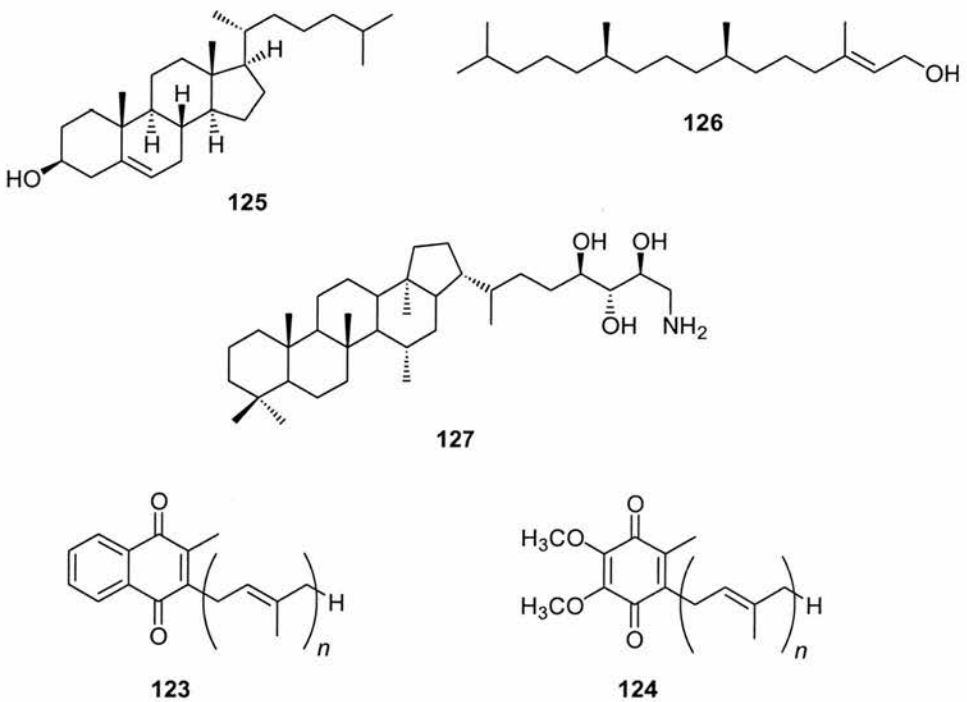

Figure 5.1. Examples of isoprenoids: Cholesterol (sterol) **125**, phytol **126**, aminobacteriohopanetriol **127**, ubiquinone **124**, menaquinone **123**.[2]

However the largest number of isoprenoids belongs to the secondary metabolites with less important roles such as terpenes from plant essential oils and resins.[2]

From a chemical viewpoint, these compounds are derived from the branched C_5 carbon skeleton of isoprene. The variety of compounds that belong to this family derive from the number of repetitions of this motif, cyclization reactions, rearrangements and oxidation of the carbon skeleton.[2] Isopentenyl diphosphate **17** and dimethylallyl diphosphate **18**, the two bio-equivalent forms of isoprene, are the building blocks for isoprenoids biosynthesis, as shown from studies with yeast and animal cells.[1]

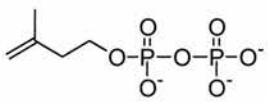

17

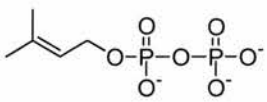

18

The biosynthesis of **17** and **18** occurs through two pathways: the mevalonate route in humans and the non-mevalonate route in certain bacteria, plastids of algae and chloroplasts of higher plants.[2]

5.2 Isoprenoids biosynthesis

5.2.1 The mevalonate route to isopentyl pyrophosphate 17 and dimethylallyl pyrophosphate 18

Early studies have shown that isopentenyl diphosphate **17** is biosynthesised from acetyl-CoA **128** via mevalonate **129**.[1,3] As shown in Scheme 5.1, in the first step two molecules of acetyl-CoA **128** condense to form acetoacetyl-CoA **130**.[4] This molecule then condenses with another molecule of acetyl-CoA **128** to give 3-hydroxy-3-methylglutaryl-CoA **131** (HMG-CoA) mediated by the HMG-CoA synthase. In the third step HGM-CoA **131** undergoes two NADPH-dependent reductions to produce (3*R*)-mevalonate **129**; this is the

rate-limiting step in steroid biosynthesis, and is catalyzed by a HGM-CoA reductase. In the following two steps, two molecules of ATP **59** are consumed to form the pyrophosphate unit at the 5-position, and another molecule of ATP **59** is needed in the third step to carry out a decarboxylation reaction to give isopentenyl pyrophosphate **17**. Dimethylallyl pyrophosphate **18** is produced by enzyme mediated isomerization of the double bond.

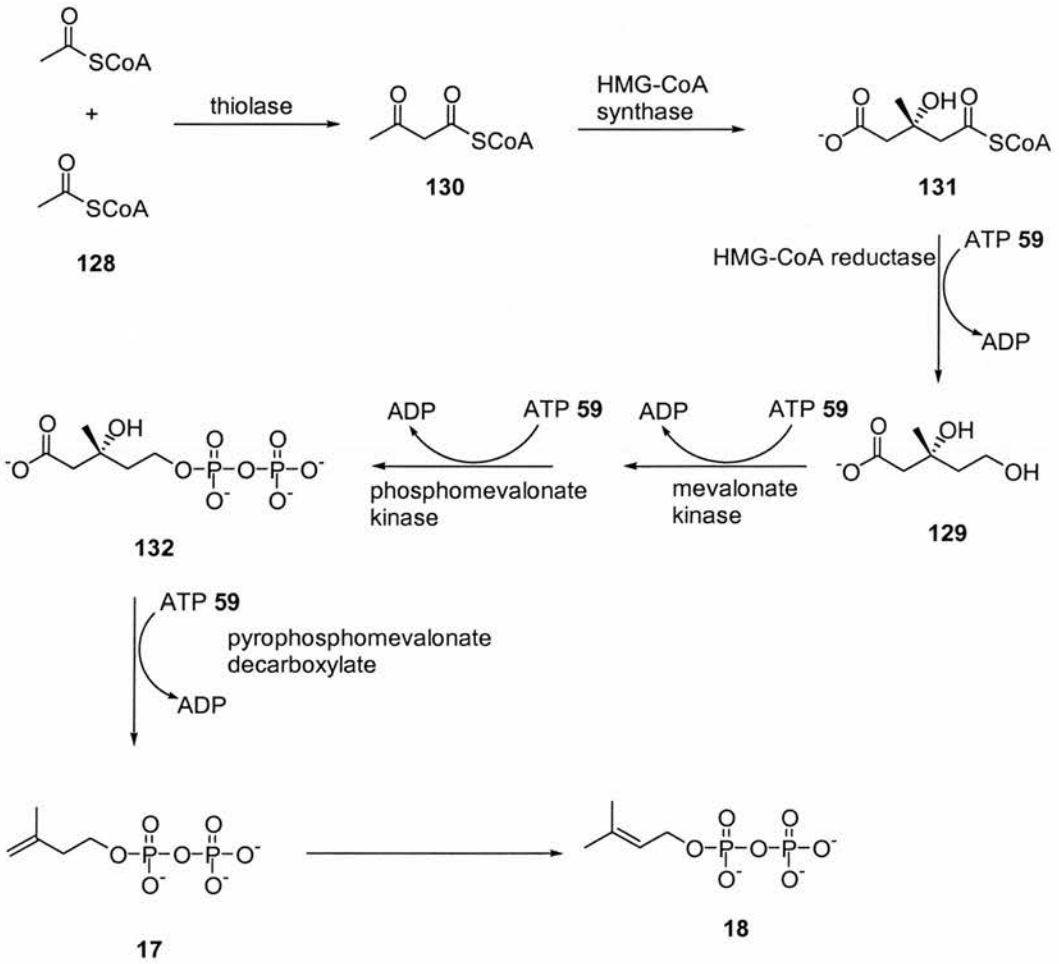

Scheme 5.1. The mevalonate pathway for the biosynthesis of isopentyl pyrophosphate **17** and dimethylallyl pyrophosphate **18**: acetyl-CoA **128**, acetoacetyl-CoA **130**, 3-hydroxy-3-methylglutaryl-CoA **131** (HMG-CoA), (3*R*)-mevalonate **129**, (3*R*)-diphosphomevalonate **132**.

5.2.2 The mevalonate-independent route to isopentyl pyrophosphate 17 and dimethylallyl pyrophosphate 18

In the early 90's, a second pathway for the formation of isopentyl pyrophosphate **17** and dimethylallyl pyrophosphate **18** was discovered after studies on bacterial hopanoid biosynthesis.[2,5] This route was found to operate in certain bacteria, plastids of plants and protozoa.[1,6] The biosynthetic pathway, which has been revealed over the last decade (Scheme 5.2), comprises of seven enzymatic steps. It begins with the condensation of pyruvate **45** and D-glyceraldehyde-3-phosphate **51** to form 1-deoxy-D-xylulose-5-phosphate **19** (DXP);[7] in the second step DXP **19** undergoes to a carbon skeletal rearrangement followed by reduction to form 2-*C*-methyl-D-erythritol-4-phosphate **20** (MEP); both of these reactions are catalyzed by the enzyme 1-deoxy-D-xylulose-5-phosphate reductoisomerase (DXR).[8] The resulting product MEP **20** is then converted into the cyclic diphosphate **136** *via* 4-diphosphocytidyl-2-*C*-methyl-D-erythritol **134** and its 2-phosphate **135** by three consecutive enzymatic reactions.[9,10,11] Intermediate **136** is then converted to 1-hydroxy-2-methyl-2-(E)-butenyl-4-diphosphate **137** by a reductive ring-opening reaction.[1] This product is the direct precursor of isopentyl pyrophosphate **17** and dimethylallyl pyrophosphate **18**.

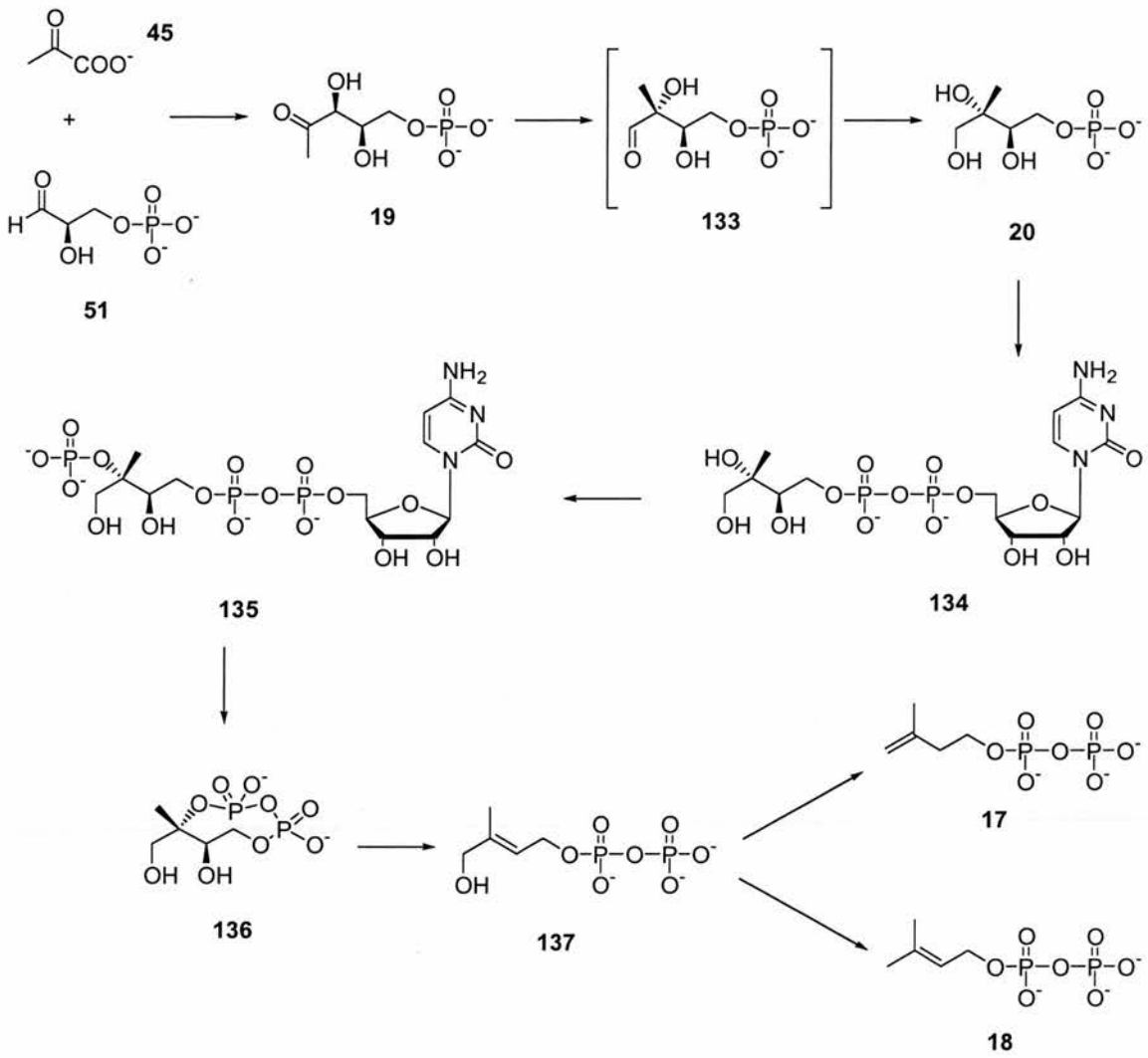

Scheme 5.2. The non-mevalonate pathway for the biosynthesis of isopentyl pyrophosphate **17** and dimethylallyl pyrophosphate **18**: pyruvate **45**, D-glyceraldehyde-3-phosphate **51**, 1-deoxy-D-xylulose 5-phosphate **19** (DXP), 2-*C*-methyl-D-erythrose-4-phosphate **133**, 2-*C*-methyl-D-erythritol 4-phosphate **20** (MEP), 4-diphosphocytidyl-2-*C*-methyl-D-erythritol **134**, 4-diphosphocytidyl-2-*C*-methyl-D-erythritol 2-phosphate **135**, 2-*C*-methyl-D-erythritol 2,4-cyclodiphosphate **136**, 1-hydroxy-2-methyl-2-(E)-butenyl-4-diphosphate **137**.

5.3 1-Deoxy-D-xylulose 5-phosphate reductoisomerase (DXR)

5.3.1 DXR characterization

The first committed intermediate of the non-mevalonate pathway is MEP **20**, which is formed from DXP **19** by the reductoisomerase (DXR). This rearrangement, as the name implies, requires two consecutive steps: an isomerization followed by a reduction. The *E. coli dxr* gene and the successful expression of the recombinant protein were first reported in 1998.[8,12] Incubation of the overexpressed protein with DXP **19** resulted in the production of MEP **20**, which revealed for the first time a single enzyme promoted isomerization and reduction steps.[12] The co-factor NADPH and a divalent cation (Mg^{2+}, Mn^{2+}, Co^{2+}) are required for the activity.[7] Based on the stereochemical features of the NADPH-dependent reduction, DXR is classified as a B dehydrogenase, delivering the *pro-S* hydride from NADPH.[13,14] The importance of this co-factor is not just related to the reduction step. Experiments have shown that in absence of NADPH, the isomerization step doesn't take place, and therefore it is crucial to the integrity of both steps.[15,16] It was suggested that NADPH first binds the DXR inducing a conformational change of the enzyme that allows the binding of DXP **19**. The divalent ion is required for the reduction step but whether it is required for the initial isomerization step has not been determined.[14] The $K_{m(DXP)}$ values vary from 42 to 720 μM depending on the enzyme source, while $K_{m(NADPH)}$ varies from 0.5 to 190 μM.[7] It has been shown that DXR are also capable of catalysing the reverse reaction, even though the equilibrium lies heavily in favour of the formation of MEP **20**.[7,15] The enzyme typically has a pH optimum between 7 and 8, operating most efficiently at 50-60 °C.[7]

5.3.2 The role of 2-*C*-methyl-D-erythrose 4-phosphate 133

By analogy to the biosynthesis of amino acids with branched side-chains, compound 2-*C*-methyl-D-erythrose-4-phosphate **133** was proposed as a transient intermediate of the isomerization, as a result of an α-ketol rearrangement of DXP **19**.[15,16] Attempts to detect this intermediate directly, however, were unsuccessful. The preparation of a sample of 2-*C*-methyl-D-erythrose-4-phosphate **133**, allowed researchers to show its important role as an intermediate in the DXR reaction. Not only it's conversion on MEP **20** was demonstrated, but when 2-*C*-methyl-D-erythrose-4-phosphate **133** was incubated with DXR in the presence of $NADP^+$, a small amount of DXP **19** was detected (~7%), indicating that methylerythrose-phosphate **133** is an intermediate in the enzymatic reaction.[7,15] It has also been shown that the methyl group of **133** is essential for turnover. When D-erythrose-4-phosphate **138** was incubated with DXR, neither reaction nor inhibition was detected.[15]

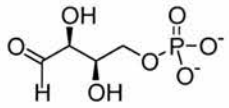

138

5.3.3 Crystal structures of DXR

The first crystal structure of DXR, obtained from *E. coli*, has been determined as the apo-enzyme without bound substrate (Figure 5.2).[18] Other crystal structures reported of *E. coli* DXR, have been determined as a binary complex with NADPH,[19] a complex with the fosmidomycin inhibitor **139** and manganese,[20] and a complex with biphosphonate inhibitors and manganese.[21] Also, Sweeney *et. al.* have determined a ternary complex of the wild-type and selenomethionine-labelled DXR with NADPH and fosmidomycin **139**, and a ternary complex of DXR/NADPH/DXP **19**.[14] The crystal structure of *Z. mobilis* DXR has recently

been reported as an apoenzyme and a binary complex with NADPH.[22] The structures revealed that DXR enzymes are homodimers with monomeric molecular weights of 42-45 kDa. Each monomer displays a V-like shape and it is composed of an amino-terminal dinucleotide binding domain, a carboxyl-terminal four-helix bundle domain, and a connective domain which is responsible for dimerization and harbors most of the active site.[18]

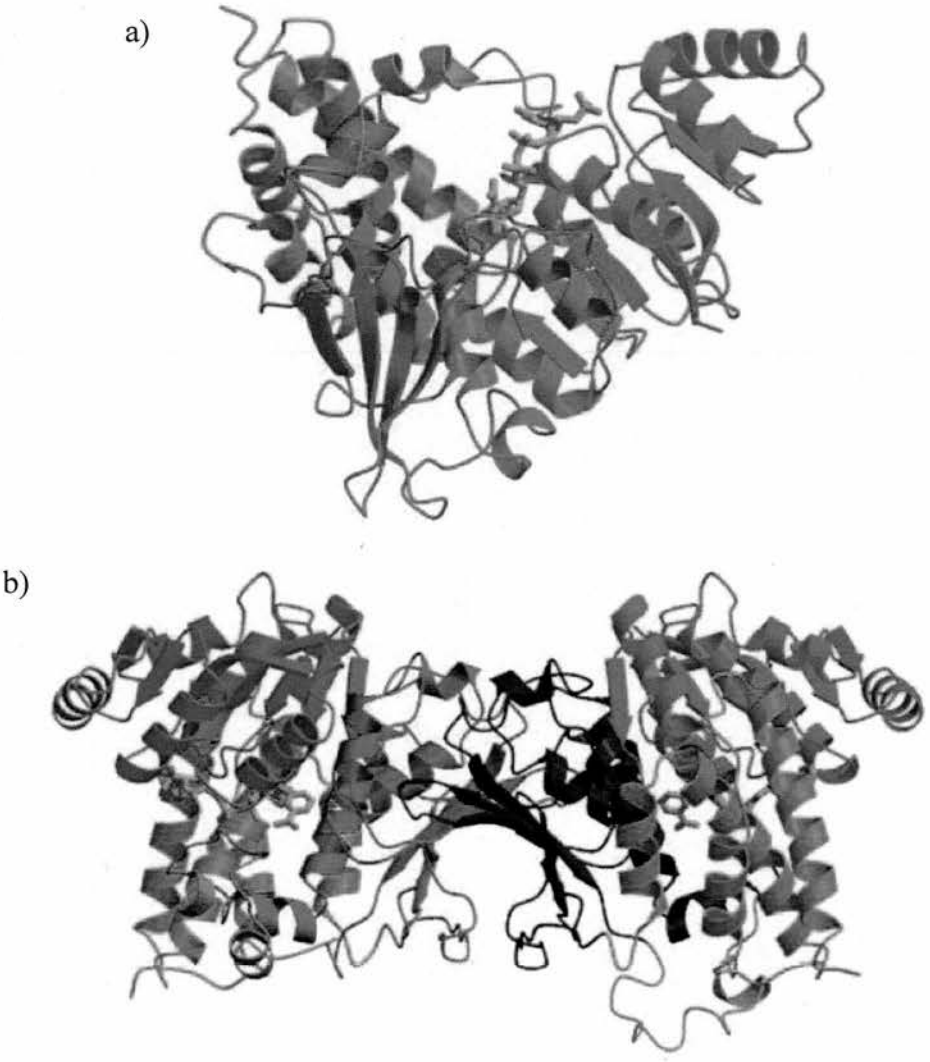

Figure 5.2. Crystal structure of apo-DXR: a) monomer; b) dimer. A molecule of NADPH (coloured yellow) has been modelled at the enzyme surface.[18]

The V-shaped protein displays an intrinsic flexibility, which reflects the necessity to undergo induced fit upon substrate binding. This has been confirmed in a ternary complex of selenomethionine-labelled DXR with NADPH and fosmidomycin **139**. The inhibitor binds to both the connective and C-terminal domains inducing a dramatic conformational change of the DXR enzyme, which has a closed conformation.[14] The flexible loop involving residues 206-216, which connects both domains, functioning as a "lid" over the active site shielding it from the solvent.[14] This results in a hydrophobic active site. Figure 5.3 shows the inhibitor fosmidomycin **139** binding at the surface of the enzyme.[14] Three crucial regions are evident for binding: a positively charged pocket, which binds the phosphonate moiety of fosmidomycin **139**, a hydrophobic region around the carbon backbone and an amphipathic region, which binds the hydroxamic acid function. In this crystallization study no divalent ion was observed, which was explained with a reduced metal-binding affinity of DXR under the low pH of the crystallization buffer (5.0).[14] The phosphonate of fosmidomycin **139** is not involved in any hydrogen bond with His-209, which appears to play an important role in the catalysis by binding the substrate in the correct orientation.[14,23] This interaction was instead observed in the crystal structure of DXR with DXP **19** (Figure 5.4).[14] The C-3 hydroxyl group of DXP **19** forms hydrogen bonds with Lys-125 and Glu-231, while the C-4 hydroxyl group is hydrogen bonded to Glu-125, Asn-227 and Lys-228. The co-factor NADPH adopts the correct conformation to deliver the *pro*-S hydrogen of C-4 of the nicotinamide ring to the carbonyl group of the proposed intermediate 2-C-methylerythrose-4-phosphate **133**.

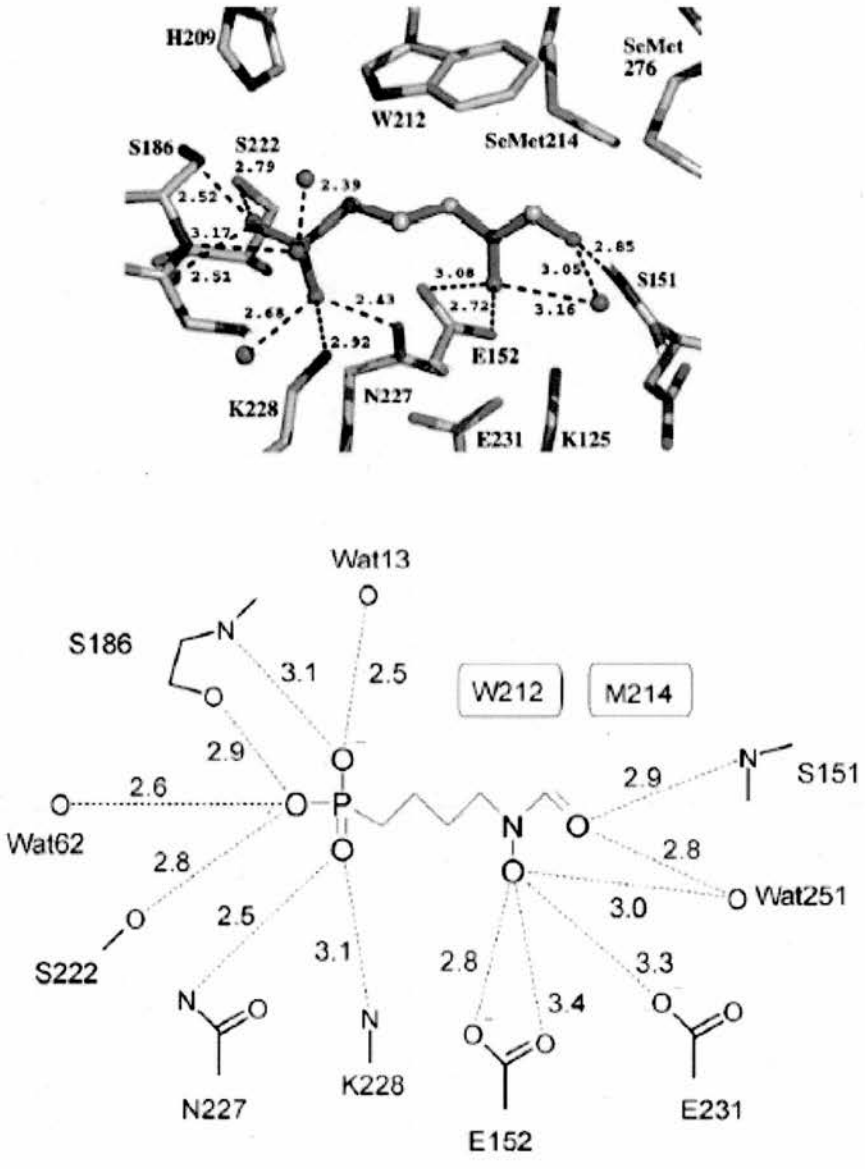

Figure 5.3. Representation of fosmidomycin **139** binding to DXR.[14]

The electron density of the ternary complex DXR, DXP **19** and NADPH showed the presence of a second diastereoisomer of **19** in the active site. This structure has not, however, advanced our understanding of the mechanism of the enzyme.

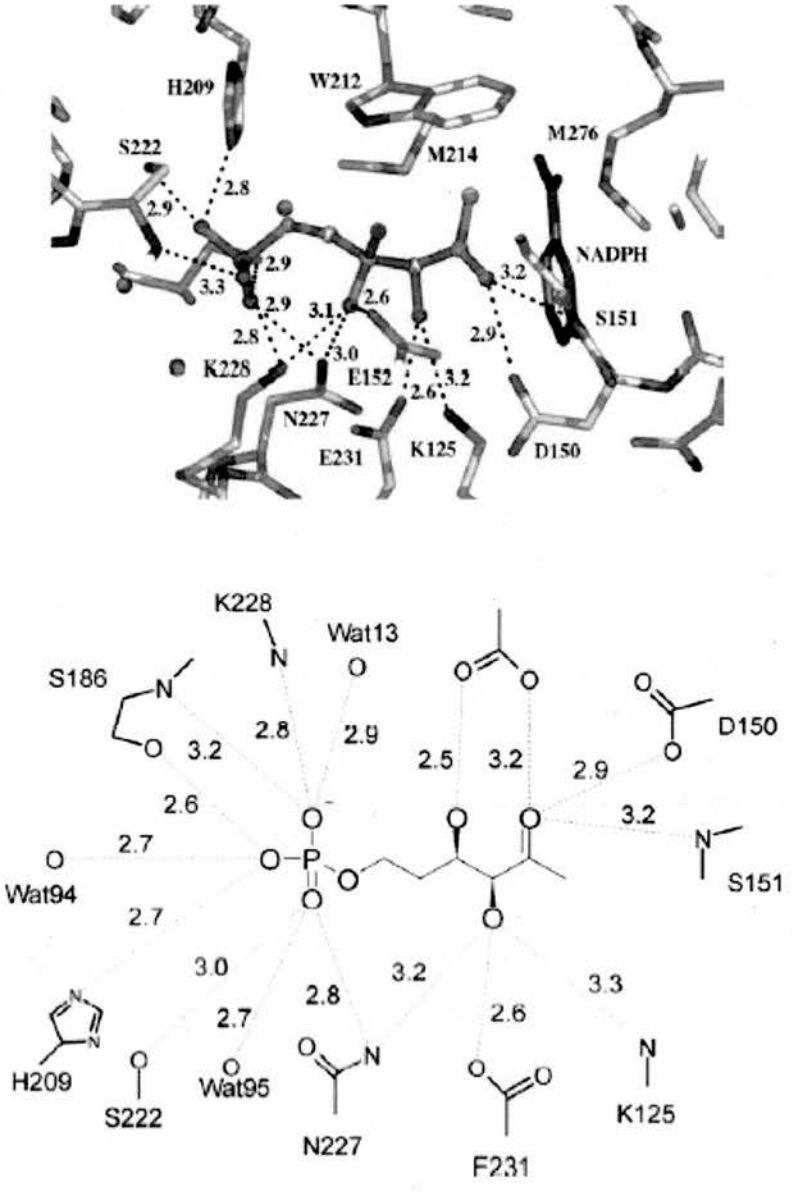

Figure 5.4. Representation of DXP **19** binding to DXR. The electron density showed the presence of a second diastereoisomer at C4 (hydroxyl depicted in green).[14]

5.3.4 Mechanism for the rearrangement of DXP 19 to 2-*C*-methyl-D-erythrose-4-phosphate 133

Three mechanisms for the rearrangement of 1-deoxy-D-xylulose-5-phosphate **19** to 2-*C*-methyl-D-erythrose-4-phosphate **133** have been proposed (Scheme 5.3).

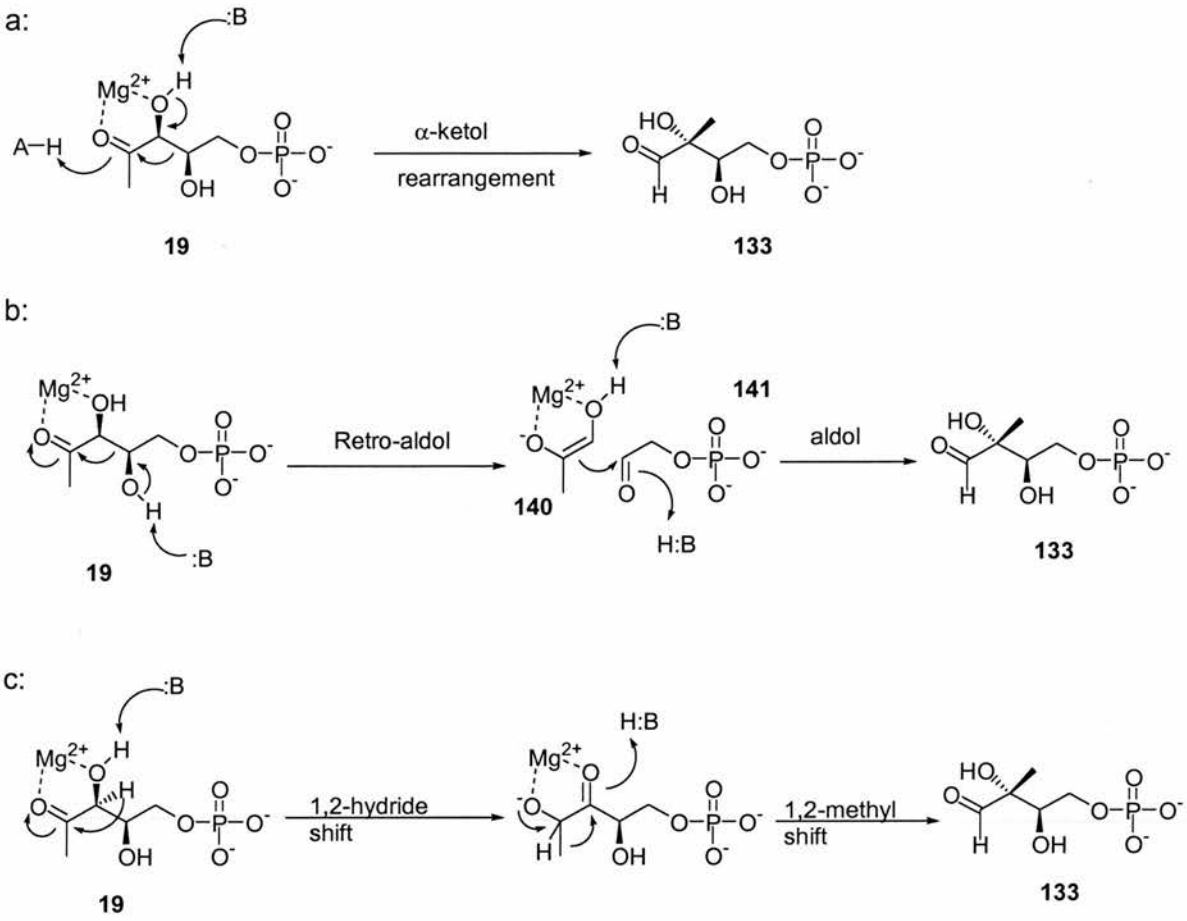

Scheme 5.3. Proposed mechanisms for DXR enzyme.[7]

The first mechanism proposed (a) is an α-ketol rearrangement.[15] This involves the deprotonation of the hydroxyl group at C-3 of DXP **19**, followed by migration of the phosphate-bearing C_2 subunit to afford the methylerythrose-phosphate **133**. This rearrangement has been proposed by analogy with the biosynthesis of the amino acids with branched side-chains (Scheme 5.4).[16]

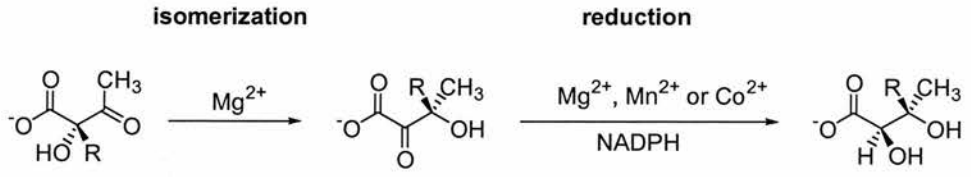

Two substrates:
R= -CH_3, (2*S*)-acetolactate
R= -CH_2CH_3, (2*S*)-2-aceto-2-hydroxybutyrate

Scheme 5.4. The α-ketol rearrangement reported for acetohydroxy acid isomeroreductase (AHIR).[16]

The second mechanism involves a retro-aldol/aldol reaction sequence.[15] The DXP **19** undergoes a retro-aldol reaction to give an enolate of hydroxyacetone **140** and glycolaldehyde phosphate **141**, then a consecutive aldol reaction affords **133**. A retroaldol/aldol sequence has been reported in the literature for the enzyme L-ribulose 5-phosphate 4 epimerase (Scheme 5.5).[24]

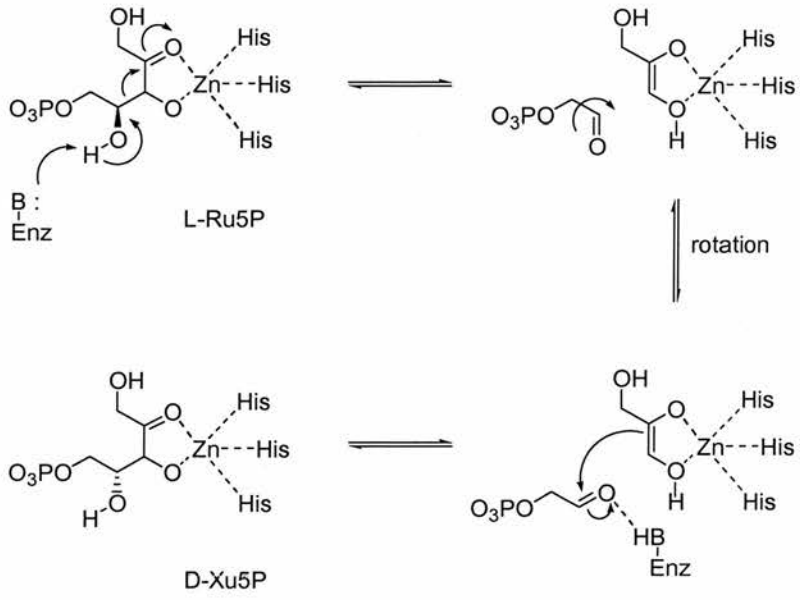

Scheme 5.5. The retroaldol/aldol rearrangement reported for L-ribulose 5-phosphate 4 epimerase.[24]

The last mechanism (c) consists on an hydride/methyl shift.[25] However, this has not received any experimental support and it is inconsistent with labelling studies.[26,27]

5.3.5 Exploring the mechanism. An α-ketol rearrangement or a retroaldol/aldol reaction?

Although the DXR enzyme has been widely studied and is fully characterised, it remains elusive whether catalysis is better described by the α-ketol rearrangement or by the retroaldol/aldol mechanism. In order to gain more insight into the mechanism of this enzyme, Liu and co-workers[28] explored the fluorinated substrate analogues **142**, **143** and **144** as potential substrates/inhibitors of *E. coli* DXR.

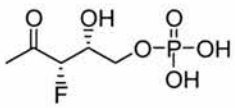

142

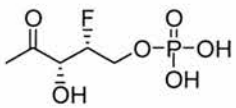

143

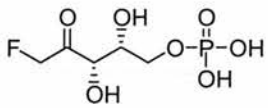

144

Compounds **142** and **143** were both inhibitors of DXR with Ki values of 0.44 mM and 0.73 mM, respectively. This result may be considered as preliminary evidence supporting that the retro-aldol/aldol sequence is operative.[28] In fact, according to this mechanism both hydroxyl groups are fundamental for the mechanism [C4-OH is involved in the retroaldol step, while C3-OH takes part to the aldol step (Scheme 5.3)] and their replacement with an inert fluorine atom causes inhibition. If the α-ketol rearrangement was operative, the inhibition might be expected only for compound **142**, as the fluorine atom replaces the C3-OH which is involved in the mechanism (Scheme 5.3). In compound **143** the fluorine atom replaces the C4-OH which is not involved in the rearrangement, and thus **143** would be expected to act as an alternate substrate. Compound **144** was a substrate for DXR with a k_{cat} value of 4.5 s^{-1}. This value is lower compared to the rate of the natural substrate, $k_{cat(DXP)}$

($21.3\ s^{-1}$). This result is also consistent with a retroaldol/aldol mechanism, as the fluorine at C-1 may stabilize the enolate anion intermediate **140** (deriving from the retroaldol step) reducing its capability as a nucleophile and, hence, suppressing the aldol step. A similar result with compound **144** was reported by C. D. Poulter and D. T. Fox.[29]

Rohmer and co-workers explored the mechanism of *E. coli* DXR with (3*S*)-hydroxypentan-2-one-5-phosphate **145**, which could potentially undergo the rearrangement by the α-ketol process, but would be incapable of participating in the retroaldol/aldol mechanism.[7,15] However, this compound acts as a mixed type inhibitor (K_i= 0.12 mM) and is not an alternate substrate.[15] This experiment, did not prove the mechanism, but was important because it showed the importance of the 3-hydroxyl group for the enzymatic process.

Other experiments exploring the retroaldol/aldol mechanism have been reported.[7,15] Detection of hydroxyacetone **140** was attempted by incubation of [1-^{13}C]-DXP and following the reaction by ^{13}C-NMR spectroscopy.[15] However no ^{13}C-NMR signal corresponding to the C-3 of hydroxyacetone **140** was observed. A further study was carried out by incubation of the enolate of hydroxyacetone **140** and glycolaldehyde phosphate **141** with DXR.[7] However, no evidence of MEP **20** was detected.

5.3.6 Inhibitors of DXR

Only few inhibitors have been reported for DXR. The antibacterial agent fosmidomycin **139** has been shown to be a mixed inhibitor of *E. coli* DXR with K_i of 38 nM.[30] Kinetic analysis with *E. coli* DXR revealed that fosmidomycin **139** initially binds with a relatively low affinity to the active site, thereby inducing alterations in the enzyme conformation that result in a significantly higher affinity for **139**.[17,31] Thus **139** undergoes quasi-irreversible

binding to the enzyme. Although fosmidomycin **139** was initially proposed to inhibit DXR by binding in a similar fashion to the intermediate aldehyde **133**, the crystal structures of *E. coli* DXR with fosmidomycin **139** bound provided evidence that **139** binds in a fashion more similar to the substrate DXP **19**.[7,14,20]

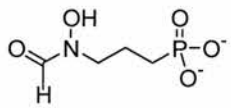

139

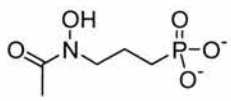

146

The discovery that **139** has significant antimalarial activity has increased the interest on finding new DXR inhibitors.[30,31,32] For its antimalarial activity, a combination of fosmidomycin **139** and clindamycin is currently employed for clinical studies in Gabon and Thailand.[31] The clear advantages of fosmidomycin **139** are its remarkably low toxicity (LD_{50} in rats (oral) ~12 g kg^{-1}) and its activity against multiresistant parasite strains.[31] Limitations arise from the short plasma half-life (~2.5 h) and the moderate absorption rate (~30%) as consequence of the low lipophilicity of the molecule.[31] The fosmidomycin derivative FR900098 **146**, showed approximately twice the antimalarial activity *in vitro* and in mice infected with *P. vinckei*.[31] The two fosmidomycin-like inhibitors **147** and **148** have recently been reported by Rohmer and co-workers.[33] These two compounds conserve the hydroxamate chelating moiety of **139**, but they differ in the connectivity as the nitrogen atom and the carbonyl group switched their relative position.

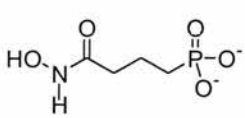

147

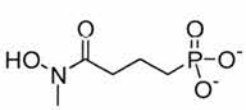

148

Both compounds showed a good inhibitory potency in the nM range, with **148** having similar Ki value compared to fosmidomicyn **139**. However, as far as antimicrobial activity

is concerned, DXR inhibitors **147** and **148** are less efficient against *E. coli* than fosmidomycin **139**.[33] Two DXP analogs lacking a hydroxyl group, [(3*S*)-hydroxypentan-2-one-5-phosphate **145** and (4*S*)-hydroxypentan-2-one-5-phosphate **149**], were also found to be inhibitors of *E. coli* DXR, but are less efficient than fosmidomycin **139**.[7,15] The 4-deoxy analog was 6.7-fold more potent than the 3-deoxy analog and both had values greater than the K_m for DXP **19**.[7,15]

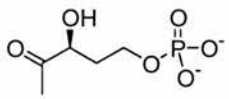

4-Deoxy-DXP **145**
Ki= 120 μM

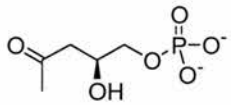

3-Deoxy-DXP **149**
Ki= 800 μM

The experiments with these two molecules showed the importance of the 3- and 4-hydroxyl groups for the rearrangement process. Proteau and co-workers[34] explored **145** and **149** and other compounds reported in Figure 5.5, as potential substrates/inhibitors for *Synechocystis* DXR.

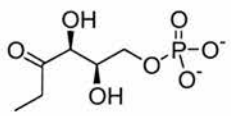

150
Ki= 630 μM

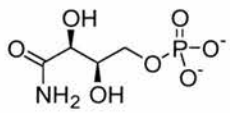

151
Ki= 90 μM

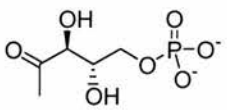

19a
Ki= 180 μM

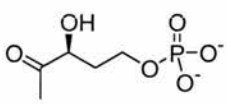

145
Ki= 30 μM

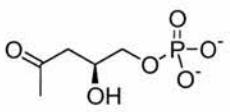

149
Ki= 150 μM

Figure 5.5. Examples of *Synechocystis* DXR inhibitors and relative Ki values reported by Proteau: 1-Methyl-DXP **150**, DXP carboxiamide **151**, 4-*epi*-DXP **19a**, 4-deoxy-DXP **145**, 3-deoxy-DXP **149**.[34]

These compounds were not alternate substrates, but proved to be weak inhibitors with Ki values in the μM range and hence not important from a clinical viewpoint. Interestingly, compounds **145** and **149** resulted as competitive inhibitors for *Synechocystis* DXR, while a mixed-type inhibition was found against *E. coli* DXR, as described above. The functional groups modified on DXP **19** structure (coloured) and their effect on enzyme activity are summarised on Table 5.1.

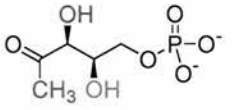

K_m= 170 μM

19

CH_3—	$\underline{NH_2}$— Amide less electrophilic than ketone, it causes inhibition; increased affinity for the active site ($Ki<K_{m(DXP)}$).	$\underline{CH_3CH_2}$— Big group, it causes inhibition; reduced affinity for the active site ($Ki>K_{m(DXP)}$).
3-OH	<u>3-Deoxy</u> 3-OH is essential for catalysis, but not for binding ($Ki\sim K_{m(DXP)}$).	
4-OH	<u>4-Deoxy</u> 4-OH is essential for catalysis, not critical for binding ($Ki<K_{m(DXP)}$).	<u>4-*epi*-DXP</u> Stereochemistry at C4 is not critical for binding, but essential for catalysis ($Ki<K_{m(DXP)}$).

Table 5.1.

Since the non-mevalonate pathway for the biosynthesis of isoprenoids appears to operate in bacteria, algae and plastids of plants, but not in humans, DXR enzymes become an excellent target for the development of new antibiotics. The use of the current crystal structures of *E. coli* DXR and *Z. mobilis* DXR, combined with mechanistic considerations opens up the opportunity to design new and more potent inhibitors for the DXR enzymes. The objective of this project is the preparation of potential inhibitors of the DXR enzyme based on mechanistic studies. In particular, we designed the synthetic target **152** based on the retroaldol/aldol mechanism. A full discussion on the preparation and evaluation of inhibitor **152** is reported in the next chapter.

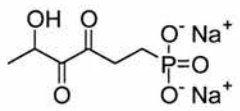

152

References Chapter 5

1. M. Gabrielsen, F. Rohdich, W. Eisenreich, T. Gräwert, S. Hecht, A. Bacher and W. N. Hunter, *Eur. J. Biochem.*, 2004, **271**, 3028.

2. M. Rohmer, *Nat. Prod. Rep.*, 1999, **16**, 565.

3. D. A. Bochar, J. A. Friesen, C. V. Stauffacher and V. W. Rodwell," Comprehensive Natural product Chemistry", Elsevier: Oxford, 1999, Vol. 2, pp. 15-44.

4. R. Garrett and C. Grisham, "Biochemistry", 2nd Ed. (1999), Saunders College Publishing

5. M. Rohmer, M. Knani, P. Simonin, B. Sutter and H. Sahm, *Biochem. J.*, 1993, **295**, 517.

6. W. Eisenreich, A. Bacher, G. Arigoni and F. Rohdich, *Cell. Mol. Life Sci.*, 2004, **61**, 1401.

7. P. J. Proteau, *Bioorg. Chem.*, 2004, **32**, 483.

8. S. Takahaschi, T. Kuzuyama, W. Watanabe and H. Seto, *Proc. Natl. Acad. Sci. USA*, 1998, **95**, 9879.

9. F. Rohdich, J. Wungsintaweekul, M. Fellermeier, S. Sagner, K. Kis, W. Eisenreich, A. Bacher and M. H. Zenk, *Proc. Natl. Acad. Sci. USA*, 1999, **96**, 11758.

10. H. Lüttgen, F. Rohdich, S. Herz, J. Wungsintaweekul, S. Hecht, C. A. Schuhr, M. Fellermeier, S. Sagner, M. H. Zenk, A. Bacher and W. Eisenreich, *Proc. Natl. Acad. Sci. USA*, 2000, **97**, 1062.

11. S. Herz, J. Wungsintaweekul, C. A. Schuhr, S. Hecht, H. Lüttgen, S. Sagner, M. Fellermeier, W. Eisenreich, M. H. Zenk, A. Bacher and F. Rohdich, *Proc. Natl. Acad. Sci. USA*, 1999, **96**, 2486.

12. T. Kuzuyama, S. Takahaschi, W. Watanabe and H. Seto, *Tetrahedron Lett.*, 1998, **38**, 4509.

13. P. J. Proteau, Y. H. Woo, R. T.Williamson and C. Phaosiri, *Org. Letters*, 1999, **1**, 921.

14. A. Mac Sweeney, R. Lange, R. P. M. Fernandes, H. Schulz, G. E. Dale, A. Douangamath, P. J. Proteau and C. Oefner, *J. Mol. Biol*, 2005, **345**, 115.

15. J.-F. Hoeffler, D. Tritsch, C. Grosdemange-Billiard and M. Rohmer, *Eur. J. Biochemistry*, 2002, **269**, 4446.

16. R. Dumas, V. Biou, F. Halgand, R. Douce and R. G. Duggleby, *Acc. Chem Res.*, 2001, **34**, 399.

17. A. T. Koppisch, D. T. Fox, B. S. J. Blagg and C. D. Poulter, *Biochemistry*, 2002, **41**, 236.

18. K. Reuter, S. Sanderbrand, H. Jomaa, J. Wiesner, I. Steinbrecer, E. Beck, M. Hints, G. Klebe and M. T. Stubbs, *J. Biol. Chem.*, 2002, **277**, 5378.

19. S. Yajima, T. Nonaka, T. Kuzuyama, H. Seto and K. Ohsawa, *J. Biochem. (Tokio)*, 2002, **131**, 313.

20. S. Steinbacher, J. Kaiser, W. Eisenreich, R. Hubert, A. Bacher and F. Rohdich, *J. Biol. Chem.*, 2003, **278**, 18401.

21. S. Yajima, K. Hara, J. M. Sanders, F Yin, K. Ohsawa, J. Wiesner, H. Jomaa and E. Oldfield, *J. Am. Chem. Soc.*, 2004, **126**, 10824.

22. S. Ricagno, S. Grolle, S. Bringer-Meyer, H. Sahm, Y. Lindqvist and G. Schneider, *Biochim. Biophys. Acta*, 2004, **1698**, 37.

23. T. Kuzuyama, S. Takahaschi, M. Takagi and H. Seto, *J. Biol. Chem.*, 2000, **275**, 19928.

24. A. E. Johnson and M. E. Tanner, *Biochemistry*, 1998, **43**, 37, 5746.

25. A. Argyrou and J. S. Blanchard, *Biochemistry*, 2004, **43**, 4375.

26. M. Rohmer, M. Seemann, S. Horbach, S. Bringer-Meyer and H. Sahm, *J. Am. Chem. Soc.*, 1996, **118**, 2564.

27. D. Arigoni, S. Sagner, C. Latzel, W. Eisenreich, A. Bacher and M. H. Zenk, *Proc. Natl. Acad. Sci. USA*, 1997, **94**, 10600.

28. A. Wong, J. W. Munos, V. Devasthali, K. A. Johnson and H. Liu, *Org. Lett.*, 2004, **6**, 3625.

29. D. T. Fox and C. D. Poulter, *J. Org. Chem.*, 2005, **70**, 1978.

30. T. Kuzuyama, T. Shimizu, S. Takahaschi and H. Seto, *Tetrahedron Lett.*, 1998, **39**, 7913.

31. J. Wiesner, R. Ortmann, H. Jomaa and M. Schlitzer, *Angew. Chem. Int. Ed.*, 2003, **42**, 5274.

32. H. Jomaa, J. Wiesner, S. Sanderbrand, B. Altincicek, C. Weidemeyer, M. Hintz, I. Turbachova, M. Eberl, J. Zeidler, H. K. Lichetenthaler, D. Soldati and E. Beck, *Science*, 1999, **285**, 1573.

33. L. Kuntz, D. Tritsch, C. Grosdemange-Billiard, A. Hemmerlin, A. Willem, T. Bach and M. Rohmer, *Biochem. J.*, 2005, **386**, 127.

34. C. Phaosiri and P. J. Proteau, *Bioorg. & Med. Chem. Lett.*, 2004, **14**, 5309.

Chapter 6

Synthesis of DXR inhibitors

6.1 Introduction

As described in the previous chapter, DXR is an important enzyme involved in the biosynthesis of isoprenoids *via* the non-mevalonate pathway. This enzyme catalyses a crucial step of the pathway in which the DXP substrate **19** undergoes to a skeletal rearrangement to form 2-*C*-methyl-D-erythrose-4-phosphate **133**, which is then reduced to MEP **20**. The two mechanisms currently considered plausible to explain such rearrangement have been described in chapter 5. These are summarised in Scheme 6.1.

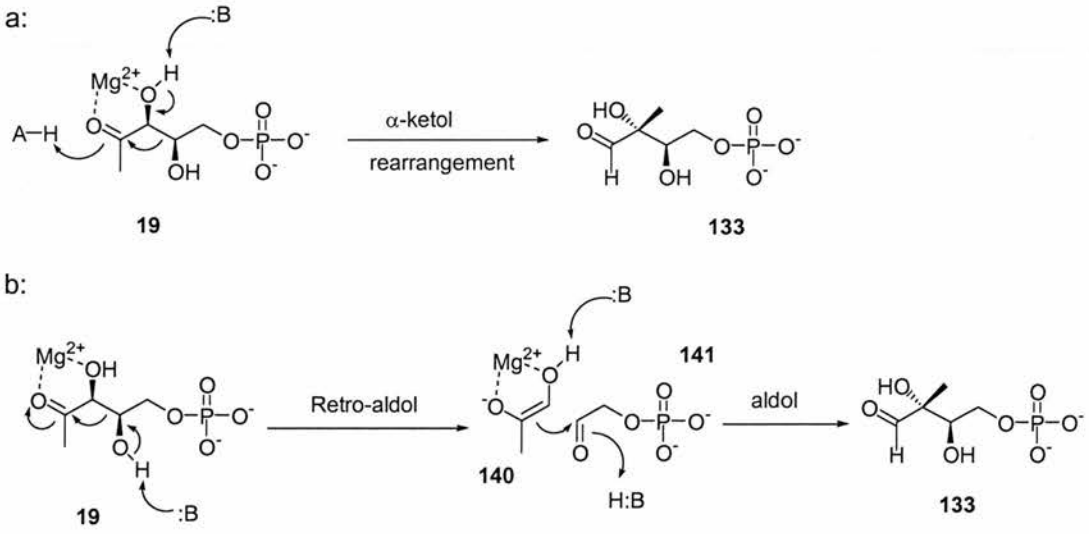

Scheme 6.1. The two mechanisms proposed for the rearrangement of DXP **19** to 2-*C*-methyl-D-erythrose-4-phosphate **133**: a) α-Ketol rearrangement; b) retroaldol/aldol sequence mechanism.

Mechanistic investigation of enzymes is an important aspect for the development of potential inhibitors. A common strategy is the design of inhibitors that act as transition state mimics. The transition state of the α-ketol rearrangement can be represented by a

cyclopropane ring bearing three hydroxyl moieties, while the transition state geometry of the retroaldol/aldol mechanism involves the formation of the enolate of hydroxyacetone **140** and glycolaldehyde phosphate **141** (Scheme 6.2).

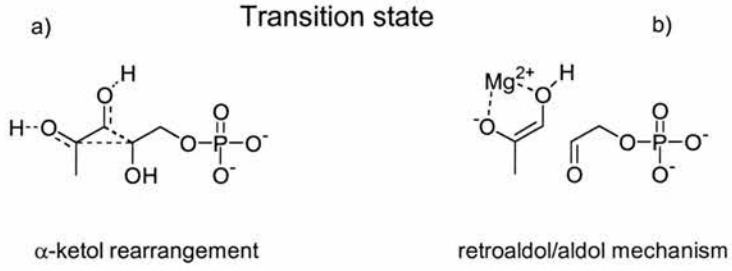

Scheme 6.2. Transition state or intermediates for a) the α-ketol rearrangement, and for b) the retroaldol/aldol mechanism involved in DXR enzymes.

Based on this concept, and considering mechanism (b) operating during the rearrangement of **19** to **133** mediated by the DXR enzyme, we identified the preparation of 5-hydroxy-3,4-dioxo-hexyl-phosphonate **152** as a potential DXR inhibitor.

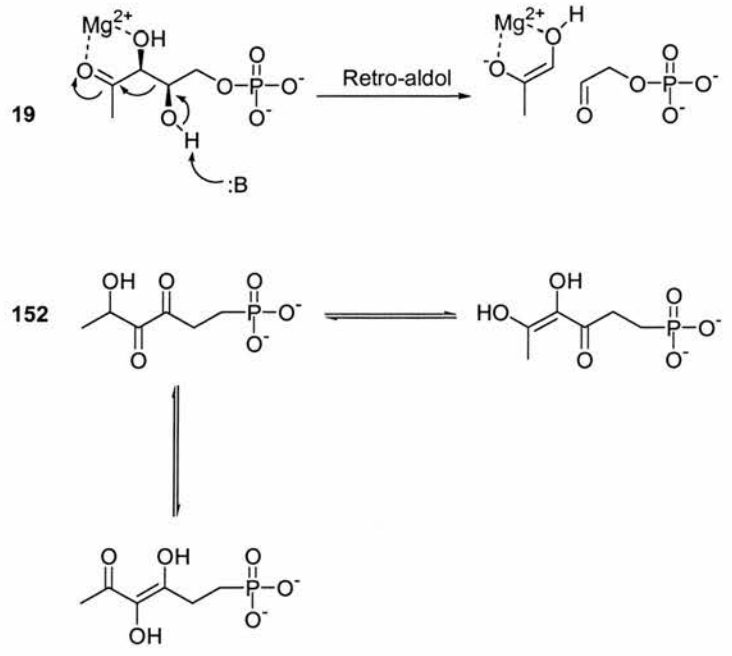

Scheme 6.3. 5-Hydroxy-3,4-dioxo-hexyl-phosphonate **152** as potential inhibitor of the DXR enzyme.

In fact, compound **152** can be represented by one of the tautomeric forms shown in Scheme 6.3, and one of them approximates the transition state geometry of the retroaldol/aldol mechanism.

6.2 Approach to the synthesis of 5-hydroxy-3,4-dioxo-hexyl-phosphonate 152: General remarks

The preparation of 5-hydroxy-3,4-dioxo-hexyl-phosphonate **152** emerged as a synthetic target. The compound contains a phosphonate moiety and an α-diketo functional group vicinal to an hydroxyl group.

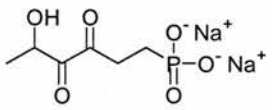

152

Furthermore, a search to identify structural motifs similar to our target molecule and in particular the diketone moiety, revealed that some of these compounds are characterised by high reactivity which makes them unstable and difficult to obtain in a pure form. Such systems exist often in an equilibrium with their hydrate forms, which can cause problems for characterization, e.g. the NMR's of these compounds are often complex. Probably, the compound in the literature that is most similar to **152** was reported by Page *et al.*[1] This compound, 3,5-dioxo-butyl-1-phosphonic acid **153**, was obtained from intermediate **154** after hydrolysis of its protecting groups (Scheme 6.4).

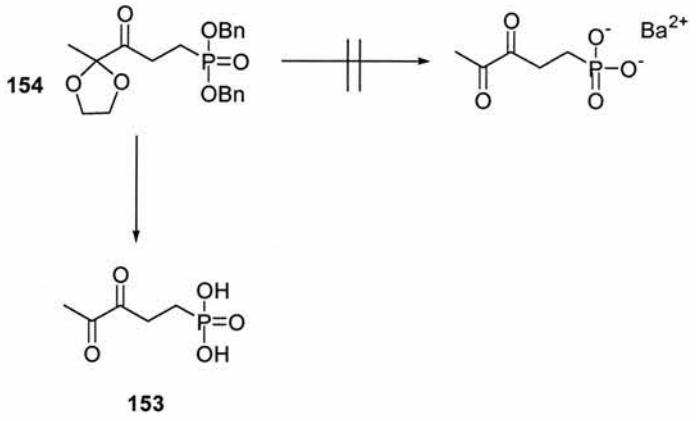

Scheme 6.4. 3,4-Dioxo-butyl-1-phosphonic acid **153** was shown to be unstable in the barium salt form.

Interestingly, when they tried to obtain the barium or the sodium salt of **153**, a complex mixture of products was formed. This result was unexpected as the salt was anticipated to be more stable then the free acid. It was tentatively suggested that the decomposition of the salt form of **153** could be due to possible reaction of the phosphonate anion with one of the two carbonyl groups.

A search of the literature for compounds containing the 1,2-diketo-3-hydroxyl motif **155**, did not reveal any clear examples of stable compounds.

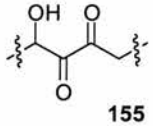

155

However, Ohloff *et al.*[2] described the synthesis of 2,5-dihydroxy-3,4-dioxohexane **156** by ozonolysis of the corresponding acetylene **157**. This product was never isolated in a pure form as it exists as a polymer most probably as a result of dimerization and then equilibrium to oligomers as shown in Scheme 6.5.

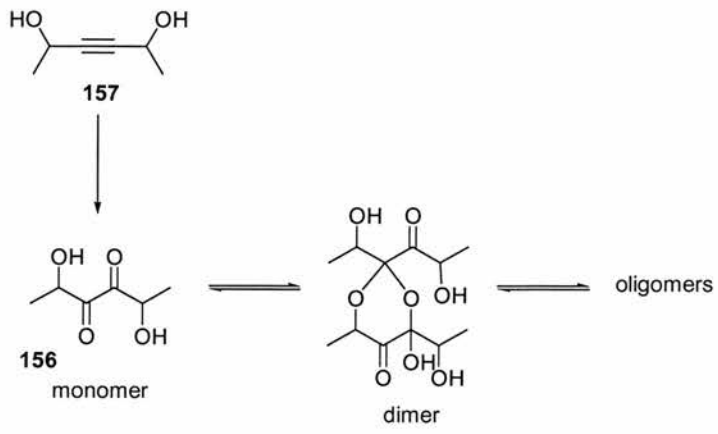

Scheme 6.5. 2,5-Dihydroxy-3,4-dioxoexane **156** was found to exist in a complex oligomeric form.

Similar synthetic problems have been reported during the synthesis of 4,5-dihydroxypentane-2,3-dione **158** (DPD).[3,4,5] This molecule, derived from the catabolism of SAH **70** in many bacteria, has been proposed as the penultimate precursor of AI-2, an important molecule involved in inter-species communication (*quorum sensing*) in the bacterial world.[3] DPD **158** has been reported to be susceptible to rearrangement and oligomerization.[3,4] The synthesis of **158** has been accomplished only recently by Janda and co-workers and the characterization was tentatively obtained from a dilute solution.[5] The characterization was complex as this molecule can exist as an equilibrium mixture of the linear and the two anomeric cyclised forms, and it becomes an even more complex scenario if the hydrate forms are considered (Scheme 6.6).

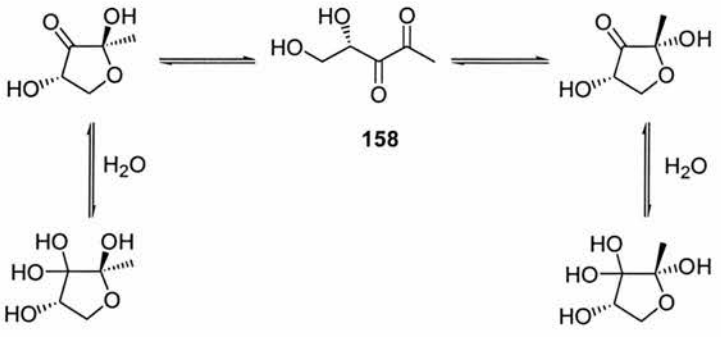

Scheme 6.6. Equilibrium of DPD **158** with its cyclic forms.

It is interesting to note that, in this work, the first synthetic attempt afforded **158** only as a mixture of products. Janda *et al.*[5] were able to isolate a constituent of the mixture in a crystalline form. The X-ray analysis of this material showed DPD **158** in a dimeric triacetal combination with one of its two anomeric furanone isomers (Figure 6.1).

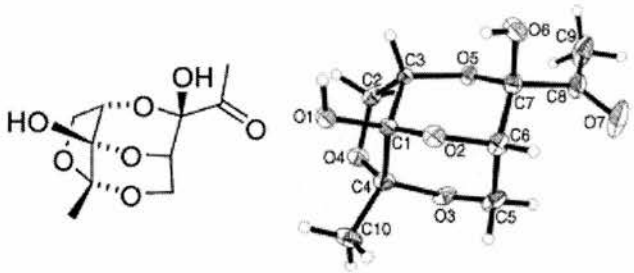

Figure 6.1. X-ray structure of a dimeric form of DPD **158** with one of its anomeric furanose isomers.[5]

This clearly shows the high reactivity and susceptibility to oligomerization of such systems.

At first glance the synthesis of a small molecule such as **152** may appear to be straightforward. However, the examples reported above suggested that potential problems could derive from the intrinsic reactivity of these systems. In the event, our synthesis proved successful but the nature of the final product was complex.

6.2.1 Retrosynthetic analysis

The strategy envisaged in our retrosynthesis of **152** called for the preparation of an acetylene (fragment **A**) as an immediate precursor for oxidation to the corresponding α-diketone (Scheme 6.7). We anticipated that the required acetylene could derive from the coupling of two fragments, an appropriate alkyne and a phosphonate, according to one of the three possible routes represented in Scheme 6.7.

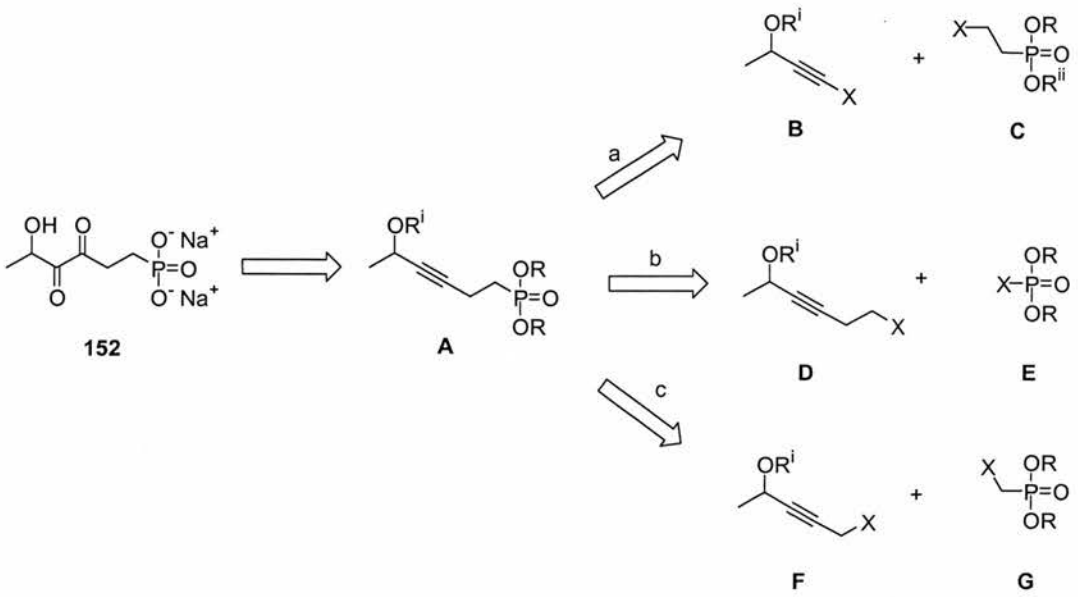

Scheme 6.7. Retrosynthetic analysis for the preparation of 5-hydroxy-3,4-dioxo-hexyl-phosphonate **152**.

Clearly, the success of the synthesis is dependent on a viable method for the preparation of fragment **A** and on an appropriate method of oxidation of the acetylene to the corresponding α-diketone.

6.2.2 Coupling of the acetylene and the phosphonate moieties

An examination of the literature was carried out to explore previous precedent for the coupling of an acetylene and a phosphonate, by the routes outlined in our retrosynthetic analysis. An interesting approach to generate fragment **A** could involve a β-metallated phosphonate generated by zinc-mediated methodology as described by Retherford *et al.* (Scheme 6.8).[6] According to this strategy, the β-bromophosphonates **159** are first treated with zinc dust to afford the alkylzinc bromide, which is transmetallated with copper to generate **160** after addition of the CuCN•2LiCl salt. The copper-zinc reagent **160** was found to react with various electrophiles in high yield. A coupling reaction with an alkynyl bromide derivative was also described, which made the route more attractive for our synthesis.

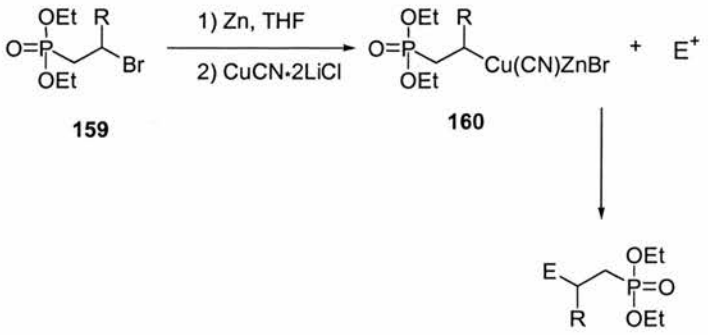

Scheme 6.8. Electrophilic addition to β-phosphonates *via* a copper-zing reagent **160**.[6]

An alternative strategy to carry out this step could involve the coupling of alkyl halide **161** with a trialkyl phosphite in a classical Michaelis-Arbuzov type reaction [route a)], or of course with the sodium salt of a dialkyl phosphite [route b)] (Scheme 6.9).[7]

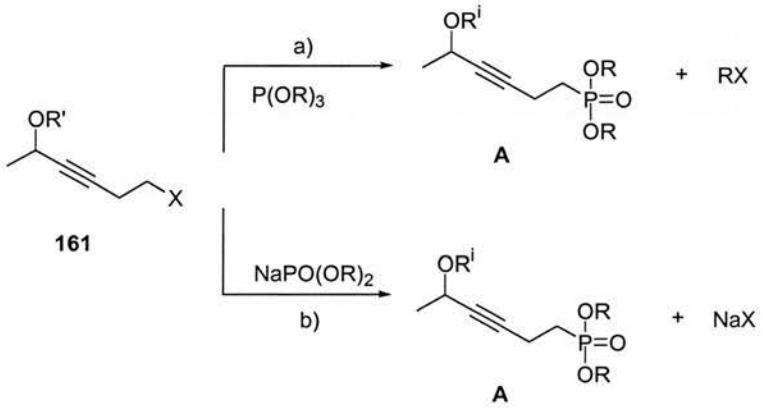

Scheme 6.9. Coupling reactions to generate the alkyne-phosphonate **A** *via* a) a Michaelis-Arbuzov reaction; or b) sodium salt of dialkyl phosphite.

The Michaelis-Arbuzov methodology usually requires high temperatures, while the use of the dialkyl phosphite usually allows the reaction to be carried out under milder conditions. An alternative procedure described in the literature involved a tosyl leaving group in place of the halide.[7,8] Interestingly, tosylates are quite reactive toward sodium diethyl phosphite as the order of reactivity with respect to alkyl chlorides and bromides was found to be Br > OTs > Cl.[8]

Finally, an approach for the preparation of the fragment **A** *via* route c) could involve an α-lithiated phosphonate. α-Metallated phosphonate reagents are versatile intermediates and have found numerous applications in organic synthesis.[6] In our case, it was anticipated that nucleophilic addition of the α-lithiated phosphonate (fragment **G**) to the acetylene derivative (fragment **F**) would be appropriate for a straightforward construction of the carbon skeleton.

6.2.3 Oxidation of a triple bond to the corresponding α-diketone

The oxidation of a triple bond to the corresponding α-diketone is widely described in the literature. Some of the reagents employed for this transformation are reported in Table 6.1.[2,9-18]

Oxidant	Ref.	Oxidant	Ref.
$KMnO_4$/aq. acetone	9	RuO_2/NaOCl or $NaIO_4/CCl_4/H_2O$	13
$OsO_4/KClO_3$	10	$(HMPA)MoO(O_2)_2/Hg(OAc)_2$	14
O_3/MeOH/Ph_3P	2	$Tl(NO_3)_3/HClO_4$	15
$RuCl_2(Ph_3P)_3$/PhIO	11	DMD or TFD	17
$RuO_2 \cdot 2H_2O$(cat.)/aq. NaCl CCl_4, 6.1-13.4 F	12	MTO/H_2O_2	18

Table 6.1. Some of the reagents commonly used to oxidise a triple bond to an α-diketone.[16]

All these reagents have proven effective in different reactions. Over-oxidation of the triple bond and/or the production of α,β-unsaturated ketones are often encountered in these oxidative transformations and these constitute a limitation of the methodology.[12,18] A method to overcome over-oxidation involves the indirect electro-oxidation with RuO_4 as a mediator.[12] RuO_2 is generally oxidised to RuO_4 *in situ* by the action of sodium

hypochlorite (NaOCl), sodium periodate ($NaIO_4$) or iodosylbenzene (PhIO).[11,13] The presence of these co-oxidants in the reaction mixture, however, could probably cause further oxidation of the substrate.[12] The *in situ* generation of RuO_4 by electrolysis in a two phase system (aq. buffered $NaCl/CCl_4$) was reported to reduce the formation of over-oxidised compounds. Dimethyl dioxirane (DMD), trifluoromethyl dioxirane (TFD) and methyltrioxorhenium-hydrogen peroxide (MTO/H_2O_2) can be also employed for this oxidation, but usually they give a more complex mixture of products depending on the nature of the substrate and the reaction conditions.[17,18] Of all the reagents reported in Table 1, the metal peroxide complex hexamethylphosphoramido molybdenum (VI) oxide diperoxide [$(HMPA)MoO(O_2)_2$] in the presence of $Hg(OAc)_2$, is the only one that does not require strictly controlled conditions to afford the α-diketones and generally products are generated in good yields.[14] It has also been described as an effective reagent for the oxidation of terminal alkynes to the corresponding α-oxoaldehydes.[14]

In our case, in order to establish the right conditions for the oxidation of a triple bond system adjacent to a protected hydroxyl group, the reaction procedures were first applied to a model compound.

6.3 Oxidation of a model system

2-(*tert*-Butyldiphenylsilanoyloxy)-oct-3-yne **162** was chosen as an appropriate model compound. It could be prepared in just two steps and involved an inexpensive starting material (Scheme 6.10). The synthesis commenced with hexyne **163**. Treatment of **163** with BuLi, followed by addition of acetaldehyde **57**, generated 2-hydroxyoct-3-yne **164** after work up and in a good yield (~62%).[19,20]

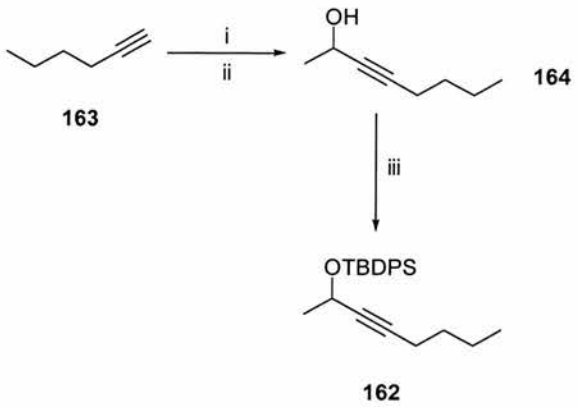

Scheme 6.10. i. BuLi, THF; ii. acetaldehyde **57** (~62%); iii. TBDPS-Cl, Pyr/THF/$AgNO_3$ (70%).

The hydroxyl group of alcohol **164** was then protected as a silyl ether derivative by treatment with TBDPS-Cl in DCM/Pyr and in the presence of $AgNO_3$.[21] $AgNO_3$ is generally used to improve the regioselectivity of silyl protection of alcohols, but has also been shown to increase the rate of silylation.[21,22] Thus, **162** was obtained in just 3 h in 70% yield.

With this compound in hand, we were in the position to investigate the oxidation of the triple bond to the corresponding α-diketone. Ozonolysis methodology was initially explored (Scheme 6.11).[2] Alkyne **162** was dissolved in methanol and treated with ozone gas for 40 min at ~ -20 °C. Triphenylphosphine was then added to quench peroxides and the product was purified by silica gel chromatography. This gave a yellow oil that corresponded to the α-diketo compound **165** as established by ^{1}H- and ^{13}C-NMR and ES-MS analyses. The yield was also excellent (80%), and therefore alternative oxidation conditions were not explored.

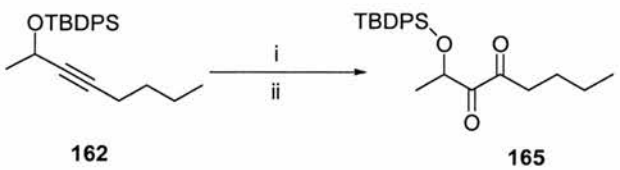

Scheme 6.11. i. O_3, MeOH, ~ -20 °C; ii. PPh_3, diethyl ether (80%).

At this point, the focus of our strategy was to identify a suitable method to couple the phosphonate derivative with the acetylene fragment. Several methods were investigated and they are described in the following section.

6.4 Preparation of 5-hydroxy-3,4-dioxo-hexyl-phosphonate 152

6.4.1 The first approach

The first synthetic attempt was based on the β-metallated phosphonate methodology described in section 6.2.2.[6] Diethyl β-bromoethylphosphonate **166** and the 3-silyl-protected 1-bromobutyne **167** were explored as starting materials for the coupling reaction. The phosphonate **166** was commercially available, while the alkynyl bromide **167** was prepared in a two step protocol starting from 3-hydroxybutyne **168** (Scheme 6.12). Thus, alcohol **168** was first protected as its *tert*-butyldiphenylsilyl ether in a similar manner to the model compound **162**.[21] Then bromination of alkyne **169** was carried out using NBS and a catalytic amount of $AgNO_3$.[23] The mechanism of this reaction is not clear. It is proposed that silver ions may activate the acetylene hydrogen to halogen exchange by formation of a π-complex with the triple bond.[23]

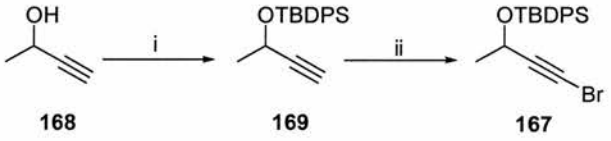

Scheme 6.12. Reagents: i. TBDPS-Cl, Pyr/THF/$AgNO_3$ (84%); ii. NBS, acetone, $AgNO_3$ (86%).

The preparation of the copper-zinc reagent **170** involved the activation of zinc dust using 1,2-dibromoethane and TMS-Cl, followed by addition of the phosphonate and then transmetallation with a solution of copper cyanide and lithium chloride.[6] The electrophilic bromoacetylene **167** was then added to this solution. However, analysis of

the crude mixture by ^{1}H-NMR spectroscopy revealed the presence of just starting material and there was no evidence of the desired product **171** (Scheme 6.13). The failure of this methodology may be due to the unsuccessful activation of the zinc, which would clearly prevent the formation of the β-metallated phosphonate **170**. Attempts to activate the metal with HCl in place of 1,2-dibromoethane and TMS-Cl gave the same negative results and this route was abandoned.

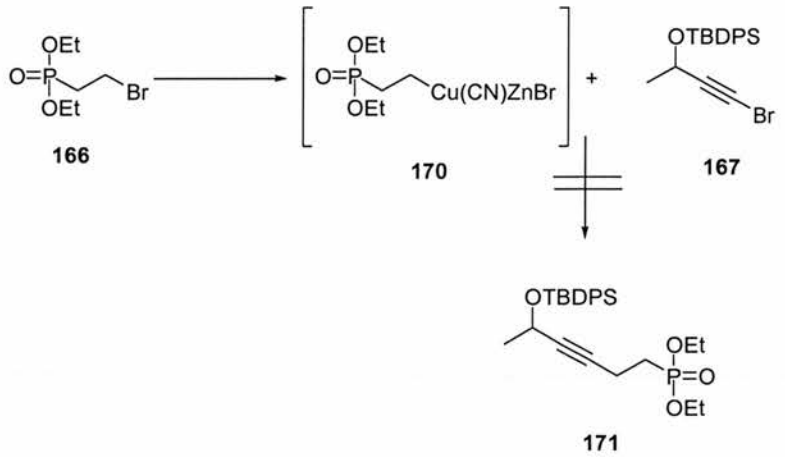

Scheme 6.13. Attempt to prepare **171** *via* a β-metallated phosphonate methodology proved unsuccessful.

6.4.2 The second attempt

The availability of compound **169** prepared in the first approach, allowed us to explore the preparation of **171** by the addition of the lithiated alkynyl **169** to either diethyl β-bromophosphonate **166** by nucleophilic displacement of bromine or by conjugate addition to the α,β-unsaturated phosphonate **172** in a Michael type reaction (Scheme 6.14). Thus, in the first experiment alkyne **169** was treated with BuLi in the presence of HMPT,[24] followed by addition of **166**, while in the second experiment, the lithium adduct of **169** was treated with **172**. After work-up, the crude material of both reactions

was analysed by ^{1}H-NMR spectroscopy. Disappointingly, the analyses showed unreacted starting material in both cases.

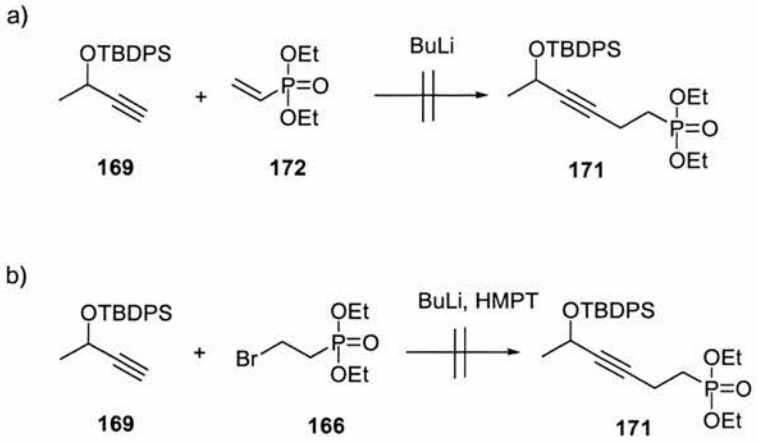

Scheme 6.14. Attempts to prepare **171** by reaction of the lithium adduct of **169** with a) diethyl vinylphosphonate **172**; and b) diethyl β-bromoethylphosphonate **166**.

6.4.3 A third approach

A third approach to the preparation of **152** involved the reaction of tosylate **173** with the sodium salt of diethyl phosphite.[7,8] The new synthetic route required the preparation of 1,5-dihydroxy-3-hexyne **174** and this was achieved by condensation of the dilithium adduct of 3-butyn-1-ol **175** with acetaldehyde **57** (Scheme 6.15). This intermediate was then selectively tosylated by taking advantage of the preferential reactivity of the primary alcohol. Thus, the corresponding derivative **176** was achieved by treatment of **174** with tosyl chloride in pyridine and a catalytic amount of DMAP.[22] Finally the secondary alcohol was protected as its triisopropylsilyl ether using the more reactive TIPS-triflate in DCM and in the presence of 2,6-lutidine,[25] affording **173** in an almost quantitative yield. The alcohol protecting group was changed with respect to the one used for the model compound **162** (TBDPS), because the TIPS was introduced more easily (the reaction was complete in just 45 min), and at the same time it was anticipated

that its removal could occur simultaneously with the hydrolysis of the diethyl phosphonate ester fragments at a later stage.

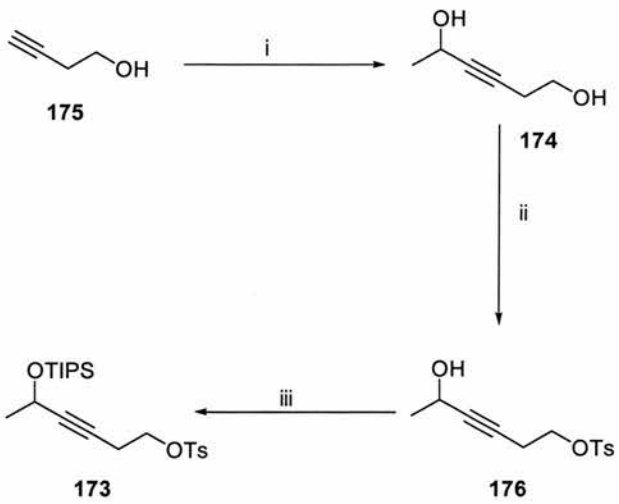

Scheme 6.15. i. 1) BuLi, THF; 2) acetaldehyde **57** (35%); ii. Tosyl-Cl, Pyr/DMAP (70%) ; iii. TIPS-triflate, DCM, 2,6-lutidine (~100%).

Compound **173** was then treated with the sodium salt of diethyl phosphite. The salt was freshly prepared just prior to reaction by treatment of diethyl phosphite with sodium hydride in dry THF (Scheme 6.16).[8]

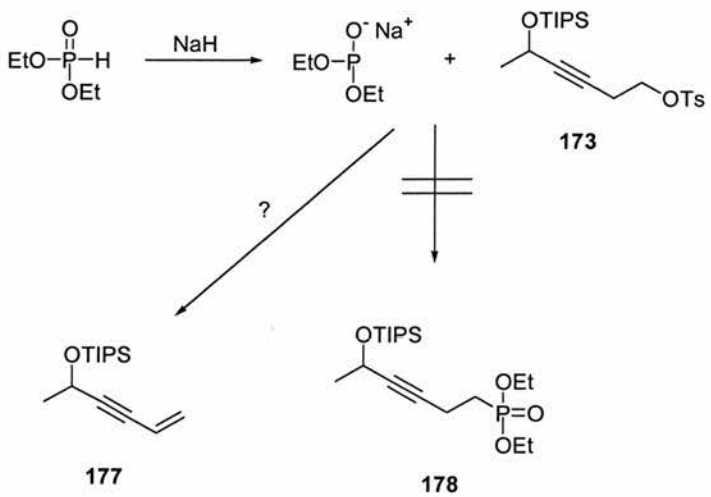

Scheme 6.16. Reaction of **173** with the sodium salt of dialkyl phosphate afforded a product which was tentatively considered **177** as result of the elimination process.

However, this reaction was unsuccessful. ^{1}H-NMR analysis of the crude product suggested that an elimination reaction was favoured over the desired nucleophilic substitution. In fact, the spectrum of the crude material showed the presence of a compound which was tentatively assigned to **177**. No evidence of **178** was apparent.

6.4.4 Fourth synthetic attempt

A fourth strategy proved successful. The target molecule **152** was prepared *via* the α-lithiated phosphonate methodology described in section 6.2.2. The route, which is shown in Scheme 6.17, started with the commercially available propargyl bromide **179**, which after sequential treatment with LDA and acetaldehyde **57** gave 1-bromo-4-hydroxy-pent-2-yne **180** in a moderate to good yield (40-60%). A limitation of this reaction was that several side products were obvious by TLC analysis and that the yield was variable with 60% the best obtained. Attempts to carry out the reaction with BuLi resulted in a lower yield and in the production of a side product which showed almost the same R_F as **180** rendering the purification more difficult. The nature of this side product was unclear.

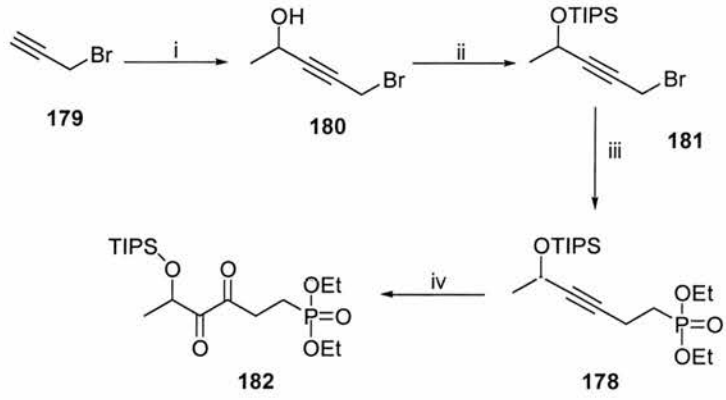

Scheme 6.17. i. 1) BuLi, THF; 2) acetaldehyde **57** (40-60%); ii. TIPS-triflate, DCM, 2,6-lutidine (~100); iii. 1) Diethyl methylphosphonate, BuLi, THF; 2) **181** (40%); iv. 1) O_3, MeOH; 2) PPh_3, diethyl ether (70%).

An alternative method to obtain **180** involved the preparation of 1,4-dihydroxypent-2-yne **183** starting from the commercially available but-3-yn-1-ol **184** and acetaldehyde **57**, followed by selective bromination of the primary over the secondary alcohol with CBr_4 in the presence of PPh_3 (Scheme 6.18).[26]

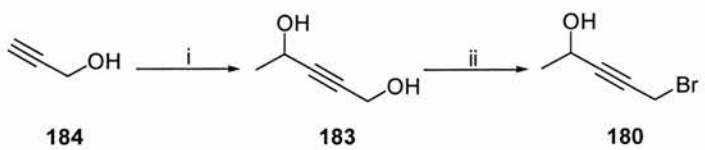

184 **183** **180**

Scheme 6.18. i. BuLi, THF; ii. acetaldehyde **57** (35%); iii. CBr_4, PPh_3, DCM (13%).

However, this route to **180** involved one extra step by comparison with the previous procedure, and the yield encountered in both steps was very poor (35% and 13%, respectively). This was clearly not a convenient alternative synthetic route and **180** was prepared as outlined in Scheme 6.17. Alcohol **180** was then protected as its triisopropylsilyl ether as described previously, affording **181** in almost quantitative yield. In the next step, diethyl methylphosphonate was α-lithiated by treatment with BuLi, and then addition of **181** generated diethyl 5-(triisopropylsilanoyloxy)-hex-3-ynyl-phosphonate **178**. This intermediate was then treated with ozone gas using the same conditions employed for the oxidation of the model compound **162**.[2] Work up and purification over silica gel afforded the α-diketo derivative **182** in a good yield (70%). The ^{1}H- and ^{13}CNMR spectra of **182** are shown in Figure 6.2

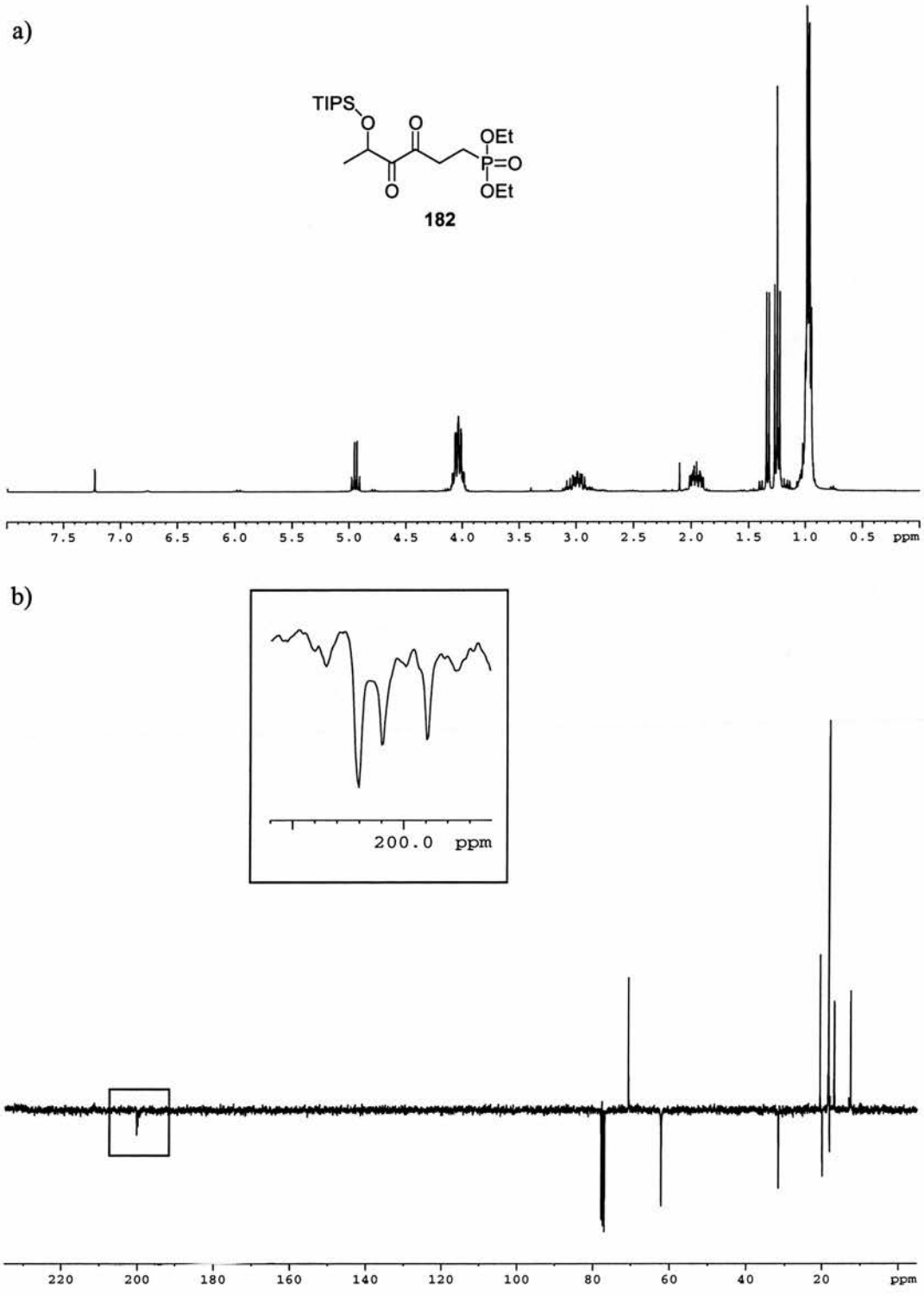

Figure 6.2. a) ^{1}H-NMR spectrum of **182**; b) ^{13}C-PENDANT spectrum of **182**. Highlighted in the box are the peaks for the two carbonyl carbons.

The carbonyl groups are clearly identified, and the one at the γ-position with respect to the phosphonate moiety is split as a doublet due to C-P coupling (15.4 Hz).

6.5 Formation of the target phosphonate 152

With α-diketo phosphonate **182** in hand, we were in a position to explore the hydrolysis of the diethyl phosphonate ester and the deprotection of the TIPS protecting group, which would then release our target molecule **152**. Phosphate ester hydrolysis was first attempted using the TMS-Br methodology described by McKenna.[27] It was anticipated that the acidic environment generated from TMS-Br would also hydrolyse the TIPS protecting group. Thus, a solution of **182** in DCM (~2 cm^3) was treated with an excess of TMS-Br (~7 eq.) (Scheme 6.19).

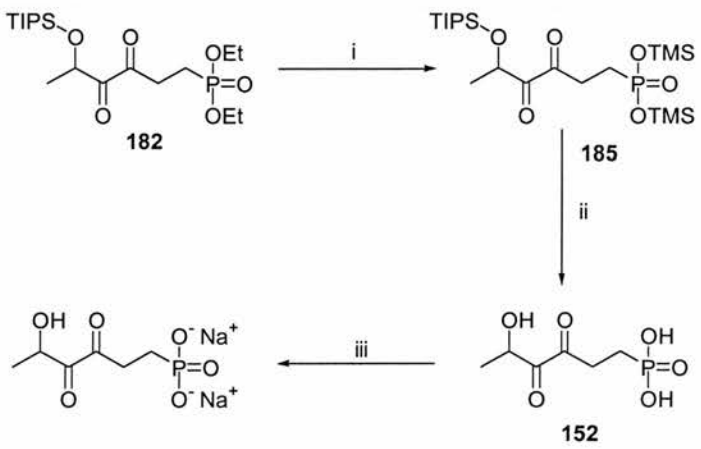

Scheme 6.19. i. TMS-Br, DCM; ii H_2O; iii. 0.2 M NaOH until pH ~7.

After 6 h volatiles were evaporated and the putative bis-trimethylsilyl ester **185** formed was treated for 20 min with a small amount of water (5 cm^3) until the solid went completely into solution. The mixture was then neutralized with a 0.2 M NaOH, and the solvent was removed by lyophilization. This product was analysed directly by ^{1}H- and ^{31}P-NMR spectroscopy. Regrettably, the NMR spectra were complex as the

deprotection of **182** mediated by TMS-Br led to a mixture of products. This result was, however, not unexpected following the discussion in section 6.2. ES-MS analysis indicated a mass of 209, which corresponded to the mono-anion form of **152** [M-H^+]. Clearly it was difficult to establish the purity of this product. In the first instance, it was considered that the simultaneous removal of the TIPS protecting group and the diethyl phosphonate ester under acidic conditions, may have favored side reactions which gave rise to more complex NMR spectra. In order to obtain a clearer insight into this, an alcohol protecting group which was able to survive the TMS-Br treatment and which could be removed in a subsequent step, was explored.

6.6 Preparation of dimethyl 5-(acetyloxy)-3,4-dioxohexyl-phosphonate 186

This new strategy involved protecting the alcohol as an acetyl ester in place of TIPS. The secondary alcohol, after hydrolysis of the phosphonate ester, could then be unmasked under basic conditions, or alternatively, by enzymatic reaction using a lipase. In the event, the phosphonate was employed as the dimethyl ester, as its hydrolysis was expected to occur a little faster than the ethyl ester. This circumvented a longer exposure of the acetyl ester to an acidic environment, which could clearly cause a problem. Thus, starting from **180**, treatment with acetic anhydride in DCM and pyridine[19,22] afforded the acetyl ester **187** (Scheme 6.20).

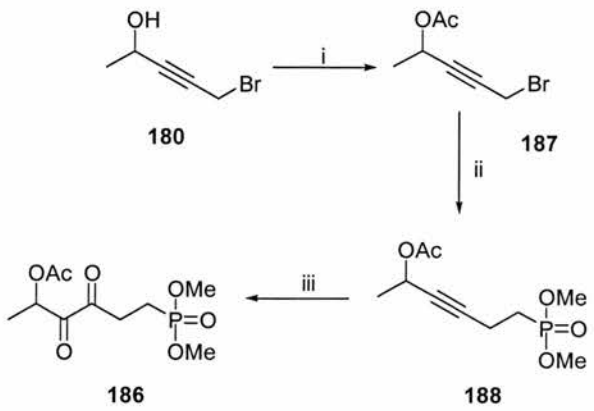

Scheme 6.20. i. Acetic anhydride, DCM/Pyr/DMAP (60%); ii. 1) Dimethyl methylphosphonate, BuLi, THF; 2) **187** (40%); iii. 1) O_3, CCl_4/acetic acid (4:1); 2) PPh_3, diethyl ether (70%).

This ester was then reacted with the α-lithiated dimethyl methylphosphonate in a similar manner as that described for **181**. The product **188** was purified by chromatography and was obtained in a modest yield of 40%. Acetylene **188** was then oxidised using ozone gas, but in this case the reaction conditions were modified and the reaction was carried out in a CCl_4/acetic acid (4:1) mixture.[2] The oxidation afforded **186** in a good yield (70%), similar to that obtained for **182**. However, in this case the purification of the product revealed some problems as phosphinoxide side products, formed from quenching of the peroxides, showed similar polarity to **186** and could be removed only after several (2/3) consecutive chromatographic processes. Also, in one case a side product was generated, which was tentatively assigned to **189** by ^{1}H- and ^{13}C-NMR analyses.

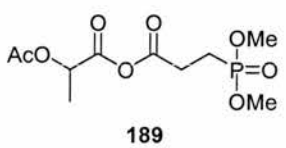

189

In Figure 6.3 are reported the ^{1}H- and ^{13}CNMR spectra of **186**. Again, the carbonyl carbons are identified, and the γ-carbonyl carbon is again split as a doublet with a C-P coupling constant of 14.4 Hz.

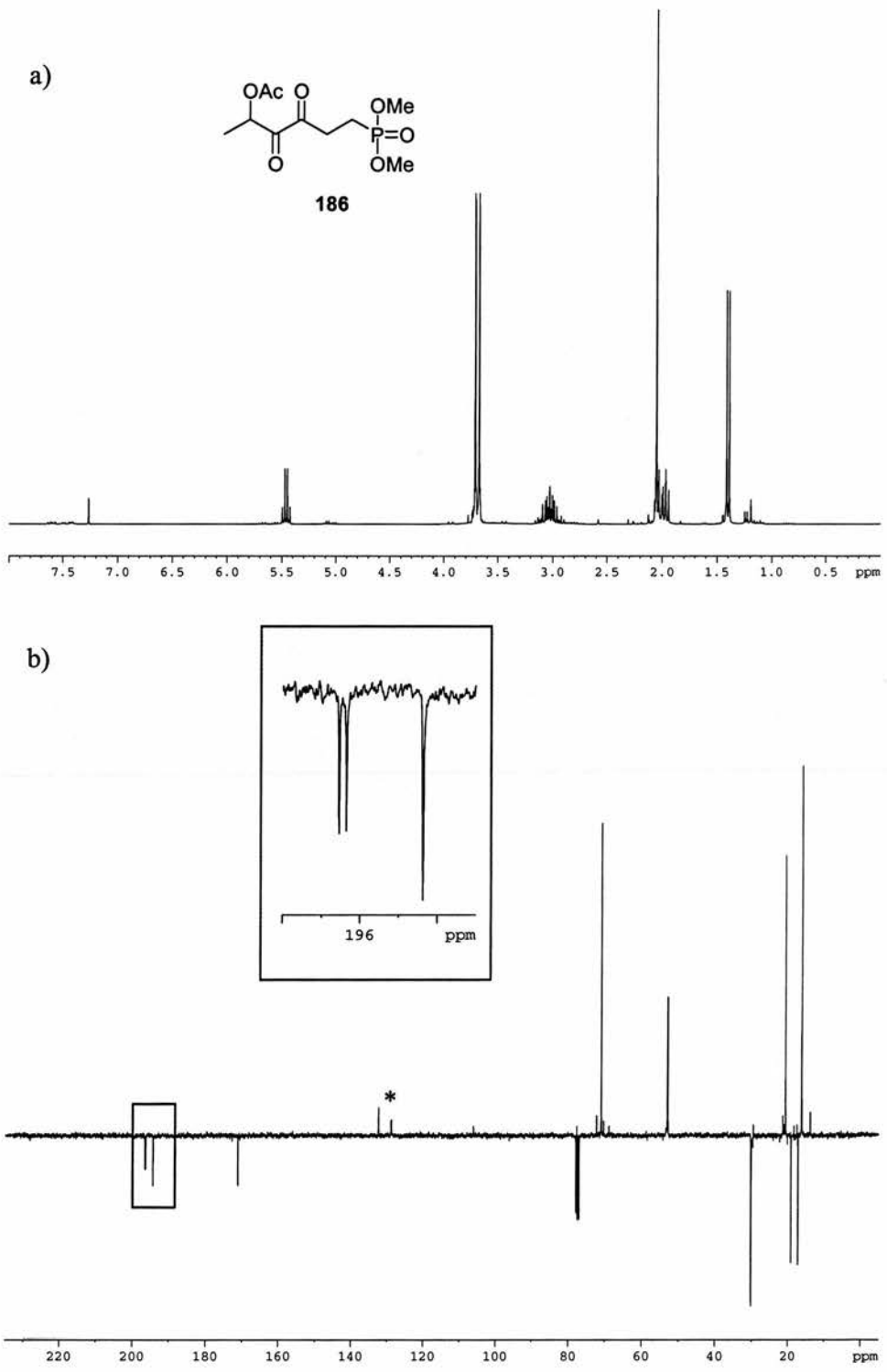

Figure 6.3. a) ^{1}H-NMR spectrum of **186**; b) ^{13}C-PENDANT spectrum of **186**. Highlighted in the box are the peaks for the two carbonyl carbons. The ^{13}C-NMR spectrum was obtained from a less pure sample of **186** and the asterisk indicates peaks from phosphineoxide impurities.

6.7 Formation of 152 from 186

With the dimethyl phosphonate ester **186** in hand, we proceeded to the hydrolysis step following the previous protocol used for the hydrolysis of **182** (Scheme 6.21). In this case, in order to have a clearer insight in the hydrolysis process, every intermediate formed was analysed by ^{1}H-NMR spectroscopy.

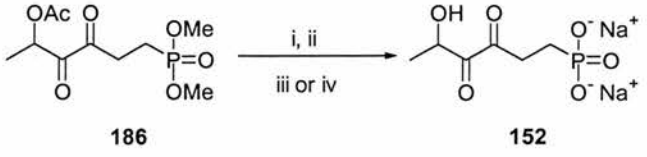

186 **152**

Scheme 6.21. i. TMS-Br, DCM; ii. H_2O; iii. NaOH (3 eq.) or iv. Lipase, phosphate buffer.

Thus, **186** was initially treated with an excess of TMS-Br and, after removal of volatiles, the intermediate **190** formed was analysed by ^{1}H-NMR spectroscopy (Figure 6.4). The spectrum shows clearly the presence of the peak relative to the TMS group while the doublet at 3.7 ppm, relative to the methyl ester moieties, disappeared. The acetate ester (2 ppm) is still intact.

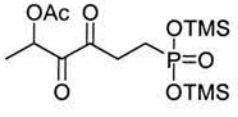

190

Figure 6.4. Formation of **190** as result of a *trans*-esterification reaction of **186** with TMS-Br.

This intermediate was then treated with a small amount of water (~5 cm^3) until the solid went completely into solution. Subsequently, the solvent was removed by lyophilization and the solid was analysed again by ^{1}H-NMR spectroscopy (Figure 6.5a).

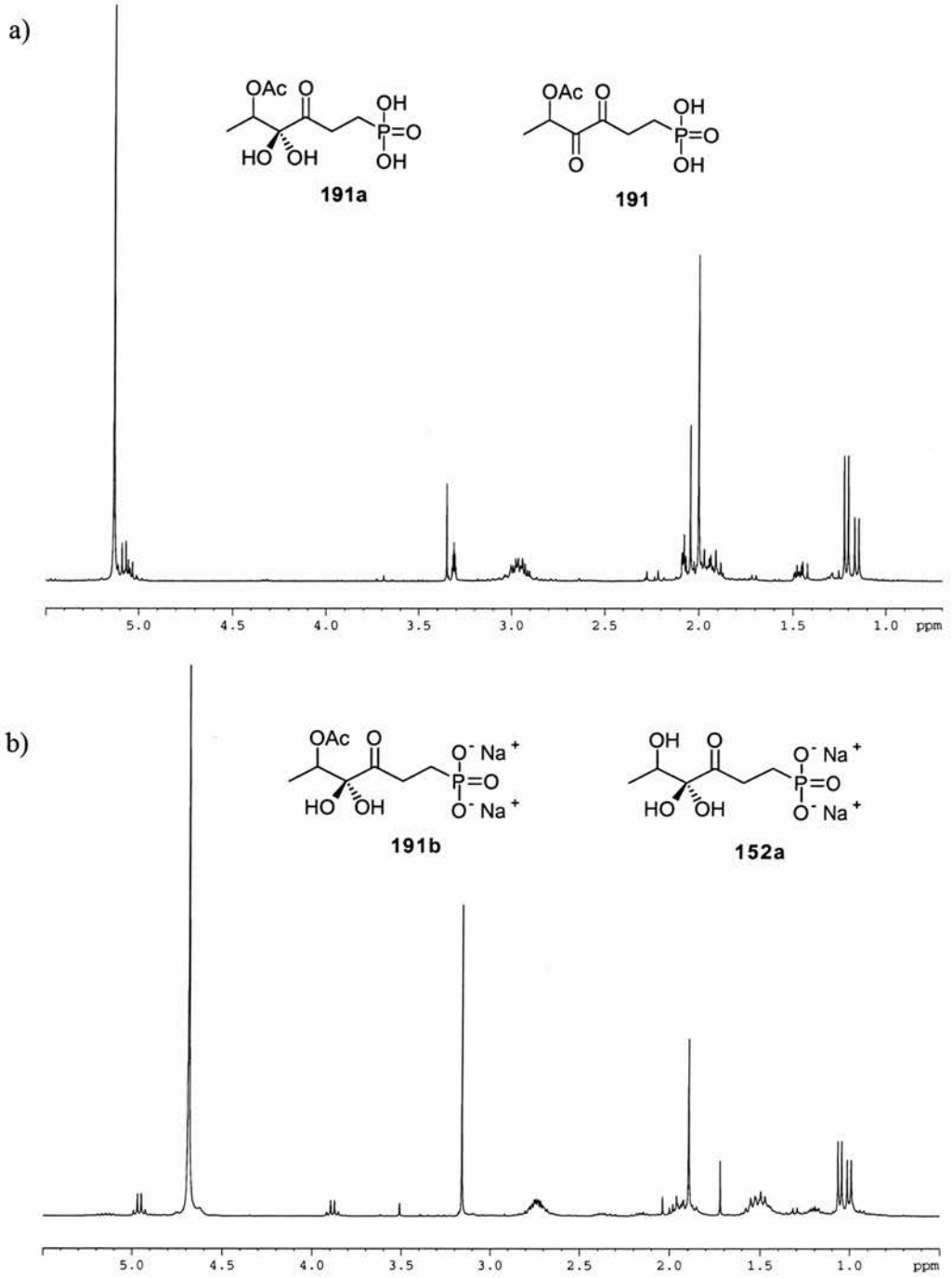

Figure 6.5. ^{1}H-NMR spectra obtained after treatment of **186** with H_2O a) and subsequently b) with 3 eq. of NaOH.

The spectrum shows clearly the presence of two compounds in approximately a 2:1 *ratio*, as established by integration of the two doublets at 1.13 and 1.2 ppm. These two products may correspond to **191** and its hydrate form **191a**. In order to hydrolyse the acetyl moiety, this material was treated with 3 eq. of NaOH. Analysis of the product by ^{1}H-NMR spectroscopy, after removal of water by lyophilization, showed still the presence of two compounds (Figure 6.5b). The spectrum suggests the presence of **191b** and also the formation of our target molecule **152**, present in its hydrate form **152a** as indicated from the shift of the proton at ~5 ppm to ~4 ppm. This material was then treated with an excess of NaOH. After 4 h, the mixture was neutralized with a HCl solution (pH ~6.5-7.0) and the solvent was removed again by lyophilization. The crude product was then analysed by ^{1}H-NMR spectroscopy (Figure 6.6).

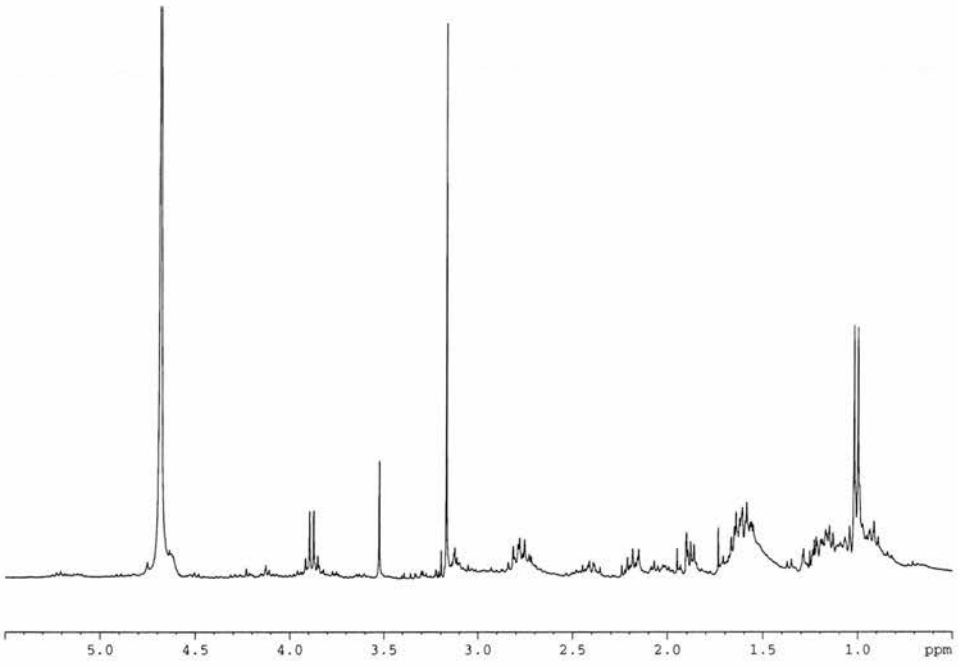

Figure 6.6. ^{1}H-NMR spectrum of the mixture obtained after hydrolysis of **186**.

Disappointingly, the spectrum was complex as a mixture of products was formed The doublet at 1.0 ppm and the quartet at 3.9 ppm may be indicative of the presence of the

desired phosphonate **152**. Also, ES-MS analysis showed again a mass of 209 which suggests **152** as a component of the product.

An alternative method to hydrolyse the acetyl group involved the use of an enzymatic reaction. Thus, after treatment of **186** with TMS-Br and subsequent removal of the solvent, the residue was suspended in a phosphate buffer solution (5 cm^3, pH ~7.4), in the presence of a lipase (*Candida rugosa*).[28] After work up, the crude material was analysed by ^1H-, ^{31}P-NMR and ES-MS spectroscopy. The outcome was similar to that shown in Figure 6.5a. Clearly, the acetyl protecting group survived to enzymatic hydrolysis, and this alternative method proved unsuccessful.

6.8 DXR incubation assays

The product obtained after hydrolysis of **182** was tested as an inhibitor for the DXR enzyme derived from *E. coli*. The test assays were carried out by Dr. U. Wong in Dr. R. Cox's laboratory at Bristol University. The assays were carried out in a tris phosphate buffer solution (1 cm^3, pH= 8) at 37 °C using 40 nM of enzyme, 0.35 mM of substrate, 1 mM of Mg^{2+}, and with varying the concentrations of **152** (Figure 6.7).

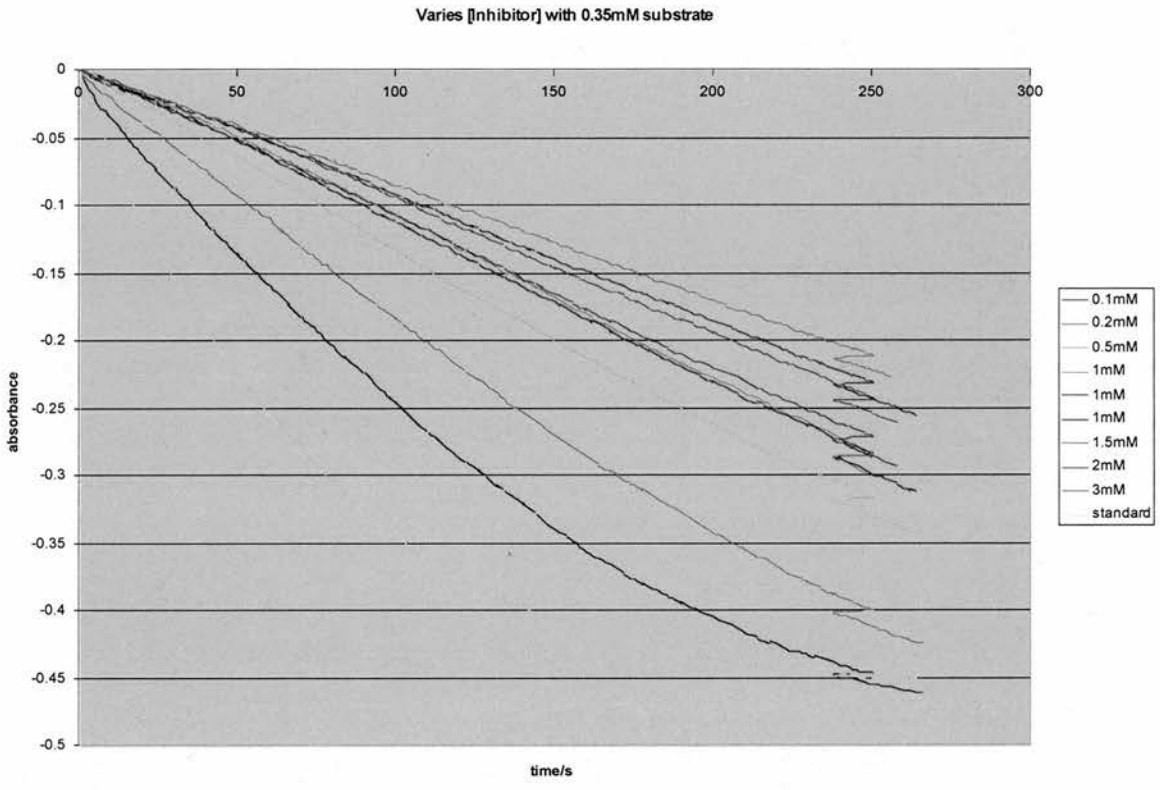

Figure 6.7. Incubation of the DXR enzyme at varying concentrations of **152**.

A time course assay was carried out where **152** was incubated with the enzyme and the reaction was assayed at intervals (T10 = time 10 min) (Figure 6.8). Interestingly, the preliminary results showed signs of inhibition. At 1.0 mM **152** showed about 80% inhibition with a tentative Ki of ~0.5 mM. Compound **152** appears not to be a very potent inhibitor, with a similar affinity with the enzyme as the natural substrate (~0.34 mM). However, as the purity of the compound tested was difficult to establish, a more accurate assessment warrants more material.

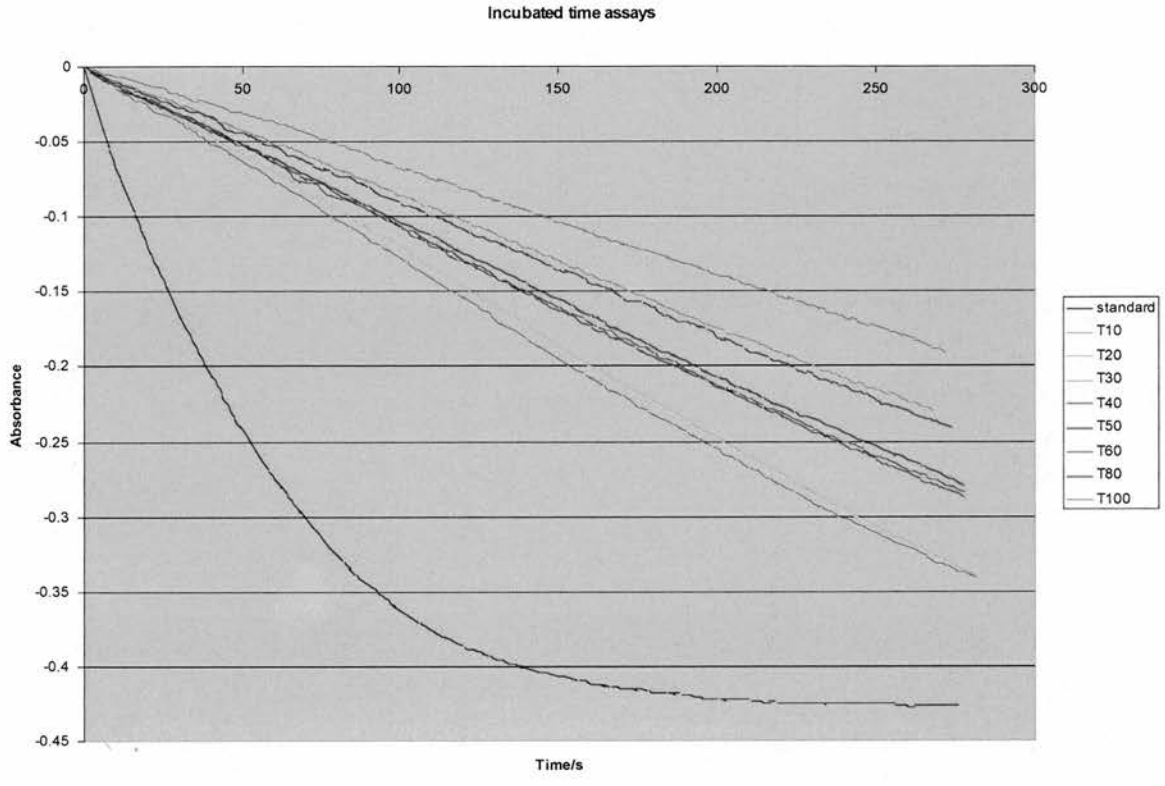

Figure 6.8. Time dependent inhibition assay.

6.9 Conclusion

The aim of the present project was the preparation of DXR inhibitors based on mechanistic studies. 5-Hydroxy-3,4-dioxo-hexyl-phosphonate **152** was designed as a transition state inhibitor of the retroaldol/aldol mechanism. This compound was obtained according to two different synthetic routes, both involving five step protocols. This first route involved the protection of the hydroxyl moiety as its triisopropylsilyl ether, while in the second route this group is masked as an acetyl ester. In both cases the product **152** gave complex NMR spectra. In the case of the silyl derivative **182** the hydrolysis occurs faster and simultaneous with the removal of diethyl phosphonate ester moieties. A preliminary biological assay suggested that **152** is a modest inhibitor of *E. coli* DXR enzyme. However, a definitive conclusion cannot be draw as the compound was tested as a crude product, and also its purity was not established. The tentative Ki is

similar to the Km of the natural substrate, perhaps suggesting no particular transition state inhibition character. Attempts to prepare **152** in a purer form and also analogues of **152** is under investigation in our laboratory. Clearly, successes here will provide a better insight into the nature of inhibition of such compounds and may contribute understanding on the mechanism of this intriguing enzyme.

References Chapter 6

1. P. Page, C. Blonski and J. Périé, *Bioorg. & Med. Chem.*, 1999, **7**, 1403.

2. L. Re, B. Maurer and G. Ohloff, *Helv. Chim. Acta*, 1973, **56**, 1882.

3. M. F. Semmelhack, S. R. Campagna, M. J. Federle and B. L. Bassler, *Org. Lett.*, 2005, **7**, 569.

4. M. F. Semmelhack, S. R. Campagna, C. Hwa, M. J. Federle and B. L. Bassler, *Org. Lett.*, 2004, **6**, 2635.

5. M. M. Meijler, L. G. Hom, G. F. Kaufmann, K. M. McKenzie, C. Sun, J. A. Moss, M. Matsushita and K. D. Janda, *Angew. Chem. Int. Ed.*, 2004, **43**, 2106.

6. C. Retherford, T. Chou, R. M. Schelkun and P. Knochel, *Tetrahedron Lett.*, 1990, **31**, 1833.

7. T. C. Myers, S. Preis and E. V. Jensen, *J. Am. Chem. Soc.*, 1954, **76**, 4172.

8. R. G. Harvey, T. C. Myers, H. I. Jacobson and E. V. Jensen, *J. Am. Chem. Soc.*, 1957, **79**, 2612.

9. N. S. Srinivasan and D. G. Lee, *J. Org. Chem.*, 1979, **44**, 1574.

10. L. Bassignani, A. Brandt, V. Caciagli and L. Re, *J. Org. Chem.*, 1978, **43**, 4245.

11. P. Müller and J. Goody, *Helv. Chim. Acta*, 1981, **64**, 2531.

12. S. Torii, T. Inokuchi and Y. Hirata, *Synthesis*, 1987, 377.

13. H. Gopal and A. J. Gordon, *Tetrahedron Lett.*, 1971, 2941.

14. F. P. Ballistreri, S. Failla, G. A. Tomaselli and R. Curci, *Tetrahedron. Lett.*, 1986, **27**, 5139.

15. A. McKillop, O. H. Oldenziel, B. P. Swann, E. C. Taylor and R. L. Robey, *J. Am. Chem. Soc.*, 1973, **95**, 1296.

16. R. Zibuck and D. Seebach, *Helv. Chim. Acta*, 1998, **71**, 237.

17. L. D'Accolti, M. Fiorentino, C. Fusco, P. Crupi and R. Curci, *Tetrahedron. Lett.*, 2004, **45**, 8575.

18. Z. Zhu and J. H. Espenson, *J. Org. Chem.*, 1995, **60**, 7728.

19. A. S. Kalgutkar, K. R. Kozak, B. C. Crews, G. P. Hochgesang Jr. and L. J. Marnett, *J. Med. Chem.*, 1998, **41**, 4800.

20. M. Nicoletti, "Novel approach to asymmetric synthesis in organic and organo-fluorine chemistry", PhD Thesis, University of St. Andrews, 2004.

21. R. K. Bhatt, K. Chauhan, P. Wheelan, R. C. Murphy and J. R. Falk, *J. Am. Chem. Soc.*, 1994, **116**, 5050.

22. T. W. Greene and P. G. M. Wuts, "Protective groups in organic synthesis", 3rd Ed. Wiley Inter-Science.

23. H. Hofmeister, K. Annen, H. Laurent and R. Wiechert, *Angew. Chem. Int. Ed.*, 1984, **23**, 727.

24. W. R. Roush and A. P. Spada, *Tetrahedron. Lett.*, 1982, **23**, 3773.

25. K. Tanaka, H. Yoda, Y. Isobe and A. Kaji, *J. Org. Chem.*, 1986, **51**, 1856.

26. S. L. Cobb, "The origin and metabolism of 5'-FDA in S. Cattleya", PhD Thesis, University of St. Andrews, 2005.

27. C. E. McKenna, M. T. Higa, N. H. Cheung and M. McKenna, *Tetrahedron. Lett.*, 1977, **18**, 155.

28. P. Beier, "Partially fluorous molecules and lipase mediated enantiomeric resolutions in fluorous solvent", PhD Thesis, University of St. Andrews, 2004.

Chapter 7

Chemical and biochemical experiments

7.1 Chemical syntheses: General methods

7.1.1 Reaction conditions

Air and moisture sensitive reactions were carried out under a nitrogen atmosphere using oven-dried glassware (140 °C). All reagents of synthetic grade were used as supplied. If further purification was required the procedures are detailed in Armarego and Perrin, "*Purification of laboratory chemicals*" 4th Ed. Ambient temperature refers to 20-25 °C. Reaction temperatures of -78 °C to -10 °C were obtained using solid carbon dioxide pellets and acetone, and temperatures of -10 °C to +4 °C were obtained in a ice/water/NaCl bath. Reactions requiring reflux or heating were carried out using an oil bath equipped with a contact thermometer.

7.1.2 Chromatography

Thin layer chromatography (TLC) was performed using Merck, Kieselgel 60 plates. Compounds were detected by either UV or by the use of a molybdenum based staining agent. Column chromatography was performed using Merck Kieselgel 60 silica gel (230-400 nm mesh). HPLC analysis was carried out using a Varian series 9012 pump/9050 UV-lamp; analytical HPLC was performed using a Hypersil ODS C-18 column, 5 μm (250•mm; 4.6 mm ID); semi-preparative HPLC was performed using a Phenomenex Hypersil C-18 column, 5 μm (250•mm; 10 mm ID). Cation exchange procedures were carried out using Dowex 50W (X8) resin with 50-100 mesh particles.

7.1.3 Nuclear magnetic resonance spectroscopy (NMR)

Nuclear magnetic resonance (NMR) spectra were obtained using several instruments. A Bruker Av-300 machine operating at 300 MHz for ^{1}H, 75 MHz for ^{13}C, 282 MHz for ^{19}F and 181 MHz for ^{31}P. A Varian Unity Plus 300 machine operating at 300 MHz for ^{1}H, 75 MHz for ^{13}C, 282 MHz for ^{19}F and Varian Unity Plus 500 machine operating at 499.90 MHz for ^{1}H, 125.71 MHz for ^{13}C, 470.26 MHz for ^{19}F. All chemical shifts (δ) are reported in parts per million (ppm) and are quoted relative to the residual proton peak of $CDCl_3$, d_6-DMSO, D_2O, or CD_3OH or to the internal standard $CFCD_3$ for ^{19}F. Coupling constants (J) are given in Hertz (Hz). Spectral coupling patterns are designated as follows; d: doublet; t: triplet; q: quartet; m: multiplet and br s: broad signal. ^{13}C-NMR, ^{19}F-NMR and ^{31}P-NMR spectra were ^{1}H decoupled.

7.1.4 Ozonolysis

Ozonolysis reactions were carried out using a Fischer ozone-Generator 500 using commercial-grade oxygen as a source.

7.1.5 Melting point analyses

Melting points were determined in Pyrex capillaries using a Gallenkamp Griffin MPA350.BM2.5 melting point apparatus.

7.1.6 Fourier transform infra red spectra (FT-IR)

All infra red (IR) spectra were recorded in the range 4000-440 cm^{-1} on a Nicolet Avatar 360 FT-IR as a thin film on NaCl plates.

7.1.7 Elemental analysis

The elemental analysis for compounds N^6-benzoyl-2',3'-*O*-isopropylideneadenosine **111** and for 2',3'-*O*-isopropylidene-5'-*O*-nitroadenosine **99** were obtained using a CE Instrument EA 1110 CHNS analyzer.

7.1.8 Mass spectrometry

High-mass resolution spectrometry (HRMS) and low resolution mass spectrometry (LRMS) were performed using a Micromass LCT (Manchester, UK) mass spectrometer with electrospray ionization (ESI) operating in both positive and negative mode. High-mass resolution spectrometry for 2-(*tert*-butyldiphenylsilanoyloxy)-octane-3,4-dione **165** and diethyl 5-(triisopropylsilanoyloxy)-3,4-dioxo-hexyl-phosphonate **182** was obtained in CI operating system.

7.1.9 Liquid crystal NMR sample preparation

Chiral ^{2}H-NMR analyses were carried out by Dr. A. Meddour (at Orsay, Paris) in Prof. J. Courtieu's laboratory.

PBLG **109** (0.151 g, Mol. Wt. 70.000-150.000 purchased from Sigma-Aldrich) was weighted into a 5 mm o.d. NMR tube. DMF (240 µl) was added and the mixture was then heated to 80-100 °C until complete dissolution of the polymer. Chloroform (30µl) and a solution of 5'-FDA (0.40 to 2.0 mg) in DMF (40 µl) was introduced to the NMR tube. In order to homogenize the viscous mixture, the NMR tube was repeatedly centrifuged (20 times) on a low speed (600rpm) bench top centrifuge, turning the tube upside-down between each centrifugation.

7.1.10 ^{2}H-NMR measurements in PBLG/DMF ($CHCl_3$) liquid crystal

^{2}H-{^{1}H} NMR spectra were recorded at 61.4 MHz on a Bruker DRX-400 spectrometer equiped with a selective deuterium probe. The temperature was held at 330 K using a BVT3000 variable temperature unit. Proton broad-band decoupling was achieved using the WALTZ-16 composite pulse sequence.

7.2 Synthetic experiments

7.2.1 2',3'-*O*-Isopropylideneadenosine-5'-carboxylic acid 89[1]

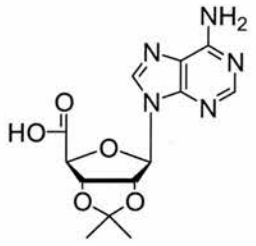

89

2',3'-*O*-Isopropylideneadenosine **100** (2.05 g, 6.67 mmol) was dissolved in water (700 cm^3). The solution was cooled to ambient temperature and then KOH (1.12 g, 20 mmol) was added followed by $KMnO_4$ (4.29 g, 27 mmol) over 2 h. After 24 h, the excess of $KMnO_4$ was destroyed with a 37% H_2O_2 solution. After removal of the resultant solid by filtration, the solution was concentrated (150 cm^3) and then cooled to 0 °C. HCl (1 N) was added until pH= 4.6 and the product precipitated. After filtration, the solid was recrystallized from water to afford **89** as an amorphous white material (1.50 g, 69%); mp: 249 °C dec. (lit.[2] 246-249 °C); δ_H (300 MHz; d_6-DMSO) 1.37 (3 H, s, CH_3), 1.54 (3 H, s, CH_3), 4.70 (1 H, d, *J* 2.1, 4'-H), 5.47 (1 H, d, *J* 5.9, 2'-H), 5.54 (1 H, dd, *J* 2.1 and 5.9, 3'-H), 6.35 (1 H, s, 1'-H), 7.32 (2 H, br s, NH_2), 8.11 (1 H, s, 8-H), 8.28 (1 H, s, 2-H); δ_C (75 MHz; d_6-DMSO) 25.2 (CH_3), 26.8 (CH_3), 83.8, 84.1, 85.8, 89.8 (C-1', C-2', C-3', C-4'), 112.97 ($\underline{C}Me_2$), 119.1 (C-5), 140.7 (C-8), 149.4 (C-4), 152.7 (C-2), 156.3 (C-6), 171.1 (COOH); ***m/z*** (ESI+) 322.12 [M+H] (40%).

7.2.2 N^6-Benzoyl-2',3'-*O*-isopropylideneadenosine 111[3]

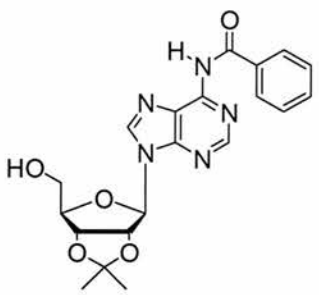

111

Benzoyl chloride (9.0 cm^3, 77.5 mmol) was added to a solution of 2',3'-*O*-isopropylideneadenosine **100** (6.14 g, 20.0 mmol) in pyridine (50 cm^3) at 0 °C, and the mixture was allowed to warm to ambient temperature over 2 h. After addition of cold water, the mixture was evaporated, the solid redissolved in DCM and washed with aqueous $NaHCO_3$ and then water. Following evaporation of the DCM, the residue was dissolved in pyridine (50 cm^3) and a solution of KOH (8.0 g in 50 cm^3 of H_2O) was added and the mixture stirred for 40 min. Acetic acid (7.0 cm^3) was then added with cooling, the solids were evaporated under reduced pressure, and the residue was partitioned between DCM and water. The organic phase was further washed with aqueous $NaHCO_3$ and water, dried and evaporated leaving a yellowish residue that was triturated with ethyl acetate. The resulting white precipitate was washed with ether and dried *under vacuum*. The solid was further washed with DCM. Crystallization from ethanol gave **111** as a white crystalline solid (4.1 g; 50%); mp: 150-152 °C (lit.[4] 151-153 °C); elemental analysis; Found C, 58.13, H, 5.16, N, 16.8. $C_{20}H_{21}N_5O_5$ requires C, 58.39, H, 5.14, 17.02; δ_H (300 MHz; $CDCl_3$) 1.36 (3 H, s, CH_3), 1.61 (3 H, s, CH_3), 3.80 (1 H, dd, *J* 12.5 and 2.0, 5'-H_a), 3.97 (1 H, dd, *J* 12.5 and 1.8, 5'-H_b), 4.52-4.55 (1 H, m, 4'-H), 5.10 (1 H, dd, *J* 5.9 and 1.3, 3'-H), 5.23 (1 H, dd,

J 4.8 and 5.9, 2'-H), 5.96 (1 H, d, *J* 4.8, 1'-H), 7.5 and 8.0 (5 H, m, aromatic), 8.08 (1 H, s, 8-H), 8.70 (1 H, s, 2-H), 9.20 (1 H, br s, NHCOAr); δ_C (75 MHz; $CDCl_3$) 25.6 (CH_3), 27.9 (CH_3), 63.6 (C-5'), 82.0, 83.5, 86.7, 94.4 (C-1', C-2', C-3', C-4'), 114.6 ($\underline{C}Me_2$), 128.3 (CH Ar), 129.2 (CH Ar), 133.3 (CH *para*-Ar), 133.8 (C Ar), 124.7 (C-5), 143.0 (C-8), 150.6, 150.9 (C-4, C-6), 152.7 (C-2), 164.9 (N$\underline{C}$OAr); ***m/z*** (ESI-) 410.02 [M-H] (100%).

7.2.3 N^6-Benzoyl-5'-deoxy-2',3'-*O*-isopropylidene-5',5'- (*N,N'*-diphenylethylenediamino)-adenosine 114[4]

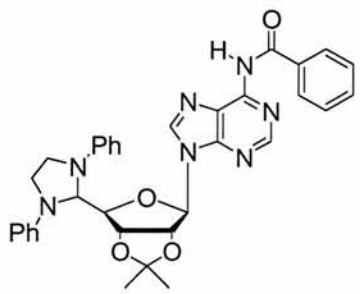

114

Dichloroacetic acid (0.36 cm^3, 4.37 mmol, 0.5, eq.) was added to a solution of N^6-benzoyl-2',3'-*O*-isopropylideneadenosine **111** (3.59 g, 8.75 mmol) and DCC (5.42 g, 26.3 mmol, 3.0 eq.) in DMSO (20 cm^3). The mixture was then stirred at ambient temperature for 90 min. A solution of oxalic acid dihydrate (2.20 g, 17.5 mmol, 2 eq.) in MeOH (7.0 cm^3) was slowly added and after 30 min was filtered and the crystalline residue of dicyclohexyl-urea was washed with cold MeOH. *N,N'*-Diphenylethylenediamine (2.21 g, 10.4 mmol, 1.2 eq.) was added to the combined filtrate and washings and the resulting solution was stirred at room temperature for 2 h. Water was then added to form a white amorphous solid. The suspension so formed was then filtered and washed with water. The mother liquors were partitioned between water and DCM and the organic phase was washed twice with water and evaporated. The residue was added to the solid material previously isolated. Crystallization from ethanol gave **114** as a colourless crystalline solid (4.0 g, 76%); mp: 127-130 °C (lit.[4] 132-135 °C); δ_H (300 MHz; $CDCl_3$) 1.34 (3 H, s, CH_3), 1.51 (3 H, s, CH_3), 3.56-3.77 (4 H, m, NCH_2CH_2N), 4.64 (1 H, dd, *J*2.5 and 4.6, 4'-H), 5.15-5.25 (2 H, m, 2'-H, 3'-H), 5.76 (1 H, d, *J*2.5, 5'-H), 6.18 (1 H, d, *J*2.3, 1'-H), 6.70 and 7.20 (10 H, m, ArNRNAr) 7.5 and 8.08 (5 H, m, NHCOAr), 7.80 (1 H, s, 8-H), 8.70 (1 H, s, 2-H), 9.04 (1

H, br s, NHCOAr); δ_C (75 MHz; $CDCl_3$) 26.1 (CH_3), 27.8 (CH_3), 47.1 and 48.1 (NCH_2CH_2N), 73.5 (C-5'), 83.4, 84.1, 87.3, 88.7 (C-1', C-2', C-3', C-4'), 115.4 ($\underline{C}Me_2$), 113.8 (CH Ar), 113.9 (CH Ar), 118.6 (CH Ar), 118.7 (CH Ar), 128.2 (CH Ar), 129.2 (CH Ar), 129.5 (CH Ar), 129.8 (CH Ar), 133.2 (CH Ar), 134.0 (C Ar), 146.8 (C Ar), 123.3 (C-5), 149.9, 151.6 (C-4, C-6), 142.0 (C-8), 153.6 (C-2), 164.9 (N$\underline{C}$OAr); ***m/z*** (ESI+) 604.25 [M+H] (100%).

7.2.4 N^6-benzoyl-2',3'-*O*-isopropylideneadenosine-5'-aldehyde hydrate 115[4]

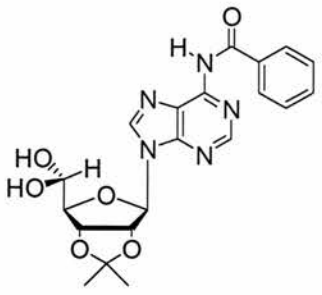

115

Dowex H^+ resin (5.8 g) was added to a solution of **114** (3.80 g, 6.3 mmol) in THF/H_2O (340 cm^3; 1:1), and then stirred at ambient temperature for 1 h. The resin was then removed by filtration, and the solvent evaporated until an amorphous solid was formed. The residual solvent was removed by syringe and the white residue washed with water, and finally dried *under vacuum* to afford N^6-benzoyl-2',3'-*O*-isopropylideneadenosine-5'-aldehyde as hydrate form **115** (1.88 g, 70%); δ_H (300 MHz; d_6-DMSO) 1.35 (3 H, s, CH_3), 1.56 (3 H, s, CH_3), 4.11 (1 H, dd, *J* 4.7 and 1.8, 4'-H), 4.87 (1 H, d, *J* 4.7, 5'-H), 5.08 (1 H, dd, *J* 6.1 and 1.8, 3'-H), 5.36 (1 H, dd, *J* 6.1 and 2.8, 2'-H), 6.27 (1 H, d, *J* 2.8, 1'-H), 7.6 and 8.0 (5 H, m, Ar), 8.64 and 8.74 (2 H, s, 8-H/2-H), 11.4 (1 H, br s, NH); δ_C (75 MHz; d_6-DMSO) 24.9 (CH_3), 26.9 (CH_3), 80.7, 83.6, 88.5, 89.0, 90.3 (C-1', C-2', C-3', C-4', C-5') 112.8 ($\underline{C}Me_2$), 128.3 (CH Ar), 128.5 (CH Ar), 132.5 (CH Ar), 133.1 (C Ar), 125.2 (C-5), 150.0, 152 (C-4, C-6), 143.1 (C-8), 151.6 (C-2), 165.7 (NH$\underline{C}$OAr); ***m/z*** (ESI+) 450.03 (M+Na) (100%).

7.2.5 N^6-Benzoyl-2',3'-*O*-isopropylidene-adenosine-5'-aldehyde 113[4]

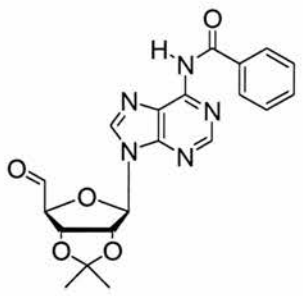

113

A suspension N^6-benzoyl-2',3'-*O*-isopropylideneadenosine-5'-aldehyde hydrate **115** (0.4 g, 0.88 mmol) in ethanol (20 cm^3) was heated at 60 °C for 20 min. This operation was repeated several times until the amorphous solid was dissolved. The solvent was then removed on a rotary evaporator to give the free aldehyde **113** as a white foam. This material* was used directly for further transformation; ***m/z*** (ESI-) 407.97 [M-H] (100%), without complete analysis.

*This compound shows a complex ^{1}H-NMR spectrum due to the simultaneously presence of the hydrate **115** and the aldehydic form **113**, and small amount of unknown side products. However the singlet due to the proton of the aldehyde at 9.30 δ ppm was very distinctive.[4]

7.2.6 (5'*R*)-[$^2H_1$]-N^6-Benzoyl-2',3'-*O*-isopropylideneadenosine 111a

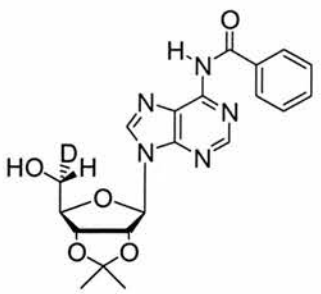

111a

Procedure A:

$NaBD_4$ (0.027 g; 0.64 mmol) was added to a solution of N^6-benzoyl-2',3'-*O*-isopropylideneadenosine-5'-aldehyde **113** (0.180 g, 0.42 mmol) in ethanol (26 cm^3) at 0 °C. After 6 h, the solvent was evaporated and the residue concentrated under reduced pressure. The compound was purified over silica gel using DCM/IPA/Acetone (86:4:10) as eluent to give **111a** (0.12 g, 66%) as a white amorphous solid; mp: 148-150 °C (lit.[4] 151-153 °C for the corresponding unlabeled compound); δ_H (300 MHz; $CDCl_3$) 1.36 (3 H, s, CH_3), 1.61 (3 H, s, CH_3), 3.79 (0.2 H, d, *J* 1.8, 5'-H_a), 3.98 (0.8 H, d, *J* 1.5, 5'-H_b), 4.51-4.54 (1 H, m, 4'-H), 5.10 (1 H, dd, *J* 5.9 and 1.3, 3'-H), 5.23 (1 H, dd, *J* 4.8 and 5.9, 2'-H), 5.96 (1 H, d, *J* 4.8, 1'-H), 7.5 and 8.0 (5 H, m, Ar), 8.08 (1 H, s, 8-H), 8.70 (1 H, s, 2-H), 9.20 (1 H, br s, NHCOAr); δ_C (75 MHz; $CDCl_3$) 25.6 (CH_3), 27.9 (CH_3), 63.0 (t, *J* 18, C-5'), 81.9, 83.7, 86.7, 94.2 (C-1', C-2', C-3', C-4'), 114.6 ($\underline{C}Me_2$), 128.4 (CH Ar), 129.1 (CH Ar), 133.2 (CH Ar), 133.8 (C Ar), 124.5 (C-5), 142.9 (C-8), 150.7, 151.0 (C-4, C-6), 152.7 (C-2), 165.3 (NH$\underline{C}$OAr); ***m/z*** (ESI+) 413.38 [M+H] (100%).

Procedure B:[5]

A solution of N^6-benzoyl-2',3'-*O*-isopropylideneadenosine-5'-aldehyde **113** (0.90 g, 2.2 mmol) and LiI (3.6 g, 26.9 mmol) in THF (20 cm^3) was stirred at ambient temperature for 10 min and then at -78 °C for 50 min. *t*-Amyl alcohol (2.9 cm^3, 26.6 mmol) was added to a suspension containing $LiAlD_4$ (0.37 g; 8.9 mmol) in THF (50 cm^3) and the mixture was stirred at ambient temperature for 20 min and then at -78 °C for an additional 20 min. This solution was then added to the adenosine solution by syringe, and the reaction mixture was stirred at -78 °C over 3 h. After 15 min, 2 N NaOH (3 cm^3) was added and the resultant mixture was stirred for an additional 20 min. The precipitate was filtered and the solution was concentrated under reduced pressure. The residue was partitioned between water and DCM and the organic phase dried over $MgSO_4$ and then concentrated. The residue was then purified over silica gel using DCM/IPA/Acetone (86:4:10) as the eluent to give **111a** (0.32 g, 35%) as an amorphous white solid. Physical and spectroscopic properties were identical to that previously given for **111a** (7.2.6 procedure A).

7.2.7 (5'*R*)-[$^2H_1$]-2',3'-*O*-Isopropylideneadenosine 100a[3]

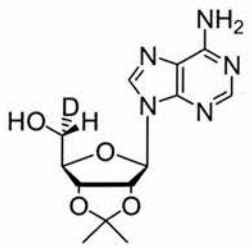

100a

A solution of (5'*R*)-[$^2H_1$]-N^6-benzoyl-2',3'-*O*-isopropylideneadenosine **111a** (0.125 g, 0.30 mmol) in methanolic ammonia (50%, 15 cm^3) was kept at ambient temperature for 24 h and then evaporated to dryness. The residue was purified over silica gel using DCM/IPA/Acetone (84:6:10) as eluent to give **100a** (0.080 g, 86%) as a white amorphous solid. mp: 220-222 °C (lit.[6] 220-221 °C); δ_H (300 MHz; CD_3OD) 1.38 (3 H, s, CH_3), 1.62 (3 H, s, CH_3), 3.70 (1 H, d, *J* 3.8, 5'-H_a), 3.78 (1 H, d, *J* 3.4, 5'-H_b), 4.35-4.39 (1 H, m, 4'-H), 5.04 (1 H, dd, *J* 6.1 and 2.3, 3'-H), 5.28 (1 H, dd, *J* 3.6 and 6.1, 2'-H), 6.15 (1 H, d, *J* 3.6, 1'-H), 8.20 (1 H, s, 8-H), 8.34 (1 H, s, 2-H); δ_C (75 MHz; CD_3OD) 25.5 (CH_3), 27.6 (CH_3), 63.2 (t, *J* 22.0, C-5'), 83.0, 85.3, 88.0, 92.9 (C-1', C-2', C-3', C-4'), 115.3 ($\underline{C}Me_2$), 141.7 (C-8), 153.8 (C-2), 120.7 (C-5), 150.0 (C-4), 157.5 (C-6); ***m/z*** (ESI+) 309.14 [M+H] (100%).

7.2.8 (5'*R*)-[$^2H_1$]-2',3'-*O*-isopropylidene-5'-*O*-mesyladenosine 116a[7]

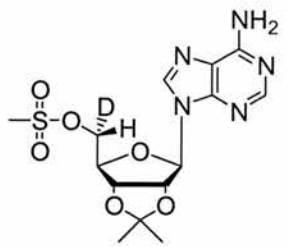

116a

Methanesulfonyl chloride (0.19 cm^3, 2.44 mmol) was added dropwise to a solution of (5'*R*)-[$^2H_1$]-2',3'-*O*-isopropylideneadenosine **100a** (0.375 g, 1.22 mmol) in anhydrous pyridine (20 cm^3) at 0 °C. The reaction mixture was left to warm to ambient temperature over 3 h. Cold water (20 cm^3) was added and the reaction mixture was concentrated and partitioned between DCM and water. The organic layer was washed with water, dried over $MgSO_4$ and concentrated. Purification over silica gel eluting with DCM/IPA/Acetone (84:6:10) afforded the mesylate **116a** (0.344 g, 73%) as a white amorphous solid; m.p.: 140 °C dec.; δ_H (300 MHz; $CDCl_3$) 1.36 (3 H, s, CH_3), 1.59 (3 H, s, CH_3), 2.89 (3 H, s, SO_2CH_3), 4.39 (0.2 H, d, *J* 6.2, 5'-H_a), 4.45 (0.8 H, d, *J* 4.6, 5'-H_b), 4.49-4.53 (1 H, m, 4'-H), 5.13 (1 H, dd, *J* 6.3 and 3.2, 3'-H), 5.44 (1 H, dd, *J* 6.3 and 2.0, 2'-H), 5.87 (2 H, br s, NH_2), 6.13 (1 H, d, *J* 2.0, 1'-H), 7.90 (1 H, s, 8-H), 8. 31 (1 H, s, 2-H); δ_C (75 MHz; $CDCl_3$) 25.3 (CH_3), 27.0 (CH_3), 37.5 (SO_2-CH_3), 68.3 (t, *J* 23.0, CH_2), 81.3, 84.0, 84.7, 90.8 (C'-1, C'-2, C'-3, C'-4), 114.7 ($\underline{C}Me_2$), 120.1 (C-5), 139.9 (C-8), 149.0 (C-4) 153.1 (C-2), 155.9 (C-6); ***m/z*** (ESI+) 387.1197 [M+H. $C_{14}H_{18}DN_5O_6S$ requires 387.1204] (7%).

7.2.9 (5'*S*)-[$^2H_1$]-2',3'-*O*-Isopropylidene-5'-fluoro-5'-deoxyadenosine 118[8]

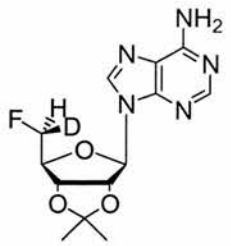

118

A solution of TBAF in THF (1 M, 1.2 cm^3, 1.2 mmol, 2.6 eq.) was added to a solution of (5'*R*)-[$^2H_1$]-2',3'-*O*-isopropylidene-5'-*O*-mesyladenosine **116a** (0.18 g, 0.46 mmol) in acetonitrile (20 cm^3) at ambient temperature and the resulting solution was heated under reflux for 3 h. The reaction was cooled to ambient temperature and concentrated and the resultant oil was partitioned between chloroform and water. The organic layer was washed with water and dried over $MgSO_4$, and the product was purified over silica gel eluting with DCM/Acetone/IPA (84:10:6) to afford the title compound **118** (0.050 g, 35%) as a light brown powder; mp: 157-159 °C (lit.[9] 159-160 °C for the corresponding unlabelled compound); δ_H (300 MHz; $CDCl_3$) 1.40 (3 H, s, CH_3), 1.64 (3 H, s, CH_3), 4.35-4.65 (2 H, m, 4'-H and 5'-H_a/5'-H_b), 5.10 (1 H, dd, *J* 6.3 and 3.8, 3'-H), 5.37 (1 H, dd, *J* 6.3 and 1.9, 2'-H), 5.68 (2 H, br s, NH_2), 6.19 (1 H, d, *J* 1.9, 1'-H), 7.93 (1 H, s, 8-H) and 8.36 (1 H, s, 2-H); δ_F (500 MHz; $CDCl_3$); -229.3 (t, *J* 6.7, 0.8F-$D_{5'b}$), -229.27 (t, *J* 7.3, 0.2F-$D_{5'a}$); δ_C (75 MHz; $CDCl_3$) 25.7 (CH_3), 27.5 (CH_3), 81.5 (d, *J* 6.7, C-3'), 82.5 (dt, *J* 170 and 23, C-5') 84.9 (C-2'), 85.9 (d, *J* 19.5, C-4'), 91.3 (C-1'), 115.0 (CMe_2), 120.4 (C-5), 139.7 (C-8), 149.7 (C-4), 153.1 (C-2) and 155.7 (C-6); ***m/z*** (ES+) 311.1378 [M + H. $C_{13}H_{15}DN_5O_3F$ requires 311.1380] (100%).

7.2.10 (5'*S*)-[$^2H_1$]-5'-Fluoro-5'-deoxyadenosine 60a {(5'*S*)-[$^2H_1$]-5'-FDA}[3]

60a

A solution of (5'*S*)-[$^2H_1$]-2',3'-*O*-isopropylidene-5'-fluoro-5'-deoxyadenosine **118** (0.047 g, 0.15 mmol) in trifluoroacetic acid-water (9:1; 7 cm^3) was stirred at ambient temperature for 25 min and then evaporated to dryness. The residue was co-evaporated with ethanol several times, then triturated with ether and finally crystallised from methanol to give **60a** as a white solid (0.033 g, 81%); m.p.: 206-207 °C (lit.[10] 205-206 °C for the corresponding unlabelled compound); δ_H (300 MHz; D_2O) 4.35 (1 H, ddd, *J* 30.0, 5.0 and 3.30, 4'-H), 4.49 (1 H, t, *J* 5.0, 3'-H), 4.70 (1 H, t, *J* 5.0, 2'-H), 4.68 (0.8 H, dd, *J* 3.30 and 45.9, 5'-H_a), 4.73 (0.2 H, dd, *J* 2.50 and 47.60, 5'-H_b), 6.11 (1 H, d, *J* 5.0, 1'-H), 8.25 (1 H, s, 8-H), 8.33 (1 H, s, 2-H); δ_F (282 MHz; D_2O): -232.3 (br s); δ_C (HSQC-HMBC; 75 MHz; CD_3OD) 69.3 (C-3'), 73.9 (C-2'), 81.4 (d, *J* 180, C-5'), 82.6 (C-4'), 88.4 (C-1'), 119.2 (C-5), 139.0 (C-8), 148.8 (C-4), 152.3 (C-2) and 155.9 (C-6); ***m/z*** (ES+) 271.1062 [M+H. $C_{10}H_{11}DN_5O_3F$ requires 271.1065] (100%).

7.2.11 (5'*R*)-[$^2H_1$]-Adenosine triphosphate 59a {(5'*R*)-[$^2H_1$]-ATP}[11,12]

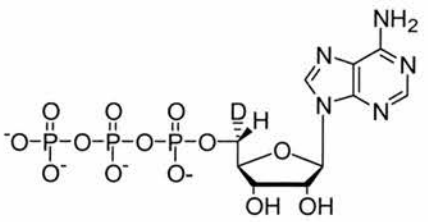

59a

A solution of 2-chloro-4*H*-1,2,3-benzodioxaphosphorin-4-one in dioxane (1 M, 0.52 cm^3, 0.52 mmol), was added to a solution of (5'*R*)-[$^2H_1$]-2',3'-*O*-isopropylideneadenosine **100a** in pyridine (0.4 cm^3) and dioxane (1.2 cm^3). After 20 min, a solution of tributyl-ammonium pyrophosphate[19] in DMF (0.5 M, 1.28 cm^3, 0.64 mmol) and tri-ethylamine (0.52 cm^3) was added. The reaction mixture was stirred for 30 min and then a solution of 1% iodine (8 cm^3, 0.31 mmol) in pyridine/water (98:2) was added. After 20 min, the excess iodine was destroyed by addition of 5% aq. $NaHSO_3$. The resultant residue was dissolved in water and the aq. layer washed with DCM. After evaporation of the organic solvent the residue was dissolved in water (37.5 cm^3) and an aq. solution of 50% TFA (10 cm^3) was added. The mixture was stirred for 30 min, adjusted to pH 8.5 by addition of aq. 0.1 N NaOH, and the solvent was evaporated to dryness. The residue was then washed with EtOAc and the crude product **59a** was dried under reduced pressure; δ_P (121.5 MHz; D_2O): δ= - 8.9 (d, *J* 21.16, Pγ), -9.4 (d, *J* 18.4, Pα), -19.5 (t, Pβ); ***m/z*** (ES-) 551.3 [M+2Na-H; unlabelled 550] (32%).

7.2.12 2',3'-*O*-Isopropylidene-5'-*O*-nitroadenosine 99

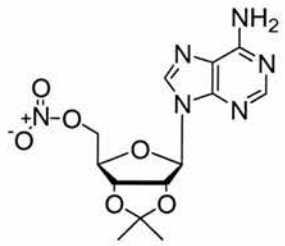

99

Procedure A:[13]

60% Nitric acid (2.5 cm^3) was added gradually to acetic anhydride (20 cm^3) with stirring, while keeping the temperature between 15-20 °C by external cooling. With continued vigorous stirring the mixture was cooled to -30 °C and 2',3'-*O*-isopropylideneadenosine **100** (0.615 g, 2 mmol) was added. After 15 min at -30 °C the slurry formed was poured into ice-water (50 cm^3), which after addition of EtOAc (100 cm^3) was neutralized by portionwise addition of $NaHCO_3$, until carbon dioxide formation ceased. The organic phase was dried over $MgSO_4$, evaporated and finally the residue was purified over silica gel eluting with DCM/IPA (92:8) to afford **99** as a white amorphous solid (0.35 g, 50%); mp: 136 °C (lit.[13] 137-138 °C); elemental analysis Found C, 43.75, H, 4.57, N, 23.71. $C_{12}H_{16}N_6O_6$ requires C, 44.32, H, 4.58, N, 23.85; δ_H (300 MHz; $CDCl_3$) 1.34 (3 H, s, CH_3), 1.55 (3 H, s, CH_3), 4.43-4.50 (1 H, m, 4'-H), 4.62-4.77 (2 H, m, 5'-$H_{a/b}$), 5.15 (1 H, dd, *J* 6.2 and 3.4, 3'-H), 5.42 (1 H, dd, *J* 6.2 and 1.7, 2'-H), 6.08 (1 H, d, *J* 1.7, 1'-H), 6.92 (2 H, br s, NH_2), 7.85 (1 H, s, 8-H), 8.25 (1 H, s, 2-H); δ_C (75 MHz; $CDCl_3$) 25.6 (CH_3), 27.4 (CH_3), 72.5 (CH_2), 82.1, 84.1, 84.4, 91.2 (C-1', C-2', C-3', C-4'), 115.1 ($\underline{C}Me_2$), 120.5 (C-5), 140.3 (C-8), 153.4 (C-2), , 149.2 (C-4), 156.5 (C-6); ***m/z*** (ESI+) 353.06 [M+H] (100%).

Procedure B:[14,15]

Triflic acid (0.33 cm^3, 0.56 g, 3.7 mmol) was added slowly to a solution of 2',3'-*O*-isopropylideneadenosine **100** (0.77 g, 2.5 mmol) and 1-nitropyrazole (0.42 g, 3.7 mmol) in dry CH_3CN (30 cm^3) at ambient temperature and under a nitrogen atmosphere. Stirring was continued for 24 h, volatiles were then evaporated and the residue was dissolved in $CHCl_3$. The solution was washed with water, dried over $MgSO_4$, evaporated and finally the residue purified over silica gel eluting with DCM/IPA (92:8) to afford **99** as an amorphous white solid (0.15 g, ~12%). Physical and spectroscopic properties were identical to that previously given for **99** (7.2.12 procedure A).

7.2.13 2',3'-*O*-Isopropylidene-9-(β-D-*erythro*-furanosyl)adenosine 104[14]

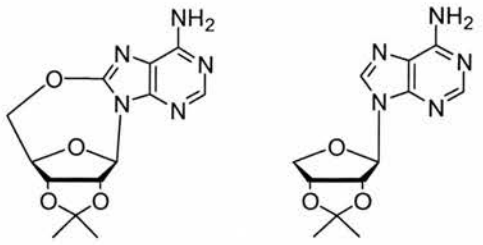

105 104

A solution of 2',3'-*O*-isopropylidene-5'-*O*-nitroadenosine **99** (0.24 g, 0.68 mmol), AIBN (0.02 g, 0.12 mmol) and Bu_3SnH (0.92 cm^3, 0.99 g, 3.4 mmol) in dried *o*-xylene was de-oxygenated for 30 min under nitrogen and was then heated under reflux for 1 h. Volatiles were evaporated and the residue was purified over silica gel eluting with DCM/IPA (88:12) to afford **1004** contaminated with **105** (*ratio* **104**:**105** varies from 40:60% to 60:40%). The contaminant **105** was removed from the mixture by several crystallizations from methanol which afforded **104** with ~95% of purity as an amorphous white solid; δ_H (300 MHz; $CDCl_3$) 1.42 (3 H, s, CH_3), 1.59 (3 H, s, CH_3), 4.24 (1 H, d, *J* 10.2, 4'-H), 4.32 (1 H, dd, *J* 10.2 and 3.5, 4'-H), 5.29 (1 H, dd, *J* 6.0 and 3.5, 3'-H), 5.51 (1 H, d, *J* 6.0, 2'-H), 5.78 (2 H, br s, NH_2), 6.03 (1 H, s, 1'-H), 7.86 (1 H, s, 8-H), 8.33 (1 H, s, 2-H); δ_C (HSQC-HMBC; 75 MHz; $CDCl_3$) 24.7 (CH_3), 26.5 (CH_3), 75.7 (C-4'), 81.5 (C-3'), 84.2 (C-2'), 91.2 (C-1'), 113.0 ($\underline{C}Me_2$), 119.9 (C-5), 139.9 (C-8), 149.5 (C-4), 153.4 (C-2), 155.0 (C-6); ***m/z*** (ESI+) 278.13 [M+H] (10%).

7.2.14 9-(β-D-*Erythro*-furanosyl)adenosine 83[14]

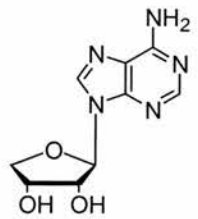

83

A suspension of 2',3'-*O*-isopropylidene-erythroadenosine **104** (0.040 g, 70 to 90% purity) in 50:50 TFA/H_2O (7 cm^3) was stirred at ambient temperature for 15 min and then the solution was evaporated. Several re-evaporations from ethanol gave a colourless residue which was purified over silica gel eluting with EtOAc/MeOH (85:15) to afford **83** (0.010 g) as an amorphous white solid; mp: 230-231 °C (lit.[16] 230-232 °C); δ_H (300 MHz; D_2O) 4.01-4.08 (1 H, m, 4'-H_S), 4.45-4.57 (2 H, m, 4'-H_R/3'-H), 4.85-4.95 (1 H, m, 2'-H), 6.0 (1 H, d, *J* 7.0, 1'-H), 8.15 (1 H, s, 8-H), 8.27 (1 H, s, 2-H); δ_C (HSQC-HMBC; 75 MHz; CD_3OD) 71.9 (C-3'), 75.1 (C-4'), 76.2 (C-2'), 90.1 (C-1'), 119.2 (C-5), 141.8 (C-8), 150.9 (C-4), 154 (C-2), 157.5 (C-6); ***m/z*** (ES+) 238.0945 [M+H. $C_9H_{12}N_5O_3$ requires 238.0940] (30%).

7.2.15 2-Hydroxy-oct-3-yne 164[17,18]

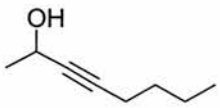

164

A solution of *n*-BuLi (2.5 M in hexane, 2.44 cm^3, 6.10 mmol) was added to a THF (30 cm^3) solution of 1-hexyne **163** (0.5 g, 6.09 mmol) at -78 °C, and the mixture was stirred for 20 min. Acetaldehyde **57** (0.308 g, 7.0 mmol) was then added, and the reaction mixture was warmed to 0 °C and stirred for 2 h. A sat. NH_4Cl solution (25 cm^3) was then added and the mixture extracted into EtOAc (2 x 50 cm^3). The organic layer was dried over $MgSO_4$, evaporated and the organic residue purified over silica gel eluting with hexane:EtOAc (90:10) to afford **164** as colourless oil (0.475 g, 62%); δ_H (300 MHz; $CDCl_3$) 0.87 (3 H, t, *J* 7.2, $CH_2C\underline{H}_3$), 1.38 (3 H, d, *J* 6.5, $CHC\underline{H}_3$), 1.29-1.50 (4 H, m, CH_2CH_2), 2.15-2.20 (2 H, m, $C{\equiv}CCH_2$), 2.40 (1 H, br s, OH), 4.47 (1 H, qt, *J* 6.5 and 1.9, CH); δ_C (75 MHz; $CDCl_3$) 13.9 (CH_3), 18.6 (CH_2), 22.2 (CH_2), 25.1 ($CH\underline{C}H_3$), 31.1 ($C{\equiv}C\underline{C}H_2$), 58.8 (CH), 82.7 ($\underline{C}{\equiv}CCHOH$), 84.8 ($C{\equiv}\underline{C}CHOH$); ***m/z*** (ES+) 149.0948 [M + Na. $C_8H_{14}ONa$ requires 149.0942] (15%).

7.2.16 2-(*tert*-Butyldiphenylsilanoyloxy)-oct-3-yne 162[19]

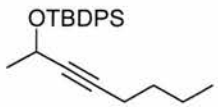

162

Anhydrous pyridine (0.85 g, 10.8 mmol) was added to a stirred solution of **164** (0.271 g, 2.15 mmol) in THF (10 cm^3) under a nitrogen atmosphere, followed by $AgNO_3$ (0.441 g, 2.60 mmol). After 10 min in the dark, *tert*-butylchlorodiphenylsilane (0.77 g, 2.80 mmol) was added, and stirring continued for an additional 3 h. The reaction mixture was filtered, and the filter cake washed with ether (30 cm^3). The combined filtrate was washed with water (20 cm^3), saturated $CuSO_4$ solution (20 cm^3) and water (20 cm^3). The organic layer was then dried over $MgSO_4$, evaporated and the organic residue purified over silica gel eluting with hexane:EtOAc (90:10) to afford **162** as colourless oil (0.548 g, 70%); δ_H (300 MHz; $CDCl_3$) 0.91 (3 H, t, *J* 7.20, $CH_2C\underline{H}_3$), 1.11 (9 H, s, 3 x CH_3), 1.41 (3 H, d, *J* 6.45, $CHC\underline{H}_3$), 1.32-1.47 (4 H, m, CH_2CH_2), 2.08-2.16 (2 H, m, $C{\equiv}CCH_2$), 4.51 (1 H, qt, *J* 6.45 and 1.93, CH), 7.36-7.49 (6 H, m, 2 x 3 H aromatic), 7.70-7.84 (4 H, m, 2 x 2 H aromatic); δ_C (75 MHz; $CDCl_3$) 14.1 (CH_3), 18.7 (CH_2), 19.6 [$\underline{C}(CH_3)_3$], 22.3 (CH_2), 26.0 ($CH\underline{C}H_3$), 27.3 [$C(\underline{C}H_3)_3$], 31.0 ($C{\equiv}C\underline{C}H_2$), 60.6 (CH), 83.0 ($\underline{C}{\equiv}CCHOH$), 84.6 ($C{\equiv}\underline{C}CHOH$) 127.7 (CH Ar), 127.9 (CH Ar), 129.9 (CH Ar), 130.0 (CH Ar), 134.4 (C Ar), 134.5 (C Ar), 136.2 (CH Ar), 136.4 (CH Ar); ***m/z*** (ESI+) 387.2114 [M + Na. $C_{24}H_{32}OSiNa$ requires 387.2120] (100%); ν_{max} (neat)/cm^{-1} 3072, 2932, 2235 (C≡C), 1955, 1888, 1821, 1589, 1427, 1106, 701.

7.2.17 2-(*tert*-Butyldiphenylsilanoyloxy)-octane-3,4-dione 165[20]

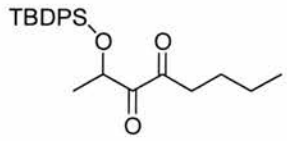

165

A solution of 2-(*tert*-butyldiphenylsilanoyloxy)-oct-3-yne **162** (0.13 g, 0.357 mmol) in methanol (10 cm^3) was treated with ozone gas at -18/-20 °C. After 40 min, a solution of PPh_3 (0.112 g, 0.428 mmol, 1.2 eq.) in ether (5 cm^3) was added to the mixture, and the reaction was stirred for 20 min at -20 °C. It was then warmed to ambient temperature and left for 24 h. The solvent was then evaporated and the residue purified over silica gel eluting with hexane:EtOAc (30:70) to afford **165** as yellow oil (0.113 g, 80%); δ_H (300 MHz; $CDCl_3$) 0.90 (3 H, t, *J* 7.2, $CH_2C\underline{H}_3$), 1.10 (9 H, s, 3 x CH_3), 1.41 (3 H, d, *J* 6.8, $CHC\underline{H}_3$), 1.22-1.36 (2 H, m, $C\underline{H}_2CH_3$), 1.42-1.54 (2 H, m, $C\underline{H}_2CH_2CH_3$), 2.45-2.67 (2 H, m, CH_2CO), 4.92 (1 H, q, *J*6.8, CH), 7.34-7.49 (6 H, m, 2 x 3 H aromatic), 7.61-7.71 (4 H, m, 2 x 2 H aromatic); δ_C (75 MHz; $CDCl_3$) 14.2 (CH_3), 19.6 [$\underline{C}(CH_3)_3$], 20.3 ($CH\underline{C}H_3$), 22.6 (CH_2), 25.1 (CH_2), 27.2 [$C(\underline{C}H_3)_3$], 37.3 ($CO\underline{C}H_2$), 71.1 (CH), 128.1 (CH Ar), 128.2 (CH Ar), 130.3 (CH Ar), 130.4 (CH Ar), 133.2 (C Ar) 133.8 (C Ar), 136.1 (CH Ar), 136.3 (CH Ar), 200.4 (CO), 201.9 (CO); ***m/z*** (CI+) 397.2210 [M + H. $C_{24}H_{33}O_3Si$ requires 397.2199] (100%); ν_{max} (neat)/cm^{-1} 3072, 2933, 1714 (C=O), 1428, 1112, 703.

7.2.18 3-(*tert*-Butyldiphenylsilanoyloxy)-butyne 169[19,21]

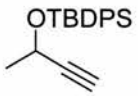

169

Pyridine (0.85 g, 10.75 mmol) was added to a stirred solution of 3-butyn-2-ol **168** (0.151 g, 2.15 mmol) in THF (8 cm^3) under a nitrogen atmosphere, followed by $AgNO_3$ (0.441 g, 2.60 mmol). After 10 min in the dark, *tert*-butylchlorodiphenylsilane (0.77 g, 2.80 mmol) was added, and stirring continued for an additional 3 h. The reaction mixture was filtered, and the filter cake washed with ether (30 cm^3). The combined filtrate was washed with water (20 cm^3), saturated $CuSO_4$ solution (20 cm^3) and again water (20 cm^3). The organic layer was then dried over $MgSO_4$, evaporated and the organic residue purified over silica gel eluting with hexane:EtOAc (90:10) to afford **169** as colourless oil (0.556 g, 84%); δ_H (300 MHz; $CDCl_3$) 1.11 (9 H, s, 3 x CH_3), 1.42 (3 H, d, *J* 6.5, $CHC\underline{H}_3$), 2.36 (1 H, d, *J* 2.1, C≡CH), 4.48 (1 H, dq, *J* 6.5 and 2.1, $C\underline{H}CH_3$), 7.36-7.50 (6 H, m, 2 x 3 Ar), 7.68-7.80 (2 H, m, 2 x 2 Ar); δ_C (75 MHz; $CDCl_3$) 19.6 [$\underline{C}(CH_3)_3$], 25.6 ($CH\underline{C}H_3$), 27.2 [$C(\underline{C}H_3)_3$], 60.2 ($\underline{C}HCH_3$), 71.9 (C≡$\underline{C}$H) 86.5 ($\underline{C}$≡CH), 127.9 (CH Ar), 128.0 (CH Ar), 130.1 (CH Ar), 130.2 (CH Ar), 133.8 (C Ar), 134.1 (C Ar), 136.2 (CH Ar), 136.4 (CH Ar); ***m/z*** (ESI+) 331.1484 [M + Na. $C_{20}H_{24}OSiNa$ requires 331.1494] (100%). ν_{max} (neat)/cm^{-1} 3305 (≡C-H), 2932, 2117 (C≡C, weak), 1960, 1891, 1824, 1474, 1058, 740, 702.

7.2.19 3-(*tert*-Butyldiphenylsilanoyloxy)-1-bromobutyne 167[22]

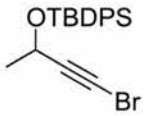

167

A solution of 3-(*tert*-butyldiphenylsilanoyloxy)-butyne **169** (0.57 g, 1.85 mmol) in acetone (20 cm^3) was treated at ambient temperature with *N*-bromosuccinimide (0.4 g, 2.25 mmol) and $AgNO_3$ (0.025 g, 0.147 mmol). After 40 min, cold water was slowly added and then the mixture was concentrated and the residue partitioned between EtOAc (20 cm^3) and water (20 cm^3). The organic layer was further washed with water (20 cm^3), dried over $MgSO_4$, evaporated and finally purified over silica gel eluting with hexane/EtOAc (90:10), to give **167** as yellowish oil (0.614 g, 86%); δ_H (300 MHz; $CDCl_3$) 1.11 (9 H, s, 3 x CH_3), 1.42 (3 H, d, *J* 6.5, $CHC\underline{H}_3$), 4.48 (1 H, q, *J* 6.5, $C\underline{H}CH_3$), 7.36-7.50 (6 H, m, 2 x 3 Ar), 7.68-7.80 (2 H, m, 2 x 2 Ar); δ_C (75 MHz; $CDCl_3$) 19.6 [$\underline{C}(CH_3)_3$], 25.4 ($CH\underline{C}H_3$), 27.3 [$C(\underline{C}H_3)_3$], 61.2 ($\underline{C}HCH_3$), 44.3 ($C\equiv\underline{C}Br$) 82.7 ($\underline{C}\equiv CBr$), 128.0 (CH Ar), 128.1 (CH Ar), 130.1 (CH Ar), 130.2 (CH Ar), 133.7 (C Ar), 133.9 (C Ar), 136.2 (CH Ar), 136.4 (CH Ar); ***m/z*** (ESI+) 409.0589 [M + Na. $C_{20}H_{23}{}^{79}BrONaSi$ requires 409.0599] (80%) and 411.0586 [M + Na. $C_{20}H_{23}{}^{81}BrONaSi$ requires 411.0579] (100%); ν_{max} (neat)/cm^{-1} 3072, 2931, 2208 (C≡C), 1960, 1891, 1825, 1589, 1427, 1105, 739, 701.

7.2.20 1,5-Dihydroxyhex-3-yne 174[17,18]

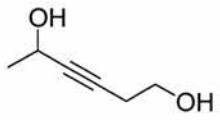

174

A solution of *n*-BuLi (2.5 M in hexane, 5.7 cm^3, 14.3 mmol) was added to a THF (30 cm^3) solution of 3-butyn-1-ol **175** (0.5 g, 7.13 mmol) at -78 °C, and the mixture was stirred for 20 min. Acetaldehyde **57** (0.314 g, 7.13 mmol) was then added, and the reaction mixture was warmed to 0 °C and stirred for 2 h. A sat. NH_4Cl solution (25 cm^3) was then added and the mixture was extracted into EtOAc (2 x 50 cm^3). The organic layer was dried over $MgSO_4$, evaporated and the organic residue purified over silica gel eluting with hexane:EtOAc, (50:50) to afford **174** as colourless oil (0.285 g, 35.0%); δ_H (300 MHz; $CDCl_3$) 1.37 (3 H, d, *J* 6.6, $CHC\underline{H}_3$), 2.39 (2 H, dt, *J* 6.1 and *J* 2.0, $C{\equiv}CC\underline{H}_2$), 3.65 (2 H, t, *J* 6.1, $C{\equiv}CCH_2C\underline{H}_2$), 4.45 (1 H, qt, *J* 6.6 and *J* 2.0, $C\underline{H}CH_3$); δ_C (75 MHz; $CDCl_3$) 22.9 ($C{\equiv}C\underline{C}H_2$), 24.4 ($CH_3$), 58.1 (CH), 60.7 ($CH_2OH$), 81.4 ($\underline{C}{\equiv}CCHOH$), 84.0 ($C{\equiv}\underline{C}CHOH$); ***m/z*** (ESI+) 137.0580 [M + Na. $C_6H_{10}O_2Na$ requires 137.0578] (100%); ν_{max} (neat)/cm^{-1} 3333 (br OH), 2980, 2249 (C≡C), 1420, 1331, 1155, 1046.

7.2.21 Toluene-4-sulfonic acid 5-hydroxy-hex-3-ynyl ester 176[23]

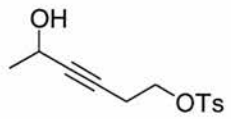

176

Tosyl chloride (0.40 g, 2.1 mmol) was added to a solution of 1,5-dihydroxyhex-3-yne **174** (0.20 g, 1.75 mmol) in pyridine (10 cm^3), followed by catalytic amount of DMAP (0.010 g, 0.082 mmol, ~5 %). The reaction was stirred under nitrogen for 5 h. After addition of a small amount of water, the solvent was evaporated. The residue was then dissolved in EtOAc (20 cm^3) and was washed with water (20 cm^3), saturated $CuSO_4$ solution (20 cm^3) and water (20 cm^3). The organic layer was then dried over $MgSO_4$, evaporated and the organic residue purified over silica gel eluting with hexane:EtOAc (60:40) to afford **176** as colourless oil (0.328 g, 70%); δ_H (300 MHz; $CDCl_3$) 1.38 (3 H, d, *J* 6.6, $CHC\underline{H}_3$), 2.45 (3 H, s, CH_3Ar), 2.57 (2 H, dt, *J* 7.0 and *J* 1.9, $C{\equiv}CCH_2$), 4.98 (2 H, t, *J* 7.0, $C{\equiv}CCH_2C\underline{H}_2$), 4.44 (1 H, qt, *J* 6.6 and *J* 1.90, $C\underline{H}CH_3$), 7.36 (2 H, d, *J* 8.1, Ar), 7.80 (2 H, d, *J* 8.1, Ar); δ_C(75 MHz; $CDCl_3$) 19.7 ($C{\equiv}C\underline{C}H_2$), 21.7 ($CH_3$), 24.4 ($CH_3$), 58.3 (CH), 67.7 ($CH_2OH$), 78.4 ($\underline{C}{\equiv}CCHOH$), 84.6 ($C{\equiv}\underline{C}CHOH$), 128.0 (CH Ar), 130.0 (CH Ar), 132.8 (C Ar), 145.1 (C Ar); ***m/z*** (ESI+) 291.0666 [M + Na. $C_{13}H_{16}O_4SNa$ requires 291.0667] (100%); ν_{max} (neat)/cm^{-1} 3387 (br OH), 2982, 2252 (C≡C), 1925, 1810, 1720, 1598, 1451, 1361, 1177, 1096, 981, 770.

7.2.22 Toluene-4-sulfonic acid 5-(triisopropylsilanoyloxy)-hex-3-ynyl ester 173[24]

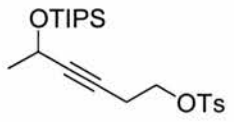

173

TIPS-triflate (0.408 g, 1.33 mmol) was added dropwise to a solution of toluene-4-sulfonic acid 5-hydroxyhex-3-ynyl ester **176** (0.30 g, 1.12 mmol) in DCM (10 cm^3) and 2,6-lutidine (0.517 g, 4.44 mmol), at 0 °C and under nitrogen atmosphere. The mixture was left to warm to ambient temperature and after 45 min the reaction was worked up. After addition of a small amount of water, the solvent was evaporated and the residue was dissolved in EtOAc (20 cm^3) and washed with water (20 cm^3). The organic layer was then dried over $MgSO_4$, evaporated and the organic residue purified over silica gel eluting with hexane:EtOAc (95:5) to give **173** as colourless oil (~100%); δ_H (300 MHz; $CDCl_3$) 1.02-1.08 [21 H, m, 3 x $CH(CH_3)_2$)], 1.37 (3 H, d, *J* 6.4, $CHC\underline{H}_3$), 2.45 (3 H, s, CH_3Ar), 2.55 (2 H, dt, *J* 7.30 and 1.86, $C{\equiv}C\underline{C}H_2$), 4.05 (2 H, t , *J* 7.3, CH_2OTs), 4.54 (1 H, qt, *J* 6.4 and 1.9, $C\underline{H}CH_3$), 7.35 (2 H, d, *J* 8.2, Ar), 7.80 (2 H, d, *J* 8.2, Ar); δ_C (75 MHz; $CDCl_3$) 12.5 [3 x $\underline{C}H(CH_3)_2$], 18.32 and 18.35 [3 x $CH(\underline{C}H_3)_2$], 20.0 ($C{\equiv}C\underline{C}H_2$), 22.1 ($\underline{C}H_3Ar$), 26.0 ($CH\underline{C}H_3$), 59.3 ($\underline{C}HCH_3$), 68.1 ($\underline{C}H_2OTs$), 77.5 ($C{\equiv}\underline{C}CH_2$), 85.9 ($C{\equiv}\underline{C}CHOH$), 128.3 (CH Ar), 130.3 (CH Ar), 133.3 (C Ar), 145.3 (C Ar); ***m/z*** (ESI+) 447.2013 [M + Na. $C_{22}H_{36}O_4SSiNa$ requires 447.2001] (100%); ν_{max} (neat)/cm^{-1} 2943, 2235 (C≡C, weak), 1464, 1367, 1178, 1100, 984, 760.

7.2.23 1-Bromo-4-hydroxypent-2-yne 180[25]

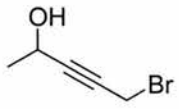

180

Procedure A

A solution of LDA (2.0 M in THF/*n*-heptane, 8.4 cm^3, 16.8 mmol) was added to a THF (30 cm^3) solution of propargyl bromide **179** (80% solution in toluene, 2.0 g, 16.80 mmol) at – 78 °C, and the mixture was stirred for 5 min. Acetaldehyde **57** (0.75 g, 17.03 mmol) was then added, and the reaction mixture was warmed to 0 °C and stirred for 2 h. A sat. NH_4Cl solution (25 cm^3) was then added and the mixture was extracted into EtOAc (2 x 50 cm^3). The organic layer was dried over $MgSO_4$, evaporated and the organic residue purified over silica gel eluting with hexane:EtOAc (90:10) to afford **180** as dark yellow oil (1.64 g, 60%); δ_H (300 MHz; $CDCl_3$) 1.42 (3 H, d, *J* 6.6, $CHC\underline{H}_3$), 3.93 (2 H, d, *J* 1.8, CH_2Br), 4.57 (1 H, qt, *J* 6.6 and 1.8, $C\underline{H}CH_3$); δ_C (75 MHz; $CDCl_3$) 14.4 (CH_2), 24.0 (CH_3), 58.2 (CH), 79.1 ($C\equiv\underline{C}CH_2$), 90.1 ($C\equiv\underline{C}CHOH$); ***m/z*** (ESI+) 184.93 (Br^{79}, 90%) and 186.93 (Br^{81}, 100%) [M + Na]; ν_{max} (neat)/cm^{-1} 3345 (O-H, broad), 2983, 2252 (C≡C, weak), 1079.

Procedure B:[8]

183 180

Triphenylphosphine (3.15 g, 12 mmol) and CBr_4 (3.31 g, 10 mmol) were added to a solution of 1,4-dihydroxypent-2-yne* **183** (0.50 g, 5 mmol) in anhydrous DCM (30 cm^3) at ambient temperature and the reaction was left to stir. After 2 h additional CBr_4 (3.31 g, 10 mmol) was added and the reaction was then left to stir for a further 12 h. The solvent was removed under reduced pressure and purification over silica eluting with hexane:EtOAc (90:10) afforded **180** as dark yellow oil (0.106 g, 13%). Physical and spectroscopic properties were identical to that previously given for **180** (7.2.23 procedure A).

*The preparation of this compound has not been reported as it was characterised just by ^{1}H-NMR spectroscopy.

7.2.24 4-(Triisopropylsilanoyloxy)-1-bromopent-2-yne 181[24]

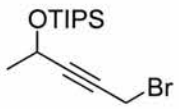

181

TIPS-triflate (0.408 g, 1.33 mmol) was added dropwise to a solution of 1-bromo-4-hydroxypent-2-yne **180** (0.183 g, 1.12 mmol) in DCM (10 cm^3) and 2,6-lutidine (0.517 g, 4.44 mmol), at 0 °C and under nitrogen. The mixture was left to warm to ambient temperature. After 45 min the reaction was completed. After addition of a small amount of water, the solvent was evaporated. The residue was dissolved in EtOAc (20 cm^3) and was washed with water (20 cm^3). The organic layer was then dried over $MgSO_4$, evaporated and the organic residue purified over silica gel eluting with hexane/EtOAc (98:2) to give **181** as colourless oil (~100%); δ_H (300 MHz; $CDCl_3$) 1.05-1.12 [21 H, m, 3 x $CH(CH_3)_2$)], 1.45 (3 H, d, *J* 6.5, $CHC\underline{H}_3$), 3.94 (2 H, d, *J* 1.9, CH_2Br), 4.66 (1 H, qt, *J* 6.5 and 1.9, $C\underline{H}CH_3$); δ_C (75 MHz; $CDCl_3$) 12.5 [3 x $\underline{C}H(CH_3)_2$], 15.0 ($\underline{C}H_2Br$), 18.3 and 18.4 [3 x $CH(\underline{C}H_3)_2$], 26.6 ($CH\underline{C}H_3$), 59.4 ($\underline{C}HCH_3$), 78.4 ($C\equiv\underline{C}CH_2$), 90.1 ($C\equiv\underline{C}CHOTIPS$); ***m/z*** (ESI+) 341.0924 [M + Na. $C_{14}H_{27}$ ^{79}BrONaSi requires 341.0912] (55%) and 343.0901 [M + Na. $C_{14}H_{27}$ ^{81}BrONaSi requires 343.0892] (52%); ν_{max} (neat)/cm^{-1} 2944, 2235 (C≡C, weak), 1464, 1104, 1029, 761, 682.

7.2.25 Diethyl 5-(triisopropylsilanoyloxy)-hex-3-ynyl-phosphonate 178

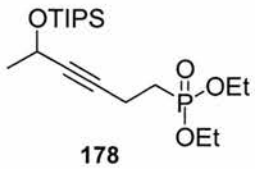

178

A solution of *n*-BuLi (2.5 M in hexane, 0.40 cm^3, 1.0 mmol) was added to a THF (20 cm^3) solution of diethyl methylphosphonate (0.152 g, 1.0 mmol) at -78 °C, and the mixture was stirred for 15 min. A solution of 4-(triisopropylsilanoyloxy)-1-bromopent-2-yne **181** (0.319 g, 1.0 mmol) in THF was then added, and the reaction mixture was warmed to ambient temperature and stirred for 2 h. A sat. NH_4Cl solution (25 cm^3) was then added and the mixture was extracted into EtOAc (2 x 50 cm^3). The organic layer was then dried over $MgSO_4$, evaporated and the organic residue purified over silica gel eluting with hexane:EtOAc (30:70) to afford **178** as colourless oil (0.156 g, 40%); δ_H (300 MHz; $CDCl_3$) 1.00-1.08 [21 H, m, 3 x $CH(CH_3)_2$)], 1.30 (6 H, t, *J* 7.1, 2 x $CH_2C\underline{H}_3$), 1.38 (3 H, d, *J* 6.4, $CHC\underline{H}_3$), 1.88-2.00 (2 H, m, CH_2P), 2.40-2.52 (2 H, m, $C{\equiv}CC\underline{H}_2$), 4.00-4.15 (4 H, m, 2 x $C\underline{H}_2CH_3$), 4.54 (1 H, qt, *J* 6.4 and 1.9, $C\underline{H}CH_3$); δ_C (75 MHz; $CDCl_3$) 12.5 [3 x $\underline{C}H(CH_3)_2$], 13.1 (d, *J* 3.1, $\underline{C}H_2CH_2P$), 16.8 [d, *J* 6.0, 2 x $POCH_2\underline{C}H_3$], 18.3 and 18.4 [3 x $CH(\underline{C}H_3)_2$], 25.3 (d, *J* 140.7, CH_2P), 26.1 ($CH\underline{C}H_3$), 59.4 ($\underline{C}HCH_3$), 62.1 (d, *J* 6.4, 2 x $PO\underline{C}H_2CH_3$), 81.9 (d, *J* 23.0, $C{\equiv}\underline{C}CH_2CH_2P$), 84.1 ($C{\equiv}\underline{C}CHOH$); δ_P (121.5 MHz; $CDCl_3$) 30.6; ***m/z*** (ESI+) 413.2247 [M + Na. $C_{19}H_{39}O_4NaPSi$ requires 413.2253] (100%); ν_{max} (neat)/cm^{-1} 2941, 2229 (C≡C, weak), 1463, 1247 (P=O), 1099, 1029.

7.2.26 Diethyl 5-(triisopropylsilanoyloxy)-3,4-dioxohexyl-phosphonate 182[20]

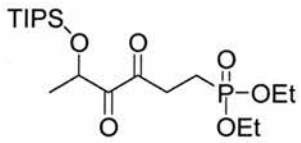

182

Diethyl 5-(triisopropylsilanoyloxy)-hex-3-ynyl-phosphonate **178** (0.13 g, 0.33 mmol) was dissolved in methanol (10 cm^3), and treated with ozone gas at -18/-20 °C. After 40 min, a solution of PPh_3 (0.131 g, 0.5 mmol) in ether (5 cm^3) was added to the mixture. The reaction was stirred for 20 min at -20 °C, and was then warmed to ambient temperature and left for 24 h. The solvent was then evaporated and the residue purified over silica gel eluting with EtOAc/hexane (80:20) to afford **182** as yellow oil (0.11 g, 80%); δ_H (300 MHz; $CDCl_3$) 0.99-1.09 [21 H, m, 3 x $CH(CH_3)_2$)], 1.31 (6 H, t, *J* 7.1, 2 x $CH_2C\underline{H}_3$), 1.40 (3 H, d, *J* 6.8, $CHC\underline{H}_3$), 1.94-2.08 (2 H, m, CH_2P), 2.90-3.08 (2 H, m, CH_2CO), 4.03-4.15 (4 H, m, 2 x $C\underline{H}_2CH_3$) 5.00 (1 H, q, *J* 6.8, $C\underline{H}CH_3$); δ_C (75 MHz; $CDCl_3$) 12.6 [3 x $\underline{C}H(CH_3)_2$], 16.8 (d, *J* 6.0, 2 x $POCH_2\underline{C}H_3$), 18.2 and 18.3 [3 x $CH(\underline{C}H_3)_2$], 19.0 (d, *J* 146.0, CH_2P), 20.5 ($CH\underline{C}H_3$), 37.3 (d, *J* 3.5, $\underline{C}H_2CH_2P$), 62.2 (d, *J* 6.0, 2 x $PO\underline{C}H_2CH_3$), 70.7 ($\underline{C}HCH_3$), 200.0 (d, *J* 15.4, $\underline{C}OCH_2CH_2P$), 200.2 (CO); δ_P (121.5 MHz; $CDCl_3$) 31.4; ***m/z*** (CI+) 445.2149 [M + Na. $C_{19}H_{39}O_6NaPSi$ requires 445.2151] (5%).

7.2.27 4-(Acetyloxy)-1-bromopent-2-yne 187[17,23]

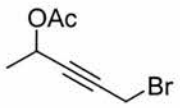

187

Pyridine (0.29 g, 3.66 mmol) was added to a stirred solution of 1-bromo-4-hydroxy-pent-2-yne **180** (0.20 g, 1.22 mmol) in DCM (5 cm^3), followed by acetic anhydride (0.142 cm^3, 1.5 mmol) and a catalytic amount of DMAP (0.010 g, 0.082 mmol). After 3 h the mixture was diluted with EtOAc (20 cm^3) and washed with water (20 cm^3), saturated $CuSO_4$ solution (20 cm^3) and again water (20 cm^3). The organic layer was then dried over $MgSO_4$, evaporated and the organic residue purified over silica gel eluting with hexane/EtOAc (90:10) to afford **187** as colourless oil (0.15 g, 60%); δ_H (300 MHz; $CDCl_3$) 1.45 (3 H, d, *J* 6.7, $CHC\underline{H}_3$), 2.05 (3 H, s, CH_3CO), 3.90 (2 H, d, *J* 1.8, CH_2Br), 5.45 (1 H, qt, *J* 6.7 and 1.8, $C\underline{H}CH_3$); δ_C (75 MHz; $CDCl_3$) 13.9 (CH_2), 21.0 (CH_3), 21.02 (CH_3), 60.1 (CH), 79.8 ($C\equiv\underline{C}CH_2$), 84.9 ($C\equiv\underline{C}CHOAc$), 169.8 (CO); ***m/z*** (ESI+) 226.9578 [M + Na. C_7H_9 $^{79}BrO_2Na$ requires 226.9684] (100%) and 228.9660 [M + Na. C_7H_9 $^{81}BrO_2Na$ requires 228.9663] (100%); ν_{max} (neat)/cm^{-1} 2991, 2078 (C≡C, weak), 1741 (C=O), 1239, 1063.

7.2.28 Dimethyl 5-(acetyloxy)-hex-3-ynyl-phosphonate 188

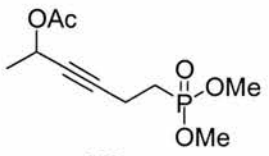

188

A solution of *n*-BuLi (2.5 M in hexane, 0.40 cm^3, 1.0 mmol) was added to a THF (20 cm^3) solution dimethyl methylphosphonate (0.124 g, 1.0 mmol) at -78 °C, and the mixture was then stirred for 15 min. A solution of 4-(acetyloxy)-1-bromopent-2-yne **187** (0.205 g, 1.0 mmol) in THF was then added, and the reaction mixture was warmed to ambient temperature and stirred for 2 h. A sat. NH_4Cl solution (25 cm^3) was then added and the mixture was extracted into EtOAc (2 x 50 cm^3). The organic layer was dried over $MgSO_4$, evaporated and the organic residue purified over silica gel eluting with EtOAc/ethanol (95:5) to afford **188** as colourless oil (0.10 g, 40%); δ_H (300 MHz; $CDCl_3$) 1.38 (3 H, d, *J* 6.7, $CHC\underline{H}_3$), 1.86-1.98 (2 H, m, CH_2P), 1.99 (3 H, s, CH_3CO), 2.37-2.49 (2 H, m, $C{\equiv}CCH_2$), 3.68 (6 H, d, *J* 10.8, 2 x CH_3O) 5.34 (1 H, qt, *J* 6.7 and 1.9, $C\underline{H}CH_3$); δ_C (75 MHz; $CDCl_3$) 13.0 (d, *J* 3.66, $\underline{C}H_2CH_2P$), 21.4 (CH_3), 21.9 (CH_3), 24.5 (d, *J* 141.6, $CH_2\underline{C}H_2P$), 52.8 (d, *J* 6.5, 2 x CH_3O), 60.8 (CH), 79.8 ($C{\equiv}\underline{C}CHOAc$), 83.6 (d, *J* 19.9, $C{\equiv}\underline{C}CH_2$), 170.2 (CO); δ_P (121.5 MHz; $CDCl_3$) 32.9; ***m/z*** (ESI+) 271.0717 [M + Na. $C_{10}H_{17}O_5NaP$ requires 271.0711] (100%).

7.2.29 Dimethyl 5-(acetyloxy)-3,4-dioxohexyl-phosphonate 186[20]

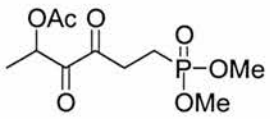

186

Dimethyl 5-(acetyloxy)-hex-3-ynyl-phosphonate **188** (0.124 g, 0.5 mmol) was dissolved in CCl_4/acetic acid (10 cm^3; 4:1), and treated with ozone gas at -18/-20 °C. After 30 min, a solution of PPh_3 (0.18 g, 0.69 mmol) in ether (5 cm^3) was added to the mixture. The reaction was stirred for 20 min at -20 °C, and was then warmed to ambient temperature and left for 24 h. The solvent was evaporated and the residue purified over silica gel eluting with EtOAc/ethanol (90:10) to afford **186** as yellow oil (0.098 g, 70%); δ_H (300 MHz; $CDCl_3$) 1.40 (3 H, d, *J* 7.1, CHC<u>H</u>$_3$), 1.94-2.07 (2 H, m, CH_2P), 2.05 (3 H, s, CH_3COO), 2.88-3.16 (2 H, m, CH_2CO), 3.68 (3 H, d, *J* 10.8, CH_3OP), 3.69 (3 H, d, *J* 10.8, CH_3OP), 5.46 (1 H, q, *J* 7.1, C<u>H</u>CH_3); δ_C (75 MHz; $CDCl_3$) 16.1 (CH<u>C</u>H_3), 18.0 (d, *J* 145.8, <u>C</u>H_2P), 20.6 (<u>C</u>H_3COO), 30.2 (d, *J* 3.6, <u>C</u>H_2CH_2P), 52.9 (d, *J* 6.5, CH_3O), 53.0 (d, *J* 6.5, CH_3O), 71.0 (CH), 171.2 (CH_3<u>C</u>OO), 194.4 (CH<u>C</u>O), 196.4 (d, *J* 14.4, <u>C</u>OCH_2CH_2P); δ_P (121.5 MHz; $CDCl_3$) 34.2; ***m/z*** (ESI+) 303.0605 [M + Na. $C_{10}H_{17}O_7NaP$ requires 303.0610] (100%).

7.2.30 Deprotection of diethyl 5-(triisopropylsilanoyloxy)-3,4-dioxohexyl-phosphonate 182[26]

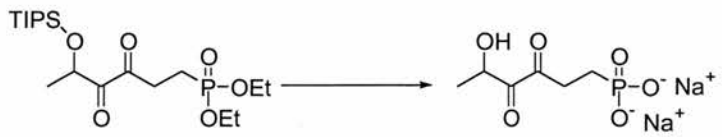

182 **152**

TMS-bromide (0.109 cm^3, 0.829 mmol) was added to a solution of diethyl 5-(triisopropylsilanoyloxy)-3,4-dioxohexyl-phosphonate **182** (0.05 g, 0.118 mmol) in DCM (2 cm^3) at ambient temperature and under an inert atmosphere. After 6 h the solvent was removed and the residue dried *under vacuum* for 3 h. Water (5 cm^3) was then added and the mixture was stirred for 20 min until the solid went completely into solution. The solution was then neutralized with 0.2 N NaOH until pH= ~7 and the solvent was finally removed by lyophilisation to afford **152** as crude product; ***m/z*** (ESI-) 209 {mono-anion form of **152**} [M-H] (30%).

7.2.31 Deprotection of dimethyl 5-(acetyloxy)-3,4-dioxohexyl-phosphonate 186

186 152

TMS-bromide (0.109 cm^3, 0.829 mmol) was added to a solution of dimethyl 5-(acetyloxy)-3,4-dioxohexyl-phosphonate **186** (0.033 g, 0.118 mmol) in DCM (2 cm^3) at ambient temperature and under an inert atmosphere. After 2 h the solvent was removed and the residue dried *under vacuum* for 3 h. Water (5 cm^3) was then added and the mixture was stirred for 20 min until the solid went completely into solution. The solvent was then evaporated and the solid was treated with an excess of NaOH solution (0.2 N). After 4 h, the solution was neutralised with a 0.2 N HCl solution (pH ~6.5-7.0). The solvent was finally removed by lyophilisation to afford **152** as crude product; ***m/z*** (ESI-) 209 {mono-anion form of **152**} [M-H] (60%).

7.3 Biochemical experiments

7.3.1 Purification of SAM Synthase[27]

Bakers' yeasts (*Saccromyces cerevasiae*) was grown in a conical flask (2 L) containing a defined medium (500 cm^3) consisting of yeast extract (0.9%), peptone (1.8%) and D-glucose (2%). After incubation (37 °C at 200 rpm) for 12 h, the cells were harvested, washed with Tris-HCl buffer (50 mM, pH = 7.8) and then resuspended in the same buffer. A cell-free extract was prepared by sonication (5x1 min, 60% duty cycle) and centrifugation of the cell debris (20,000 x g for 20 min at 4 °C). Typically the protein cencentration was 3.5 mg/mL. The enzyme activity was partially purified by adding solid $(NH_4)_2SO_4$ to the cell free extract at 4 °C until 60% saturation followed by centrifugation. The supernatant was adjusted to 80% saturation with solid $(NH_4)_2SO_4$ and the precipitate was collected after centrifugation. The pellet was dialysed in Tris-HCl buffer (50 mM, pH = 7.8) (12 h at 4 °C) and the protein was eluted from an anion exchange column (Bio-RAD Macro-prep High Q) at 2 mL/min using an AKTA Prime FPLC system (Amersham Pharmacia Biotech), initially with 40 cm^3 Tris-HCl buffer and then a linear gradient from 0 to 0.35 M KCl in Tris-HCl buffer (50mM, pH=7.8) to a final volume of 80 cm^3. The fractions containing SAM synthase were concentrated (3 cm^3) using a 10 kDa Macrosep (Pall Folton) centrifugal concentrator.

7.3.2 HPLC conditions for the SAM synthase / fluorinase assay and purification for (5'*R*)-[$^2H_1$]-FDA 60b

Partially-purified SAM synthase fractions (150 μL) were incubated at 37 °C for 6 h with ATP (20 mM, 50 μL), L-methionine (100 mM, 25 μL), $MgSO_4$ (1 M, 50 μL) and KCl (1

M, 25 μL), in final volume of 0.2 mL. The over-expressed fluorinase solution (3 mg/ cm^3, 500 μL) and KF (2 M, 200 μL) was then added and the coupled enzyme reaction left at 37 °C for 12 h. Aliquotes for HPLC analyses were treated at 95 °C (3 min) and the precipitated protein was removed by centrifugation. An aliquot (20 μL) of the clear supernatant was injected onto a Hypersil 5 μM C-18 column (250x4.6 mm, Macherey-Nagel) equilibrated with KH_2PO_4 (50 mM) and acetonitrile (95:5 v/v). Runs were monitored by UV detection at 260 nm by gradient elution starting from KH_2PO_4 (50 mM) and acetonitrile (95:5 v/v) to a final mobile phase consisting of KH_2PO_4 (50 mM) and acetonitrile (80:20 v/v). Samples were introduced through a high-pressure injector fitted with a 100-μL loop and the flow rate was maintained at 1.0 mL/min with a total time of elution of 20 min.

The isotopically labelled sample of (5'*R*)-[$^2H_1$]-FDA **60b** derived from the enzymatic reactions was purified by semi-preparative HPLC using a C-18 column (Phenomenex Hypersil 5, 250x10.00 mm, 5 μm) under the same conditions described for analytical HPLC. Samples were introduced through a high-pressure injector fitted with a 1 mL loop and the flow rate was maintained at 5.0 mL/min with a total time of elution of 30 min. The fractions were collected and the solvent was removed by lyophilization to afford a mixture of phosphate salts and (5'*R*)-[$^2H_1$]-FDA **60b**. The salts were removed by trituration of the mixture with CH_3CN and then filtration. Removal of the solvent on a rotary evaporator afforded **60b** (0.40 mg).

7.3.3 Crystallization of 83 co-complex with the fluorinase

The fluorinase was purified by a slightly modified protocol to that previously described. The enzyme was treated with TEV protease to remove the His tag and it was then treated with adenine deaminase, to remove any endogenous adenosine, by conversion to inosine which binds to the enzyme. This generated an apo-fluorinase which was more amenable to binding substrate analogues. Fluorinase at a concentration of 4 mg mL^{-1} was incubated with 9-(β-D-*erythro*-furanosyl)adenosine **83** (20 mM), L-methionine **61** (20 mM) and choride ion at different concentrations (from 20 mM up to 150 mM) at 298 K for 4 h. A similar experiment was carried in the absence of L-methionine **61**. These solutions were then crystallised by vapour diffusion against a reservoir containing 32% PEG 1000, 0.1 M phosphate-citrate pH 4.2 and 0.2 M Li_2SO_4. A single crystal was selected and flash cooled to 100 K in a nitrogen stream. Data were recorded to 2.0 Å, on PX14.1 at the SRS beamline (DARSEBURY) (λ= 0.87) on a Q4 ADSC detector. Data were indexed and integrated using MOSLFM and scaled using SCALA. The structure was solved by molecular replacement, using MOLREP, from the original FDAS structure (1 rqr) and refined using Refmac. The final R-factor was 22.4% with a R-free of 28.6%. The PDB entry code is 2cbx. This work was done in collaboration with Professor J. H. Naismith lab at St. Andrews.

7.3.4 DXR assays

The DXR assays have been carried out by Dr. U. Wong in Dr. R. Cox's laboratory at Bristol University, using a DXR enzyme purified from *E. coli*. Each assay was run for 5 min at 340 nm wavelength, and was carried out in a tris phosphate buffer solution (1 cm^3,

pH= 8) at 37 °C using 40 nM of enzyme, 0.35 mM of substrate, 1 mM of Mg^{2+}, and varying the concentrations of **152** (0.1, 0.2, 0.5, 1, 1.5 2 and 3 mM). A time course assay was evaluated at intervals T (10, 20, 30, 40, 50, 60, 80 and100 min).

References Chapter 7

1. R. R. Schmidt, U. Schloz and D. Schwille, *Chem. Ber.*, 1968, **101**, 590.

2. J. B. Epp and T. S. Widlanski, *J. Org. Chem.*, 1999, **64**, 293.

3. I. D. Jenkis, J. P. H. Verheyden and J. G. Moffatt, *J. Am. Chem. Soc.*, 1976, **98**, 3346.

4. R. S. Ranganathan, G. H. Jones and J. G. Moffatt, *J. Org. Chem.*, 1974, **39**, 290.

5. Y. Oogo, A. M. Ono and M. Kainosho, *Tetrahedron Lett.*, 1998, **39**, 2873.

6. D. C. Baker and D. Horton, *Carbohydr. Res.*, 1972, **21**, 393.

7. D. Giani and A. W. Johnson, *J. Chem. Soc., Perkin Trans. I*, 1982, 1197.

8. S. L. Cobb, "The origin and metabolism of 5'-FDA in S. Cattleya", PhD Thesis, University of St. Andrews, 2005.

9. C. Schaffrath, S. L. Cobb and D. O'Hagan, *Angew. Chem. Int. Ed.*, 2002, **41**, 3913.

10. H. M. Kissman and M. J. Weiss, *J. Am. Chem. Soc.*, 1958, **80**, 5559.

11. E. Trevisol, E. Defrancq, J. Lhomme, A. Laayoun and P. Cros, *Eur. J. Org. Chem.*, 2000, 211.

12 J. Ludwig and F. Eckstein, *J. Org. Chem.*, 1989, **54**, 631.

13. F. W. Lichtenthaler and H. J. Müller, *Synthesis*, 1974, 199.

14. M. J. Robins, Z. Guo, M. C. Samano and S. F. Wnuk, *J. Am. Chem. Soc.*, 1999, **121**, 1425.

15. J. Giziewicz, S. F. Wnuk and M. J. Robins, *J. Org. Chem.*, 1999, **64**, 2149.

16. P. C. Kline and A. S. Serianni, *J. Org. Chem.*, 1992, **57**, 1772.

17. A. S. Kalgutkar, K. R. Kozak, B. C. Crews, G. P. Hochgesang Jr. and L. J. Marnett, *J. Med. Chem.*, 1998, **41**, 4800.

18. M. Nicoletti, "Novel approach to asymmetric synthesis in organic and organo-fluorine chemistry", PhD Thesis, University of St. Andrews, 2004.

19. R. K. Bhatt, K. Chauhan, P. Wheelan, R. C. Murphy and J. R. Falk, *J. Am. Chem. Soc.*, 1994, **116**, 5050.

20. L. Re, B. Maurer and G. Ohloff, *Helv. Chim. Acta*, 1973, **56**, 1882.

21. M. Yoshida, Y. Ohsawa and M. Ihara, *J. Org. Chem.*, 2004, **69**, 1590.

22. H. Hofmeister, K. Annen, H. Laurent and R. Wiechert, *Angew. Chem. Int. Ed.*, 1984, **23**, 727.

23. T. W. Greene and P. G. M. Wuts, "Protective groups in organic synthesis", 3rd Ed. Wiley Interscience.

24. K. Tanaka, H. Yoda, Y. Isobe and A. Kaji, *J. Org. Chem.*, 1986, **51**, 1856.

25. S. Hu and L. P. Hager, *J. Am. Chem. Soc.*, 1999, **121**, 872.

26. C. E. McKenna, M. T. Higa, N. H. Cheung and M. McKenna, *Tetrahedron. Lett.*, 1977, **18**, 155.

27. T. C. Chou and P. Talalay, *Biochemistry*, 1972, **11**, 1065.

Appendix I

X-ray data for **105**

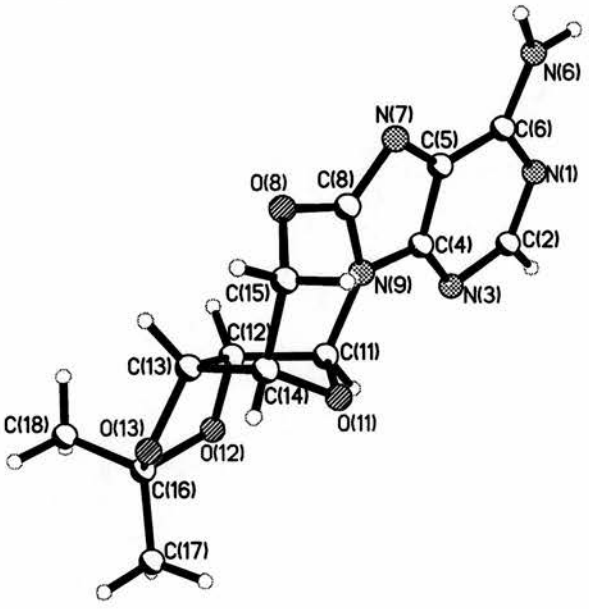

Table 1. Crystal data and structure refinement for **105**

Empirical formula	C14 H19 N5 O5	
Formula weight	337.34	
Temperature	93(2) K	
Wavelength	0.71073 Å	
Crystal system	Monoclinic	
Space group	P2(1)	
Unit cell dimensions	a = 16.365(6) Å	α= 90°.
	b = 8.486(3) Å	β= 102.537(5)°.
	c = 17.132(7) Å	γ = 90°.
Volume	2322.6(15) $Å^3$	
Z	6	
Density (calculated)	1.447 Mg/m^3	
Absorption coefficient	0.112 mm^{-1}	
F(000)	1068	
Crystal size	0.2000 x 0.0500 x 0.0500 mm^3	
Theta range for data collection	2.44 to 25.35°.	
Index ranges	-16<=h<=19, -10<=k<=7, -20<=l<=20	
Reflections collected	17900	
Independent reflections	7776 [R(int) = 0.0522]	
Completeness to theta = 25.35°	98.0 %	
Absorption correction	Multiscan	
Max. and min. transmission	1.0000 and 0.7121	
Refinement method	Full-matrix least-squares on F^2	
Data / restraints / parameters	7776 / 7 / 681	
Goodness-of-fit on F^2	1.069	
Final R indices [I>2sigma(I)]	R1 = 0.0693, wR2 = 0.1624	
R indices (all data)	R1 = 0.0952, wR2 = 0.1843	
Absolute structure parameter	0.4(15)	
Extinction coefficient	0.0022(13)	
Largest diff. peak and hole	0.748 and -0.371 $e.Å^{-3}$	

Table 2. Atomic coordinates (x 10^4) and equivalent isotropic displacement parameters ($Å^2$x 10^3) for **105**. U(eq) is defined as one third of the trace of the orthogonalized U^{ij} tensor.

	x	y	z	U(eq)
N(1)	5159(2)	7561(5)	13058(2)	24(1)
C(2)	5652(3)	8033(6)	13738(3)	24(1)
N(3)	6087(2)	7141(5)	14343(2)	26(1)
C(4)	5939(3)	5597(6)	14178(3)	23(1)
C(5)	5467(3)	4944(6)	13490(3)	23(1)
C(6)	5046(3)	5991(6)	12905(3)	23(1)
N(6)	4529(3)	5579(5)	12221(2)	24(1)
N(7)	5444(2)	3306(5)	13544(2)	24(1)
C(8)	5922(3)	3041(6)	14256(3)	21(1)
O(8)	6143(2)	1585(4)	14538(2)	27(1)
N(9)	6236(2)	4363(5)	14674(2)	24(1)
C(11)	6722(3)	4469(6)	15495(3)	26(1)
O(11)	6291(2)	3676(5)	16019(2)	30(1)
C(12)	7570(3)	3661(6)	15612(3)	25(1)
O(12)	8134(2)	4455(5)	16246(2)	29(1)
C(13)	7432(3)	2027(6)	15974(3)	28(1)
O(13)	7934(2)	2083(5)	16773(2)	31(1)
C(14)	6511(3)	2020(6)	15999(3)	29(1)
C(15)	5961(3)	1167(6)	15308(3)	28(1)
C(16)	8537(3)	3302(6)	16808(3)	26(1)
C(17)	8708(4)	4005(7)	17636(3)	37(1)
C(18)	9305(3)	2684(7)	16564(3)	35(1)

Table 3. Bond lengths [Å] and angles [°] for **105**

N(1)-C(2)	1.327(6)
N(1)-C(6)	1.363(6)
C(2)-N(3)	1.354(6)
C(2)-H(2A)	0.9500
N(3)-C(4)	1.351(7)
C(4)-N(9)	1.369(7)
C(4)-C(5)	1.378(7)
C(5)-N(7)	1.394(6)
C(5)-C(6)	1.403(7)
C(6)-N(6)	1.335(6)
N(6)-H(6A)	0.9800(11)
N(6)-H(6B)	0.9800(11)
N(7)-C(8)	1.318(6)
C(8)-O(8)	1.348(6)
C(8)-N(9)	1.369(6)
O(8)-C(15)	1.457(6)
N(9)-C(11)	1.461(6)
C(11)-O(11)	1.425(6)
C(11)-C(12)	1.521(7)
C(11)-H(11A)	1.0000
O(11)-C(14)	1.453(6)
C(12)-O(12)	1.432(6)
C(12)-C(13)	1.555(7)
C(12)-H(12A)	1.0000
O(12)-C(16)	1.430(6)
C(13)-O(13)	1.436(6)
C(13)-C(14)	1.518(7)
C(13)-H(13A)	1.0000
O(13)-C(16)	1.421(6)
C(14)-C(15)	1.507(7)
C(14)-H(14A)	1.0000
C(15)-H(15A)	0.9900
C(15)-H(15B)	0.9900
C(16)-C(18)	1.503(7)

C(16)-C(17)	1.507(7)
C(17)-H(17A)	0.9800
C(17)-H(17B)	0.9800
C(17)-H(17C)	0.9800
C(18)-H(18A)	0.9800
C(18)-H(18B)	0.9800
C(18)-H(18C)	0.9800
C(2)-N(1)-C(6)	119.6(4)
N(1)-C(2)-N(3)	128.5(5)
N(1)-C(2)-H(2A)	115.8
N(3)-C(2)-H(2A)	115.8
C(4)-N(3)-C(2)	110.0(4)
N(3)-C(4)-N(9)	126.1(4)
N(3)-C(4)-C(5)	127.6(5)
N(9)-C(4)-C(5)	106.3(4)
C(4)-C(5)-N(7)	111.3(5)
C(4)-C(5)-C(6)	117.0(5)
N(7)-C(5)-C(6)	131.4(5)
N(6)-C(6)-N(1)	117.3(5)
N(6)-C(6)-C(5)	125.5(5)
N(1)-C(6)-C(5)	117.2(4)
C(6)-N(6)-H(6A)	123(4)
C(6)-N(6)-H(6B)	125(4)
H(6A)-N(6)-H(6B)	111(5)
C(8)-N(7)-C(5)	102.2(4)
N(7)-C(8)-O(8)	123.2(4)
N(7)-C(8)-N(9)	115.1(4)
O(8)-C(8)-N(9)	121.5(4)
C(8)-O(8)-C(15)	117.2(4)
C(8)-N(9)-C(4)	105.1(4)
C(8)-N(9)-C(11)	128.2(4)
C(4)-N(9)-C(11)	126.5(4)
O(11)-C(11)-N(9)	109.7(4)
O(11)-C(11)-C(12)	105.4(4)
N(9)-C(11)-C(12)	112.9(4)
O(11)-C(11)-H(11A)	109.6

N(9)-C(11)-H(11A)	109.6
C(12)-C(11)-H(11A)	109.6
C(11)-O(11)-C(14)	106.4(4)
O(12)-C(12)-C(11)	107.9(4)
O(12)-C(12)-C(13)	104.0(4)
C(11)-C(12)-C(13)	104.4(4)
O(12)-C(12)-H(12A)	113.2
C(11)-C(12)-H(12A)	113.2
C(13)-C(12)-H(12A)	113.2
C(16)-O(12)-C(12)	108.4(4)
O(13)-C(13)-C(14)	109.9(4)
O(13)-C(13)-C(12)	104.4(4)
C(14)-C(13)-C(12)	104.2(4)
O(13)-C(13)-H(13A)	112.6
C(14)-C(13)-H(13A)	112.6
C(12)-C(13)-H(13A)	112.6
C(16)-O(13)-C(13)	108.2(4)
O(11)-C(14)-C(15)	112.0(4)
O(11)-C(14)-C(13)	104.4(4)
C(15)-C(14)-C(13)	114.0(4)
O(11)-C(14)-H(14A)	108.8
C(15)-C(14)-H(14A)	108.8
C(13)-C(14)-H(14A)	108.8
O(8)-C(15)-C(14)	113.0(4)
O(8)-C(15)-H(15A)	109.0
C(14)-C(15)-H(15A)	109.0
O(8)-C(15)-H(15B)	109.0
C(14)-C(15)-H(15B)	109.0
H(15A)-C(15)-H(15B)	107.8
O(13)-C(16)-O(12)	104.8(4)
O(13)-C(16)-C(18)	110.4(4)
O(12)-C(16)-C(18)	110.0(4)
O(13)-C(16)-C(17)	108.3(4)
O(12)-C(16)-C(17)	109.1(4)
C(18)-C(16)-C(17)	113.8(5)
C(16)-C(17)-H(17A)	109.5

C(16)-C(17)-H(17B)	109.5
H(17A)-C(17)-H(17B)	109.5
C(16)-C(17)-H(17C)	109.5
H(17A)-C(17)-H(17C)	109.5
H(17B)-C(17)-H(17C)	109.5
C(16)-C(18)-H(18A)	109.5
C(16)-C(18)-H(18B)	109.5
H(18A)-C(18)-H(18B)	109.5
C(16)-C(18)-H(18C)	109.5
H(18A)-C(18)-H(18C)	109.5
H(18B)-C(18)-H(18C)	109.5
C(19)-O(19)-H(19)	109.5
O(19)-C(19)-H(19A)	109.5
O(19)-C(19)-H(19B)	109.5
H(19A)-C(19)-H(19B)	109.5
O(19)-C(19)-H(19C)	109.5
H(19A)-C(19)-H(19C)	109.5
H(19B)-C(19)-H(19C)	109.5

Table 4. Anisotropic displacement parameters ($Å^2 x\ 10^3$) for **105**. The anisotropic displacement factor exponent takes the form: $-2\pi^2[\ h^2\ a^{*2}U^{11} + ... + 2\ h\ k\ a^*\ b^*\ U^{12}\ ]$

	U^{11}	U^{22}	U^{33}	U^{23}	U^{13}	U^{12}
N(1)	24(2)	18(3)	26(2)	-5(2)	-1(2)	-3(2)
C(2)	23(2)	21(3)	26(3)	-3(2)	0(2)	3(2)
N(3)	26(2)	21(3)	26(2)	-4(2)	-5(2)	-1(2)
C(4)	24(3)	17(3)	28(3)	-4(2)	4(2)	-1(2)
C(5)	22(2)	22(3)	25(3)	-3(2)	5(2)	-1(2)
C(6)	21(2)	19(3)	31(3)	-5(2)	8(2)	-5(2)
N(6)	21(2)	25(3)	21(2)	-1(2)	-4(2)	1(2)
N(7)	23(2)	23(3)	25(2)	0(2)	6(2)	2(2)
C(8)	26(2)	9(3)	26(3)	-1(2)	4(2)	-2(2)
O(8)	35(2)	19(2)	26(2)	3(2)	7(2)	-1(2)
N(9)	31(2)	19(2)	21(2)	-3(2)	3(2)	-2(2)
C(11)	36(3)	16(3)	23(2)	1(2)	3(2)	-5(2)
O(11)	36(2)	30(2)	27(2)	-2(2)	13(2)	-1(2)
C(12)	30(3)	23(3)	18(2)	1(2)	-4(2)	-3(2)
O(12)	33(2)	28(2)	22(2)	0(2)	-6(2)	-1(2)
C(13)	41(3)	21(3)	19(2)	2(2)	2(2)	-3(2)
O(13)	36(2)	32(2)	21(2)	7(2)	0(2)	-2(2)
C(14)	37(3)	22(3)	28(3)	0(2)	9(2)	-8(2)
C(15)	36(3)	23(3)	26(3)	8(2)	10(2)	-4(2)
C(16)	31(3)	19(3)	26(3)	1(2)	1(2)	-2(2)
C(17)	47(3)	37(4)	25(3)	-5(2)	6(2)	-4(3)
C(18)	40(3)	33(3)	30(3)	5(2)	3(2)	7(3)

Table 5. Hydrogen coordinates (x 10^4) and isotropic displacement parameters ($Å^2$x 10^3) for **105**.

	x	y	z	U(eq)
H(2A)	5707	9141	13810	29
H(6A)	4270(40)	6340(60)	11820(30)	80(20)
H(6B)	4350(40)	4500(30)	12070(30)	60(20)
H(11A)	6803	5601	15655	31
H(12A)	7783	3585	15109	30
H(13A)	7588	1131	15656	33
H(14A)	6446	1513	16509	35
H(15A)	6038	17	15391	34
H(15B)	5368	1416	15299	34
H(17A)	8183	4385	17755	55
H(17B)	9100	4887	17663	55
H(17C)	8953	3201	18027	55
H(18A)	9150	2253	16021	52
H(18B)	9560	1852	16935	52
H(18C)	9708	3543	16576	52
H(19)	7050	8515	14814	75
H(19A)	8416	8637	14157	83
H(19B)	7529	7816	13823	83
H(19C)	8218	6953	14493	83

Table 6. Torsion angles [°] for ccdh1.

C(6)-N(1)-C(2)-N(3)	-0.2(8)
N(1)-C(2)-N(3)-C(4)	-1.6(7)
C(2)-N(3)-C(4)-N(9)	-176.2(4)
C(2)-N(3)-C(4)-C(5)	3.8(7)
N(3)-C(4)-C(5)-N(7)	-178.8(5)
N(9)-C(4)-C(5)-N(7)	1.2(6)
N(3)-C(4)-C(5)-C(6)	-4.0(8)
N(9)-C(4)-C(5)-C(6)	175.9(4)
C(2)-N(1)-C(6)-N(6)	178.4(4)
C(2)-N(1)-C(6)-C(5)	0.2(7)
C(4)-C(5)-C(6)-N(6)	-176.4(5)
N(7)-C(5)-C(6)-N(6)	-2.9(9)
C(4)-C(5)-C(6)-N(1)	1.7(7)
N(7)-C(5)-C(6)-N(1)	175.2(5)
C(4)-C(5)-N(7)-C(8)	-1.6(5)
C(6)-C(5)-N(7)-C(8)	-175.3(5)
C(5)-N(7)-C(8)-O(8)	-173.9(4)
C(5)-N(7)-C(8)-N(9)	1.4(5)
N(7)-C(8)-O(8)-C(15)	-125.5(5)
N(9)-C(8)-O(8)-C(15)	59.4(6)
N(7)-C(8)-N(9)-C(4)	-0.8(5)
O(8)-C(8)-N(9)-C(4)	174.7(4)
N(7)-C(8)-N(9)-C(11)	174.4(4)
O(8)-C(8)-N(9)-C(11)	-10.2(7)
N(3)-C(4)-N(9)-C(8)	179.7(5)
C(5)-C(4)-N(9)-C(8)	-0.3(5)
N(3)-C(4)-N(9)-C(11)	4.4(8)
C(5)-C(4)-N(9)-C(11)	-175.5(4)
C(8)-N(9)-C(11)-O(11)	-52.9(6)
C(4)-N(9)-C(11)-O(11)	121.3(5)
C(8)-N(9)-C(11)-C(12)	64.4(6)
C(4)-N(9)-C(11)-C(12)	-121.4(5)
N(9)-C(11)-O(11)-C(14)	84.2(5)
C(12)-C(11)-O(11)-C(14)	-37.7(5)

O(11)-C(11)-C(12)-O(12)	-89.3(5)
N(9)-C(11)-C(12)-O(12)	150.9(4)
O(11)-C(11)-C(12)-C(13)	20.9(5)
N(9)-C(11)-C(12)-C(13)	-98.8(5)
C(11)-C(12)-O(12)-C(16)	129.5(4)
C(13)-C(12)-O(12)-C(16)	19.0(5)
O(12)-C(12)-C(13)-O(13)	0.1(5)
C(11)-C(12)-C(13)-O(13)	-113.0(4)
O(12)-C(12)-C(13)-C(14)	115.3(4)
C(11)-C(12)-C(13)-C(14)	2.3(5)
C(14)-C(13)-O(13)-C(16)	-130.5(4)
C(12)-C(13)-O(13)-C(16)	-19.2(5)
C(11)-O(11)-C(14)-C(15)	-84.7(5)
C(11)-O(11)-C(14)-C(13)	39.1(5)
O(13)-C(13)-C(14)-O(11)	87.2(5)
C(12)-C(13)-C(14)-O(11)	-24.2(5)
O(13)-C(13)-C(14)-C(15)	-150.3(4)
C(12)-C(13)-C(14)-C(15)	98.3(5)
C(8)-O(8)-C(15)-C(14)	-70.8(5)
O(11)-C(14)-C(15)-O(8)	72.3(5)
C(13)-C(14)-C(15)-O(8)	-46.0(6)
C(13)-O(13)-C(16)-O(12)	31.3(5)
C(13)-O(13)-C(16)-C(18)	-87.1(5)
C(13)-O(13)-C(16)-C(17)	147.7(4)
C(12)-O(12)-C(16)-O(13)	-31.4(5)
C(12)-O(12)-C(16)-C(18)	87.3(5)
C(12)-O(12)-C(16)-C(17)	-147.2(4)

Symmetry transformations used to generate equivalent atoms:

Table 7. Hydrogen bonds for **105** [Å and °].

D-H...A	d(D-H)	d(H...A)	d(D...A)	<(DHA)
N(6)-H(6A)...N(47)#1	0.9800(11)	2.15(3)	3.077(6)	158(6)
N(6)-H(6B)...N(41)#2	0.9800(11)	1.970(16)	2.932(6)	166(5)
O(19)-H(19)...N(3)	0.98	1.99	2.867(6)	148.4
N(26)-H(26A)...N(27)#1	0.9800(11)	2.256(7)	3.234(6)	176(4)
N(26)-H(26B)...N(21)#2	0.9800(11)	2.000(19)	2.925(6)	156(4)
O(39)-H(39)...N(23)	0.98	1.97	2.932(6)	165.9
N(46)-H(46A)...N(7)#1	0.9800(11)	2.178(13)	3.151(6)	171(7)
N(46)-H(46B)...N(1)#2	0.9800(11)	1.876(12)	2.849(6)	172(7)
O(59)-H(59)...N(7)	0.98	2.23	3.103(6)	148.4

Symmetry transformations used to generate equivalent atoms:

#1 -x+1,y+1/2,-z+2 #2 -x+1,y-1/2,-z+2

Appendix II

List of publications

Cosimo D. Cadicamo, Jacques Cortieu, Hai Deng, Abdelkrim Meddour and D. O'Hagan: "Enzymatic Fluorination in Streptomyces cattleya takes place with an inversion of configuration consistent with an S_N2 reaction mechanism", *ChemBioChem*, 2004, **5**, 685-690 (Front Cover).

Awards

1st Prize for the Best Poster presentation at the Graduate Symposium (Bristol, 16th June 2004): "The Chemsitry and Biology of Natural Product Biosynthesis".

Conferences attended

- 2nd RSC Fluorine Subject Group Postgraduate Meeting,

University of Manchester (5th-6th Sept 2002).

- 31st Scottish Regional Perking Division Meeting,

Dundee University (18th Dec 2002).

- Enzyme mechanism. A structural perspective,

University of St Andrews (12th-14th Jan 2003)

- 14th Scottish Graduate Symposium on novel organic chemistry,

University of Aberdeen (9th April 2003).

- 3rd RSC Fluorine Subject Group Postgraduate Meeting,

University of St Andrews (4th-5th Sept 2003).

- 1st University of Glasgow/Organon Symposium on synthetic chemistry (22nd Sept 2003)

- RSC Organic Division and Chemical Biology Forum,

University of Edinburgh (31st October 2003).

- 32nd Scottish Regional Perkin Meeting,

University of Edinburgh (17th December 2003).

- 4th RSC Fluorine Subject Group Postgraduate Meeting,

University of Durham (September 2004)

- 33rd Scottish Organic Division Meeting,

University of St Andrews (20th December 2004).

- 2nd Organic Chemistry PhD symposium,

University of St Andrews (2nd June 2005)

- The 17th Winter Fluorine Conference

St Pete Beach, Florida, USA (9th -14th January 2005)

- RSC and BBSRC symposium,'The Chemistry and Biology of Natural Product

Biosynthesis II', Bristol (15th July 2005)

- 5th Annual RSC Fluorine Subject Group Postgraduate Meeting,

University of Oxford, (1-2nd September 2005).